Advanced Pediatric Chest Computed Tomography

Safe and standardized protocols and sensitive image analysis of cystic fibrosis lung disease

WieYing Kuo – Kim

Advanced Pediatric Chest Computed Tomography

Safe and standardized protocols and sensitive image analysis
of cystic fibrosis lung disease

WieYing Kuo - Kim

The work presented in this thesis was conducted at the Erasmus University Medical Center – Sophia Children's Hospital, the Department of Pediatric Pulmonology & Allergology and the Department of Radiology & Nuclear Medicine.

The studies carried out in this thesis are supported by the Sophia Children's Hospital scientific research foundation (SSWO), through the "steun door zeevaart" fund and the Dutch Cystic Fibrosis Foundation (NCFS).

Printing of this thesis was kindly supported by Teva Netherlands B.V., the Department of Radiology & Nuclear Medicine, Erasmus MC and the Erasmus University Rotterdam.

Cover	© Kenny Rubenis
Layout	Nikki Vermeulen - Ridderprint BV
Printing	Ridderprint BV
ISBN	978-94-6299-667-0

© WieYing Kuo, 2017
All rights reserved. For articles published or accepted for publication, the copyright has been transferred to the respective publisher. No part of this publication may be reproduced, stored in a retrieval system or transmitted, in any form or by any means, without prior permission of the author, or when appropriate, of the publishers of the manuscript.

Advanced Pediatric Chest Computed Tomography

Safe and standardized protocols and sensitive image analysis
of cystic fibrosis lung disease

Geavanceerde thorax computertomografie

Veilig en gestandaardiseerde protocollen en sensitieve beeld analyse
van longziekten door cystische fibrose

Proefschrift

ter verkrijging van de graad van doctor aan de
Erasmus Universiteit Rotterdam
op gezag van de
rector magnificus

Prof.dr. H.A.P. Pols

en volgens besluit van het College voor Promoties.

De openbare verdediging zal plaatsvinden op
woensdag 18 oktober 2017 om 13.30 uur

door

WieYing Kuo - Kim
geboren te Rotterdam

Erasmus University Rotterdam

PROMOTIECOMMISSIE

Promotor:
Prof.dr. H.A.W.M. Tiddens

Overige leden:
Prof.dr. M. de Hoog
Prof.dr. G.G.O. Brusselle
Prof.dr. C.K. van der Ent

Copromotoren:
Dr. M. de Bruijne
Dr. ir. M. van Straten

"The good life is one inspired by love and guided by knowledge."

Bertrand Russel

CONTENTS

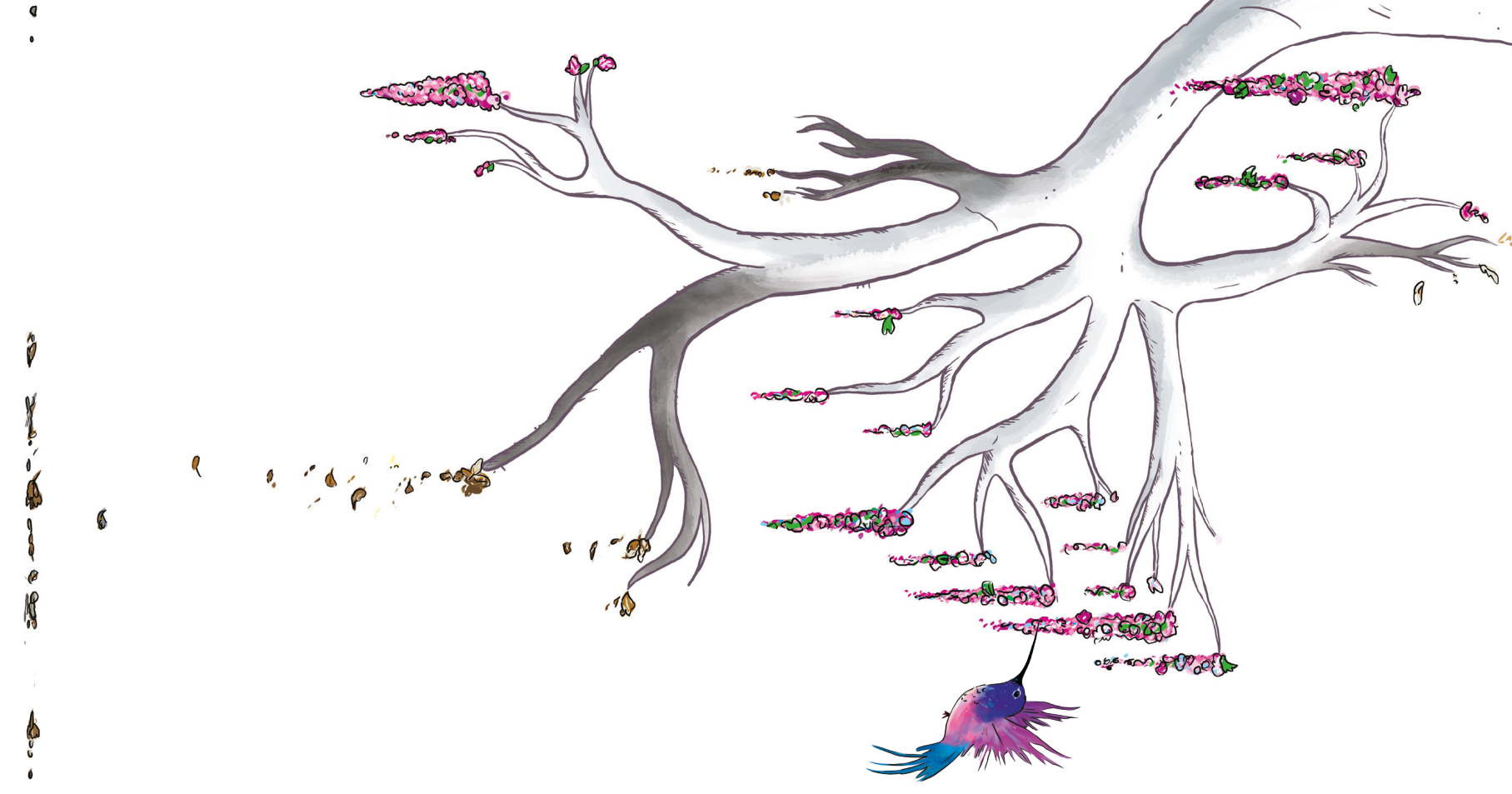

CHAPTER 1

GENERAL INTRODUCTION

Cystic fibrosis

Cystic fibrosis (CF) is the most common life limiting autosomal recessive disorder in Caucasians. Genetic mutations can cause dysfunctional or absent cystic fibrosis transmembrane conductance regulator (CFTR) protein. The CFTR protein is present in many organs, so a dysfunctional or absent CFTR can impact many organ systems. One of the major systems affected are the lungs.[1] When the CFTR is defective or absent, the chloride secretion is reduced or absent causing a hyperabsorption of sodium and water across the airway epithelial cells. This imbalance leads to reduced airway surface liquid and more viscous mucous, impairing mucociliary clearance.[2] This results in chronic bacterial infections and inflammation of the airways. Chronic respiratory disease is the leading cause of mortality and morbidity in patients with CF.[3]

Monitoring early CF lung disease with chest computed tomography

CF lung disease and progressive structural lung changes starts early in life. Lung function and symptom based parameters have mostly been used as outcome measures for intervention studies in CF. Unfortunately in the children with CF aged of 5 and younger, lung function outcome measures are cumbersome to execute and to date not sensitive enough to quantify structural lung disease.[4] The most sensitive modality to detect and monitor structural lung changes in the younger children is computed tomography (CT). CT can visualize the lung parenchyma and airways in more detail than conventional chest X-ray and magnetic resonance imaging.[5] Structural changes on chest CT can be detected as early as three months and can be present in children without any symptoms.[6,7] Due to the silently progressive nature of CF lung disease it is essential to intervene at a young age, before any permanent and irreversible lung changes have established.[4]

To evaluate the effectiveness of early CF treatment there is a need for sensitive CT image analysis methods to quantify structural lung disease in young children. In order to sensitively monitor early CF lung disease with the aid of CT, radiation risk and standardization have to be addressed.

Radiation risk of routine chest CT

Chest CT became an essential imaging technique in clinical practice for the detection and monitoring of CF lung disease in children since the nineties. [8,9] The use of chest CT has increased over the past years among pediatric CF patients. A downside of CT scanning, however, is the exposure to ionizing radiation. This is especially important for children as they are more sensitive to radiation and generally have longer life expectancies to develop radiation induced cancer.[10] The potential risks associated with

radiation exposure have for long been a hurdle for implementation of routine chest CT in clinical practice and for clinical studies.[11] Routine chest CT introduces accumulative radiation exposure and should only be applied if the benefits are greater than the risks. The risks of routine chest CT have been estimated previously, [12] but these estimates were highly conservative and are now outdated thanks to the lower radiation output of modern CT scanners. Additionally, to fully comprehend the risk to benefit ratio, there is a need to put potential radiation risk estimates into perspective of daily life risks.

Chest CT in clinical trials

The improved sensitivity of chest CT for the detection of structural lung disease in CF has opened up the possibility of its use as an outcome measure in clinical trials.[13] Traditional functional outcome measures for clinical trials in CF lung disease are relatively insensitive to measure progression of CF lung disease, particularly in children. The need for more sensitive outcome measures became more urgent as promising but very expensive disease modifying agents were developed recently.[1] Functional outcome measures require a large number of study subjects to demonstrate an effect, causing the clinical trials to be very expensive. More multi-center clinical trials are needed to test all the different new compounds developed, leading to an increased challenge to enroll large numbers of patients.

The use of chest CTs in clinical trials is a promising outcome measure for children with CF, but standardization of CT protocols across CF centers is needed before such trials can be executed. Large differences in CT protocols and CT scanners used across centers are present. This leads to variability in image quality, radiation dose, and lung volume levels. [14] As with any other outcome measure, detailed standardization is needed across centers and across CT vendors to allow for the use of chest CT in multicenter clinical trials.

Image analysis

The most important structural changes related to CF lung disease that can be detected on chest CTs are bronchiectasis, airway wall thickening, mucous plugging and hypoperfusion. Bronchiectasis is defined as an abnormal widening of the airways in combination with a lack of tapering. In adults an airway to artery ratio larger than 1 is classified as bronchiectasis.[15] The inner airway diameter is mostly used nowadays for comparison with the accompanying artery.[16–18] There is however no clear consensus based on objective quantification on whether the inner or outer airway diameter should be used for the diagnosis of bronchiectasis. Additionally, the definition of bronchiectasis has not well been investigated in children. In healthy subjects, the airway to artery ratio is thought to increase with age and a smaller ratio has been suggested

in children.[19,20] Lack of tapering is present if the airway diameter remains unchanged for at least 2 cm after branching,[15] but has not previously been quantified objectively. Tapering could also be quantified by comparing the airway diameter before branching to the airway diameter after branching and has been objectified previously as the homothety ratio. [21,22] Airway wall thickening is present when the airway wall diameter occupies more than 20% of the total outer airway diameter.[23] To date, the presence of CF related bronchiectasis and airway wall thickening are primarily determined visually by radiologists without measuring tools. For detection of more subtle lung changes in children an objective quantification of airway dimensions was considered necessary to allow unbiased assessment of bronchiectasis and airway wall thickening.

Several semi-quantitative scoring techniques were developed to assess structural CF lung disease on chest CT more objectively. Most scoring techniques were developed to quantify moderate to severe lung disease in adults with CF.[24,25] These scoring systems were however not sensitive for young children with CF. For this reason a scoring technique was recently developed specifically for young children with early CF lung disease.[26] These scoring techniques measure disease severity in a semi quantitative subjective way, and have not been compared to objective dimensions of the airways.

More objective quantitative methods to assess airway dimensions were first proposed 10 years ago[27] and repeated in children with volumetric CT recently.[7] These methods assessed the airway and artery dimensions on a limited number of axial CT slices using digital calipers. A disadvantage of this approach is that it causes inaccuracy due to projection error, [28] i.e. the airway and artery dimensions can be perceived larger or smaller depending on the plane in which the airway is visualized, causing an incorrect measurement. In addition, relatively few airway artery pairs can be detected on these axial slices. Ideally, airway and artery dimensions should be measured perpendicular to the longitudinal airway axis. Nowadays, anatomical sizes of the airways can be assessed by reformatting and three-dimensional (3D) rendering the airways with advanced CT image analysis software. Cross-sectional areas of the central and peripheral airways can be visualized. Using the 3D segmented bronchial tree, all visible airway artery pairs can be measured. Such systems have the potential to detect more subtle changes and may be more sensitive to detect early lung disease. A disadvantage of such system is that the manual quantification of a large number of airway and artery dimensions is very time consuming. However, in the current era such measurements can potentially be automated offering fast, inexpensive and sensitive analysis.[29] In addition, automatic quantification would eliminate intra- and inter-observer variability related to manual scoring. Lastly, automated analysis can objectively assess tapering and define the objective dimensions of the airway along the entire airway branch without extremely tedious and time-consuming manual labour.

Reference values

Chest CT is widely used in the pediatric population to diagnose chest disorders and to monitor progression of thoracic abnormalities. To determine pulmonary abnormalities it is essential to have pediatric reference values for thoracic structures. The size and orientation of thoracic structures are known to be dependent on age and gender in the pediatric population.[30,31] A known limitation for the establishment of pediatric CT reference values is that it is not justified to acquire chest CTs in a healthy population and expose healthy children to ionizing radiation to establish reference values.[32] Therefore the availability of CT reference values in the pediatric population is scarce. Normative dimensions of the trachea are currently based on studies with small sample sizes,[33] studies in adults[34] or on studies more than 30 years old using older generation CT scanners.[30,35] Normative data of the airway and artery dimensions are currently based on studies with small sample sizes [19,21] or values determined in adults.[36] Evidently, attempts should be made to obtain pediatric reference values based on larger sample sizes than currently available. This could be based for instance on patients in need for a CT scan due to several clinical indications, but afterwards assessed as normal by the radiologist.

Objectives and outline of this thesis

The following objectives in this thesis have been established to address the issues introduced above:

- To estimate the risks of radiation exposure due to CT scanning and to put these risks into perspective in relation to other risks
- To characterize and standardize pediatric chest CT across CF centers
- To develop an objective method for quantification of airway abnormalities in infants, children and adolescents with CF
- To compare CF scoring methods with objectively quantified airway and artery dimensions
- To provide reference values for key thoracic structures on chest CT of children

The studies addressing these objectives are outlined in this thesis as follows:

Part 1 is about the safety and standardization of pediatric chest CT.
Chapter 2 describes the fundamentals related to CT radiation and estimates the lifetime risk of cancer mortality due to CT related radiation exposure. In addition it puts the risks of radiation exposure in perspective by comparing them with other medical and non-medical risks.
Chapter 3 describes the approach to standardize pediatric chest CT across 16 centers participating in an international network. CT scanners are characterized and the performances of these scanners are compared.

Part 2 focusses on the assessment of CF lung disease on chest CT of pediatric patients with CF.

Chapter 4 describes a sensitive quantitative method for the assessment of airway and artery dimensions to quantify structural lung disease in children and adolescents with CF and the comparison with airway and artery dimensions of control patients.

Chapter 5 entails the same objective airway and artery quantification applied in a longitudinal CT dataset of younger children with early CF lung disease and the cross-sectional comparison with an age matched control patient cohort.

Chapter 6 compares two semi quantitative CF scoring systems with the objective airway and artery quantification method in children and adolescents with CF.

Chapter 7 investigates automated quantification of airway and artery dimensions and validates tapering as a sensitive biomarker for bronchiectasis. In addition, reference tapering values are provided for a control group with and without lung volume control.

Part 3 describes the CT reference values in control pediatric patients.

Chapter 8 presents the normative CT defined central airways.

Chapter 9 presents the normative CT defined airway and artery dimensions.

REFERENCES

1. Wainwright CE, Elborn JS, Ramsey BW, Marigowda G, Huang X, Cipolli M, Colombo C, Davies JC, De Boeck K, Flume P a, et al. Lumacaftor-Ivacaftor in Patients with Cystic Fibrosis Homozygous for Phe508del CFTR. The New England journal of medicine. 2015:1–12.
2. Davies JC. The future of CFTR modulating therapies for cystic fibrosis. Current Opinion in Pulmonary Medicine. 2015;21(6):579–584.
3. Foundation CF. Cystic Fibrosis Foundation Patient Registry Annual Data Report 2014. Accessed March 31, 2016. 2014.
4. Stick S, Tiddens H, Aurora P, Gustafsson P, Ranganathan S, Robinson P, Rosenfeld M, Sly P, Ratjen F. Early intervention studies in infants and preschool children with cystic fibrosis: are we ready? The European respiratory journal. 2013;42(2):527–38.
5. Ciet P, Serra G, Bertolo S, Spronk S, Ros M, Fraioli F, Quattrucci S, Assael MB, Catalano C, Pomerri F, et al. Assessment of CF lung disease using motion corrected PROPELLER MRI: a comparison with CT. European Radiology. 2016;26(3):780–787.
6. Sly PD, Brennan S, Gangell C, De Klerk N, Murray C, Mott L, Stick SM, Robinson PJ, Robertson CF, Ranganathan SC. Lung disease at diagnosis in infants with cystic fibrosis detected by newborn screening. American Journal of Respiratory and Critical Care Medicine. 2009;180(2):146–152.
7. Mott LS, Park J, Murray CP, Gangell CL, de Klerk NH, Robinson PJ, Robertson CF, Ranganathan SC, Sly PD, Stick SM. Progression of early structural lung disease in young children with cystic fibrosis assessed using CT. Thorax. 2012;67(6):509–516.
8. Bhalla M, Turcios N, Aponte V, Jenkins M, Leitman BS, McCauley DI, Naidich DP. Cystic fibrosis: scoring system with thin-section CT. Radiology. 1991;179(3):783–788.
9. Maffessanti M, Candusso M, Brizzi F, Piovesana F. Cystic fibrosis in children: HRCT findings and distribution of disease. Journal of thoracic imaging. 1996;11(1):27–38.
10. Brenner DJ, Elliston CD, Hall EJ, Berdon WE. Estimated Risks of Radiation- Induced Fatal Cancer from Pediatric CT. American Journal of Roentgenology. 2001;176(2):289–296.
11. Lee DW, Levy F. The sharp slowdown in growth of medical imaging: An early analysis suggests combination of policies was the cause. Health Affairs. 2012;31(8):1876–1884.
12. De Jong PA, Mayo JR, Golmohammadi K, Nakano Y, Lequin MH, Tiddens HAWM, Aldrich J, Coxson HO, Sin DD. Estimation of cancer mortality associated with repetitive computed tomography scanning. American Journal of Respiratory and Critical Care Medicine. 2006;173(2):199–203.
13. Wainwright CE, Vidmar S, Armstrong DS, Byrnes CA, Carlin JB, Cheney J, Cooper PJ, Grimwood K, Moodie M, Robertson CF, et al. Effect of bronchoalveolar lavage-directed therapy on Pseudomonas aeruginosa infection and structural lung injury in children with cystic fibrosis: a randomized trial. JAMA : the journal of the American Medical Association. 2011;306(2):163–171.
14. Boedeker KL, McNitt-Gray MF, Rogers SR, Truong D a, Brown MS, Gjertson DW, Goldin JG. Emphysema: effect of reconstruction algorithm on CT imaging measures. Radiology. 2004;232(1):295–301.
15. Newell JD. Bronchiectasis. In: Contemporary Medical imaging. CT of the. 2008. p. 213–235.

16. Mott LS, Graniel KG, Park J, De Klerk NH, Sly PD, Murray CP, Tiddens HAWM, Stick SM. Assessment of early bronchiectasis in young children with cystic fibrosis is dependent on lung volume. Chest. 2013;144(4):1193–1198.

17. Brody AS, Kosorok MR, Li Z, Broderick LS, Foster JL, Laxova A, Bandla H, Farrell PM. Reproducibility of a scoring system for computed tomography scanning in cystic fibrosis. Journal of thoracic imaging. 2006;21(1):14–21.

18. Gaillard EA, Carty H, Heaf D, Smyth RL. Reversible bronchial dilatation in children: comparison of serial high-resolution computer tomography scans of the lungs. European Journal of Radiology. 2003;47(3):215–220.

19. Kapur N, Masel JP, Watson D, Masters IB, Chang AB. Bronchoarterial ratio on high-resolution CT scan of the chest in children without pulmonary pathology: Need to redefine bronchial dilatation. Chest. 2011;139(6):1445–1450.

20. Milliron B, Henry TS, Veeraraghavan S, Little BP. Bronchiectasis: Mechanisms and imaging clues of associated common and uncommon diseases. RadioGraphics. 2015;35:1011–1030.

21. Montaudon M, Desbarats P, Berger P, Dietrich G de, Marthan R, Laurent F. Assessment of bronchial wall thickness and lumen diameter in human adults using multi-detector computed tomography: comparison with theoretical models. Journal of anatomy. 2007;211(July):579--588.

22. Tawhai MH, Hunter P, Tschirren J, Reinhardt J, McLennan G, Hoffman E a. CT-based geometry analysis and finite element models of the human and ovine bronchial tree. Journal of applied physiology. 2004;97(6):2310–2321.

23. Naidich DP, Webb WR, Muller NL, Vlahos I, Krinsky GA. Chapter 5. Airways. In: Computed Tomography and Magnetic Resonance of the thorax. Lippincott Williams & Wilkins; 2007. p. 453–556.

24. Calder AD, Bush A, Brody AS, Owens CM. Scoring of chest CT in children with cystic fibrosis: state of the art. Pediatric radiology. 2014;44(12):1496–506.

25. de Jong PA, Ottink MD, Robben SGF, Lequin MH, Hop WCJ, Hendriks JJE, Paré PD, Tiddens HAWM. Pulmonary disease assessment in cystic fibrosis: comparison of CT scoring systems and value of bronchial and arterial dimension measurements. Radiology. 2004;231(2):434-439.

26. Rosenow T, Oudraad MCJ, Murray CP, Turkovic L, Kuo W, de Bruijne M, Ranganathan SC, Tiddens HAWM, Stick SM. PRAGMA-CF. A Quantitative Structural Lung Disease Computed Tomography Outcome in Young Children with Cystic Fibrosis. American journal of respiratory and critical care medicine. 2015;191(10):1158–1165.

27. De Jong PA, Nakano Y, Hop WC, Long FR, Coxson HO, Paré PD, Tiddens H a. Changes in airway dimensions on computed tomography scans of children with cystic fibrosis. American Journal of Respiratory and Critical Care Medicine. 2005;172(2):218-224.

28. Dournes G, Laurent F. Airway Remodelling in Asthma and COPD: Findings, Similarities, and Differences Using Quantitative CT. Pulmonary Medicine. 2012;2012:1–8.

29. Petersen J, Nielsen M, Lo P, Nordenmark LH, Pedersen JH, Wille MMW, Dirksen A, de Bruijne M. Optimal surface segmentation using flow lines to quantify airway abnormalities in chronic obstructive pulmonary disease. Medical Image Analysis. 2014;18(3):531–541.

30. Griscom NT, Wohl MEB. Dimensions of the growing trachea related to age and gender. American Journal of Roentgenology. 1986;146(2):233–237.

31. Abbassi V. Growth and normal puberty. Pediatrics. 1998;102(2 Pt 3):507–11.

32. Brody AS, Frush DP, Huda W, Brent RL. Radiation risk to children from computed tomography. Pediatrics. 2007;120(3):677–682.

33. Chen SJ, Shih TTF, Liu KL, Chiu IS, Wu MH, Chen HY, Lee WJ. Measurement of tracheal size in children with congenital heart disease by computed tomography. Annals of Thoracic Surgery. 2004;77(4):1216–1221.

34. Diaz AA, Rahaghi FN, Ross JC, Harmouche R, Tschirren J, San Jose Estepar R, Washko GR. Understanding the contribution of native tracheobronchial structure to lung function: CT assessment of airway morphology in never smokers. Respiratory research. 2015;16:23.

35. Griscom NT, Wohl MEB. Dimensions of the growing trachea related to body height. The American Review of Respiratory Disease. 1985;131:840–844.

36. Smith BM, Hoffman EA, Rabinowitz D, Bleecker E, Christenson S, Couper D, Donohue KM, Han MK, Hansel NN, Kanner RE, et al. Comparison of spatially matched airways reveals thinner airway walls in COPD. The Multi-Ethnic Study of Atherosclerosis (MESA) COPD Study and the Subpopulations and Intermediate Outcomes in COPD Study (SPIROMICS). Thorax. 2014;69(11):987–96.

PART I

SAFETY AND STANDARDIZATION OF CHEST CT IN THE PEDIATRIC CYSTIC FIBROSIS POPULATION

CHAPTER 2

MONITORING CYSTIC FIBROSIS LUNG DISEASE USING COMPUTED TOMOGRAPHY: RADIATION RISK IN PERSPECTIVE

Wieying Kuo, Pierluigi Ciet, Harm A.W.M. Tiddens, Wei Zhang, R. Paul Guillerman, Marcel van Straten

American Journal of Respiratory and Critical Care Medicine. 2014;189(11):1328–1336.

ABSTRACT

Computed tomography (CT) is a sensitive technique to monitor structural changes related to cystic fibrosis (CF) lung disease. It detects structural pulmonary abnormalities such as bronchiectasis and trapped air, in an early stage, before they become apparent with other diagnostic tests. Clinical decisions may be influenced by knowledge of these abnormalities. CT imaging, however, comes with risk related to ionizing radiation exposure.

The aim of this review is to discuss the risk of routine CT imaging in CF patients using current models of radiation-induced cancer and to put this risk into perspective with other medical and non-medical risks. The magnitude of the risk is a complex, controversial matter. Risk analyses have largely been based on a linear no-threshold model and excess relative and excess absolute risk estimates mainly derived from atomic bomb survivors. The estimates have large confidence intervals. Our risk estimates are in concordance with previously reported estimates. A large proportion of radiation, to which humans are exposed to, is from natural background sources and varies widely depending on geographical location. The risk differences due to variation in background radiation can be larger than the risks associated with CF lung disease monitoring using CT.

We conclude that the risk related to routine usage of CT in clinical care is small. In addition, a life limiting disease, such as CF lowers the risk of radiation-induced cancer. Nonetheless, the use of CT should always be justified and the radiation dose should be kept as low as reasonably achievable.

INTRODUCTION

The number of computed tomography (CT) scans performed in the USA increased by 600% over the past 20 years.[1-3] In 2007, nearly 70 million CT procedures were performed in the USA, of which 7 million were performed in the pediatric population.[4] Since 2007, CT usage in pediatrics has plateaued or even declined in some locales, likely related to multiple factors including economic cost constraints and increased awareness of cancer risks in the pediatric population, but the technique is still in frequent use.[5,6]

A downside of CT imaging is that it involves exposure to ionizing radiation. Even though CT imaging represents only 17% of radiological examinations, it accounts for half of the collective dose from medical sources in some countries. As a consequence of the increased use of CT, the overall radiation exposure from medical procedures has increased as well.[7] Recent studies have shown a small but statistically significant association between pediatric CT scanning and cancer incidence.[1,8] Every CT procedure should be justified by weighing the perceived benefits against the potential risks.[9,10] CT imaging has multiple roles, such as diagnosing disease, monitoring disease progression, assessing response to therapy, detecting complications of therapy, and detecting disease recurrence. It provides detailed anatomic information from multiple organ systems simultaneously.[3,11] These benefits improve health care and can be lifesaving in certain conditions.[12]

Cystic fibrosis (CF) is the most common life-limiting autosomal recessive disorder in the white population. Chronic respiratory disease accounts for more than 80% of mortality in CF patients.[13] Chest CT imaging is increasingly used both for patient management and clinical trials in CF, since chest CT is the most sensitive modality to assess and monitor CF-related changes in lung structure.[14] Chest CT can detect changes in lung structure before they become apparent by pulmonary function testing[15] or other imaging techniques such as MRI and chest radiography.[14,16,17] Pulmonary abnormalities, such as bronchiectasis, air trapping, bronchial wall thickening and mucous plugging can be observed with chest CT imaging.[18,19] Importantly, bronchiectasis and trapped air, defined by CT, are well-validated outcome measures.[20] These abnormalities can be identified by CT in early infancy.[21-23] The diagnosis of bronchiectasis can be delayed by three years in CF patients without CT scans.[13] Early detection of lung abnormalities is essential, because further irreversible lung damage may be prevented by treatment. Additionally, as a secondary benefit, patients and parents could have better compliance to their medication, when shown the results of their lung images.[24] Hence, the ability and benefits of chest CT to detect and monitor CF lung disease are clear.

However, the enthusiasm for the routine use of CT is tempered by the ongoing debate over carcinogenic risks.[1,25] This is especially important for patients with chronic diseases like CF, where the cumulative radiation risks of repetitive CT scans must be taken into

consideration. On one hand there is the risk of radiation exposure that may increase the likelihood of developing malignancies. On the other hand there is the risk of undetected progression of CF lung disease eventually leading to severe lung disease and reduced life expectancy.

For the optimal and safe use of chest CT, an understanding of the basic concepts related to diagnostic use of ionizing radiation is important for CF care givers. Our aim is to provide a better understanding of the factors related to monitoring CF lung disease with chest CT scans. We will discuss what is known about the possible risks of ionizing radiation, the radiation dose, and the risks associated with chest CT in CF patients. Furthermore, we will put these risks into perspective by comparisons with other medical and non-medical risks.

General introduction to effects of radiation

The adverse effects of ionizing radiation can be regarded as either deterministic or stochastic. Table 1 provides a brief overview of the terminology used in radiology and radiation protection. A deterministic effect is the direct consequence of tissue damage due to radiation. Such effects include epilation and skin erythema. Deterministic effects are highly dose dependent and only occur after exceeding a threshold dose.[3] The threshold values are high and beyond the range typically associated with CT imaging used for monitoring CF-related lung disease.

A stochastic effect is a random, probabilistic effect due to genomic damage. Stochastic effects include carcinogenesis and mutagenesis, and lack an obvious threshold. Stochastic genomic damage by radiation can increase the risk for developing cancer, but not the cancer's severity.[26]

An important risk modifier is the age at the time of radiation exposure. Pediatric patients are more sensitive to radiation-induced cancer than adult patients.[27] The estimated additional lifetime cancer mortality risk due to radiation increases steeply with younger ages at exposure.[28] This is presumed to be related to the larger proportion of proliferative tissue stem cells and the longer time for a potential cancer to develop in children compared to adults.[11,15]

Terminology for CT radiation dose

Several terms define the radiation dose related to the CT scan. The absorbed dose describes how much energy from ionizing radiation has been absorbed per unit mass and is expressed in units of Grays (Gy), with 1 Gy equal to 1 Joule/kilogram. To express the absorbed dose in relation to a specific CT protocol, the most commonly used descriptors are the Computed Tomography Dose Index (CTDI) and the dose-length-product (DLP).[29]

TABLE 1. Definitions of radiology dose and risk terms

Term	Definition
Absorbed dose	Amount of ionizing radiation energy absorbed in per unit mass
CTDI (Computed Tomography Dose Index)	A CT radiation dose descriptor used to characterize exposure to standardized reference phantoms for acceptance testing, quality control and protocol comparisons
$CTDI_{vol}$	A CTDI measure that approximates the average dose to a slice of the reference phantom, taking the helical pitch into account
Deterministic effect	Tissue damage due to exceeding a threshold dose of radiation, with the severity proportionate to dose
DLP (Dose Length Product)	A CT radiation dose descriptor that consists of the product of the $CTDI_{vol}$ and scan length, and measures the total radiation exposure for the whole series of images
EAR (Excess Absolute Risk) model	A risk model that expresses the excess risk as the difference between the total risk and the background risk
Effective dose	Weighted sum of doses to irradiated tissues used to describe total risk of stochastic effects for radiation protection purposes
ERR (Excess Relative Risk) model	A risk model that expresses the excess risk as a ratio relative to the background risk
LNT (Linear No Threshold) model	A risk model in which any radiation dose is potentially harmful and the probability of cancer is linearly related to dose
Organ dose	Radiation absorbed dose for a specific organ
Stochastic effect	An event such as carcinogenesis or mutagenesis that occurs by chance depending on the radiation dose without an obvious threshold

The CTDI is a descriptor of the energy absorbed within a dose profile deposited within the nominal collimated beam width and is used for quality control and comparison of the radiation dose of various CT protocols. To calculate the CTDI the radiation output of the CT scanner is measured with an ionization chamber using either a 16 cm diameter head phantom or a 32 cm body phantom.[30] The volumetric CTDI ($CTDI_{vol}$) expressed in milligrays (mGy), is the most commonly used descriptor and represents the average dose over the scanned volume. A product of the $CTDI_{vol}$ and the scan length is known as the DLP which is reported in units of milligray times cm (mGy·cm).[31]

Changes of scanning protocol parameters on a CT scanner (e.g. tube voltage, tube current, pitch, bowtie filter, scan length) are reflected by changes in the $CTDI_{vol}$ and/or the DLP value. Every CT scanner provides the $CTDI_{vol}$ and DLP to the user for each scanning procedure, a feature that facilitates comparison of different CT scanners and scanning protocols. However, the $CTDI_{vol}$ and the DLP only provide information regarding CT scanner radiation output and absorbed dose in standardized phantoms. These measures neither take the size of the patient into consideration, nor do they describe the radiation dose absorbed by any individual patient. This is an important aspect to keep in mind, especially in the pediatric population. To conclude, the CTDI

value is important for comparison of different CT scanners and scanning protocols but is not an accurate measure of the absorbed radiation dose for the individual pediatric patient[32] and should not be directly used to calculate the accompanying radiation risk.[3]

Effective dose

The effective dose, measured in units of Sievert (Sv), was developed as a quantity for radiation protection purposes.[33,34] The effective dose takes into account where the radiation dose is being absorbed, as well as the relative radiosensitivity of different tissues.[11] It is calculated by summing the weighted dose to exposed tissues using sex- and age- averaged tissue weighting factors derived from estimates of risk and lethality of cancer and effect on quality of life. Thus the effective dose characterizes the radiation burden to a sex- and age-averaged "reference person" from a given radiation exposure, but it does not provide the dose specific to a patient from an individual study. Therefore, the effective dose should not be calculated or used for risk assessment of an individual patient, especially children who may differ greatly from the "reference person".[30,34]

From CT dose to organ dose

The organ dose is defined as the average radiation energy absorbed in an individual organ, usually expressed in mGy units in diagnostic CT.[11] The size specific dose estimate (SSDE) is a measure that approximates the dose that the individual patient absorbs from the CT scan, by using the $CTDI_{vol}$ multiplied by a conversion factor based on patient cross-sectional size.[35] The SSDE may be useful as a first approximation of some organ doses, depending on organ location and size. However, organ doses can be estimated more accurately for specific CT scanners and scanning protocols using specialized Monte Carlo dose calculation software.[36,37] These estimates become more accurate when more information, such as the energy spectra, x-ray beam or the type of filter used to shape the x-ray beam, are incorporated. Monte Carlo organ dose estimates can be expressed per unit $CTDI_{vol}$ or DLP.[38]

From organ dose to cancer risk in patients with CF

As discussed previously, the effective dose is not appropriate for estimations of radiation risk in individual patients. For a given dose, there is a discrepancy in cancer risk from radiation exposure between children and adults.[11] Therefore, it is recommended to use the organ absorbed dose to estimate radiation risk.[34] Organ dose in combination with age- and sex-specific risk coefficients provided by the BEIR VII report can be used to estimate lifetime attributable risks of cancer incidence and mortality.[39]

As an example, consider a CF chest CT protocol without contrast for a 5-year-old

consisting of inspiratory and expiratory series on a Philips Brilliance 64 CT scanner with a total radiation output corresponding to a $CTDI_{vol32\,cm}$ of 2.1 mGy. The total dose of 2.1 mGy for the two series is very similar to a single volumetric chest CT dose recommendation at the age of 5 years by Nievelstein and colleagues,[40] and compared to several European surveys, the total dose is up to four times lower.[41] During a chest CT scan, several organs (including the thyroid, breasts, esophagus, lungs, thymus, and portions of the upper abdominal viscera) are irradiated. Thus to determine cancer risk, multiple organ doses have to be taken into consideration. Organ doses can be estimated with CT-Expo, a dose calculation software.[36,37] Each organ dose is multiplied with the corresponding lifetime attributable risk of cancer mortality for an exposure at the age of 5 as described in the BEIR VII report.[39] In our example, we estimate a sex-averaged lifetime cancer mortality risk of 0.023% attributable to the radiation output associated with a $CTDI_{vol32\,cm}$ of 2.1 mGy. Note that for our CF chest CT protocol, the organ doses and thus the corresponding risk estimates are much lower than the doses and corresponding risks for a typical non-CF chest CT scan. For example, our lung dose estimate of 4 mGy compares to a lung dose of 10-15 mGy for a chest CT scan previously reported in the literature.[6]

If a patient with CF is routinely monitored for progression of structural lung disease with biennial CT scans, from birth till the age of 17, they will typically undergo 9 chest CT scans. The radiation dose used for CT at relatively older ages is typically higher than the 2.1 mGy in our previous example, because the x-ray beam is attenuated more by the thicker tissues of larger children.[42] At younger ages the dose is less than 2.1 mGy. The total $CTDI_{vol32\,cm}$ for these 9 scans combined is calculated to be approximately 20 mGy. Organ doses at various ages were estimated by estimating organ doses for the baby, child and adult phantom with CT Expo. The values for the intermediary ages were estimated with linear interpolation. Lifetime attributable risks at various ages were estimated by linear interpolation of the tabulated risk values in the BEIR VII report.[39] This results into a cancer mortality risk of 0.2% for a radiation output of 20 mGy in total. Meaning that for every 1000 people exposed to 9 chest CT scans during childhood, two will possibly die of cancer due to these CT scans.

It should be noted that for this risk estimate it is assumed that radiation dose for each scan will not change over the coming 17 years period. Advances in CT dose reduction technology would likely result in lower radiation doses and correspondingly lower estimated risks.[43]

Complexities of estimating radiation risk

To estimate radiation risks, models are needed. A model is by definition a simplification of reality and always comes with limitations. Calculating radiation risk is complex and comes with large uncertainties.

Often overlooked is the fact that estimations of radiation-induced cancer from CT have largely been theoretical calculations extrapolated from findings in subjects who received radiation doses many times greater than what is currently used in diagnostic CT.[25] Radiation risk estimates are mainly derived from longitudinal cohort studies of populations exposed to moderate to high doses of radiation, including Japanese survivors of the atomic bombs and radiotherapy patients. It is unsure how applicable the findings from these groups are to the relatively low doses of radiation exposure from CT scans in a mainly white group of children and adolescents with CF.[1]

Most radiation risk analyses are based on excess relative risk (ERR) and excess absolute risk (EAR) values applied to a linear no-threshold (LNT) dose-response model. ERR expresses the additional risk of radiation exposure relative to the background risk, while EAR expresses the additional risk as the difference in the total risk and the background risk.[39] The LNT model assumes that any radiation dose, no matter how small, is potentially harmful and that the probability of cancer is linearly related to dose (see Figure 1). The LNT model does not take radiation damage repair mechanisms into consideration, which exhibit non-linear dose-response properties, and that may even function to provide a practical threshold at low dose levels. Compared to the mean exposures of the exposed cohort of atomic bomb survivors, the dose of a chest CT scan is relatively low. In addition, risk estimates have large confidence intervals.[44] Despite its limitations, the LNT model is currently dominant in public policy guidelines for risk assessment and radiation protection.

Our cancer mortality risk estimate of 0.2% comes with uncertainties as well. The BEIR VII committee subjectively provides 95% confidence intervals for lifetime attributable risk of solid cancer mortality for persons of mixed ages exposed to radiation. These subjective intervals indicate that for lung cancer risk factors may be approximately 2.5 times lower or higher. The recent American Association of Physicists in Medicine Position Statement also acknowledges these uncertainties stating that: "Risks of medical imaging at effective doses below 50 mSv for single procedures and 100 mSv for multiple procedures over short time periods are too low to be detectable and may be nonexistent".[45] Despite the large and subjective uncertainties, the risk estimate of 0.2% can be of use when putting the possible risk of radiation-induced cancer into perspective.

Recent studies of radiation exposure by CT in young populations have shown excess cancer rates similar or even higher than those for the atomic bomb survivor cohort. In a retrospective study by Pearce and colleagues, a positive association was shown between radiation dose from CT scans in childhood and development of leukemia and brain tumors.[1] In another retrospective study by Mathews and colleagues, the cancer incidence rate was found to be elevated within 10 years of follow-up after CT scanning. The incidence was greater when exposed at younger ages or in female patients.[8]

Unfortunately, the risk estimates by these two recent retrospective studies[1,8] came with large uncertainties and any actual risk is too small to estimate with any certainty at the level of the individual patient.[46]

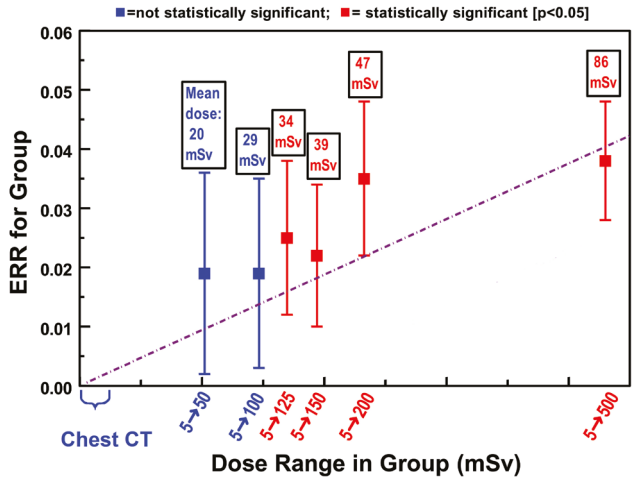

FIGURE 1. The linear no threshold model extrapolated to the lower doses received by chest CT. Estimated excess relative risk (±1 SE) of mortality from solid cancers among groups of survivors in the Life Span Study cohort of atomic bomb survivors, who were exposed to radiation. The dashed straight line represents the results of a linear fit to all the data. The line has been extrapolated to include the lower radiation exposure levels of CT scans as well. Adapted from Brenner et al.[67]

CT radiation risk into perspective

Alarming media reports spread fear and misperception of the true risks posed by radiation, while everyday risks from other sources are accepted or disregarded. Many in the general and medical field do not understand the concepts of risk or probability.[47] Risks are often overestimated or overweighted when the hazard is sensationalized, small, uncertain, delayed in effect, and not under control of the exposed; all of which are operative in the setting of medical radiation. Therefore, the risk of radiation must be put into proper perspective.

Compared to risks from other CT scan indications

Chest CT scans are used not only for monitoring purposes in CF patients, but also for many other clinical indications and diseases. We compared the risk of routine usage of CT in CF estimated in this study with the risks from other CT scans for other indications and age groups (see Table 2). If not already reported in the article, a sex-averaged, lifetime cancer mortality risk was calculated based on the BEIR VII report methodology

assuming an otherwise normal life expectancy. Unfortunately, not all studies allowed for using organ doses to estimate the risk. Some studies report the effective dose as a radiation dose parameter. If only the effective dose was described, it was converted to a homogeneous whole body irradiation for the calculations; for example, 1 mSv corresponds to an organ dose of 1 mGy for each organ.

TABLE 2. Lifetime cancer mortality risk for various CT scans and age groups

Reference	Age and size patient group	Indication of CT scan	Period that data was studied	Measure of dose	Sex-averaged lifetime cancer mortality risk based on BEIR VII
This review	5 years	CF (inspiratory and expiratory scan)	2013	$CTDI_{vol,32cm}$ = 2.1 mGy	0.023%
	0-17 years	CF monitoring (9 inspiratory and expiratory scans)	2013	Cumulative $CTDI_{vol,32cm}$=20 mGy	0.2%
Huda (67)	5 years	Routine Chest	Not specified Pub year: 2007	Effective dose 2.1 mSv	0.029%*
	5 years	Low dose CF Chest	Not specified Pub year: 2007	Effective dose 0.55 mSv	0.0075%*
Bernier et al. (68)	<1 year n=11.857	Chest	2000-2006	The reported organ doses. Including lung dose of 6 mGy.	0.038% †
	1-5 years n=15.505	Chest	2000-2006	The reported organ doses. Including lung dose of 5 mGy.	0.029% ‡
Kharbanda et al. (70)	< 19 years n=23.148	Trauma	2010	Mean dose= 12.0 mSv	0.11%§
Niemann et al. (70)	Adults 20 years n<10	Pulmonary embolism	Not specified Pub year: 2013	Reported organ doses including lung dose of 13 mGy (sex-averaged).	0.039%*
	Adults 60 years n=142	Pulmonary embolism	Not specified Pub year: 2013	Reported organ doses including lung dose of 14 mGy (sex-averaged).	0.024%*

All calculations are made using the lifetime attributable risk of cancer mortality from the BEIR VII report.[39]

* *Estimations given by the reference.*

† *Calculations made with the risk estimates for age at exposure of 0 years.*

‡ *Calculations made with the average risk estimates for age at exposure of 0 and 5 years.*

§ *Calculations made with the risk estimates for age at exposure of 10 years*.

Compared to risks from other radiation sources

A main source of ionizing radiation is the omnipresent natural background radiation from radon, cosmic rays, terrestrial sources and internal sources. Background radiation levels vary widely depending on geographic location. The annual global average from natural radiation sources for an individual is an effective dose of 2.4 mSv, with a typical range of 1 to 10 mSv.[48] The Dutch population is exposed to an average background radiation of 1.9 mSv per person per year,[49] compared to 3.0 mSv per year in the United States.[31] Moving from Nevada to Colorado increases background radiation by 1.5 mSv per year.[50] Across 75 years, this would translate into an additional life-time cancer mortality risk of approximately 0.7% based on the lifetime attributable risk estimates of the BEIR VII committee. Thus, an additional seven per 1000 people will potentially die from cancer when they are lifelong (i.e. 75 years) exposed to an additional annual 1.5 mSv of natural background radiation. In comparison, the cancer mortality risk of approximately 0.2% as calculated previously for routine chest CT scanning is thus smaller than that from geographical higher background radiation (see Figure 2). In certain parts of Brazil, India, Iran and China, natural background radiation levels of several times the US average have been recorded.[48] Despite these higher levels, no increase in the incidence of cancer has been documented in the populations residing in these areas.[25]

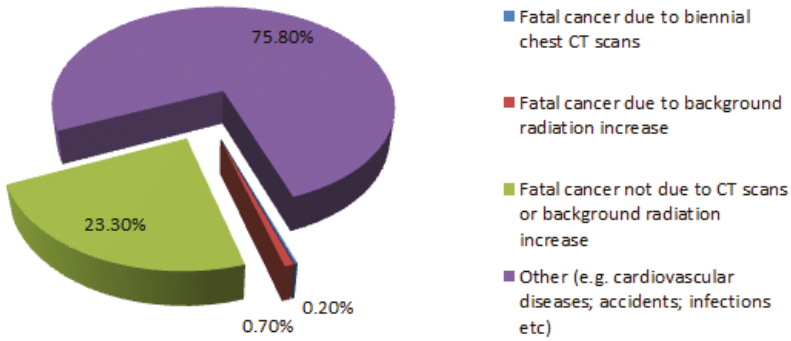

FIGURE 2. Causes of death for a group of patients receiving biennial chest CT scans until the age of 17 and receiving an additional 1.5 mSv each year during their life due to a relatively high natural background radiation level. Only a small fraction (0.2%) dies of cancer induced by the chest CT scans. In CF, the excess contribution of radiation-induced cancer mortality is expected to be even lower if the shorter life expectancy due to CF is taken into account.

The Background Equivalent Radiation Time (BERT) describes radiation doses from a source, such as from a CT scanner, in relation to the radiation dose of natural background radiation. One BERT year in the US corresponds to an effective dose of 3 mSv.[51] As mentioned previously, the concept of effective dose is not designed to be applied to

children undergoing CT scans. Therefore, one cannot easily relate the effective dose of 3 mSv natural background radiation to the organ doses (in mGy) from pediatric CT scans. Alternatively, background radiation and radiation from pediatric CT scans can be related to each other through associated risks. The effective dose of 3 mSv can be translated into organ doses in mGy assuming uniform irradiation of 3 mGy across the whole body. Using the BEIR VII report, the corresponding risk of this whole body irradiation can be estimated for various ages and both sexes. Routine biennial CT usage from birth until the age of 17 translates into an estimated BERT from birth until the age of 4 years for boys and until the age of 6 years for girls.

Compared to CF related risks

The attributable risks of mortality from (background) radiation-induced cancer as calculated above and depicted in Figure 2 are a misleading detriment measurement in patients with severe, life-limiting diseases such as CF. A large proportion of patients with CF might not survive long enough for the radiation-induced cancer to develop. Therefore, a lower lifetime radiation-induced cancer mortality risk in patients with CF than calculated above is expected.[52] The current median life expectancy of CF patients is 40 years of age[53] and increasing (see Figure 3), due to improvements in screening, treatment and medical care. We assume that life expectancy for CF patients at birth is now approximately 50 years. With the use of the previously described organ doses and data of the Surveillance, Epidemiology, and End Results (SEER) program of the National Cancer institute,[54] cancer mortality for a population with lower median survival age can be estimated. The radiation-induced cancer mortality for a patient with a median survival age of 50 years is calculated to be 0.08%. Taking the different life expectancies into account the estimated mortality risk of 0.08% for CF patients is approximately 2.5 times lower than the estimated mortality risk for a general population.

de González and colleagues also showed decreased influences of reduced life expectancies on risk estimates. Their radiation-induced cancer was approximately 4 times lower in case of annual CT scanning during lifetime, for a group with a median survival age of 36 years compared to a median survival age of 50 years.[55] Thus the importance of radiation risks in determining optimal imaging use is reduced in patients with diminished life expectancies.

In addition to the reduced life expectancy there is another possible factor affecting the validity of our risk estimates in CF patients. The BEIR VII risk factors and therefore our estimates do not adjust for the observed change in baseline cancer risk in CF patients as described by Maisonneuve and colleagues. The risk of melanoma was decreased in patients with CF, whereas the risk of lymphoid leukemia, thyroid, testicular and digestive tract cancer was increased especially in transplanted patients. Some increased risks

can be explained by genetic mechanisms. The excess in cases of thyroid cancer may be explained by the increased surveillance of the CF population.[57] Some of the tumors found in CF might be associated with excess radiation. As individual radiation exposure information is lacking, this hypothesis cannot be further investigated at present. In any case, the absolute risk of cancer in CF remains low and will not affect our risk estimates significantly. Routine biennial CT imaging seems acceptable based on our risk estimates and the known reduced life expectancy in CF.

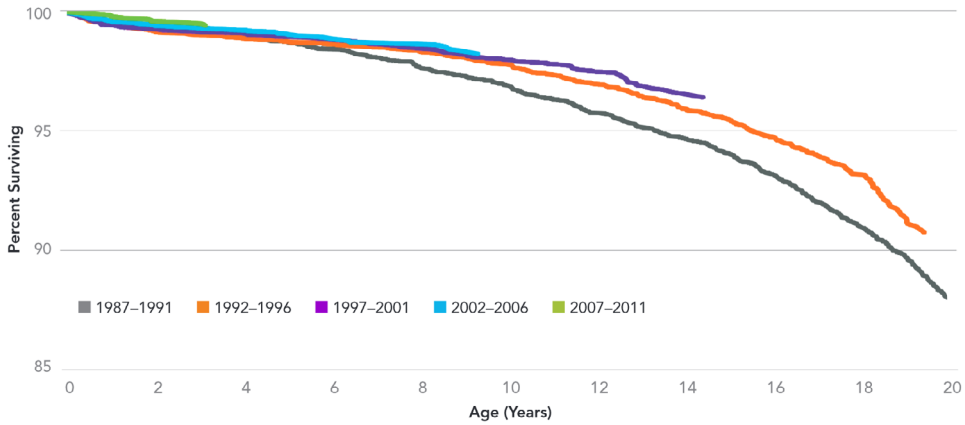

FIGURE 3. Survival by birth cohort (source: Cystic Fibrosis Foundation (US) patient registry annual data report 2011). The graph shows that of patients with CF born between 1987 and 1991 (gray line), 94.7 percent were alive at age 14. For children with CF born between 1997 and 2001 (purple line), 96.6 percent were alive at age 14. The children with CF born in a more recent cohort have a longer life expectancy.

Compared to other 'daily' risks

The overall probability of death from cancer over a typical person's lifetime is 23.3%.[11,58] This means that for every 1000 children, 233 will potentially die of cancer even if never exposed to medical radiation. Figure 2 shows this baseline cancer mortality risk in relation to the additional cancer mortality risk from chest CT scans and excess natural background radiation, as discussed previously. The possible risk of dying from cancer attributable to radiation from CT scanning is very small in comparison to the overall risk of dying from cancer. In comparison, cigarette smoking confers an 18% risk of developing smoking-related cancer, and 12% of deaths worldwide are thought to be attributable to tobacco use.[59] According to the US National Safety Council, there is an approximately 1% lifetime risk of dying from a motor vehicle accident and a 0.6% lifetime risk of dying from a fall.[60] The mortality rate in the United States for children between 1 to 19 year olds is 0.4%. The primary cause of childhood mortality is unintentional injuries with a mortality rate

of 0.15%.[61] As calculated in this paper, there is a 0.2% risk estimate of potential mortality caused by cancer due to routine biennial chest CT scans performed through childhood and adolescence, assuming a LNT model and normal life expectancy. Independent of CT scan usage, this possibility is comparable to the 0.18% risk of developing a severe reaction to intravenous contrast.[62] Lastly, it has been estimated that there is a greater than 0.1% risk of death from a medical error per hospitalization.[63]

CONCLUSIONS

This review describes the radiation risk for routine usage of chest CT scanning in pediatric CF patients with a discussion of the level of concern this should generate. Our mortality risk estimates for routine biennial pediatric chest CT scanning of 0.2% assuming a normal life expectancy, are in concordance with previous risk estimations.[6,55] As discussed by de González and colleagues, and confirmed by the risk estimates made in this review, the previous risk estimates by our colleagues, de Jong and colleagues, were highly conservative.[55,64] The risk is even lower taking into consideration the reduced life expectancy of CF patients.

Patients with CF could benefit from routine chest-CT monitoring of the progression of their lung disease and their responses to therapy. It is reasonable to believe that compensating gains in life expectancy may be expected by sensitively monitoring structural lung changes, detecting clinical relevant changes earlier, and more promptly instituting treatment and assessing response to therapy.

The additional cancer mortality risk related to the radiation received from routine CT is uncertain but small. Considering the small risk and long latency of radiation-induced cancer, the benefit-to-risk ratio of CT is very favorable, even if CT scans provide life-prolonging information in only a tiny fraction of patients with life-limiting severe disease such as CF.

Several risk models have been developed to predict the carcinogenic risks of radiation, with the LNT model being dominant for radiation protection policies. To quantify overall cancer mortality risk from radiation in the dose range of a single CT scan, a cohort of 5 million people would need to be followed over their lifetime for adequate statistical power and precision.[25] Hence, in the absence of such dauntingly large studies, risk estimates related to low dose radiation exposure remain speculative and uncertain.[31]

Undue concern over the potential risks of radiation can cause clinicians or parents to forego medically indicated CT scans, thereby imposing the very real risk of missed or delayed diagnoses. A patient's past or future exposure should not factor into current imaging decisions. Radiation risk models imply that if a patient without history of

irradiation should get a CT scan when clinically indicated, then this same patient with history of accumulative radiation exposure should as well.[65,66] This will remain true provided that for every exposure to diagnostic radiation, the anticipated benefit outweighs the potential risk, and assuming that the radiation exposure is kept as low as reasonably achievable. It is important to optimize radiation dose and CT protocols, especially in the pediatric population, by implementing dose-reducing and dose-optimizing technology in standard CT scanning protocols and by adopting a radiation registry for quality control and staff training. Radiation risk estimation is a complicated matter. The risk related to the routine use of CT in clinical care is small but not negligible. However, this risk can be outweighed by its benefits, especially in the pediatric patients with severe, chronic and life-limiting diseases, such as CF.

REFERENCES

1. Pearce MS, Salotti JA, Little MP, McHugh K, Lee C, Kim KP, et al. Radiation exposure from CT scans in childhood and subsequent risk of leukaemia and brain tumours: a retrospective cohort study. Lancet 2012 Aug 4;380(9840):499-505.
2. Smith-Bindman R, Miglioretti DL, Larson EB. Rising use of diagnostic medical imaging in a large integrated health system. Health Aff (Millwood) 2008 Nov-Dec;27(6):1491-1502.
3. Huda W, Mettler FA. Volume CT dose index and dose-length product displayed during CT: what good are they? Radiology 2011 Jan;258(1):236-242.
4. Mahesh M. Advances in CT technology and application to pediatric imaging. Pediatr Radiol 2011 Sep;41 Suppl 2:493-497.
5. Lee DW, Levy F. The sharp slowdown in growth of medical imaging: an early analysis suggests combination of policies was the cause. Health Aff (Millwood. 2012 Aug;31(8):1876-1884.
6. Miglioretti DL, Johnson E, Williams A, Greenlee RT, Weinmann S, Solberg LI, et al. The Use of Computed Tomography in Pediatrics and the Associated Radiation Exposure and Estimated Cancer Risk. JAMA Pediatr 2013 Jun 10:1-8.
7. Hendee WR, O'Connor MK. Radiation risks of medical imaging: separating fact from fantasy. Radiology 2012 Aug;264(2):312-321.
8. Mathews JD, Forsythe AV, Brady Z, Butler MW, Goergen SK, Byrnes GB, et al. Cancer risk in 680 000 people exposed to computed tomography scans in childhood or adolescence: data linkage study of 11 million Australians. BMJ 2013 May 21;346:f2360.
9. Martin CJ. Effective dose: practice, purpose and pitfalls for nuclear medicine. J Radiol Prot 2011 Jun;31(2):205-219.
10. Skinner S. Radiation safety. Aust Fam Physician 2013 Jun;42(6):387-389.
11. Brody AS, Frush DP, Huda W, Brent RL, American Academy of Pediatrics Section on Radiology. Radiation risk to children from computed tomography. Pediatrics 2007 Sep;120(3):677-682.
12. Hricak H, Brenner DJ, Adelstein SJ, Frush DP, Hall EJ, Howell RW, et al. Managing radiation use in medical imaging: a multifaceted challenge. Radiology 2011 Mar;258(3):889-905.
13. O'Connor OJ, Vandeleur M, McGarrigle AM, Moore N, McWilliams SR, McSweeney SE, et al. Development of low-dose protocols for thin-section CT assessment of cystic fibrosis in pediatric patients. Radiology 2010 Dec;257(3):820-829.
14. Barreto MM, Rafful PP, Rodrigues RS, Zanetti G, Hochhegger B, Souza AS,Jr, et al. Correlation between computed tomographic and magnetic resonance imaging findings of parenchymal lung diseases. Eur J Radiol 2013 Jun 10.
15. O'Connell OJ, McWilliams S, McGarrigle A, O'Connor OJ, Shanahan F, Mullane D, et al. Radiologic imaging in cystic fibrosis: cumulative effective dose and changing trends over 2 decades. Chest 2012 Jun;141(6):1575-1583.
16. Ciet P, Wielopolski P, Lever S, van der Wiel E, Lequin M, Tiddens H. Comparison of proton-MRI (MRI) and contrast enhanced MRI (CE-MRI. in cystic fibrosis (CF. to detect small airways disease? Presented at RSNA 2011, ECR 2011, NACFC 2010.
17. de Jong PA, Lindblad A, Rubin L, Hop WC, de Jongste JC, Brink M, et al. Progression of lung disease on computed tomography and pulmonary function tests in children and adults with cystic fibrosis. Thorax 2006 Jan;61(1):80-85.

18. Tiddens HA. Chest computed tomography scans should be considered as a routine investigation in cystic fibrosis. Paediatr Respir Rev 2006 Sep;7(3):202-208.

19. Tepper LA, Utens E, Caudri D, Bos A, Gonzalez-Graniel K, Duivenvoorden H, et al. Impact of bronchiectasis and trapped air on quality of life and exacerbations in CF. Eur Respir J 2013 Jan 11.

20. Loeve M, Krestin GP, Rosenfeld M, de Bruijne M, Stick SM, Tiddens HA. Chest computed tomography; a validated surrogate endpoint of cystic fibrosis lung disease? Eur Respir J 2012 Dec 20.

21. Mott LS, Park J, Murray CP, Gangell CL, de Klerk NH, Robinson PJ, et al. Progression of early structural lung disease in young children with cystic fibrosis assessed using CT. Thorax 2012 Jun;67(6):509-516.

22. Sly PD, Brennan S, Gangell C, de Klerk N, Murray C, Mott L, et al. Lung disease at diagnosis in infants with cystic fibrosis detected by newborn screening. Am J Respir Crit Care Med 2009 Jul 15;180(2):146-152.

23. Stick SM, Brennan S, Murray C, Douglas T, von Ungern-Sternberg BS, Garratt LW, et al. Bronchiectasis in infants and preschool children diagnosed with cystic fibrosis after newborn screening. J Pediatr 2009 Nov;155(5):623-8.e1.

24. Negarandeh R, Mahmoodi H, Noktehdan H, Heshmat R, Shakibazadeh E. Teach back and pictorial image educational strategies on knowledge about diabetes and medication/dietary adherence among low health literate patients with type 2 diabetes. Prim Care Diabetes 2013 Jul;7(2):111-118.

25. O'Connor MK, Li H, Rhodes DJ, Hruska CB, Clancy CB, Vetter RJ. Comparison of radiation exposure and associated radiation-induced cancer risks from mammography and molecular imaging of the breast. Med Phys 2010 Dec;37(12):6187-6198.

26. Preston RJ. Radiation effects. Ann ICRP 2012 Oct-Dec;41(3-4):4-11.

27. UNSCEAR 2013 Report. Annex B - Effects of radiation exposure of children. "Sources, effects and risks of ionizing radiation". 2013;Official Records of the General Assembly, Sixty-first Session, Supplement No. 46 and corrigendum (A/61/46 and Corr.1)(Volume 2):paras. 21-22.

28. Brenner D, Elliston C, Hall E, Berdon W. Estimated risks of radiation-induced fatal cancer from pediatric CT. AJR Am J Roentgenol 2001 Feb;176(2):289-296.

29. McNitt-Gray MF. AAPM/RSNA Physics Tutorial for Residents: Topics in CT. Radiation dose in CT. Radiographics 2002 Nov-Dec;22(6):1541-1553.

30. Macdougall RD, Strauss KJ, Lee EY. Managing radiation dose from thoracic multidetector computed tomography in pediatric patients: background, current issues, and recommendations. Radiol Clin North Am 2013 Jul;51(4):743-760.

31. Frush DP, Applegate K. Computed tomography and radiation: understanding the issues. J Am Coll Radiol 2004 Feb;1(2):113-119.

32. Boone JM, Strauss KJ, Cody DD, McCollough CH, McNitt-Gray MF, Toth TL. AAPM report No. 204. Size-Specific Dose Estimates (SSDE) in Pediatric and Adult Body CT Examinations. 2011;204.

33. ICRP, Khong PL, Ringertz H, Donoghue V, Frush D, Rehani M, et al. ICRP publication 121: radiological protection in paediatric diagnostic and interventional radiology. Ann ICRP 2013 Apr;42(2):1-63.

34. Menzel HG, Harrison J. Effective dose: a radiation protection quantity. Ann ICRP 2012 Oct-Dec;41(3-4):117-123.

35. Bankier AA, Kressel HY. Through the Looking Glass revisited: the need for more meaning and less drama in the reporting of dose and dose reduction in CT. Radiology 2012 Oct;265(1):4-8.

36. Deak P, van Straten M, Shrimpton PC, Zankl M, Kalender WA. Validation of a Monte Carlo tool for patient-specific dose simulations in multi-slice computed tomography. Eur Radiol 2008 Apr;18(4):759-772.

37. Stamm G, Nagel HD. CT-expo--a novel program for dose evaluation in CT. Rofo 2002 Dec;174(12):1570-1576.

38. Harrison JD, Streffer C. The ICRP protection quantities, equivalent and effective dose: their basis and application. Radiat Prot Dosimetry 2007;127(1-4):12-18.

39. National Research Council . Committee to Assess Health Risks from Exposure to Low Level of Ionizing Radiation. Health risks from exposure to low levels of ionizing radiation : BEIR VII Phase 2. Washington, D.C.: National Academies Press; 2006.

40. Nievelstein RA, van Dam IM, van der Molen AJ. Multidetector CT in children: current concepts and dose reduction strategies. Pediatr Radiol 2010 Aug;40(8):1324-1344.

41. Verdun FR, Gutierrez D, Vader JP, Aroua A, Alamo-Maestre LT, Bochud F, et al. CT radiation dose in children: a survey to establish age-based diagnostic reference levels in Switzerland. Eur Radiol 2008 Sep;18(9):1980-1986.

42. The Alliance for Radiation Safety in Pediatric Imaging. Image Gently. Available at: http://www.imagegently.org, 2013.

43. Noel PB, Renger B, Fiebich M, Munzel D, Fingerle AA, Rummeny EJ, et al. Does iterative reconstruction lower CT radiation dose: evaluation of 15,000 examinations. PLoS One 2013 Nov 26;8(11):e81141.

44. Tubiana M, Feinendegen LE, Yang C, Kaminski JM. The linear no-threshold relationship is inconsistent with radiation biologic and experimental data. Radiology 2009 Apr;251(1):13-22.

45. AAPM. AAPM Position Statement on Radiation Risk from Medical Imaging Procedures. December 2011(PP 25-A).

46. Agudo A, Bonet C, Travier N, Gonzalez CA, Vineis P, Bueno-de-Mesquita HB, et al. Impact of cigarette smoking on cancer risk in the European prospective investigation into cancer and nutrition study. J Clin Oncol 2012 Dec 20;30(36):4550-4557.

47. Krille L, Hammer GP, Merzenich H, Zeeb H. Systematic review on physician's knowledge about radiation doses and radiation risks of computed tomography. Eur J Radiol 2010 Oct;76(1):36-41.

48. Annex B Exposures from natural radiation sources. United Nations Scientific Committee on the effects of atomic radiation, UNSCEAR 200 report vol. I Sources and effects of ionizing radiaton. p. 83-141.

49. Eleveld H. Ionising radiation exposure in the Netherlands. 2003;RIVM report 861020002.

50. Moeller DW, Sun LS. Comparison of natural background dose rates for residents of the Amargosa Valley, NV, to those in Leadville, CO, and the states of Colorado and Nevada. Health Phys 2006 Oct;91(4):338-353.

51. Nickoloff EL, Lu ZF, Dutta AK, So JC. Radiation dose descriptors: BERT, COD, DAP, and other strange creatures. Radiographics 2008 Sep-Oct;28(5):1439-1450.

52. Brenner DJ, Shuryak I, Einstein AJ. Impact of reduced patient life expectancy on potential cancer risks from radiologic imaging. Radiology 2011 Oct;261(1):193-198.

53. Simmonds NJ. Ageing in Cystic Fibrosis and Long-term Survival. Paediatr Respir Rev 2013 Feb 23.

54. Surveillance Research Program, National Cancer Institute. Fast Stats: An interactive tool for access to SEER cancer statistics. Available at: http://seer.cancer.gov/faststats, 2014.

55. de Gonzalez AB, Kim KP, Samet JM. Radiation-induced cancer risk from annual computed tomography for patients with cystic fibrosis. Am J Respir Crit Care Med 2007 Nov 15;176(10):970-973.

56. Maisonneuve P, Marshall BC, Knapp EA, Lowenfels AB. Cancer risk in cystic fibrosis: a 20-year nationwide study from the United States. J Natl Cancer Inst 2013 Jan 16;105(2):122-129.

57. Murphy SL, Xu J, Kenneth D, Kochanek KD. Deaths: final data for 2010. Natl Vital Stat Rep 2013 May 8;61(4):1-118.

58. World Health Organization. WHO Global Report Mortality attributable to tobacco. 2012.

59. National safety council. Injury facts, 2012 Edition. Itasca, IL: Natoinal Safety Council; 2012.

60. Hamilton BE, Hoyert DL, Martin JA, Strobino DM, Guyer B. Annual summary of vital statistics: 2010-2011. Pediatrics 2013 Mar;131(3):548-558.

61. Lindsay R, Paterson A, Edgar D. Preparing for severe contrast media reactions in children - results of a national survey, a literature review and a suggested protocol. Clin Radiol 2011 Apr;66(4):340-348.

62. Kohn LT, Corrigan JH, Donaldson MS. To Err Is Human. Building a safer health system. Institute of Medicine Committee on quality of health care in America. Washington, D.C.: National Academy Press; 2000.

63. de Jong PA, Mayo JR, Golmohammadi K, Nakano Y, Lequin MH, Tiddens HA, et al. Estimation of cancer mortality associated with repetitive computed tomography scanning. Am J Respir Crit Care Med 2006 Jan 15;173(2):199-203.

64. Eisenberg JD, Lewin SO, Pandharipande PV. The fisherman's cards: how to address past and future radiation exposures in clinical decision making. AJR American journal of roentgenology 2014; 202: 362-367.

65. Durand DJ, Dixon RL, Morin RL. Utilization strategies for cumulative dose estimates: a review and rational assessment. J Am Coll Radiol 2012 Jul;9(7):480-485.

66. Brenner DJ, Doll R, Goodhead DT, Hall EJ, Land CE, Little JB, et al. Cancer risks attributable to low doses of ionizing radiation: assessing what we really know. Proc Natl Acad Sci U S A 2003 Nov 25;100(24):13761-13766.

67. Huda W. Radiation doses and risks in chest computed tomography examinations. Proc Am Thorac Soc 2007 Aug 1;4(4):316-320.

68. Bernier MO, Rehel JL, Brisse HJ, Wu-Zhou X, Caer-Lorho S, Jacob S, et al. Radiation exposure from CT in early childhood: a French large-scale multicentre study. Br J Radiol 2012 Jan;85(1009):53-60.

69. Kharbanda AB, Flood A, Blumberg K, Kreykes NS. Analysis of radiation exposure among pediatric trauma patients at national trauma centers. J Trauma Acute Care Surg 2013 Mar;74(3):907-911.

70. Niemann T, Zbinden I, Roser HW, Bremerich J, Remy-Jardin M, Bongartz G. Computed tomography for pulmonary embolism: assessment of a 1-year cohort and estimated cancer risk associated with diagnostic irradiation. Acta Radiol 2013 Sep;54(7):778-784.

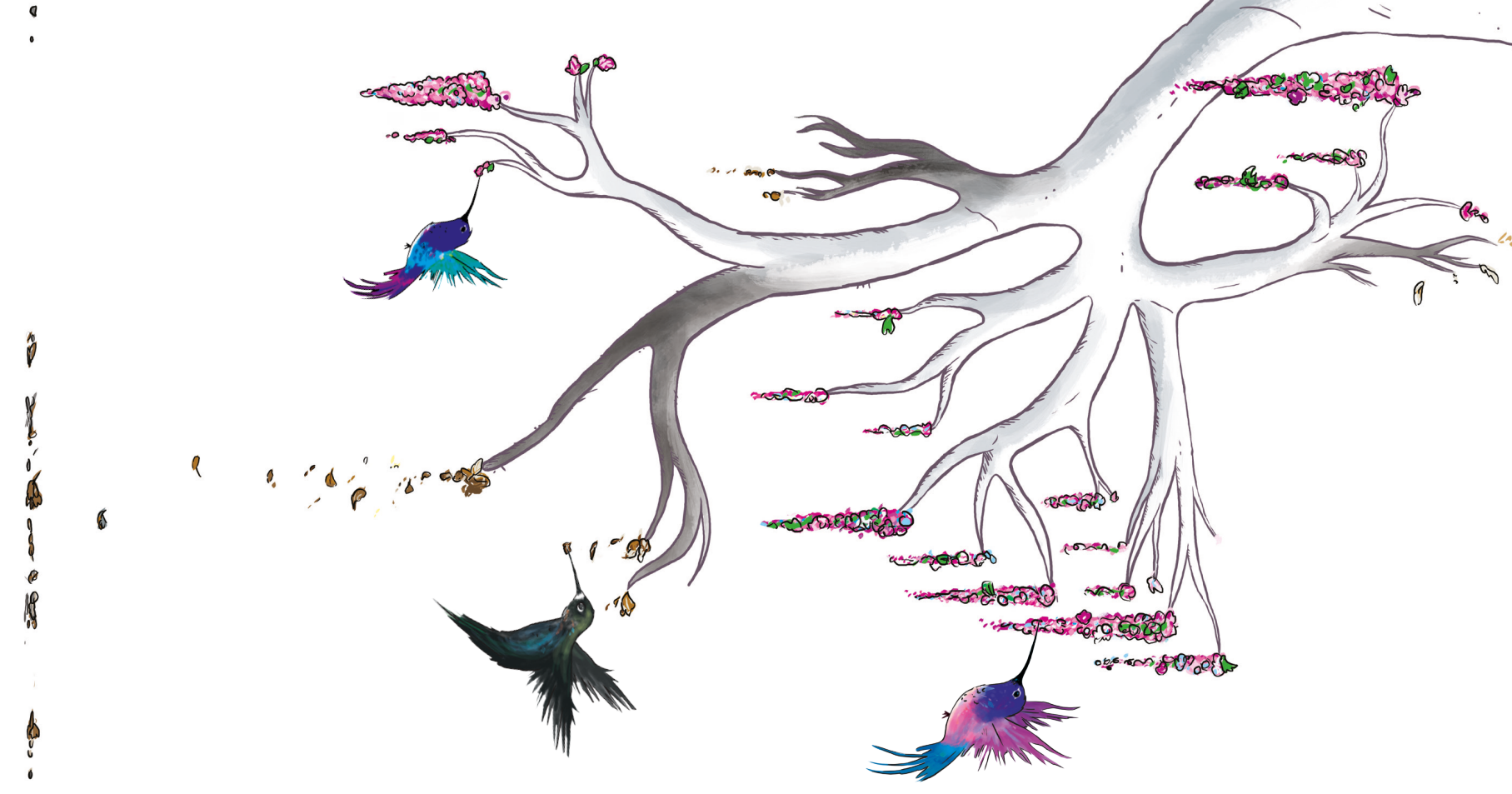

CHAPTER 3

MULTICENTER CHEST CT STANDARDISATION IN CHILDREN AND ADOLESCENTS WITH CYSTIC FIBROSIS: THE WAY FORWARD

Wieying Kuo, Mariette P.C. Kemner-van de Corput, Adria Perez-Rovira, Marleen de Bruijne, Isabelle Fajac, Harm A.W.M. Tiddens, Marcel van Straten on behalf of the SCIFI CF study group.

SCIFI CF study group (in alphabetic order):
Laureline Berteloot, Kris de Boeck, Cesare Braggion, Torkel B. Brismar, Rosaria Casciaro, Desmond Cox, Jane C. Davies, C. Kors van der Ent, Pilar Garcia Peña, Silvia Gartner, Nanko de Graaf, David Hansell, Lena Hjelte, Herma C. Holscher, Annmarie Jeanes, Pim A. de Jong, Ahmed Kheniche, Timothy Lee, Giorgio Lucigrai, Marco Di Maurizio, Anne Mehl, Anne Munck, Marianne Nuijsink, Jacqueline Payen de la Garanderie, David Rea, Isabelle Sermet, Veronika Skalicka, Florian Streitparth, Philippe Reix,

European Respiratory Journal.
2016;47(6):1706-17.

ABSTRACT

Progressive cystic fibrosis (CF) lung disease is the main cause of mortality in CF patients. CF lung disease starts in early childhood. With current standards-of-care, respiratory function remains largely normal in children and more sensitive outcome measures are needed to monitor early CF lung disease. Chest CT is currently the most sensitive imaging modality to monitor pulmonary structural changes in children and adolescents with CF. To quantify structural lung disease reliably among multiple centers, standardization of chest CT protocols is needed. The **S**tandardized **C**hest **I**maging **F**ramework for **I**nterventions and personalized medicine in **CF** (SCIFI CF) was founded to characterize chest CT image quality and radiation doses among 16 participating European CF centers in 10 different countries. We aimed to optimize CT protocols in children and adolescents among several CF centers. A large variety was found in CT protocols, image quality and radiation dose usage among the centers. However, the performance of all CT scanners was found to be very similar, when taking spatial resolution and radiation dose into account. We conclude that multicenter standardization of chest CT in children and adolescents with CF can be achieved for future clinical trials.

INTRODUCTION

Computed tomography (CT) usage has increased over the past two decades to aid with diagnostic and monitoring purposes in the pediatric population.[1] CT has become an important imaging tool for patients with cystic fibrosis (CF), who develop lung disease early in life when irreversible pulmonary abnormalities can still be prevented. Some centers start monitoring the progression of early CF lung disease with CT at a young age,[2–4] as this is currently the most sensitive imaging modality to detect and monitor the structural changes of early CF lung disease. Chest CT can detect structural abnormalities even before symptoms occur in a patient[2] and in general before it becomes apparent with spirometry[5] or any other imaging modality.[6–9] Findings on chest CT provide important timely information to CF care givers on the presence and progression of structural lung abnormalities and guides treatment aimed to prevent progressive pulmonary changes.[10]

The sensitivity of chest CT to detect structural lung changes promptly has also resulted in several clinical trials that include chest CT as an outcome measure[11–13] and more are to be anticipated to evaluate the efficacy of new costly promising disease-modifying agents. Chest CT related parameters such as bronchiectasis scores can be of use as primary or secondary outcome measures. Smaller sample sizes may suffice in studies with more sensitive CT outcome measures.[14,15] Chest CT can play an important role especially in clinical trials in young children and for children and adolescents with CF as well as in other lung diseases when sensitive outcome measures are needed.[16]

To utilize chest CT in a multi-center clinical trial, it is of great importance to standardize image acquisition of chest CT scans. Acquired CT scans require sufficient image quality at the lowest possible radiation dose. Currently, technical scanning parameters and image reconstruction techniques are chosen by each center individually, affecting image acquisition and consistency profoundly.[17] Affected image quality could indicate false disease progression or treatment effectiveness in patients. Differences can also be found in lung density measurements and airway analyses between scanners, but also within a specific CT scanner over time.[18] Studies have shown either overestimation or underestimation of emphysema and bronchiectasis depending on the reconstruction algorithm [17] and the inspiration level during CT acquisition.[19] Next to the variety in image quality and CT acquisition, a spread in amount of radiation dose used for each scanner and protocol can be expected. Radiation exposure comes with potential risks and it is therefore important to keep this as low as reasonably achievable, especially in young children as they are more sensitive to ionizing radiation [1]. The use of a sequential technique with gaps, i.e. a non-contiguous scan predates a volumetric or spiral scan. Currently sequential chest CT techniques are, however, still used as a strategy to reduce

radiation dose by some centers,[20–22] even though this strategy comes at the cost of losing information and making longitudinal follow up less sensitive.
CT techniques have improved, with the main goal to decrease the radiation exposure in patients while maintaining sufficient diagnostic image quality. Techniques such as automatic exposure control and the more recent development of iterative reconstruction techniques have been effective to lower the radiation exposure in pediatric patients.[23,24]
With rapidly improving CT technology and different CT scanners, it can be a challenge to quantify and maintain consistent image quality of CT scans during a multi-center clinical trial.
The aims of our study was to characterize CT practices and performance of CT scanners in different European CF centers involved in CF research and to optimize CT protocols for children and adolescents. Standardized chest CT was aimed to be available for future clinical trials in the pediatric CF population. For these purposes, the **S**tandardized **C**hest **I**maging **F**ramework for **I**nterventions and personalized medicine in **CF** (SCIFI CF) was founded in 2012. Site visits were conducted within European centers, most of them being part of the European Cystic Fibrosis Society-Clinical Trial Network (ECFS-CTN). We describe the current routine chest CT protocols used for children and the performance of the CT scanners using these protocols. Based on these findings, guidelines and recommendations are presented for future chest CT protocols.

MATERIAL AND METHODS

The ECFS-CTN is a European network launched by the European CF society in 2008. It was composed of 30 selected CF sites dedicated to CF clinical research in 11 countries in 2012. All 30 ECFS-CTN centers were invited to participate with the SCIFI CF initiative. In addition to the ECFS-CTN centers, 2 other centers requested to participate, as they were eager to have their CT scanners characterized for research purposes. A letter was sent to each of these centers explaining the background of the SCIFI CF initiative. In addition, a questionnaire was sent to acquire general information regarding the pediatric CF center and an inventory of the centers' CT protocols used for CF patients was requested (see Appendix for full details). Centers were selected based on the commitment of the pediatric pulmonologist and radiologist, availability of the CT scanner, availability of the employees and technicians for a site visit, and consent to compensate for the costs of the site visit. To ensure the commitment of both the department of pediatric pulmonology and the department of radiology, a letter of agreement signed by both a pediatric pulmonologist and a radiologist was required.
All participating centers and their data were anonymized for this manuscript.

Site visit

The visits to the selected centers were planned and executed over a period of 2 years starting from 2013. A SCIFI CF site visit was prepared in close collaboration with the CF coordinator of each center. During the two-day visit, a presentation about the SCIFI CF initiative was given, phantoms were scanned on the CT scanner, and training was provided concerning spirometer guided CT. The feasibilities of standardized inspiration levels acquired during CT scanning have been described separately.[25]

Evaluation of routine CT protocol

The main CT scanner and the age specific routine chest CT protocols used in clinical practice to acquire CT scans in children and adolescents with CF were studied and evaluated with three age-specific phantoms (QRM, Quality Assurance in Radiology and Medicine, Möhrendorf, Germany). These phantoms were designed to represent the average patient size of a newborn, a child (5 years old), and a young adult. The size and geometry of the adult phantom was based on measurements in a European young adult population.[26] The newborn and child phantoms are scaled down versions of this adult phantom. Based on the phantom sizes and the information available from the Image Gently campaign,[27] the newborn, child, and adult phantom correspond with a patient weight of 4, 18, and 58 kg, respectively. The materials used in these anthropomorphic phantoms mimic human tissues in the thorax with regards to the characteristics of X-ray attenuation. The tissues of the phantom include artificial lung parenchyma, bone, and soft tissue-equivalent material. In addition, inserts containing homogeneous solid water, iodine or soft tissue-equivalent material can be placed on various positions of the phantom. A tungsten wire and golden disk insert were used to determine the spatial resolution of the scanner. For the child phantom, the applied x-ray tube voltage and rotation time were noted. To assess the applied radiation dose as a function of patient size, the newborn, child, and adult phantoms were first scanned according to the centers' current CT protocol for patients with CF in these age groups. The scanner's radiation output was determined by the reported volumetric CT dose index ($CTDI_{vol}$) in the DICOM header or from the accompanying DICOM dose report image. When this information was not available, the $CTDI_{vol}$ was determined manually, with the aid of tabulated dose values in the software package CT-Expo (version 2.0), using the scanning parameters of the protocol. The $CTDI_{vol}$ value of non-contiguous sequential CT protocols was extrapolated to the corresponding dose of a continuous volumetric CT scan.

The median dose found in the child phantom in all centers, served as a reference value for the absolute dose level. It was assumed that this reference dose level provides images with sufficient image quality for diagnosis as it is based on the protocols used by the centers for their clinical routine. The dose outliers are assumed to be of too good or too

bad diagnostic quality. For each center, the ratio between the newborn and the child dose and the ratio between the adult and the child dose were determined. The median values of these ratios were multiplied by the reference value for the child phantom to obtain reference values for the newborn and young adult.

CT scanner performance characterization

The performance of each scanner was characterized by assessing the quality of the child phantom images reconstructed with the filtered back projection technique. The primary measure for image quality Q_{NOISE} was solely related to image noise:

$$Q_{NOISE} = \frac{1}{\sigma^2}$$

with σ as the standard deviation of the image noise. Image noise was determined in each slice in a 5 cm^2 region of the lung parenchyma. A relatively high Q_{NOISE} factor corresponds with an image with a relatively low noise level. Thus, for a given level of image contrast a relatively high Q_{NOISE} factor also corresponds with a better contrast-to-noise ratio.

It is important to realize that image quality and applied dose are interconnected. Moreover, several aspects of image quality, in particular image noise and spatial resolution, are closely linked. Therefore, the Q_{NOISE} factor was extended accordingly to take both spatial resolution and applied dose into account.

In general, a better spatial resolution corresponds with a higher noise level. The spatial resolution of an image can be described in-plane and out-of-plane by the pre-sampled modulation transfer function (MTF) and slice sensitivity profile (SSP), respectively. The measure $Q_{NOISE,RES}$ incorporates the previously derived relationship between image noise and spatial resolution[28–31]:

$$Q_{NOISE,RES} = \frac{1}{\sigma^2} \cdot \frac{M^2 \int \mathrm{d}f \, f^2 \, \mathrm{MTF}^2(f)}{\mathrm{FWHM}_{SSP}}$$

with M the reconstruction matrix size, $FWHM_{SSP}$ the full width at half maximum of the SSP, and f the spatial frequency. The integral runs from $-f_N$ to $+f_N$, with f_N the Nyquist frequency of the projection data. The SSP was determined by scanning the insert containing a 10 μm thick golden disk. The MTF was derived from the point spread function (PSF) that was determined from the CT scan of the tungsten wire insert.

In addition to the spatial resolution, the radiation dose applied during the CT scan influences the image noise as well. The measure $Q_{NOISE,RES,DOSE}$ incorporates both the relationship between image noise and spatial resolution and the relationship between image noise and radiation dose:

$$Q_{NOISE,RES,DOSE} = \frac{1}{\sigma^2} \cdot \frac{M^2 \int df\, f^2\, MTF^2(f)}{FWHM_{SSP}} \cdot \frac{1}{CTDI_{vol}}$$

$Q_{NOISE,RES,DOSE}$ is a figure-of-merit which is similar to the dose efficiency and imaging performance parameter used by another group.[32] The higher the Q-factor, the better the imaging performance of the CT scanner. A CT scanner with a relatively high $Q_{NOISE,RES,DOSE}$ produces images with a relatively low noise level at the same dose level and spatial resolution as another scanner with a relatively low $Q_{NOISE,RES,DOSE}$ factor. CT scanners with equal $Q_{NOISE,RES,DOSE}$ factors are able to produce images of equal quality with respect to noise and resolution at equal dose levels.

The Q values were determined for all axial slices scanned and averaged over all slices. Based on these averaged values and corresponding scan parameters, a general recommendation was made including the radiation dose to be applied as a function of patient age and the scan and reconstruction parameters to be used. These recommendations will be discussed in the final section of this guideline.

RESULTS

Study population

Twenty-three out of the 30 ECFS-CTN centers completed the questionnaires. 19 centers showed interest in participating in the SCIFI-CF study of which 13 pediatric centers fulfilled the requirements to participate. In addition, the CT scanner in our own department of radiology at Erasmus MC, Rotterdam, the Netherlands (also ECFS-CTN center) was included in this project. Aside from the 14 ECFS-CTN centers two additional European non ECFS-CTN centers were included. All 16 centers were visited in 2013 or 2014. The following manufactures of the CT scanners were involved: 8x Siemens; 5x Philips; 2x GE healthcare; 1x Toshiba.

Evaluation of routine CT protocol

Nine out of the 16 centers routinely monitored CF patients with a chest CT every two or three years. Seven centers only acquired chest CT scans on clinical indication. Twelve centers acquired volumetric inspiratory chest CTs, of which 9 centers included volumetric expiratory CT scans and 3 centers included non-contiguous expiratory CTs. Two centers acquired volumetric scans only in the first scan of the patient, followed by non-contiguous CT scans for follow-up assessment. Two centers never used volumetric CTs in clinical practice for the checkup of CF patients, but only scanned non-contiguously. Applied x-ray tube voltage for the child phantom varied between centers (range 70-120 kV, median value 100 kV). X-ray tube rotation time varied as well (range 400-750 ms, median value 500 ms).

Radiation doses applied to the 3 phantoms for each center are presented in Figure 1. On average, the applied dose ($CTDI_{vol,32\ cm}$) for the child phantom was 1.8 mGy. The median dose was 1.0 mGy (horizontal line in Figure 1a). The applied dose for the newborn and adult phantom relative to the dose for the child phantom is shown in Figure 1b. The horizontal lines in Figure 1b correspond to the median relative dose levels of 64% and 223% for the newborn and adult phantom, respectively. The deviation of the bars from these lines indicates how well the dose for a newborn child was reduced and conversely increased for an adult relative to the dose for a 5-year old child. For instance, site 10 was in agreement with the recommended dose levels for both absolute and relative values. Young children were scanned while spontaneous breathing in 14 centers and under general anesthesia in 2 centers. Starting from the age of 5-6 years old, when children can cooperate, inspiration CT's were scanned with voluntary breath hold in 15 centers and with spirometer guidance in 1 center. Expiration CT's were scanned with voluntary breath hold in 15 centers (and in lateral decubitus position in 2 centers) and with spirometer guidance in 1 center.

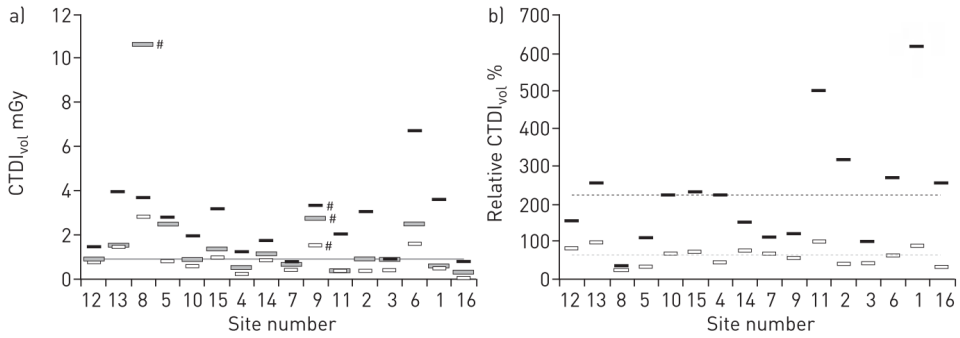

FIGURE 1. Dose levels applied in all centres. **a)** Volumetric computed tomography dose index ($CTDI_{vol}$) applied in each centre for the child phantom (grey bars) and the median dose value (grey line), the adult (black bars) and the newborn phantom (white bars). The smaller bars represent the $CTDI_{vol}$ used for the newborn (white) and a young adult (black). **b)** $CTDI_{vol}$ values relative to the dose applied to the child phantom for the phantoms representing a newborn (white bars) and young adult (black bars). Grey and black dashed lines correspond to the recommended relative dose for a newborn and young adult, respectively. The order of the centres is the same as that in in figure 2. #: extrapolated $CTDI_{vol}$ values derived from a sequential computed tomography.

CT scanner performance

The factors Q_{NOISE}, $Q_{NOISE,RES}$, and $Q_{NOISE,RES,DOSE}$ for each center are shown in Figure 2 relative to the average value for Q_{NOISE}, $Q_{NOISE,RES}$, and $Q_{NOISE,RES,DOSE}$, respectively. Large variability between scanners can be observed for Q_{NOISE} and $Q_{NOISE,RES}$. The large difference seen in Q_{NOISE} is also seen in the qualities of the phantom scans (Figure 3). The variability found

in Q_{NOISE} can partly be explained by the variability found in in-plane spatial resolution as determined by the MTF. Figure 4 shows the large variation in MTF shapes found across the centers. The influence of the MTF can for example be seen in the Q_{NOISE} factor of center number 9, which is relatively low because of the relatively sharp reconstruction kernel used (center number 9 in Figure 2a for Q_{NOISE} and the arrow in Figure 4 for MTF). After correcting for the negative influence of the sharp kernel on the image noise, the Q-factor ($Q_{NOISE,RES}$) increases and is even better than average (Figure 2b). The latter can be explained by the relatively high dose level used by this center (Figure 1a).

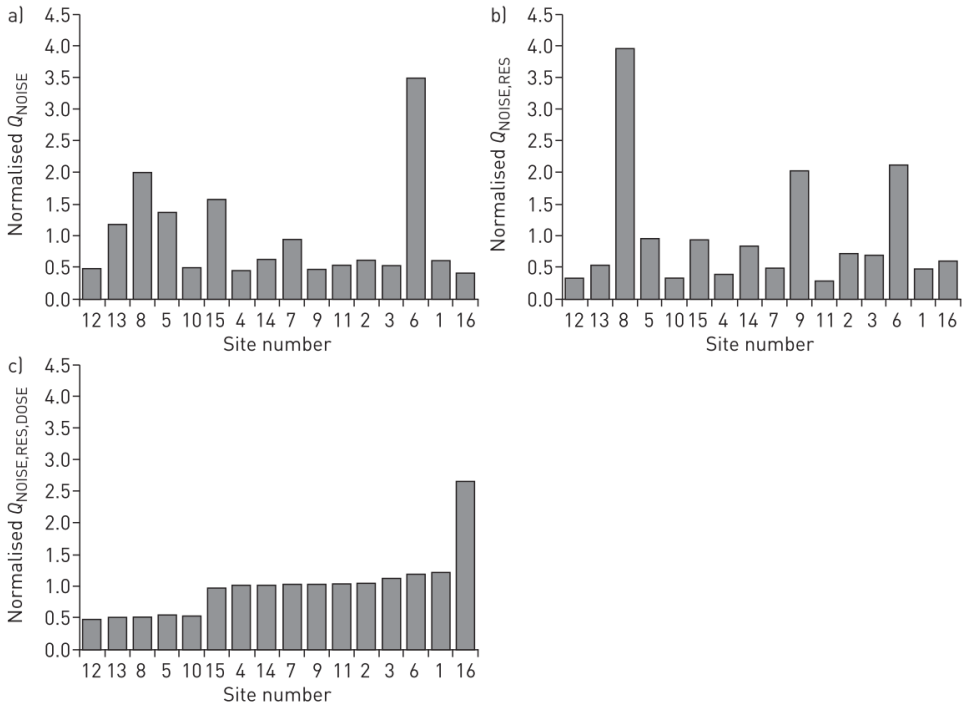

FIGURE 2. Q factors for each centre normalised to the average Q factor. **a)** Q_{NOISE} based on image noise. **b)** $Q_{NOISE,RES}$ based on image noise and compensated for differences in spatial resolution between centres. **c)** $Q_{NOISE,RES,DOSE}$ based on image noise and compensated for differences in spatial resolution and radiation dose between centres. Centres are sorted from small to large $Q_{NOISE,RES,DOSE}$.

After compensation for differences in dose, the Figure of merit $Q_{NOISE,RES,DOSE}$ shows less variation over all centers. The performances of 10 scanners (40-128 slice scanners) were approximately equal. Thus for a given dose level, the image quality can be standardized in the majority of the participating centers. A prerequisite is that equal reconstruction matrix size, a comparable in-plane spatial resolution and slice sensitivity profile is present.

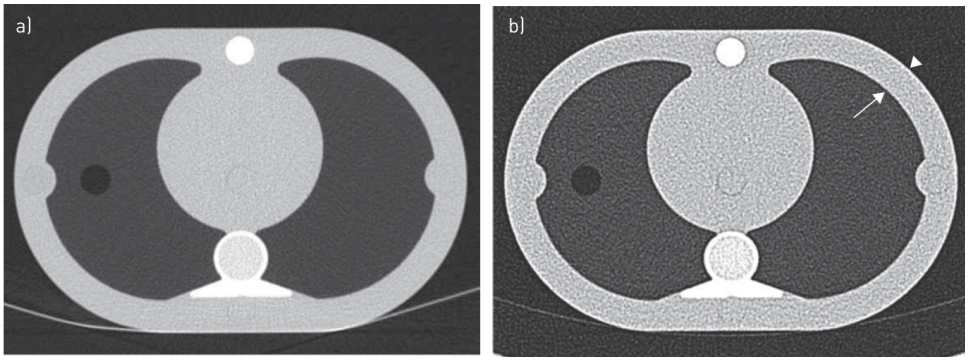

FIGURE 3. Examples of the child phantom scans made with two different CT scanners. **a)** The highest QNOISE, as seen at site 6, and b) the lowest QNOISE, seen at site 16, are both shown with window level −400 Hounsfield units (HU) and window width 1500 HU. Notice the influence of the edge enhancing reconstruction kernel in **b)**: the outer edges of the phantom appear brighter (arrowhead) and outer edges of the lung equivalent tissue appear darker (arrow).

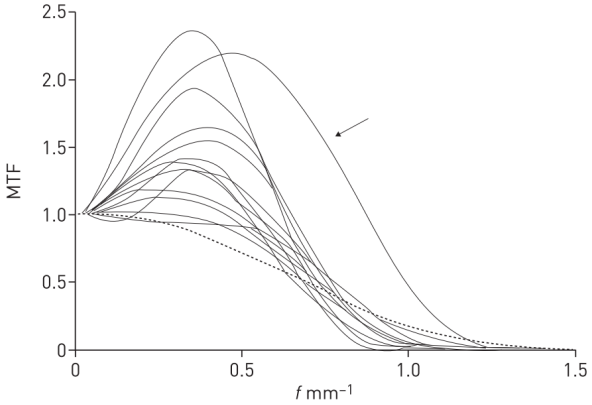

FIGURE 4. Variety of modulation transfer function (MTF) from all centres. The arrow indicates the MTF of site 9, with a relatively sharp reconstruction kernel. The dashed line shows an MTF when reconstructing with a kernel for quantitative image analysis. Such an MTF does not have values larger than unity.

Five scanners (16-64 slice scanners) performed below average and one scanner (>128 slice scanner) performed above average. No relation between applied x-ray tube voltage and scanner performance was found. These deviations from the average Q-factor might be explained by differences in in-plane sampling frequency. The scanners involved show differences in the number of detector elements per detector row and rotation time, which is directly related to the number of projection measurements per rotation. The number of detector elements per detector row is a hardware property of the scanner that cannot be changed by the user. The user can change the rotation time,

but options are limited. Longer rotation times do improve the sampling frequency and thus the performance of the scanner. This appeared to be the case for center 6 that used a rotation time of 750 ms and performed better than similar scanners from the same manufacturer at rotation times of 400-500 ms. A disadvantage of long rotation times is the correspondingly longer total scan time. Alternatively, a site specific dose level might be used at centers with scanners that perform below or above average to achieve an equal image noise level at all centers.

DISCUSSION

The SCIFI CF project aimed to compare CT scanners and optimize CT protocols for children and adolescents with CF. This study showed considerable differences within CT protocols among the 16 participating CF centers. All participating centers have received a general report and site-specific report including recommendations to optimize their CT protocol for (future) clinical trials. Table 1 shows the general guidelines recommended by the SCIFI CF. In addition to standardizing CT image quality, we explored the feasibilities of standardized lung volume levels acquired during CT scanning as observed by Salamon et al.[25]

TABLE 1. Summary of the recommended guidelines for CT protocols based on this initiative SCIFI CF findings

Data acquisition mode	Volumetric, helical scan technique
Patient positioning	Supine, with arms above the head
$CTDI_{vol}$ # for inspiratory scan	
1 year old	0.6 mGy
5 years old	1.0 mGy
young adult	2.2 mGy
Field of view	As close as possible to the entirety of the lungs, without cutting of the lung borders
$CTDI_{vol}$ for expiratory scan	50% lower than inspiratory scan
Tube voltage	Low enough such that the recommended $CTDI_{vol}$ can be reached, e.g. 80 kV
Tube current	Adapt to recommended $CTDI_{vol}$
Pitch	<1; lower limit determined by maximum scan time allowed
Slice thickness	Thinnest slice thickness e.g. 1 mm
Reconstruction increment	50% overlap e.g. 0.5 mm with 1 mm slice thickness
Kernel for automated analysis	Sharp reconstruction filter without under- or overshoot at edges preferably a dedicated kernel for quantitative image analysis
Iterative reconstruction technique	If available, iterative reconstruction techniques can be applied in addition to the requested filtered back projection techniques
Shielding	Breast shielding by bismuth for example is discouraged

SCIFI CF: Standardised Chest Imaging Framework for Interventions and Personalised Medicine in Cystic Fibrosis; $CTDI_{vol}$: volumetric computed tomography dose index expressed in mGy. #: in 32-cm body phantom.

Standardisation of CT became an important aspect in clinical trials and in clinical practice. The Quantitative Imaging Biomarkers Alliance (QIBA) working group was founded to standardize CT scanners and techniques for diseases such as chronic obstructive pulmonary disease (COPD) and asthma.[18] CT standardization has also been performed for a large observational COPD study with assessment of CT lung attenuation variation between CT scanners and the determination of longitudinal variation for individual scanners.[33,34] A custom designed phantom for adult patients was developed to perform quality control in CT scanners. Another study by Robinson et al., used a Plexiglas airway phantom to standardize CT protocols in children with CF.[35] This study, however, did not have the human equivalent study material to assess the general image quality, such as image noise. Both mentioned phantom studies also did not include pediatric sized anthropomorphic thorax phantoms to assess the automatic exposure control systems of each CT scanner.

Indication and applied scan technique

This initiative showed that 44% of the centers acquired chest CT scans only on clinical indication, while 56% of centers monitor their CF patients routinely with CT. Acquiring chest CT scans only on clinical indication could impose missed or delay in diagnosis of structural lung changes in a patient. Structural changes can be detected on chest CT scans when infants with CF do not express any clinical symptoms.[16] It is important to identify early pulmonary changes so treatment can be initiated promptly. Diagnosis of structural changes, such as bronchiectasis, was estimated to be delayed by 3 years when no routine check was performed.[36]

Another finding was that 4 centers acquired non-contiguous chest CT scans. For CF lung disease, it has been shown that structural abnormalities will be underestimated with non-contiguous acquisition.[21] In addition, the use of limited slices will make it difficult to evaluate progression of lung disease in longitudinal follow up or to reconstruct the image in different planes facilitating recognition of anatomical and abnormal structures of the lungs. Some centers aim to forego possible radiation risks and radiation exposure. However, with the recent improvements in scanning time and reduction in radiation exposure of volumetric CTs, the increased benefits of acquiring continuous CTs routinely justifies its use.[1] Based on the many advantages for the detection and monitoring of the heterogeneous CF lung disease we recommend acquiring volumetric CT scans in patients with CF and to forego sequential scanning.[37]

Finally, chest CT was acquired during spontaneous breathing in most centers when children are non-cooperative and with voluntary breath hold when children are old enough to cooperate in most centers. General anesthesia was only used in 2 centers. Since more CT scanners currently have short acquisition times, it is possible to acquire

images with sufficiently diagnostic quality in spontaneous breathing children. A disadvantage of this approach is that the lung will mostly be scanned at a volume level near functional residual capacity. Which has been recognized to reduce the sensitivity for the detection of bronchiectasis.[19]

Radiation dose

Based on the applied dose to the phantoms at various sizes for all centers, recommended dose levels were derived. As the phantoms have no shoulders, these are not very representative of actual patient anatomy. In patients, tube current modulation algorithms might increase the dose in the shoulder region. The recommended dose levels below are therefore valid for the thorax region away from the shoulder region only.

The median radiation dose of 1 mGy applied to the child phantom in all centers is in fairly good agreement with previous levels in the literature,[1] and this value was typical for an ongoing multi-center trial in Australia. We advised all centers to be aware of their applied radiation doses in comparison to the median radiation dose used within the SCIFI CF initiative. For the majority of scanners, our recommendation is to consider adjustment of the radiation dose for a 5 year old child to the median $CTDI_{vol}$ of 1 mGy. In this SCIFI CF initiative, we found 10 out of 16 centers to differ more than 40% from the median value of 1 mGy.

The recommended dose for the newborn child was based on the median dose for a 5 year old child and on the median ratio between the dose for the newborn child and the dose for the 5 year old child. Similarly, the recommended dose for the young adult was derived. Only two centers deviate 20% or less from the recommended dose for an adult CT scan and only two centers deviate 20% or less from the recommended dose for a newborn CT.

The Image Gently campaign provides dose reduction factors in order to establish pediatric patient diagnostic reference levels based on established levels for adult size patients.[27] The reduction factors are given as a function of patient size. Three series of reduction factors are provided that result in a 'limited', 'moderate' or 'aggressive' reduction of the pediatric patient dose relative to the dose for an adult patient. Based on the 'aggressive' reduction factors, the recommended dose in a newborn and adult would be 64%, and 190% of the dose in a child, respectively. Thus the relative dose recommended by Image Gently for a newborn is in agreement with our recommendations based on the median relative dose found in this study. The relative dose recommended by Image Gently for an adult patient is approximately 15% lower

than our recommendation (190% versus 223%). The reduction factors of the Image Gently campaign were designed for a community unaccustomed to adjusting the dose for children. The 'limited' and 'moderate' dose reduction factors changed less with size than what we found in clinical practice in this study. Apparently, the centers involved in this study are more accustomed to adjusting the dose for children with CF than the centers that the Image Gently campaign had in mind while developing the dose reduction factors.

Doses of expiratory CTs were recommended to be 50% lower than an inspiratory CT. A different dose level is recommended for 6 out of 16 scanners, to compensate for differences in performance of the scanner.

In 2 centers dose values were extrapolated from a non-contiguous scan. At these centers, the $CTDI_{vol}$ value was adjusted automatically in the scanner's dose report to reflect the dose reduction due to non-contiguous scanning. This adjusted value does not, however, reflect the dose used for a single image in case of a volumetric scan. Therefore the unadjusted $CTDI_{vol}$ value was used in this study instead. We do feel it is reasonable to report the relatively high unadjusted values because this makes the comparison between sites easy as if every site uses a volumetric scan protocol and these 2 extrapolated dose values did not affect the median dose level of all centers. Naturally, when we reported the DLP values as well, the sites using a non-contiguous scanning protocol would not have had such a high dose level. This report indicates however, that these sites should consider lowering the dose per image before switching from non-contiguous to volumetric scanning. The associated loss of image quality is expected to be limited as for the same exposure settings; image noise is different in sequential and spiral acquisition even for the same reconstruction kernel.

Some centers also discussed the use of breast shielding with a bismuth shield as a method to decrease the radiation exposure of the patient. This is not recommended as the use of a bismuth shield counteracts with the automatic exposure control used in most modern CT scanners, leading to higher and unpredictable radiation doses.[38] Alternatively, by reducing the tube current, similar reductions in radiation dose can be achieved with equivalent image noise levels.

Scanner performance

The SCIFI CF demonstrated large variations in image noise among centers (see Figure 2a and Figure 3) when CT scanner protocols were not standardized. After compensation for differences in spatial resolution, differences in image noise will remain (Figure 2b). When standardizing both resolution and radiation dose image quality is expected to become equal for the majority of scanners (Figure 2c). Remaining differences can be compensated for by doubling the recommended dose for the five centers with a

$Q_{NOISE,RES,DOSE}$ factor 50% below average. Before doing so, the actual influence of the reconstruction kernel should be assessed as the equations used in this manuscript were predictions on a theoretical model only. The same holds true when lowering the dose for the center with a performance above average. It should be noted that image noise, spatial resolution, and dose could not be fully characterized by the variables used in the equations. The standard deviation of the image noise reflects the noise magnitude only. It ignores the spatial correlations introduced into the noise by the reconstruction algorithm.[39] To minimize the effect of reconstruction filters on the Q factor, the images reconstructed with a typical lung reconstruction filter were used for calculating the Q values.

As no relation was found between scanner performance and applied tube voltage, no recommendations on the tube voltage to be applied are given. In practice, a relatively low tube voltage may be preferred because the relatively low dose levels technically cannot be reached at high voltages.

All the SCIFI CF related results have been discussed so far in this guideline. Following is some additional recommendations concerning chest CT in children and adolescents based on previous literature.

Selection of scan protocol for clinical studies including image analysis

The scan protocol to be selected depends on the image analysis method that will be used. CF lung disease on chest CT has become important to compare individual patients longitudinally and cross-sectionally between patients. Several scoring techniques have been developed to assess the extent and severity of CF lung disease.[15,19,40–43] It has been well recognized that adequate scoring methods require a constant image quality and standardization. Scoring techniques like the CF-CT[40] and PRAGMA[15] currently rely on visual assessment by an experienced observer, hence the image quality should be on par with clinically accepted diagnostic image quality. For the CF-CT method it is essential for CTs to be acquired volumetric in order to detect and score the complete lobes. For the SALD[41] and PRAGMA scoring methods, a volumetric CT is not required per se, as long as there are at least 10 slices between the top and bottom part of the lung. However, being able to visualize the entire part above and below the structure needed to be scored, improves the accuracy of the different lung structures. For the airway artery method,[19,43] it is crucial to have thin sliced volumetric CTs with an overlapping increment, to allow measuring the airway and artery diameters in reformatted slices perpendicular to the airway axis. Fewer slices could be an option when measuring the airway and artery dimensions in an axial, coronal, or sagittal view only. Reconstructions with 0.5 to 1 mm thickness using a sharp reconstruction filter possibly with enhancement of the edges, results in images with the impression of a higher resolution. This is needed to detect and

manually delineate the smaller airways. Selection of the scoring technique is dependent on the endpoint of the (multi-center) trial. Chest CTs of a multi-center trial should be scored centrally instead of each center separately.

Automated image analysis

Automatic image analysis methods exist and are in development for quantification of lung parenchyma,[44,45] air trapping,[44] and airway properties.[46–49] These methods can replace time-consuming manual annotations, and are capable of obtaining a much larger number of high precision measurements at any point of the airway structure or lung without additional costs. Because of their automatic nature, measurements are always performed in the exact same way and will not be influenced by inter- and intra-observer variability issues.

Automatic methods rely on mathematical models that characterize the CT image properties. A high degree of homogeneity between analyzed images is often required. Consequently, small variations in acquisition protocols or inspiration level, barely perceivable to the human eye, can largely affect the obtained measurements. Therefore standardization of inspiration level and image acquisition protocol is very important when automated image analysis methods are used, even more so than for visual inspection. The requirements to the image acquisition protocol differ for different automated analyses. Quantification of trapped air and consolidation based on CT intensity values can be performed in thicker slice and soft reconstructions, while quantification of the airway walls, identification of the lobes, and characterization of parenchymal texture patterns benefit from thin slices and a sharper reconstruction, showing more detail. For all automated image analysis purposes, we recommend to store thin-slice reconstructions (≤1 mm slice thickness) with overlapping slices with a relatively sharp reconstruction kernel. The reconstruction kernel should be as sharp as possible, without under- or overshooting (overenhancing). Then, if desired, thick-slice resampling or image denoising can be easily performed as image post-processing. Because each automatic method relies on different image assumptions, the ideal kernel may vary from technique to technique. A safe choice would be a dedicated kernel for quantitative image analysis as shown in Figure 4 with the dashed line. All the lung kernels we had analysed deviated strongly from this kernel.

To conclude, in order to optimise the image properties for automated image analysis, a careful selection of reconstruction kernel and a high level of image quality standardization are required to balance between radiation dose and image quality.

For clinical practice there are currently no automated analysis methods available. Using a spirometer controlled volumetric scan protocol allows to compare with great precision slice per slice to detect changes between the most recent scan and previous scans. It is

strongly recommended to use structured reporting to improve consistency between and within radiologists. These reports should at least include the components used in the scoring systems.[50]

Iterative reconstruction techniques

Iterative reconstruction techniques are more and more commonly applied in clinical practice. Often a dose reduction is reported when switching to these techniques.[51] Since effect of iterative reconstruction on (automated) image analysis is not yet known, it is recommended to store a second reconstruction using filtered back projection aside from the iterative reconstruction kernel. Most importantly large dose reductions should be avoided when compared to the recommended dose levels in Table 1.

CONCLUSION

In conclusion, considerable variation was found in radiation dose applied in the pediatric CF population among European centers. This difference cannot be explained by differences in scanner performance. Specific CT protocols are needed to balance between radiation dose and image quality in both clinical practice as for research purposes. With increasing demand for more sensitive outcome measures in upcoming clinical trials the SCIFI CF project shows that standardization of chest CT is required and more importantly feasible in a multi-center cohort.

ACKNOWLEDGEMENTS

The authors would like to acknowledge Elizabeth Salamon, Karla Logie, Pauline Wesselman and Els van der Wiel ((Dept of Pediatric Pulmonology, Erasmus MC – Sophia Children's Hospital, Rotterdam, The Netherlands) for their involvement in setting up the SCIFI CF project and executing the site visits.

REFERENCES

1. Kuo W, Ciet P, Tiddens HAWM, Zhang W, Guillerman RP, Van Straten M. Monitoring cystic fibrosis lung disease by computed tomography: Radiation risk in perspective. American Journal of Respiratory and Critical Care Medicine. 2014;189(11):1328–1336.
2. Sly PD, Brennan S, Gangell C, De Klerk N, Murray C, Mott L, Stick SM, Robinson PJ, Robertson CF, Ranganathan SC. Lung disease at diagnosis in infants with cystic fibrosis detected by newborn screening. American Journal of Respiratory and Critical Care Medicine. 2009;180(2):146–152.
3. Stick SM, Brennan S, Murray C, Douglas T, von Ungern-Sternberg BS, Garratt LW, Gangell CL, De Klerk N, Linnane B, Ranganathan S, et al. Bronchiectasis in Infants and Preschool Children Diagnosed with Cystic Fibrosis after Newborn Screening. Journal of Pediatrics. 2009;155(5):623–628.e1.
4. Sheikh SI, Long FR, Flucke R, Ryan-Wenger NA, Hayes D, McCoy KS. Changes in Pulmonary Function and Controlled Ventilation-High Resolution CT of Chest After Antibiotic Therapy in Infants and Young Children with Cystic Fibrosis. Lung. 2015;i.
5. de Jong PA, Nakano Y, Lequin MH, Mayo JR, Woods R, Paré PD, Tiddens H a WM. Progressive damage on high resolution computed tomography despite stable lung function in cystic fibrosis. European Respiratory Journal. 2004;23(1):93–97.
6. Sileo C, Corvol H, Boelle PY, Blondiaux E, Clement A, Ducou Le Pointe H. HRCT and MRI of the lung in children with cystic fibrosis: Comparison of different scoring systems. Journal of Cystic Fibrosis. 2014;13(2):198–204.
7. Puderbach M, Eichinger M, Gahr J, Ley S, Tuengerthal S, Schmähl A, Fink C, Plathow C, Wiebel M, Müller FM, et al. Proton MRI appearance of cystic fibrosis: Comparison to CT. European Radiology. 2007;17(3):716–724.
8. Lee KS, Primack SL, Staples CA, Mayo JR, Aldrich JE, Müller NL. Chronic infiltrative lung disease: comparison of diagnostic accuracies of radiography and low- and conventional-dose thin-section CT. Radiology. 1994;191(3):669–73.
9. Ciet P, Serra G, Bertolo S, Spronk S, Ros M, Fraioli F, Quattrucci S, Assael MB, Catalano C, Pomerri F, et al. Assessment of CF lung disease using motion corrected PROPELLER MRI: a comparison with CT. European Radiology. 2016;26(3):780–787.
10. Bortoluzzi C-F, Volpi S, D'Orazio C, Tiddens HAWM, Loeve M, Tridello G, Assael BM. Bronchiectases at early chest computed tomography in children with cystic fibrosis are associated with increased risk of subsequent pulmonary exacerbations and chronic pseudomonas infection. Journal of Cystic Fibrosis. 2014;13(5):564–571.
11. Wainwright CE, Vidmar S, Armstrong DS, Byrnes CA, Carlin JB, Cheney J, Cooper PJ, Grimwood K, Moodie M, Robertson CF, et al. Effect of bronchoalveolar lavage-directed therapy on Pseudomonas aeruginosa infection and structural lung injury in children with cystic fibrosis: a randomized trial. JAMA : the journal of the American Medical Association. 2011;306(2):163–171.
12. Robinson TE, Goris ML, Zhu HJ, Chen X, Bhise P, Sheikh F, Moss RB. Dornase alfa reduces air trapping in children with mild cystic fibrosis lung disease: A quantitative analysis. Chest. 2005;128(4):2327–2335.

13. Horsley AR, Davies JC, Gray RD, Macleod KA, Donovan J, Aziz ZA, Bell NJ, Rainer M, Mt-Isa S, Voase N, et al. Changes in physiological, functional and structural markers of cystic fibrosis lung disease with treatment of a pulmonary exacerbation. Thorax. 2013;68(6):532–9.

14. Tiddens HAWM, Puderbach M, Venegas JG, Ratjen F, Donaldson SH, Davis SD, Rowe SM, Sagel SD, Higgins M, Waltz D a. Novel outcome measures for clinical trials in cystic fibrosis. Pediatric Pulmonology. 2015;50(3):302–315.

15. Rosenow T, Oudraad MCJ, Murray CP, Turkovic L, Kuo W, de Bruijne M, Ranganathan SC, Tiddens HAWM, Stick SM. PRAGMA-CF. A Quantitative Structural Lung Disease Computed Tomography Outcome in Young Children with Cystic Fibrosis. American journal of respiratory and critical care medicine. 2015;191(10):1158–1165.

16. Stick S, Tiddens H, Aurora P, Gustafsson P, Ranganathan S, Robinson P, Rosenfeld M, Sly P, Ratjen F. Early intervention studies in infants and preschool children with cystic fibrosis: are we ready? The European respiratory journal. 2013;42(2):527–38.

17. Boedeker KL, McNitt-Gray MF, Rogers SR, Truong D a, Brown MS, Gjertson DW, Goldin JG. Emphysema: effect of reconstruction algorithm on CT imaging measures. Radiology. 2004;232(1):295–301.

18. Coxson HO. Sources of variation in quantitative computed tomography of the lung. Journal of Thoracic Imaging. 2013;28(5):272–9.

19. Mott LS, Graniel KG, Park J, De Klerk NH, Sly PD, Murray CP, Tiddens HAWM, Stick SM. Assessment of early bronchiectasis in young children with cystic fibrosis is dependent on lung volume. Chest. 2013;144(4):1193–1198.

20. Bendaoud S, Remy-Jardin M, Wallaert B, Deken V, Duhamel A, Faivre J-B, Remy J. Sequential versus volumetric computed tomography in the follow-up of chronic bronchopulmonary diseases: comparison of diagnostic information and radiation dose in 63 adults. Journal of thoracic imaging. 2011;26(3):190–195.

21. de Jong PA, Nakano Y, Lequin MH, Tiddens HAWM. Dose reduction for CT in children with cystic fibrosis: Is it feasible to reduce the number of images per scan? Pediatric Radiology. 2006;36(1):50–53.

22. Loeve M, Lequin MH, de Bruijne M, Hartmann IJC, Gerbrands K, van Straten M, Hop WCJ, Tiddens H a WM. Cystic fibrosis: are volumetric ultra-low-dose expiratory CT scans sufficient for monitoring related lung disease? Radiology. 2009;253(1):223–229.

23. Alibek S, Brand M, Suess C, Wuest W, Uder M, Greess H. Dose Reduction in Pediatric Computed Tomography with Automated Exposure Control. Academic Radiology. 2011;18(6):690–693.

24. Singh S, Kalra MK, Shenoy-Bhangle A, Saini A, Gervais D a, Westra SJ, Thrall JH. Radiation Dose Reduction with Hybrid Iterative Reconstruction for Petriatric CT. Radiology. 2012;263(2):537–546.

25. Salamon E, Lever S, Kuo W, Ciet P, Tiddens HAWM. Spirometer guided chest imaging in children: It is worth the effort! Pediatric Pulmonology. 2016;56(September 2015):48–56.

26. Mccollough CH, Ulzheimer S, Halliburton SS, White RD, Kalender WA. Coronary Artery Calcium : A Multi-institutional, Multimanufacturer International Standard for Quantification at Cardiac CT. 2007;243(2):527–538.

27. Image gently. Image Gently development of pediatric CT protocols 2014. 2014;(96).

28. Kalender WA, Fuchs T. On the Correlation of Pixel Noise, Spatial Resolution and Dose in Computed Tomography : Theoretical Prediction and Verification by Simulation and Measurement. Physica medica. 2003;XIX(2):1000–1012.

29. Baek J, Pelc NJ. The noise power spectrum in CT with direct fan beam reconstruction. Medical Physics. 2010;37(5):2074.

30. Faulkner K, Moores BM. Analysis of x-ray computed tomography images using the noise power spectrum and autocorrelation function. Physics in Medicine and Biology. 1984;29(11):1343–1352.

31. Kijewski MF, Judy PF. The noise power spectrum of CT images. Physics in Medicine and Biology. 1987;32(5):565–575.

32. Lewis M, Keat N, Edyvean S. Report 06013: 32 to 64 slice CT scanner comparison report version 14. 2006. 1-17 p.

33. Newell JD, Sieren J, Hoffman EA. Development of quantitative computed tomography lung protocols. Journal of thoracic imaging. 2013;28(5):266–71.

34. Sieren JP, Newell JD, Judy PF, Lynch DA, Chan KS, Guo J, Hoffman EA. Reference standard and statistical model for intersite and temporal comparisons of CT attenuation in a multicenter quantitative lung study. Medical Physics. 2012;39(9):5757.

35. Robinson TE, Long FR, Raman P, Saha P, Emond MJ, Reinhardt JM, Raman R, Brody AS. An Airway Phantom to Standardize CT Acquisition in Multicenter Clinical Trials. Academic Radiology. 2009;16(9):1134–1141.e1.

36. O'Connor OJ, Vandeleur M, McGarrigle AM, Moore N, McWilliams SR, McSweeney SE, O'Neill M, Ni Chroinin M, Maher MM. Development of low-dose protocols for thin-section CT assessment of cystic fibrosis in pediatric patients. Radiology. 2010;257(3):820–829.

37. Loeve M, de Bruijne M, Hartmann ICJ, Van Straten M, Hop WCJ, Tiddens H a. Three-section Expiratory CT: Insufficient for Trapped Air Assessment in Patients with Cystic Fibrosis? Radiology. 2012;262(3):969–976.

38. AAPM Position Statement on the Use of Bismuth Shielding for the Purpose of Dose Reduction in CT scanning. 2012:7–10.

39. Boedeker KL, Cooper VN, McNitt-Gray MF. Application of the noise power spectrum in modern diagnostic MDCT: part I. Measurement of noise power spectra and noise equivalent quanta. Physics in medicine and biology. 2007;52(14):4027–46.

40. Brody AS, Kosorok MR, Li Z, Broderick LS, Foster JL, Laxova A, Bandla H, Farrell PM. Reproducibility of a scoring system for computed tomography scanning in cystic fibrosis. Journal of thoracic imaging. 2006;21(1):14–21.

41. Loeve M, van Hal PTW, Robinson P, de Jong PA, Lequin MH, Hop WC, Williams TJ, Nossent GD, Tiddens HAWM. The spectrum of structural abnormalities on CT scans from patients with CF with severe advanced lung disease. Thorax. 2009;64(10):876–882.

42. De Jong PA, Nakano Y, Hop WC, Long FR, Coxson HO, Paré PD, Tiddens H a. Changes in airway dimensions on computed tomography scans of children with cystic fibrosis. American Journal of Respiratory and Critical Care Medicine. 2005;172(2):218–224.

43. Kuo W, de Bruijne M, Nasserinejad K, Ozturk H, Chen Y, Perez-Rovira A, Tiddens HAWM. Assessment of bronchiectasis in children with cystic fibrosis by comparing airway and artery dimensions to normal controls on inspiratory and expiratory spirometer guided chest computed tomography. Insights Imaging. 2015;6(1):S197, NaN-168.

44. Ciompi F, Palaioroutas A, Loeve M, Pujol O, Radeva P, Tiddens H, de Bruijne M. Lung tissue classification in severe advanced cystic fibrosis from CT scans. Fourth International Workshop on Pulmonary Image Analysis. 2011;(1):57–68.

45. Galbán CJ, Han MK, Boes JL, Chughtai K a, Charles R, Johnson TD, Galbán S, Rehemtulla A, Kazerooni E a, Martinez FJ, et al. CT-based biomarker provides unique signature for diagnosis of COPD phenotypes and disease progression. Nature Medicine. 2012;18(11):1711–1715.

46. Lo P, Van Ginneken B, Reinhardt JM, Yavarna T, De Jong PA, Irving B, Fetita C, Ortner M, Pinho R, Sijbers J, et al. Extraction of airways from CT (EXACT'09). IEEE Transactions on Medical Imaging. 2012;31(11):2093–2107.

47. Petersen J, Nielsen M, Lo P, Nordenmark LH, Pedersen JH, Wille MMW, Dirksen A, de Bruijne M. Optimal surface segmentation using flow lines to quantify airway abnormalities in chronic obstructive pulmonary disease. Medical Image Analysis. 2014;18(3):531–541.

48. Wielpütz MO, Eichinger M, Weinheimer O, Ley S, Mall MA, Wiebel M, Bischoff A, Kauczor H-U, Heußel CP, Puderbach M. Automatic airway analysis on multidetector computed tomography in cystic fibrosis: correlation with pulmonary function testing. Journal of thoracic imaging. 2013;28(2):104–13.

49. Fetita C, Brillet P-Y, Hartley R, Grenier PA, Brightling C. 3D mapping of airway wall thickening in asthma with MSCT: a level set approach. In: Aylward S, Hadjiiski LM, editors. SPIE Medical Imaging. International Society for Optics and Photonics; 2014. p. 90352I.

50. Larson DB, Towbin AJ, Pryor RM, Donnelly LF. Improving consistency in radiology reporting through the use of department-wide standardized structured reporting. Radiology. 2013;267(1):240–50.

51. Kalmar PI, Quehenberger F, Steiner J, Lutfi A, Bohlsen D, Talakic E, Hassler EM, Schöllnast H. The impact of iterative reconstruction on image quality and radiation dose in thoracic and abdominal CT. European Journal of Radiology. 2014;83(8):1416–1420.

APPENDIX

QUESTIONNAIRE SCIFI-CF

Name of CF-center	
Total number of CF patients between 0-5:	
Diagnosis through Newborn Screening:	
Total number of patients between 5 and 18 years:	
Total number of adults:	
Describe <u>current use</u> of chest CT in your center:	
When using routinely, what is the age of first chest CT?	
Additional comments in relation to chest CT routine	…… …… ……
For young children … yrs what CT protocol is used	□ General anaesthesia + Pressure controlled expiration 0 cm H_2O And / Or □ General anaesthesia + pressure controlled inspiration ….. cm H_2O And / Or □ Spontaneous breathing with sedation
For expiratory CT in children ≥ … is used:	Voluntary breath hold/ Spirometer controlled
For inspiratory CT in children ≥ … is used:	Voluntary breath hold/ Spirometer controlled
Which scan protocol is used for expiratory scan:	Volumetric or limited slices
Which scan protocol is used for inspiratory scan:	Volumetric or limited slices

APPENDIX FIGURE 1. Questionnaire sent to all 30 ECFS-CTN centers for inventory and participation with the SCIFI CF initiative.

PART II

OBJECTIVE QUANTIFICATION OF LUNG DISEASE ON CHEST CTS OF PEDIATRIC CF PATIENTS

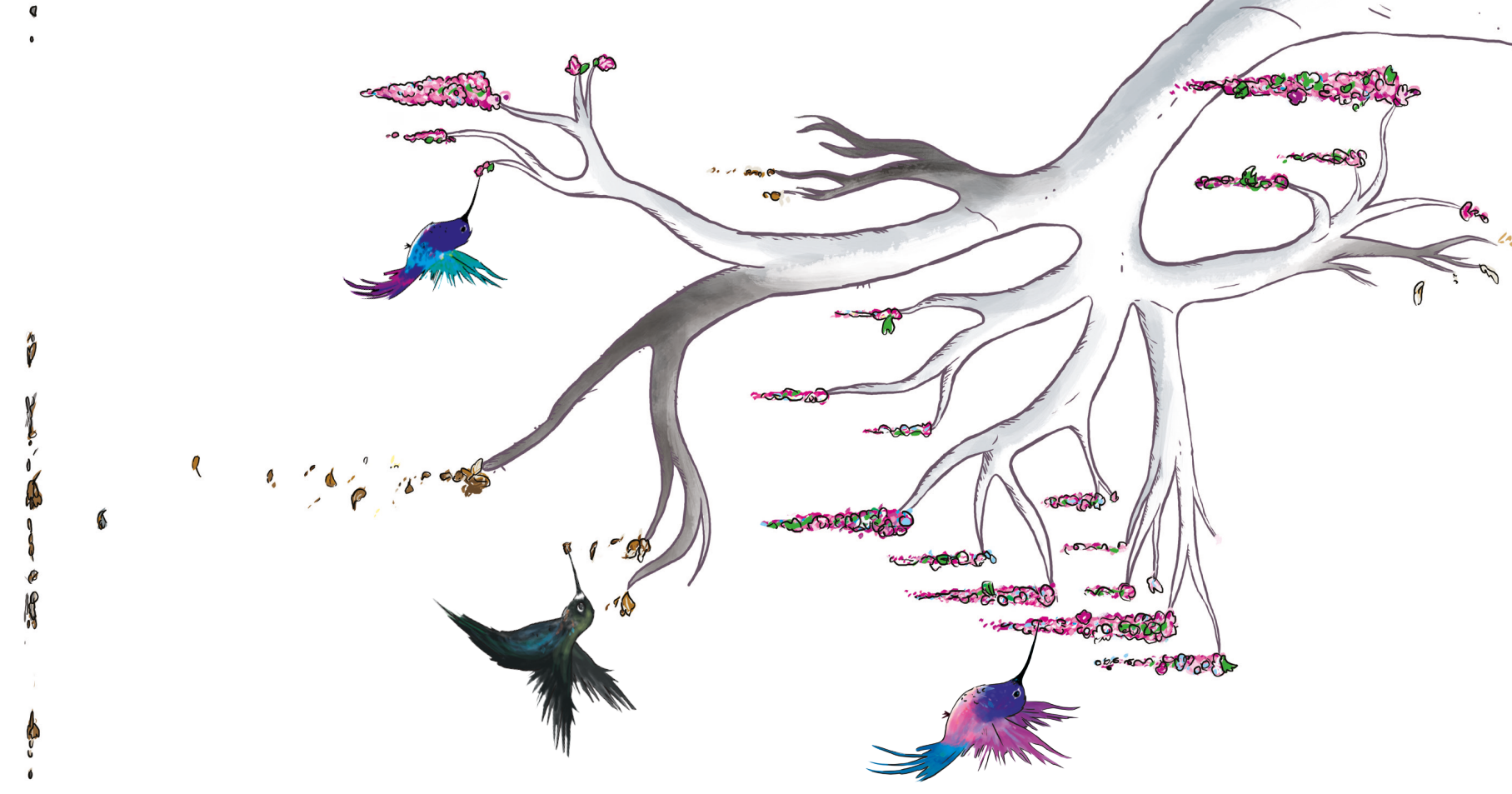

CHAPTER 4

DIAGNOSIS OF BRONCHIECTASIS AND AIRWAY WALL THICKENING IN CHILDREN WITH CF: OBJECTIVE AIRWAY-ARTERY QUANTIFICATION

Wieying Kuo, Marleen de Bruijne, Jens Petersen, Kazem Nasserinejad, Hadiye Ozturk, Yong Chen, Adria Perez-Rovira, Harm A.W.M. Tiddens

European Radiology.
2017; in press

ABSTRACT

Objectives

To quantify airway and artery (AA)-dimensions in CF and control patients, for objective CT diagnosis of bronchiectasis and airway wall thickness (AWT).

Methods

Spirometer guided inspiratory and expiratory CTs of 11 CF and 12 control patients were collected retrospectively. Airway pathways were annotated semi-automatically to reconstruct 3-Dimensional bronchial trees. All visible AA-pairs were measured perpendicular to the airway axis. Inner, outer, and AWT (outer minus inner) diameter were divided by the adjacent artery diameter to compute A_{in}A-, A_{out}A-, and A_{WT}A-ratios. AA-ratios were predicted using mixed-effects models including disease status, lung volume, gender, height, and age as covariates.

Results

Demographics did not differ significantly between cohorts. Mean AA-pairs CF: 299 inspiratory; 82 expiratory. Controls: 131 inspiratory; 58 expiratory. All ratios were significantly larger in inspiratory compared to expiratory CTs for both groups ($p<0.001$). A_{out}A-, and A_{WT}A-ratios were larger in CF than in controls, independent of lung volume ($p<0.01$). Difference of A_{out}A-, and A_{WT}A-ratios between patients with CF and controls increased significantly for every following airway generation ($p<0.001$).

Conclusion

Diagnosis of bronchiectasis is highly dependent on lung volume and more reliably diagnosed using outer airway diameter. Difference in bronchiectasis and AWT severity between the two cohorts increased with each airway generation.

INTRODUCTION

In cystic fibrosis (CF), lung disease is characterized by progressive bronchiectasis (BE) and airway wall thickening (AWT).[1–3] Chest computed tomography (CT) is the most sensitive tool to diagnose BE and AWT, which are important outcome measures for both clinical and research purposes.[1,4]

BE is defined as destructive and irreversible widening of airways with a ratio between airway and accompanying artery (AA) above 1 in adults.[5,6] Currently, the inner airway dimensions are mostly used for comparison with the artery.[7–9] However, no clear consensus, based on objective quantitative measures, exists on whether inner or outer airway diameter should be compared with the artery for the diagnosis of BE.[10] Nonetheless, the approximate ratio of one was based on the outer airway diameter.[11] In addition, it is not clear whether identical AA-ratios cutoffs can be used to define BE in children, where smaller AA-ratio has been suggested.[5] Lastly, the AA-ratio is thought to increase with age in healthy subjects.[12]

AWT like BE is associated to airway inflammation.[13,14] AWT is presumed present when the airway wall diameter occupies more than 20% of the total outer airway diameter[15] or takes up more than 33% of the adjacent arterial diameter.[8] CT assessments of BE and AWT are mostly performed in the axial or coronal plane by comparing airway diameter, to the accompanying artery diameter. However, to avoid inaccuracy caused by the parallax or projection error, the AA dimensions should ideally be evaluated in a view perpendicular to the airway centerline.[16–18]

Airway dimensions are routinely evaluated on inspiratory CT.[19] Unfortunately lung volume levels during inspiratory CT acquisition have shown to vary widely between 55 and 106 % of the measured total lung capacity (TLC) obtained via body plethysmograph.[20] This variability is caused by a lack of breath hold standardization and influences the AA-ratio and therefore diagnosis of bronchiectasis.[7,21,22] Airway dimensions assessed on axial view were shown to be highly dependent on the lung volume levels in children below the age of 5 years with CF [7], in adults with COPD,[23,24] and in healthy controls.[22] Hence, suboptimal lung volume levels negatively impact objective evaluation of BE and AWT.

The purpose of our study was to develop objective criteria to diagnosis BE and AWT in children by comparing AA dimensions between CF patients and control patients with spirometer guided CTs. We hypothesized that AA-ratios are increased in pediatric CF patients and more prominent on inspiratory CTs. To investigate this, we aimed to assess 1) AA dimensions in control patients; 2) use of inner or outer airway diameter as a more sensitive biomarker to diagnose BE; 3) influence of inspiratory and expiratory CTs on AA dimensions. Between CF and control patients we aimed to assess: 4) differences in number of visible AA-pairs and AA dimensions; 5) differences by airway location (e.g. lobes and airway generations).

MATERIALS AND METHODS

This study was approved by institutional review board (MEC-2014-254). Written informed consent was waived for all patients because of the retrospective nature of the study.

Study population

Spirometer guided inspiratory and expiratory chest CTs of 11 CF patients and 12 control patients without lung abnormalities on CT made between 2007 and 2012 were selected retrospectively. All patients were treated at [blinded].

CF patients. Inclusion criteria: diagnosis of CF; age between age 6 and 16 years, spirometer guided chest CT acquired with SOMATOM® Definition Flash CT scanner (Siemens Healthcare, Forchheim, Germany); Slow vital capacity during CT for inspiratory CT ≥85% and expiratory CT ≥80% as recommended and described by Salamon et al.[25] Exclusion: poor image quality due to motion artifacts; poor breath hold performance as judged by lung function technician. 12 CF patients were randomly selected out of all patients that met the selection criteria.

Control patients. Inclusion criteria: good or excellent spirometer guided chest CT acquired with SOMATOM® Definition Flash scanner; clinical reason for CT other than CF; report by [blinded] radiologist stating chest CT to be normal; defined normal on second reading by an independent radiologist (CY, 20 years of experience in thoracic imaging) blinded to patient identifiers and information. Out of 16 control chest CTs that met above mentioned criteria, 12 CTs were selected with best matched ages of CF group. More detailed control group characteristics are provided in Table 1.

CT scanning

End-inspiratory and end-expiratory volumetric chest CTs were obtained in supine position. Details of scan parameters are provided in Table 2.

Quantitative analysis of airways and arteries

All CTs were scored in random order using the CF-CT scoring system, to quantify structural CT abnormalities in CF and controls as described in more detail separately.[26] Dimensions of AA-pairs were measured using Myrian® (v1.16.2, Lung XP module) image analysis platform (Intrasense, Montpelier, France) and described previously.[26] In summary, airway pathways were indicated automatically. Pathways of additional lobar, segmental and subsegmental airways not automatically indicated were added manually. The bronchial tree was reconstructed in a 3D-view (Appendix video-E1), and cross-sectional CT reconstructions were generated based on the airway's centerline (Figure 1). One measurement per branch was made when both airways and artery were clearly

visible. AA-pairs with movement artefacts or too much noise for reliable measurements were excluded. In addition, AA-pairs of airways that did not show a visible inner lumen (e.g. due to mucous plugging) and airways without a clear identifiable adjacent artery (e.g. due to atelectasis or severe cystic bronchiectasis without a traceable artery) were excluded.

Inner and outer airway diameters were divided by artery diameter to compute $A_{in}A$ and $A_{out}A$-ratio, respectively. Wall thickness (difference between outer and inner airway diameter) was divided by outer airway diameter to compute A_{WT}-ratio; and divided by artery diameter to compute $A_{WT}A$-ratio.

TABLE 1. Diagnosis of control subjects

Clinical diagnosis	Reason for CT	Findings	No of subjects
Asthma	Air trapping, bronchiectasis, malacia?	No air trapping, no bronchiectasis, no malacia	8
Recurrent respiratory infections	Air trapping, bronchiectasis, malacia?	No air trapping, no bronchiectasis, no malacia	3
Condition after esophageal atresia	Tracheomalacie?	No tracheomalacie	1

TABLE 2. Scan parameters used to obtain the CTs

	CF subjects		Control subjects	
Scan acquisition	Insp	Exp	Insp	Exp
Tube voltage (kV)	80	80	(80-120)	(80-120)
Pitch	0.85	0.85	0.85	0.85
Slice thickness (mm), median (range)	1 (0.75-1)	1 (0.75-1)	1	1
Reconstruction increment (mm), median (range)	0.6 (0.3-1)	0.6 (0.3-1)	0.8 (0.6-0.8)	0.8 (0.6-0.8)
Reconstruction kernel	B70f;B75f	B70f;B75f	B75f; I70f	B75f;I50f
Collimation	128x0.6	128x0.6	128x0.6	128x0.6
Current-time product (mAs), median (range)	46 (36-52)	44 (35-53)	28 (11-61)	23 (8-65)
$CTDI_{vol,32\ cm}$ (mGy), median (range)	0.74 (0.57-0.83)	0.71 (0.56-0.84)	0.76 (0.32-1.13)	0.56 (0.24-1.05)
DLP(mGy * cm), median (range)	21 (14-28)	17 (11-25)	22.5 (7-38)	14.5 (5-30)

Location of airway artery measures

The lung lobes (right upper (RUL), right middle (RML), right lower (RLL), left upper (LUL), left lower lobe (LLL) and lingula (LING)), segmental bronchi (nomenclature as depicted by Netter [27]), and airway generations were annotated for each AA measurement. Airway generation started at the trachea as 0, the main stem bronchi as 1 and continuing after

each time the bronchi bifurcates. The upper segmental bronchi begins at generation 3-4 and lower segmental bronchi begins at generation 4-7. The generation from each segmental bronchi as described in Appendix Figure E2a was subtracted from the airway generation to compute the segmental generation starting at 1 (see Figure 2). Segmental generation ≥ 4 were defined as peripheral airways for the purpose of this paper.

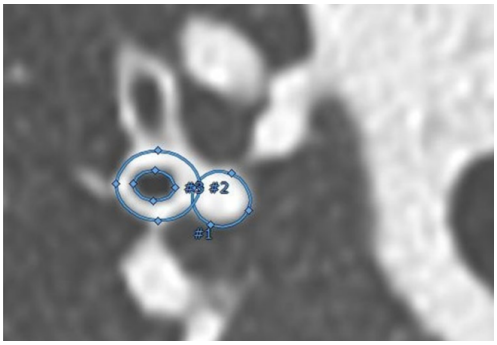

FIGURE 1. The three measurements of the airway and accompanying artery in a perpendicular view to the pathway centerline, using an ellipse image analysis tool (Myrian®). The annotated surface areas of the inner (#3) and outer (#2) airway and of the artery (#1) were used to estimate diameters and to calculate the AA-ratios. The location of all AA-pairs was determined by the use of the 3D segmentation (videos of rotating 3D segmentations in color can be found in Appendix E2).

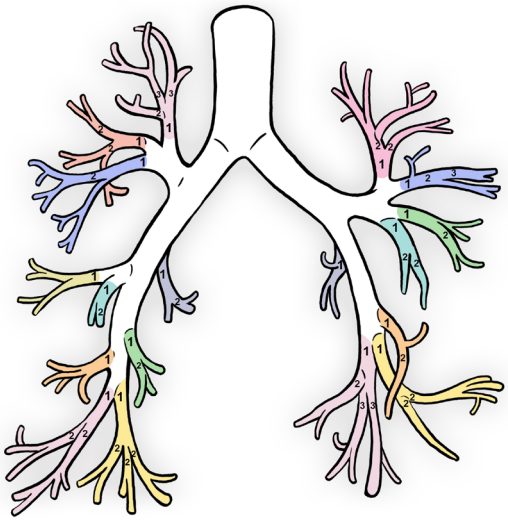

FIGURE 2. The segmental branches are shown in the different colors and the numbering stands for each segmental airway generation. The segmental generation ensured all segmental bronchi to start at segmental generation 1 avoiding discrepancies in the upper and lower segmental airway generations as demonstrated in Appendix Figure E2 (Artist: K. Rubenis).

Observer reliability

CTs of all patients were anonymized and randomized before scoring. The scorers were blinded to all clinical information. All AA measurements were conducted by the first observer (WK, 3 years of experience). After 3 months, a total of 386 measurements were repeated in one randomly selected segmental branch of every patient to establish intra-observer variability. A second observer measured a total of 2945 AA dimensions in a random subset of 25 CTs (HO, 1 year of experience) in order to determine inter-observer variability.

Statistical Analysis

Difference between patients' characteristics in the two cohorts were assessed with Mann-Whitney U test. Difference in number of AA-pairs visible was assessed using Wilcoxon signed-rank test. Relationship between number of AA-pairs visible with height and age was evaluated with linear regression analysis. Mixed-effect models were used to predict AA-ratios using disease status and lung volume. Influence of other covariates (i.e. gender, age, and height) on AA-ratios was assessed univariately. Univariate covariates found to be significant were added with interaction to the main model. Variable selection in the main model was performed with a likelihood ratio test. Mixed-effect models were used to evaluate differences between CF and controls and volume level predicting AA-ratios for each segmental generation and lung lobes. Random-effects of lobes and individuals were included in all mixed-effect models to capture heterogeneity. For diagnosis of bronchiectasis receiver operating characteristics (ROC) curves with the corresponding area under curves (AUCs) and 95% confidence interval (CI) were plotted to identify the threshold values for $A_{in}A$ and $A_{out}A$-ratios with the highest combined sensitivity and specificity. The intraclass correlation coefficient (ICC) was used to measure inter- and intra-observer agreement, with the use of mixed-effects models. In these mixed-effects models the structure was taken into account specifically the segmental branches within generation within patients. ICC values between 0.4 and 0.6, 0.6 and 0.8 or ≥ 0.8 were considered to indicate moderate, good and very good agreement, respectively.[28]

Results were expressed as median, interquartile range (IQR). A p-value of 0.05 or less was considered significant. All analysis were conducted using R version 3.1.0.[29]

RESULTS

Study population

A detailed description of the group characteristics is shown in Table 3. One subject in the CF group was excluded after image analysis since the patient appeared to be mislabeled and diagnosed with common variable immunodeficiency. Hence, 11 patients with CF (6 males) were included for further analysis with a median age of 11 years. 12 control patients with normal CTs (7 males) were included with a median age 13.9 years. All but one control patient had spirometry performed on the same day or maximally one month apart from the CT scan. One control patient did not have a recent spirometry available, so spirometry of 8 months prior to the CT was used. Re-analysis without this subject did not influence difference between the groups in demographics or spirometry. No significant difference was found in age, gender, height, weight, and PFT's between the two groups. All CF-CT scores were significantly higher in CF compared to the control group.

TABLE 3. Demographics of the CF and normal cohort

	Patients with CF, median (IQR)	Control patients, median (IQR)	P –value
Age at CT (years)	11 (9.3-11.1)	13.9 (8.7-15)	0.385
Age at PFT (years)	11 (9.3-13)	13.9 (8.7-15)	0.385
Time between CT and PFT (months)	0.0 (0.0-0.0)	0.5 (0.1-0.7)	0.011*
Gender	6 males; 5 females	7 males; 5 females	0.808
Height (cm)	144.4 (138.2-146.8)	149 (136.6-170.9)	0.296
Weight (kg)	34.5 (30.4-45.3)	40.1 (28.6-65.8)	0.461
BMI	17.5 (15.5-19.4)	18.1 (15.9-20.2)	0.435
CF-CT BE score (%)	5.2 (1.4-12.1)	0.0 (0.0-0.7)	<0.001*
CF-CT AWT score (%)	5.6 (0.0-19.3)	0.0 (0.0-0.0)	<0.001*
CF-CT MP score (%)	2.8 (0.0-22.9)	0.0 (0.0-0.0)	<0.001*
CF-CT AT score (%)	51.2 (25.9-66.7)	3.7 (0.0-8.3)	<0.001*
CF-CT total score (%)	7.8 (6.2-18.4)	1.2 (0.4-1.4)	<0.001*
FEV_1 (z-scores)	-1.3 (-2.2-0.1)	-1.7 (-2.1- -0.4)	0.668
FVC (z-scores)	-0.1 (-1.2-0.8)	-0.4 (-2.3-0.8)	0.409
FEV_1/FVC	0.82 (0.76-0.83)	0.82 (0.70-0.91)	0.385
FEF_{25-75} (z-scores)	-1.8 (-2.3- -0.6)	-1.4 (-2.5- -1)	0.939

Wilcoxon signed rank test to test the difference in demographics between the CF and control group. CF-CT scores of mucous plugging (MP), air trapping (AT), and the total score were compared as well as CF-CT scores of BE and AWT. Spirometry was compared using Z-scores according to Quanjer et al. [41]. PFT: pulmonary function test, BMI: body mass index, FEV_1: forced expiratory flow in 1 s, FVC: forced vital capacity, FEF_{25-75}: forced expiratory flow during the 25-75% portion of the FVC

Quantitative analysis of airways and arteries

A total of 6464 AA-pairs were measured in perpendicular view of the airway axis. In CF patients a mean of 299 AA-pairs were measured on end-inspiration and 82 AA-pairs on the end-expiration CTs. In control patients a mean of 131-pairs were measured on end-inspiration and 58 AA-pairs on the end-expiration CTs. Number of visible AA-pairs was significantly higher in inspiration compared to expiration CTs in both CF and control group ($p<0.001$). This difference is especially prominent after segmental generation 4 (Figure 3). CF patients had significantly more visible AA-pairs ($p<0.001$) than controls in inspiratory CTs, but not in expiratory CTs ($p=0.54$). As seen in Figure 3, patients with CF have a large number of visible AA-pairs in higher generations (8 to 12), whereas control patients had none. Number of AA-pairs counted was not correlated with age ($p=0.72$) or height ($p=0.77$).

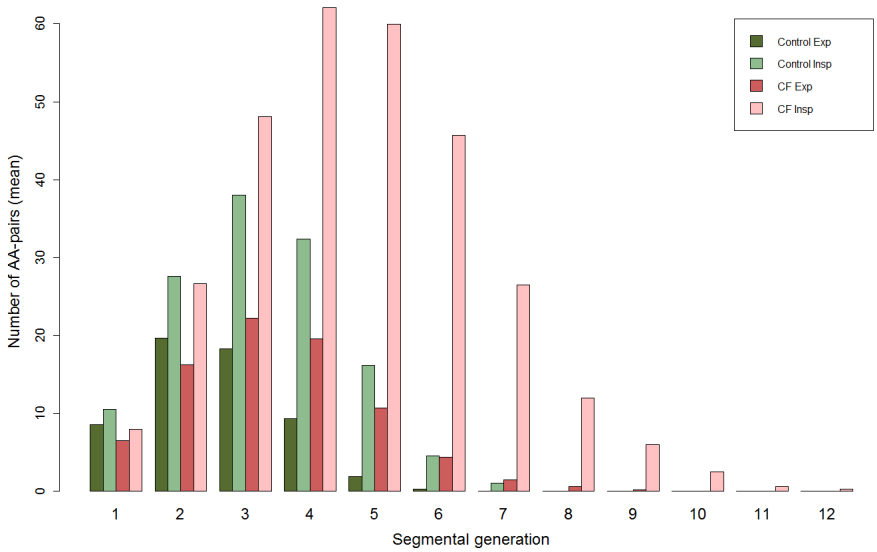

FIGURE 3. Average number of AA-pairs visible per segmental generation for controls (green) and CF patients (red), separated by inspiratory (light colors) and expiratory (dark colors) CT. Note that the total number of visible airways on the inspiratory scans in CF is increased relative to controls.

Airway-artery dimensions

Median (range) of the inner, outer, wall and vessel diameter were 1.65 (0.36-6.58), 3.74 (1.00-9.84), 2.08 (0.50-6.28), and 3.42 (0.94-11.99) mm respectively (Appendix Figure E3). $A_{in}A$- and $A_{out}A$-ratio was independent of age in both CF and controls (Figure 4). Gender, age and height were not significantly related with $A_{in}A$, $A_{out}A$ or $A_{WT}A$-ratio in an univariate mixed-effect model. Height, but not gender and age, was found to be

significant in the mixed-effect model with A_{WT}-ratio (p=0.001), so height was included in the model describing A_{WT}-ratio.

$A_{in}A$, $A_{out}A$, A_{WT} and $A_{WT}A$-ratios differed significantly on inspiratory CTs compared to expiratory CTs for both CF and control groups (P<0.001). The significant differences in AA- and AWT-ratios between CF and control patients are shown in Table 4.

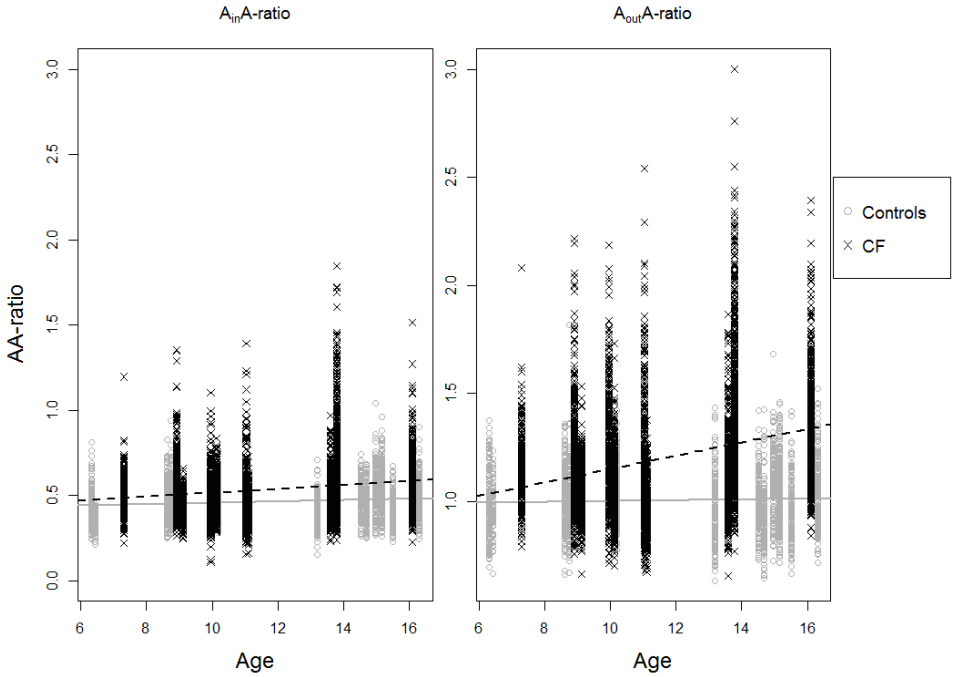

FIGURE 4. The AA-ratio is plotted as a function of age, for $A_{in}A$ (left) and $A_{out}A$ (right). The CF patients are depicted as black X and dashed line and the control patients as gray O and solid lines. $A_{in}A$-ratio remained constant with increasing age in the CF (value=0.010, p=0.28), and control group (value=0.006, p=0.22). The $A_{out}A$-ratio in the CF group (value=0.026, p=0.10), and control group (value=0.002, p=0.52) do not increase significantly either with age.

TABLE 4. Comparison of airway dimensions between CF patients and controls

Significant difference between disease status (Control/CF)	$A_{in}A$-ratio	$A_{out}A$-ratio	$A_{WT}A$-ratio	A_{WT}-ratio
Inspiration	0.156	<0.001*	<0.001*	0.215
Expiration	0.996	0.003*	<0.001*	0.036*

P-values of mixed-effect model analysis of differences between airway dimensions between CF and control patients. $A_{out}A$ and $A_{WT}A$ -ratios were higher in CF than controls in both inspiratory and expiratory scans. $A_{in}A$-ratios was not significant and the A_{WT}-ratio only in the expiratory subgroup. * *indicantes significance*

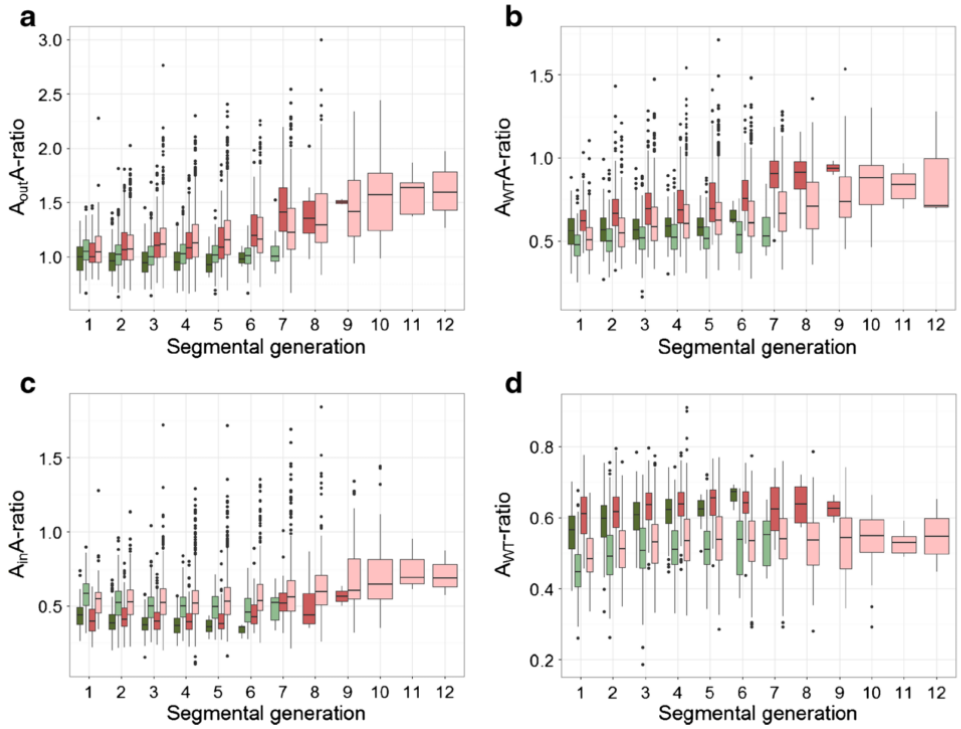

FIGURE 5. Boxplots of the AA-ratios in the control group (green) and in the cystic fibrosis (CF) group (red) for each segmental generation. Inspiratory scans are shown in light colours and expiratory scans in dark colours. Each box shows median (horizontal line), interquartile range (solid box), 1.5*interquartile range (whiskers) and outliers (points). **a** When focusing on the inspiratory scans, an increasing difference can be found in A_{out}A- ratio between the CF and control group from generation 2 to generation 6 (increasing difference of 0.08–0.19, p≤0.02). The difference between CF and the control group of the A_{out}A-ratio in the expiratory scans was found to be significant from generation 2 to 5 (difference of 0.13–0.15, p≤0.04). **b** On the inspiratory scans, a difference can be found in A_{WT}A-ratio between the cystic fibrosis (CF) and control groups starting from segmental generation 1 to 6 (difference of 0.05–0.12, p≤0.04). The difference in A_{WT}A-ratio between CFand the control group in the expiratory scans was found to be significant from generation 1 to 5 (difference of 0.08–0.13, p≤0.003). **c** There was no difference in A_{in}A-ratio between the cystic fibrosis (CF) and control groups on inspiratory CTs (p≥0.08), neither was there for the expiratory scans (p≥0.28). A difference in A_{in}A-ratio was observed between inspiration and expiration CTs of both the CF (difference of 0.12–0.20, p≤0.04) and control group (difference of 0.13–0.14, p≤0.001). **d** There was no difference in A_{WT}-ratio between the cystic fibrosis (CF) and control groups in all segmental generations on the inspiratory CTs. On expiratory CTs only a difference was found in segmental generation 1 (difference of 0.05, p=0.021). An apparent difference was found between inspiratory and expiratory scans in A_{WT}-ratio for the CF group (0.08–0.11, p≤0.001), as well for the control group (0.09– 0.15, p≤0.001) in all segmental generations (all absolute values can be found in Appendix Table E1a–d).

Comparison CF vs control group

The optimal threshold to define BE was reached at a value of 0.5 for A_{in}A-ratio and 1.11 for A_{out}A-ratio. AUC (95% CI) for A_{in}A was 0.6 (0.59-0.61) and 0.72 (0.71-0.74) for A_{out}A-ratio (Appendix Figure E4). The optimal threshold for BE of peripheral airways (segmental generation≥4) was 0.56 for A_{in}A-ratio (AUC=0.63, 95% CI=0.61-0.65) and 1.17 for A_{out}A-ratio (AUC= 0.75, 95% CI=0.73-0.77).

Location of airway and artery measures

Figure 5A and B show A_{out}A and A_{WT}A-ratio by segmental generation. The difference in A_{out}A and A_{WT}A-ratio between inspiratory CF and controls was significant for segmental generation 2 to 6 ($p \leq 0.02$). Difference of A_{out}A between patients with CF and control patients became larger with each following segmental generation. A_{in}A and A_{WT}-ratio did not differentiate significantly between CF and control group on inspiratory CT in each segmental generation (Figure 5C, D). More detail on the differences and significance values by each segmental generation can be found in Appendix Table E1a-d.

Quantitatively, bronchiectasis has an upper lobe predominance. Appendix Table E2a-d shows the detailed results of the mixed-effect model regarding the different lung lobes. In both CF and control patients, A_{out}A-, A_{WT}A-, and A_{WT}-ratio was significantly higher in RUL compared to all other lobes ($p<0.001$). In CF patients, A_{out}A- and A_{WT}A-ratio was significantly higher in LUL compared to right middle lobe (RML), right lower lobe (RLL) and left lower lobe (LLL) ($p<0.001$). LLL was significant lower than all other lobes for A_{out}A-, A_{WT}A-, and A_{WT}-ratio in CF patients ($p \leq 0.004$).

Reproducibility of airway measurements

For the inter-observer variability, ICC for AA dimensions were as follows: Inner airway (0.69), outer airway (0.72), wall (0.66) and vessel diameter (0.69). For the intra-observer variability, ICC for the different dimensions were as follows: Inner airway (0.70), outer airway (0.74), wall (0.71) and vessel diameter (0.79).

DISCUSSIONS

To our knowledge, this is the first study measuring all visible AA-pairs perpendicular to airway centerlines in maximal inspiration and expiration CTs of CF patients and control patients. Major differences were observed in number of visible AA-pairs and in AA-ratios between inspiratory and expiratory CTs and between CF patients and control patients.

Our study showed that end-inspiratory CTs were most sensitive to detect structural airway disease. Overall 2 to 3 times more AA-pairs were detected on end-inspiratory CTs of a patient with CF than on CTs of controls. Difference in number of visible AA-pairs became more striking with each generation. Beyond the 7th segmental generation, AA-

pairs were still visible in CF but not in control patients. Our study confirms that number visible of AA-pairs could be used as a surrogate outcome for bronchiectasis.[26,30–32] Nevertheless, it is important to keep in mind that the number of visible airways can be affected by patient size as well as inspiration level and scan protocol. In this study, patient size did not influence the number of AA-pairs counted and scan protocol did not play a role as inspiratory CTs of both CF and control patients were scanned using the same scanner and protocols.

$A_{out}A$ and $A_{WT}A$-ratios on inspiratory CTs progressively increased with segmental generation in CF subjects, while they remained relatively constant over generations in control subjects. Increased AA-ratios and higher number of visible peripheral airways suggests more structural abnormalities due to CF lung disease in the more peripheral airways compared to central airways. These are findings that to our knowledge have not been established by quantitative assessment previously and strongly support the importance of peripheral airways in CF lung disease.[32–35] An increase in visible AA-pairs or in AA-ratios might, however, easily be missed on visual routine CT.

AA-ratio based on outer airway diameter was more sensitive to detect BE compared to inner diameter as demonstrated by the higher AUC in the ROC curve. Furthermore, the $A_{out}A$-ratio was less influenced by the inspiration level compared the $A_{in}A$-ratio. Lastly, $A_{in}A$-ratio could not differentiate between CF and controls within all segmental generations. This can be explained by simultaneous airway wall thickening due to inflammation and mucus impaction, leading to decreased $A_{in}A$-ratio. This finding supports previous[11] and recently published guidelines[12,26] that rely on outer airway diameter for diagnosis of bronchiectasis on CT. A lower AA-ratio was reported in children by Kapur et al,[5] but this was based on inner luminal diameter instead of the outer diameter. In our dataset, an AA-ratio based on outer diameter of 1.1 was optimal to differentiate between normal and abnormal. However $A_{out}A$-ratios above 1.1 were found in the control group as well.

Number of AA-pairs visible and AA-ratios between the groups were only significantly different in end-inspiration and not in end-expiration CT. Additionally AWT values were higher in end-expiratory CTs, possibly due to folding of the airways in expiration.[33] Thus, in case an 'inspiratory' CT is performed below TLC, number of bronchiectatic airways will be underestimated. On the other hand AWT increased and became more apparent in end-expiratory. Hence, when lung volume is below TLC during CT acquisition, AWT could be overestimated. These findings strongly support the need for volume control during acquisition to allow consistent, sensitive, and objective detection of BE and AWT.[7,25]

In control patients the AA-ratio did not change significantly with age as also reported in previous studies.[5,21] In CF a trend was observed of an increasing $A_{out}A$-ratio with age, which can be due to disease progression. Nevertheless, we dealt with a small sample size, thus, a larger study population is needed to investigate changes of the AA-ratios by age.

Higher A_{out}A-ratios were observed in the upper lobes, especially the RUL. This observation is in concordance with previous publications observing more severe abnormalities and inflammation in the RUL of CF patients.[13,36,37] Hence, bronchiectasis detection most likely has to take lobes into account. Intra-subject differences in airway dimensions between lung lobes have previously been reported in COPD patients,[23,24,38] and control subjects.[22]
Our study has several limitations. First, the control patients were not healthy as they were referred for chest CT through the pediatric respiratory department. Even though all CTs were reported to be normal by two independent radiologists, we cannot exclude that subtle changes in AA dimensions could have influenced our comparisons. Secondly, scan and reconstruction parameters were not identical in all CTs of this retrospective study. In theory this could have caused a small bias, but we believe this the bias to be small at most since there was no automated post-processing involved in detecting the airway and artery dimensions, but instead they were measured manually with an ellipse tool. However, it is unlikely that these limitations can explain the large differences found between CF and control patients. Importantly, a constant AA-ratio was observed for each airway generation in control patients while this ratio steadily increased in CF. Moreover, the CF-CT scored almost no abnormalities in control subjects, except for some trapped air which can be physiologic in healthy patients.[39] A second limitation is that we only studied a relatively small population. This was due to the time needed to manually score all 48 inspiratory and expiratory CTs (average of 15 hours per scan). However, a large number of AA-pairs could be measured to test our research questions. Thirdly, radiation dose for expiratory CTs was lowered after 2012, in 5 out of 12 control patients. This reduced the sensitivity of measurements and could have reduced the number of visible AA-pairs, leading to overestimation of the effect of inspiration level in control patients. Finally, reproducibility of single AA measurements was hard to assess as repeated manual measurements were unlikely to be measured at identical anatomical locations, causing variability. However ICC's showed good inter- and intra-observer agreements.
In conclusion, the results of this study showed greater structural lung changes with each airway generation on chest CTs of children with CF. In children with CF, more airways were visible on CT due to the increase of AA-ratios in the peripheral part of the lungs. For diagnosis and quantification of BE outer airway diameter should be used, as this is a better differentiator between CF and control patients. Our findings strongly support the need for volume standardization in chest CTs of children 6 years and above, for objective and sensitive evaluation of airway dimensions.[7] To generate reference values for airway dimensions in children, a larger study population of normal chest CTs acquired at TLC is needed. Automatic methods to quantify bronchiectasis are in development to support clinicians' diagnosis and reduce the time of annotations.[40]

REFERENCES

1. Tepper LA, Caudri D, Utens EMWJ, van der Wiel EC, Quittner AL, Tiddens HAWM. Tracking CF disease progression with CT and respiratory symptoms in a cohort of children aged 6-19 years. Pediatric Pulmonology. 2014;1189(February):1182–1189.
2. Tiddens HAWM, Stick SM, Davis S. Multi-modality monitoring of cystic fibrosis lung disease: The role of chest computed tomography. Paediatric Respiratory Reviews. 2014;15(1):92–97.
3. Loeve M, van Hal PTW, Robinson P, de Jong PA, Lequin MH, Hop WC, Williams TJ, Nossent GD, Tiddens HAWM. The spectrum of structural abnormalities on CT scans from patients with CF with severe advanced lung disease. Thorax. 2009;64(10):876–882.
4. Bortoluzzi C-F, Volpi S, D'Orazio C, Tiddens HAWM, Loeve M, Tridello G, Assael BM. Bronchiectases at early chest computed tomography in children with cystic fibrosis are associated with increased risk of subsequent pulmonary exacerbations and chronic pseudomonas infection. Journal of Cystic Fibrosis. 2014;13(5):564–571.
5. Kapur N, Masel JP, Watson D, Masters IB, Chang AB. Bronchoarterial ratio on high-resolution CT scan of the chest in children without pulmonary pathology: Need to redefine bronchial dilatation. Chest. 2011;139(6):1445–1450.
6. Newell JD. Bronchiectasis. In: Contemporary Medical imaging. CT of the. 2008. p. 213–235.
7. Mott LS, Graniel KG, Park J, De Klerk NH, Sly PD, Murray CP, Tiddens HAWM, Stick SM. Assessment of early bronchiectasis in young children with cystic fibrosis is dependent on lung volume. Chest. 2013;144(4):1193–1198.
8. Brody AS, Kosorok MR, Li Z, Broderick LS, Foster JL, Laxova A, Bandla H, Farrell PM. Reproducibility of a scoring system for computed tomography scanning in cystic fibrosis. Journal of thoracic imaging. 2006;21(1):14–21.
9. Gaillard EA, Carty H, Heaf D, Smyth RL. Reversible bronchial dilatation in children: comparison of serial high-resolution computer tomography scans of the lungs. European Journal of Radiology. 2003;47(3):215–220.
10. Hansell DM, Bankier AA, MacMahon H, McLoud TC, Müller NL, Remy J. Fleischner Society: glossary of terms for thoracic imaging. Radiology. 2008;246(3):697–722.
11. Hansell DM. Thin-section CT of the lungs: the Hinterland of normal. Radiology. 2010;256(3):695–711.
12. Milliron B, Henry TS, Veeraraghavan S, Little BP. Bronchiectasis: Mechanisms and imaging clues of associated common and uncommon diseases. RadioGraphics. 2015;35:1011–1030.
13. Davis SD, Fordham LA, Brody AS, Noah TL, Retsch-Bogart GZ, Qaqish BF, Yankaskas BC, Johnson RC, Leigh MW. Computed tomography reflects lower airway inflammation and tracks changes in early cystic fibrosis. American Journal of Respiratory and Critical Care Medicine. 2007;175(9):943–950.
14. Sly PD, Gangell CL, Chen L, Ware RS, Ranganathan S, Mott LS, Murray CP, Stick SM. Risk factors for bronchiectasis in children with cystic fibrosis. The New England journal of medicine. 2013;368(21):1963–70.
15. Naidich DP, Webb WR, Muller NL, Vlahos I, Krinsky GA. Chapter 5. Airways. In: Computed Tomography and Magnetic Resonance of the thorax. Lippincott Williams & Wilkins; 2007. p. 453–556.

16. Quint LE, Whyte RI, Kazerooni EA, Martinez FJ, Cascade PN, Lynch JP, Orringer MB, Brunsting LA, Deeb GM. Stenosis of the central airways: evaluation by using helical CT with multiplanar reconstructions. Radiology. 1995;194(3):871–7.

17. Remy-Jardin M, Remy J, Deschildre F, Artaud D, Ramon P, Edme JL. Obstructive lesions of the central airways: evaluation by using spiral CT with multiplanar and three-dimensional reformations. European radiology. 1996;6(6):807–16.

18. Sundarakumar DK, Bhalla AS, Sharma R, Hari S, Guleria R, Khilnani GC. Multidetector CT evaluation of central airways stenoses: Comparison of virtual bronchoscopy, minimal-intensity projection, and multiplanar reformatted images. The Indian journal of radiology & imaging. 2011;21(3):191–4.

19. Webb WR, Muller NL, Naidich DP. Technical aspects of High-Resolution CT. In: High-Resolution CT of the lung. 5th ed. Kluwer Wolters; 2014. p. 2–47.

20. Loeve M, Lequin MH, de Bruijne M, Hartmann IJC, Gerbrands K, van Straten M, Hop WCJ, Tiddens H a WM. Cystic fibrosis: are volumetric ultra-low-dose expiratory CT scans sufficient for monitoring related lung disease? Radiology. 2009;253(1):223–229.

21. De Jong PA, Nakano Y, Hop WC, Long FR, Coxson HO, Paré PD, Tiddens H a. Changes in airway dimensions on computed tomography scans of children with cystic fibrosis. American Journal of Respiratory and Critical Care Medicine. 2005;172(2):218–224.

22. Petersen J, Wille MMW, Rakêt LL, Feragen A, Pedersen JH, Nielsen M, Dirksen A, De Bruijne M. Effect of inspiration on airway dimensions measured in maximal inspiration CT images of subjects without airflow limitation. European Radiology. 2014;24(9):2319–2325.

23. Bakker ME, Stolk J, Reiber JHC, Stoel BC. Influence of inspiration level on bronchial lumen measurements with computed tomography. Respiratory Medicine. 2012;106(5):677–686.

24. Kambara K, Shimizu K, Makita H, Hasegawa M, Nagai K, Konno S, Nishimura M. Effect of lung volume on airway luminal area assessed by computed tomography in chronic obstructive pulmonary disease. PLoS ONE. 2014;9(2):e90040.

25. Salamon E, Lever S, Kuo W, Ciet P, Tiddens HAWM. Spirometer guided chest imaging in children: It is worth the effort! Pediatric Pulmonology. 2016;56(September 2015):48–56.

26. Kuo W, Andrinopoulou E-R, Perez-Rovira A, Ozturk H, de Bruijne M, Tiddens HAWM. Objective airway artery dimensions compared to CT scoring methods assessing structural cystic fibrosis lung disease. Journal of Cystic Fibrosis. 2016;16(1):116–123.

27. Netter FH. Atlas of human anatomy. 6th ed. Saunders Elsevier; 2014. 197-198 p.

28. Portney L, Watkins M. Foundations of clinical research: applications to practice. Prentice Hall; 2000. p. 560–567.

29. R Foundation for statistical Computing. R Development Core Team. R: A Language and Environment for Statistical Computing. Vienna; 2005.

30. Kurashima K, Takaku Y, Hoshi T, Kanauchi T, Nakamoto K, Takayanagi N, Yanagisawa T, Sugita Y, Kawabata Y. Lobe-based computed tomography assessment of airway diameter , airway or vessel number , and emphysema extent in relation to the clinical outcomes of COPD. International journal of chronic obstructive pulmonary disease. 2015;10:1027–1033.

31. Smith BM, Hoffman EA, Rabinowitz D, Bleecker E, Christenson S, Couper D, Donohue KM, Han MK, Hansel NN, Kanner RE, et al. Comparison of spatially matched airways reveals thinner airway walls in COPD. The Multi-Ethnic Study of Atherosclerosis (MESA) COPD Study and the Subpopulations and Intermediate Outcomes in COPD Study (SPIROMICS). Thorax. 2014;69(11):987–96.

32. DeBoer EM, Swiercz W, Heltshe SL, Anthony MM, Szefler P, Klein R, Strain J, Brody AS, Sagel SD. Automated ct scan scores of bronchiectasis and air trapping in cystic fibrosis. Chest. 2014;145(3):593–603.

33. Tiddens HAWM, Donaldson SH, Rosenfeld M, Paré PD. Cystic fibrosis lung disease starts in the small airways: Can we treat it more effectively? Pediatric Pulmonology. 2010;45(2):107–117.

34. Ratjen F. Cystic Fibrosis: The role of the small airways. Journal of Aerosol Medicine and Pulmonary Drug Delivery. 2012;25(5):261–264.

35. Boon M, Verleden SE, Bosch B, Lammertyn EJ, McDonough JE, Mai C, Verschakelen J, Kemner-Van De Corput M, Tiddens HAW, Proesmans M, et al. Morphometric analysis of explant lungs in cystic fibrosis. American Journal of Respiratory and Critical Care Medicine. 2016;193(5):516–526.

36. Bos AC, van Holsbeke C, de Backer JW, van Westreenen M, Janssens HM, Vos WG, Tiddens H a. WM. Patient-specific modeling of regional antibiotic concentration levels in airways of patients with cystic fibrosis: are we dosing high enough? Plos One. 2015;10(3):e0118454.

37. Meyer KC, Sharma A, Assistance T, Peterson K, Brennan L. Regional variability of lung inflammation in cystic fibrosis. Am J Respir Crit Care Med. 1997;156:1536–1540.

38. Diaz AA, Come CE, Ross JC, San José Estépar R, Han MK, Loring SH, Silverman EK, Washko GR. Association between airway caliber changes with lung inflation and emphysema assessed by volumetric CT scan in subjects with COPD. Chest. 2012;141(3):736–744.

39. Silva M, Nemec SF, Dufresne V, Occhipinti M, Heidinger BH, Chamberlain R, Bankier AA. Normal spectrum of pulmonary parametric response map to differentiate lung collapsibility: distribution of densitometric classifications in healthy adult volunteers. European radiology. 2015.

40. Perez-Rovira A, Kuo W, Petersen J, Tiddens HAWM, de Bruijne M. Automatic airway–artery analysis on lung CT to quantify airway wall thickening and bronchiectasis. Medical Physics. 2016;43(10):5736–5744.

APPENDIX

MATERIAL AND METHODS

Appendix E1

CF subjects: Patients with CF were monitored routinely with a biennial chest CT. Since 2007, a protocol for spirometer guided inspiratory and expiratory chest CT was introduced for all chest CTs to optimize and standardize lung volume and reduce movement artefacts. Consequently all CTs of CF patients were spirometer guided [1].
Disease control subjects: Indication for CTs in this control group can be found in Table 1.

Pulmonary function test

Routine pulmonary function tests (PFT) were performed in all CF patients and controls. For both groups PFT closest to, or on the same day, of CT acquisition was used for analysis. The following parameters were included and expressed as Z-scores: FEV_1, FVC, forced expiratory flows between 25 and 75% of expiratory VC (FEF_{25-75}) [2]. Age at the day of the CT was used to define patient characteristics. For height and weight we used values as recorded at the time of PFT.

APPENDIX TABLE E1a. The following tables describes the mean difference and p-value as depicted by the mixed-effect model for A_{out}A-ratio in each generation as plotted in the figure 4a. * indicates significant difference.

A_{out}A-ratio	1	2	3	4	5	6	7	8	9
Control insp vs CF insp	(p=0.53)	0.08 (p=0.019)*	0.13 (p<0.001)*	0.13 (p<0.001)*	0.17 (p<0.001)*	0.19 (p=0.004)*	(p=0.15)		
Control insp vs control exp	-0.08 (p<0.001)*	-0.07 (p<0.001)*	-0.08 (p<0.001)*	-0.08 (p<0.001)*	(p=0.15)	(p=0.89)			
Control insp vs CF exp	(p=0.71)	0.08 (p=0.022)*	(p=0.09)	(p=0.21)	(p=0.17)	(p=0.06)	(p=0.34)		
Control exp vs CF exp	(p=0.06)	0.15 (p<0.001)*	0.15 (p<0.001)*	0.13 (p=0.003)*	0.14 (p=0.036)*	(p=0.30)			
CF insp vs CF exp	(p=0.16)	(p=0.98)	-0.06 (p<0.001)*	-0.08 (p<0.001)*	-0.10 (p<0.001)*	(p=0.13)	(p=0.54)	(p=0.50)	(p=0.59)

APPENDIX TABLE E1b. The following tables describes the mean difference and p-value as depicted by the mixed-effect model for A_{WT}A-ratio in each generation as plotted in the figure 4b. * indicates significant difference.

A_{WT}A-ratio	1	2	3	4	5	6	7	8	9
Control insp vs CF insp	0.05 (p=0.037)*	0.06 (p=0.004)*	0.09 (p<0.001)*	0.09 (p=0.001)*	0.12 (p<0.001)*	0.12 (p=0.004)*	(p=0.10)		
Control insp vs control exp	0.06 (p<0.001)*	0.06 (p<0.001)*	0.05 (p<0.001)*	0.06 (p<0.001)*	0.07 (p=0.049)*	(p=0.15)			
Control insp vs CF exp	0.15 (p<0.001)*	0.17 (p<0.001)*	0.18 (p<0.001)*	0.17 (p<0.001)*	0.20 (p<0.001)*	0.23 (p<0.001)*	0.22 (p=0.006)*		
Control exp vs CF exp	0.08 (p=0.002)*	0.12 (p<0.001)*	0.13 (p<0.001)*	0.12 (p<0.001)*	0.13 (p=0.003)*	(p=0.37)			
CF insp vs CF exp	0.10 (p<0.001)*	0.12 (p<0.001)*	0.09 (p<0.001)*	0.08 (p<0.001)*	0.08 (p<0.001)*	0.11 (p<0.001)*	0.11 (p=0.011)*	(p=0.26)	(p=0.58)

APPENDIX TABLE E1c. The following tables describes the mean difference and p-value as depicted by the mixed-effect model for A_{in}A-ratio in each generation as plotted in the figure 4c. * indicates significant difference.

A_{in}A-ratio	1	2	3	4	5	6	7	8	9
Control insp vs CF insp	(p=0.28)	(p=0.38)	(p=0.09)	(p=0.09)	(p=0.08)	(p=0.09)	(p=0.38)		
Control insp vs control exp	-0.14 (p<0.001)*	-0.13 (p<0.001)*	-0.13 (p<0.001)*	-0.13 (p<0.001)*	-0.14 (p<0.001)*	(p=0.08)			
Control insp vs CF exp	-0.16 (p<0.001)*	-0.09 (p=0.002)*	-0.11 (p<0.001)*	-0.12 (p<0.001)*	-0.13 (p<0.001)*	-0.09 (p=0.042)*	(p=0.48)		
Control exp vs CF exp	(p=0.58)	(p=0.28)	(p=0.45)	(p=0.72)	(p=0.85)	(p=0.50)			
CF insp vs CF exp	-0.13 (p<0.001)*	-0.12 (p<0.001)*	-0.16 (p<0.001)*	-0.17 (p<0.001)*	-0.18 (p<0.001)*	-0.16 (p<0.001)*	-0.13 (p=0.012)*	-0.20 (p=0.035)*	(p=0.21)

APPENDIX TABLE E1d. The following tables describes the mean difference and p-value as depicted by the mixed-effect model for A_{WT}-ratio in each generation as plotted in the figure 4d. * indicates significant difference.

A_{WT}-ratio	1	2	3	4	5	6	7	8	9
Control insp vs CF insp	(p=0.06)	(p=0.53)	(p=0.36)	(p=0.33)	(p=0.20)	(p=0.37)	(p=0.51)		
Control insp vs control exp	0.10 (p<0.001)*	0.09 (p<0.001)*	0.09 (p<0.001)*	0.10 (p<0.001)*	0.11 (p<0.001)*	0.15 (p<0.001)*			
Control insp vs CF exp	0.15 (p<0.001)*	0.11 (p<0.001)*	0.13 (p<0.001)*	0.13 (p<0.001)*	0.09 (p<0.001)*	0.13 (p<0.001)*	0.10 (p=0.006)*		
Control exp vs CF exp	0.05 (p=0.021)*	(p=0.19)	(p=0.07)	(p=0.12)	(p=0.20)	(p=0.67)			
CF insp vs CF exp	0.11 (p<0.001)*	0.11 (p<0.001)*	0.11 (p<0.001)*	0.11 (p<0.001)*	0.12 (p<0.001)*	0.11 (p<0.001)*	0.08 (p<0.001)*	0.11 (p<0.001)*	(p=0.11)

APPENDIX TABLE E2a. The following tables describes the mean difference and p-value for A_{out}A-ratio in each lobe computed with the mixed-effect model. * indicates significant difference.

A_{out}A-ratio	RUL		RML		RLL		LUL		LING	
	CF	Control	CF	Control	CF	Control	CF	Control	CF	Control
RUL										
RML	-0.11 (p<0.001)*	-0.02 (p=0.048)*								
RLL	-0.10 (p<0.001)*	-0.03 (p<0.001)*	(p=0.36)	(p=0.24)						
LUL	-0.06 (p<0.001)*	-0.03 (p<0.001)*	0.05 (p<0.001)*	(p=0.30)	0.04 (p<0.001)*	(p=0.97)				
LING	-0.09 (p<0.001)*	-0.03 (p=0.039)*	(p=0.28)	(p=0.65)	(p=0.58)	(p=0.71)	(p=0.20)	(p=0.72)		
LLL	-0.15 (p<0.001)*	-0.04 (p<0.001)*	-0.03 (p=0.02)*	(p=0.13)	-0.05 (p<0.001)*	(p=0.57)	-0.08 (p<0.001)*	(p=0.67)	-0.06 (p=0.004)*	(p=0.50)

APPENDIX TABLE E2b. The following tables describes the mean difference and p-value for A_{WT}A-ratio in each lobe computed with the mixed-effect model. * indicates significant difference.

A_{WT}A-ratio	RUL		RML		RLL		LUL		LING	
	CF	Control	CF	Control	CF	Control	CF	Control	CF	Control
RUL										
RML	-0.08 (p<0.001)*	-0.02 (p=0.005)*								
RLL	-0.08 (p<0.001)*	-0.03 (p<0.001)*	(p=0.67)	(p=0.44)						
LUL	-0.05 (p<0.001)*	-0.02 (p<0.006)*	0.03 (p=0.006)*	(p=0.77)	0.03 (p<0.001)*	(p=0.22)				
LING	-0.07 (p<0.001)*	-0.02 (p=0.024)*	(p=0.56)	(p=0.94)	(p=0.37)	(p=0.62)	(p=0.16)	(p=0.75)		
LLL	-0.12 (p<0.001)*	-0.03 (p<0.001)*	-0.04 (p<0.001)*	(p=0.23)	-0.04 (p<0.001)*	(p=0.52)	-0.07 (p<0.001)*	(p=0.09)	-0.05 (p<0.001)*	(p=0.39)

APPENDIX TABLE E2c. The following tables describes the mean difference and p-value for A_{in}A-ratio in each lobe computed with the mixed-effect model. * indicates significant difference.

AinA-ratio	RUL		RML		RLL		LUL		LING	
	CF	Control	CF	Control	CF	Control	CF	Control	CF	Control
RUL										
RML	-0.3 (p<0.001)*	(p=0.87)								
RLL	-0.02 (p=0.017)*	(p=0.41)	(p=0.08)	(p=0.44)						
LUL	(p=0.16)	(p=0.07)	0.02 (p=0.03)*	(p=0.11)	(p=0.48)	(p=0.23)				
LING	(p=0.18)	(p=0.64)	(p=0.31)	(p=0.60)	(p=0.90)	(p=0.99)	(p=0.61)	(p=0.46)		
LLL	-0.02 (p=0.002)*	(p=0.39)	(p=0.29)	(p=0.42)	(p=0.37)	(p=0.93)	(p=0.14)	(p=0.28)	(p=0.73)	(p=0.97)

APPENDIX TABLE E2d. The following tables describes the mean difference and p-value for A_{WT}-ratio in each lobe computed with the mixed-effect model. * indicates significant difference.

A_{WT}-ratio	RUL		RML		RLL		LUL		LING	
	CF	Control	CF	Control	CF	Control	CF	Control	CF	Control
RUL										
RML	-0.01 (p=0.005)*	(p=0.11)								
RLL	-0.02 (p<0.001)*	-0.01 (p=0.049)*	(p=0.22)	(p=0.82)						
LUL	-0.01 (p=0.007)*	(p=0.83)	(p=0.54)	(p=0.20)	0.01 (p=0.018)*	(p=0.16)				
LING	-0.02 (p=0.013)*	(p=0.33)	(p=0.68)	(p=0.80)	(p=0.68)	(p=0.91)	(p=0.37)	(p=0.44)		
LLL	-0.03 (p<0.001)*	-0.01 (p=0.024)*	-0.02 (p<0.001)*	(p=0.91)	-0.02 (p<0.001)*	(p=0.64)	-0.03 (p<0.001)*	(p=0.09)	-0.02 (p=0.008)*	(p=0.71)

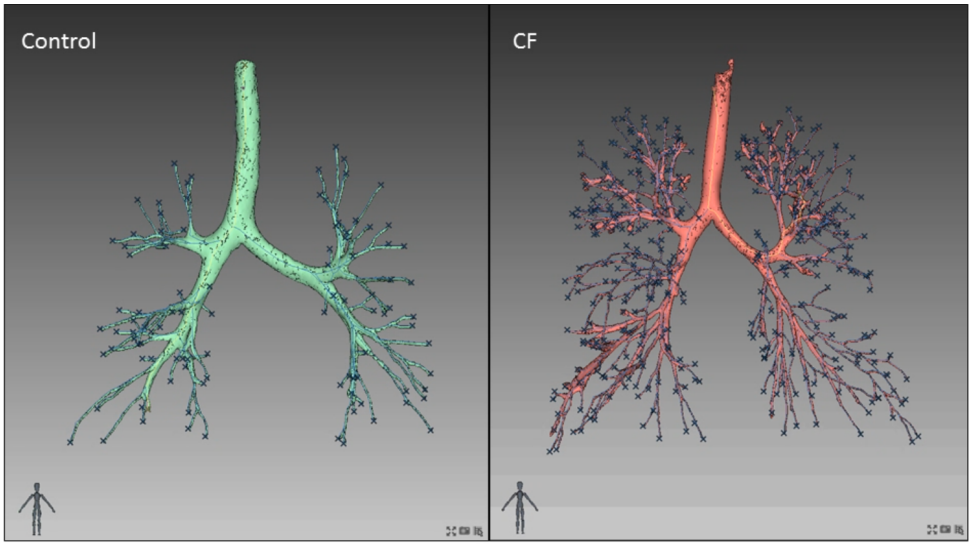

APPENDIX VIDEO E1. Screen-shot of the video with rotating 3D segmentations. The full video can be found with the published article online: https://link.springer.com/article/10.1007%2Fs00330-017-4819-7

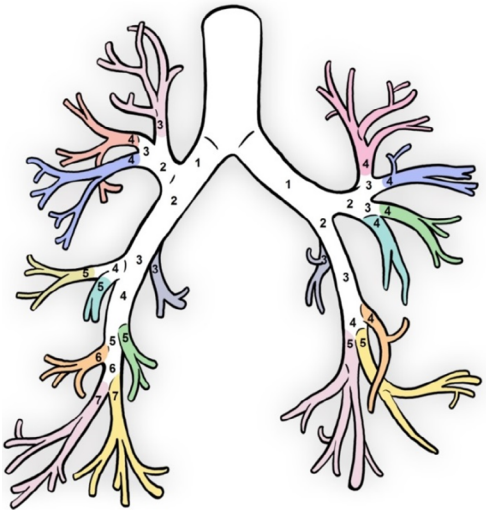

APPENDIX FIGURE E2. Anatomy of the airways. The segmental branches are shown in the different colors and the numbering stands for the airway generation. Each segmental branch starts with a different generation, eg generation 3-4 in the upper segmental branches whereas it starts at generation 4-7 in the lower segmental branches (Artist: K. Rubenis).

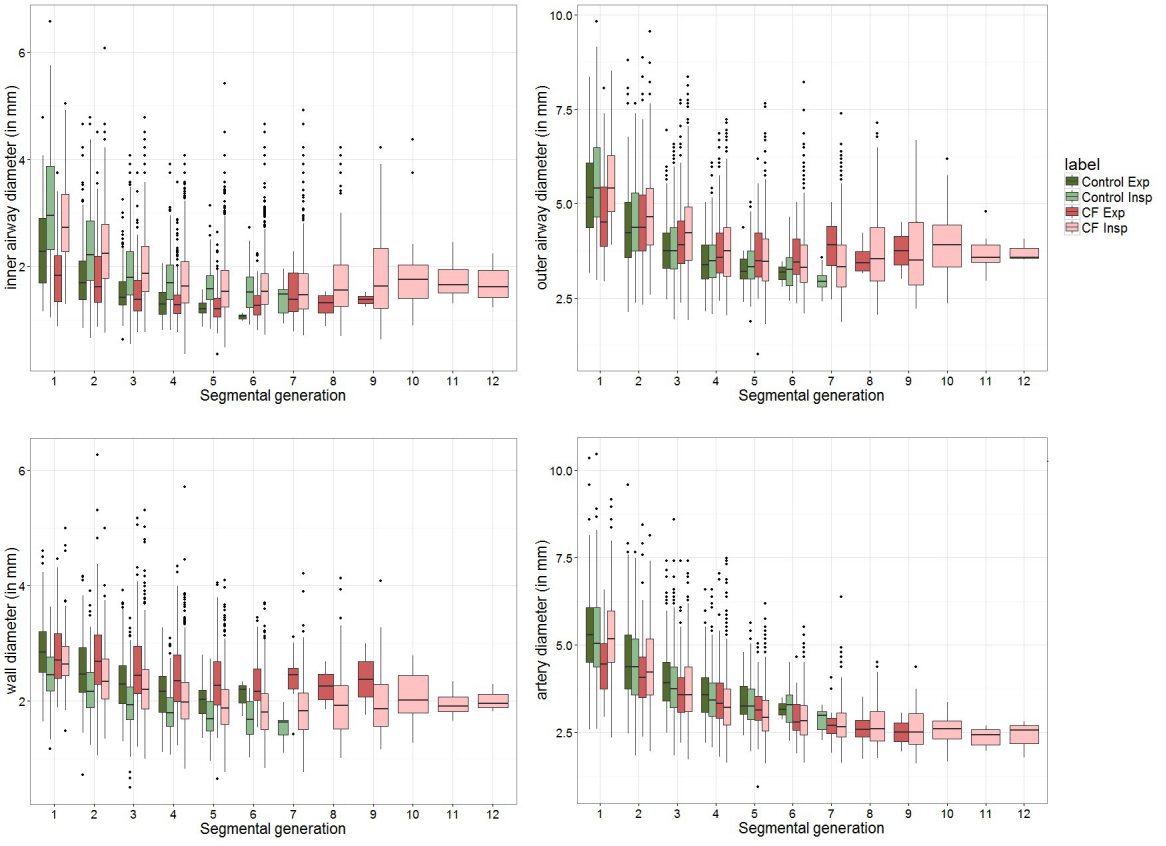

APPENDIX FIGURE E3. Boxplots of the inner and outer airway diameter (top graphs) and the airway wall and artery diameter (bottom graphs. The diameters are shown for the control group (green) and the CF group (red) for each segmental generation. Inspiratory scans are shown in light colors and expiratory scans in dark colors. Each box shows median (horizontal line), interquartile range (solid box), 1.5*interquartile range (whiskers) and outliers (points).

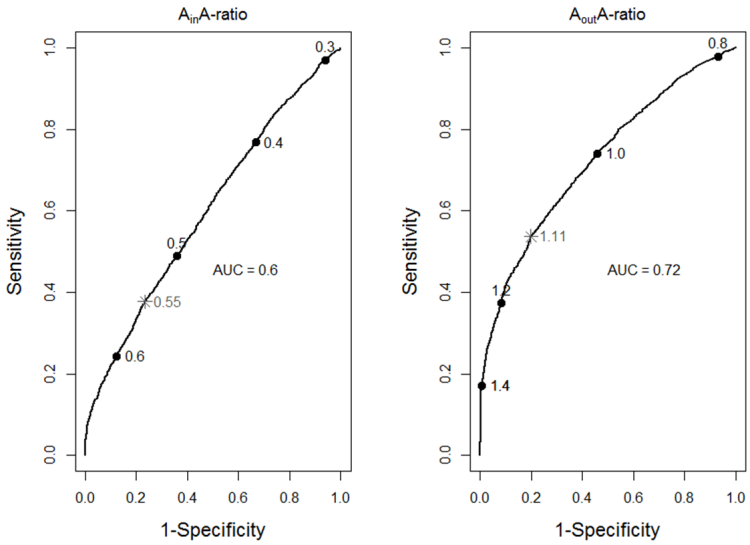

Appendix Figure E4. ROC curves to distinguish between patients with CF and control subjects show that A_{out}A-ratio (right) had better detection capability than A_{in}A-ratio (left). The gray stars indicate the AA-ratio with optimal sensitivity + specificity.

REFERENCES

1. Salamon ER, Lever S, Kuo W, Ciet P, Tiddens HAWM. Spirometer guided chest imaging in children: It is worth the effort. Pediatr Pulmonol. 2015;in Press(April):1–9.
2. Quanjer PH, Stanojevic S, Cole TJ, Baur X, Hall GL, Culver BH, et al. Multi-ethnic reference values for spirometry for the 3-95-yr age range: The global lung function 2012 equations. Eur Respir J. 2012;40(6):1324–43.

CHAPTER 5

QUANTITATIVE ASSESSMENT OF AIRWAY DIMENSIONS IN YOUNG CHILDREN WITH CYSTIC FIBROSIS LUNG DISEASE USING CHEST COMPUTED TOMOGRAPHY

Wieying Kuo, Thomas Soffers, Eleni-Rosalina Andrinopoulou, Tim Rosenow, Sarath Ranganathan, Lidija Turkovic, Stephen M. Stick, Harm A.W.M. Tiddens, on behalf of AREST CF

Pediatric Pulmonology.
2017; in press

ABSTRACT

Objective

To evaluate lung disease progression using airway and artery (AA) dimensions on chest CT over 2-year interval in young CF patients longitudinally and compare to disease controls cross-sectionally.

Methods

Retrospective analysis of pressure controlled end-inspiratory CTs: 12 routine baseline (CT_1) and follow up (CT_2) from AREST CF cohort; 12 disease controls with normal CT. All visible AA-pairs were measured perpendicular to the airway axis. Inner and outer airway diameters and wall (outer - -inner radius) thickness were divided by adjacent arteries to compute A_{in}A-, A_{out}A-, and A_{WT}A-ratios, respectively. Differences between CF and control data were assessed using mixed effects models predicting AA-ratios per segmental generation (SG). Power calculations were performed with 80% power and α=0.05.

Results

CF: median age CT_1 2 years; CT_2 3.9 years, 5 males. Controls: median age 2.9 years, 10 males. Total of 4798 AA-pairs measured. Cross-sectionally: A_{in}A-ratio showed no difference between controls and CF CT_1 or CT_2. A_{out}A-ratio was significantly higher in CF CT_1 (SG 2-4) and CT_2 (SG 2-5) compared to controls. A_{WT}A-ratio was increased for CF CT_1 (SG 1-5) and CT_2 (SG 2-6) compared to controls. CF longitudinally: A_{in}A-ratio was significantly higher at CT_2 compared to CT_1. Increase in A_{out}A-ratio at CT_2 compared to CT_1 was visible in SG≥4. Sample sizes of 21 and 58 would be necessary for 50 and 30% A_{out}A-ratio reductions, respectively, between CF CT_2 and controls.

Conclusion

AA-ratio differences were present in young CF patients relative to disease controls. A_{out}A-ratio as an objective parameter for bronchiectasis could reduce sample sizes for clinical trials.

INTRODUCTION

Most patients with cystic fibrosis (CF), develop progressive structural lung disease (SLD) early in life.[1] SLD on chest computed tomography (CT) has been observed as early as 3 months of age, and in young asymptomatic patients with CF.[2,3] Early detection of SLD is considered important for clinical studies and for treatment guidance to prevent irreversible SLD or progression.[4–6] Therefore, sensitive outcome measures are needed to monitor lung disease in young and non-cooperative patients with CF.[7]

Chest CT is currently the most sensitive imaging modality to assess SLD. The most important structural change related to CF is bronchiectasis, usually defined as an airway artery (AA)-ratio greater than one. Another important change is airway wall thickening.[8–10] Both components have been objectively quantified on chest CT by measuring airway and adjacent artery dimensions perpendicular to the airway axis[11] and showed good correlations with CF-CT and PRAGMA-CF scoring systems.[12] Using this AA-method in children with CF aged 6 years and older, major differences in AA-ratio and airway wall thickness were observed in our previous study,[11] particularly in the small airways. In addition, to diagnose bronchiectasis the outer airway diameter was more reliable than the inner airway diameter[11] and the sensitivity of inspiratory scans to diagnose bronchiectasis was better compared to expiratory CTs.[11] Airway wall thickness, however, could be detected on both inspiratory and expiratory CTs. Lastly, the number of AA-pairs was shown to be more than doubled in patients with CF relative to controls.[11] Hence, the AA-method seems to be a promising, sensitive quantitative method to detect structural airways changes that could be used as an outcome measure in clinical intervention trials. A sensitive method to detect changes is required in particular, for children below 6 years old in whom CT changes can be subtle and for whom interventions to prevent development and/or progression of disease are highly desirable. To gain further insight regarding this approach, AA-ratios on CTs were measured in a small group of pre-school children with CF and control subjects showing promising results.[3,13] Limitations of previous studies were that measurements were executed on limited number of axial slices introducing a projection error, and only a small number of detectable AA-pairs was analyzed.

The aims of this study were to objectively assess early airway changes on chest CTs of young CF patients using the same AA-method as used for children above 6 years old,[11,12] and to estimate the sensitivity of the AA-method which could be used as a sensitive outcome measure to detect structural airway changes in CF, relative to disease controls. We hypothesized that the AA-method is sensitive to detect changes in airway dimensions of small airways and that the AA-ratio is greater in young children with CF compared to disease controls.

METHODS

Study population

Chest CTs of 12 randomly selected patients with CF from the Australian Respiratory Early Surveillance Team for Cystic Fibrosis (AREST CF) cohort with two CTs 2 years apart were analyzed retrospectively. Additionally chest CTs of 12 disease control patients were included for cross-sectional comparisons to CF. All patients were treated at the Princess Margaret Hospital, Perth, Australia.

CF subjects: Patients with CF diagnosed through newborn screening were monitored routinely with annual chest CT according to AREST CF protocol.[14] Inclusion criteria were: diagnosis of CF; availability of two longitudinal pressure controlled inspiratory chest CTs; ages between 0 and 6 years old; absence of exacerbation requiring a course of intravenous antibiotics, meaning that all children were free of acute symptoms at the time of the CT scan and in the month prior to scanning. A course or maintenance with oral antibiotics for milder pulmonary symptoms were not considered an exclusion criteria for executing routine chest CT scans. In this cohort, children less than 2 years old were routinely prescribed prophylactic oral antibiotics. .

Disease control subjects: Control CTs were selected when meeting the following criteria; pressure controlled inspiratory chest CT scan; age between 0 and 6 years old; clinical indication for chest CT other than CF; CT acquired for a variety of clinical indications (Table 1) but assessed as normal with no lung abnormalities by experienced pediatric radiologist (CM, 15 years of experience). Single scans from the cross-sectional control population matched the paired CF scans with regard to average age during acquisition.

TABLE 1. clinical diagnosis and indications for chest CT of the disease control group.

Controls Clinical diagnosis	Reason for CT	No of subjects
Recurrent respiratory infections/ chronic cough/ persistent tachypnoea	Bronchiectasis? Tracheobronchomalacie?	10
Developmental delay	Aspiration?	2

CT scanning

All CTs of CF and disease control subjects were made supine, with pressure control under general anesthesia. To reduce atelectasis, alveolar recruitment maneuvers were performed consisting of 10 consecutive slow breath with inspirations pressure of 40 cm H_2O followed by a breath hold with end-inspiration pressure of 25 cm H_2O. Volumetric end-inspiratory acquisitions were obtained using a Philips Brilliance 64 scanner prior to 2012 and Siemens Definition Flash scanner from 2012 (for additional scanner information see Appendix Table E1).

Quantitative analysis of airways and arteries

AA dimensions were measured with image analysis platform Myrian®, v1.18.1 (Lung XP module, Intrasense, Montpelier, France) as described previously.[11] In short, the bronchial tree was segmented automatically in 3D and remaining visible airways were added manually. Next, AA dimensions of all AA-pairs were measured perpendicular to the airway centerline. Measurements were made using an ellipse tool surrounding the inner and outer airway and adjacent artery boundaries in a window width of 1500 HU and window level of -200 HU (see Appendix Figure E1). Short and long axis diameters of the inner-, outer airway and adjacent artery were measured preferably in the middle of each reconstructed airway branch. The mean of short and long axis of the airway and artery was used to compute airway and artery diameters, respectively. Inner and outer airway diameters were divided by artery diameter to compute $A_{in}A$-, $A_{out}A$ -ratio respectively. Wall thickness (= [outer airway - inner airway diameter] / 2) was divided by artery diameter to compute $A_{WT}A$-ratio.

Airway generation and segmental bronchi were registered for every AA-pair. Segmental bronchi were numbered according to Netter nomenclature.[15] As previously described,[11] segmental generation (SG) was computed to allow all segmental bronchi to start at SG 1, correcting for generation discrepancy in each segmental bronchi (see Appendix Figure E2).

Observer reliability

All AA measurements were conducted by one observer (TS, medical student after one month training) blinded to disease status and time of scans. Three months after completion, 10 measurements were repeated in randomly selected segmental branch in each of the 36 CTs to establish intra-observer variability. In case less than 10 AA-pairs were visible and measured in the original random selected segmental branch, the following segmental branch was executed until 10 AA-pairs were measured per CT.

Statistical Analysis

Patients' characteristics were summarized using median (range). Difference in number of AA-pairs was assessed using Wilcoxon signed-rank test and relationship between age and number of AA-pairs using linear regression. Differences in AA-ratios per SG for cross-sectional data (CF CT_1 and CT_2 versus disease controls) and longitudinal data (CF CT_1 vs CT_2) were examined with mixed effects models , accounting for correlation within patients and lobes by including random effects. Influence of gender and age on AA-ratios was assessed by including them as potential confounding variables in the original models. Bonferroni correction was applied per outcome for 16 mixed effects models to predict AA-ratios per SG, with $p \leq 0.003$ considered to be significant.

Receiver operating characteristics (ROC) curves with corresponding area under curves (AUCs) were plotted to find AA-ratios with highest combined sensitivity and specificity differentiating between CF and disease controls.

Power calculations were performed assuming clustering of AA-pairs within individual patients and presented for AA-ratios based on a range of effect sizes, estimated as relative difference between CF and disease control group with 80% power and α=0.05.[16]

Intraclass correlation coefficient (ICC) using a mixed effects model was calculated to determine intra-observer agreement with structure taken into account. The structure specifically included segmental branches within generation within patients. All analysis were conducted using R v3.1.0.[17]

IRB approved prospective collection of CTs according to AREST CF study and written informed consent was obtained for each procedure.

RESULTS

Study population

Description of group characteristics is shown in Table 2.

TABLE 2. Demographics of the CF and control cohort

	Patients with CF			Disease controls
	CT_1	CT_2	CT_1+CT_2	
N			12	12
Gender (% male)			42% (5)	83% (10)
Age (in years)	2 (0.6-3.2)	3.9 (2.6-5.2)	2.9 (0.6-5.2)	2.9 (1-5.2)
Homozygote delta F508			50% (6)	
Heterozygote delta F508			50% (6)	
Pancreatic sufficiency			25% (3)	
Pseudomonas aeruginosa infection (%)	0% (0)	8% (1)		
Pseudomonas aeruginosa infection ever (%)			25% (3)	
Inner airway diameter (in mm)	1.46 ± 0.49	1.59 ± 0.55		1.63 ± 0.53
Outer airway diameter (in mm)	2.77 ± 0.70	2.91 ± 0.76		2.78 ± 0.80
Vessel diameter (in mm)	2.58 ± 0.72	2.67 ± 0.81		2.82 ± 0.85
A_{in}A-ratio	0.57 ± 0.10	0.60 ± 0.13		0.58 ± 0.09
A_{out}A-ratio	1.09 ± 0.14	1.12 ± 0.18		1.00 ± 0.14
A_{WT}A-ratio	0.52 ± 0.11	0.52 ± 0.13		0.42 ± 0.10

Data is represented as mean ± standard deviation or percentage (absolute numbers) as appropriate, with the exception of age which is described as median (range).

Quantitative analysis of airways and arteries

A total of 4798 AA-pairs were identified in perpendicular view of the 3D airway segmentations. 37 Outliers by manual errors and 14 AA-pairs before beginning of the segmental branch were omitted (for more detail see Appendix), leaving 4747 AA-pairs for analysis. In the CF group, a mean (range) of 127 (91-185) AA-pairs were measured at CT_1 and 148 (115-277) AA-pairs at CT_2. In controls a mean (range) of 121 (47-198) AA-pairs were measured. There were no significant differences cross-sectionally in number of AA-pairs between controls and CF at CT_1 ($p=0.83$) or CT_2 ($p=0.31$) and longitudinally between CF CT_1 and CF CT_2 ($p=0.09$). Figure 1 shows the number of AA-pairs by SG. As demonstrated in Figure 2 the number of AA-pairs is correlated with age (adjusted $r^2=0.28$, $p<0.001$) for CF and control patients combined.

Overall mean (range) of the inner, outer, vessel diameter and wall thickness in all measurements in the CF and control group were 1.6 (0.3-4.4), 2.8 (1.3-6.6), 2.7 (1.1-6.8) and 0.3 (0.1-0.7) mm respectively. $A_{in}A$-, $A_{out}A$-, and $A_{WT}A$-ratio did not increase significantly with age in the CF or control group (Appendix Figure E3). Gender and age were found not to be significant in a mixed effects model with $A_{in}A$-, $A_{out}A$-, or $A_{WT}A$-ratio. In the cross-sectional analyses, $A_{in}A$-ratio did not show significant differences between control and CF CT_1 or CT_2 in any SG (Figure 3, Table 3). Difference in $A_{out}A$-ratio between CF and control (Figure 4, Table 3) was significant from SG 2-4 for CT_1 ($p\leq0.002$) and SG 2-5 for CT_2 ($p\leq0.001$). Difference in $A_{WT}A$-ratio between CF and control (Figure 5, Table 3) was significant from SG 1-5 for CT_1 ($p<0.001$) and SG 2-6 in CT_2 ($p<0.001$). Difference in $A_{out}A$-, and $A_{WT}A$-ratio between patients with CF CT_2 and disease controls became larger with each next segmental generation.

In the CF longitudinal analyses, $A_{in}A$-ratio showed small but significant differences between CT_1 and CT_2 along most SG (Figure 3, Table 3). $A_{out}A$-ratio showed an increasing difference between CT_1 and CT_2 as a function of SG, only significant in SG 6 ($p<0.001$) (Figure 4, Table 3). A significant difference in $A_{WT}A$-ratio was observed between CF CT_1 and CT_2 in SG 1 and SG 3 respectively (Figure 5, Table 3).

The optimal threshold for $A_{in}A$-ratio was 0.7 (AUC= 0.49; sensitivity=0.14; specificity=0.91) and for $A_{out}A$-ratio was determined to be 1.06 (AUC=0.69; sensitivity= 0.58; specificity= 0.69). The optimal threshold for $A_{WT}A$-ratio was 0.44 (AUC= 0.75; sensitivity=0.75; specificity=0.64). ROC curves based on $A_{out}A$- and $A_{WT}A$-ratio between the CF and control group are shown in Appendix Figure E4.

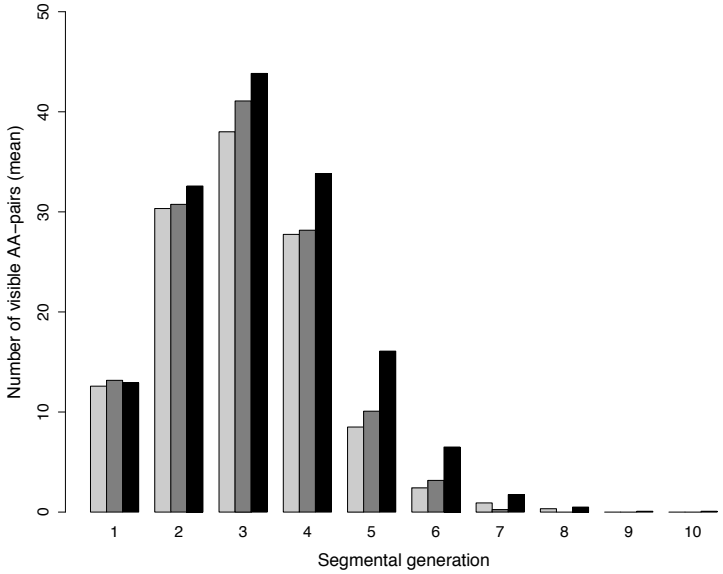

FIGURE 1. Average amount of AA-pairs visible per generation per control (light gray) and CF patients, for CT_1 (gray) and after a two-year interval for CT_2 (black).

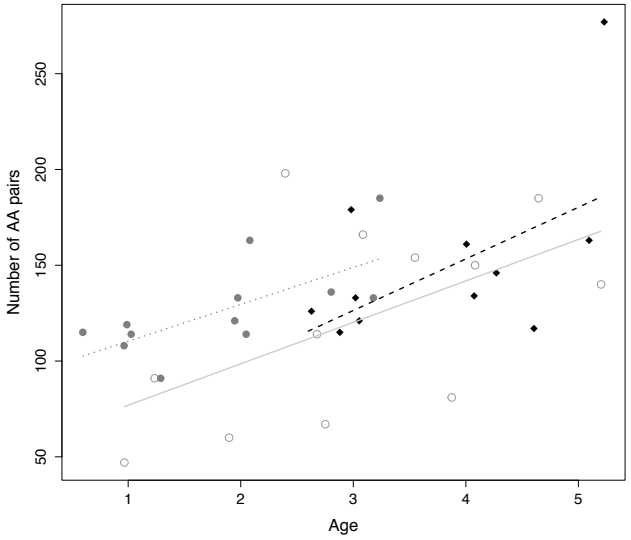

FIGURE 2. Amount of AA-pairs visible per generation per control (open circles, gray line) and CF patients, divided at CT_1 (filled circles, dotted gray line) and CT_2 (filled diamonds, black striped line). The number of AA-pairs increases significantly with age ($p<0.001$). Note that for CF we have a CT_1 and CT_2 while for controls we have only a CT at one time point

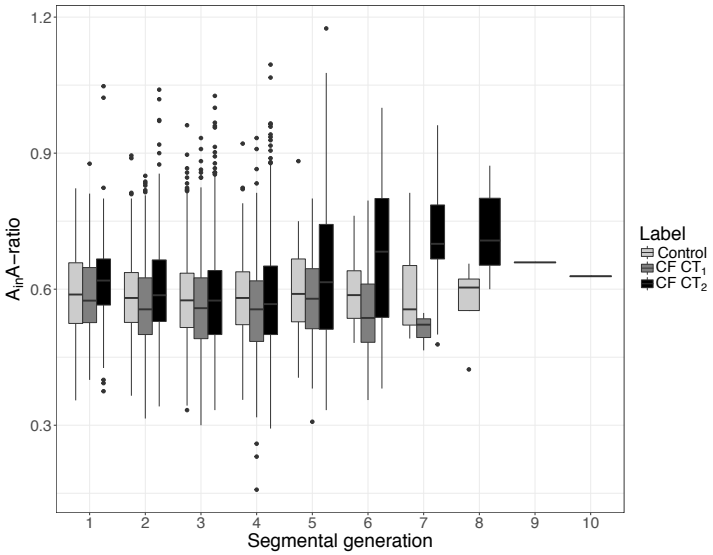

FIGURE 3. Boxplots of the A_{in}A-ratio in the control group (light gray) and in the CF group at CT_1 (gray) and CT_2 (black). Each box shows median (horizontal line), interquartile range (solid box), 1.5*interquartile range (whiskers) and outliers (points). Table 2 describes the mean differences and p-values for each generation as plotted in the A_{in}A-ratio graph.

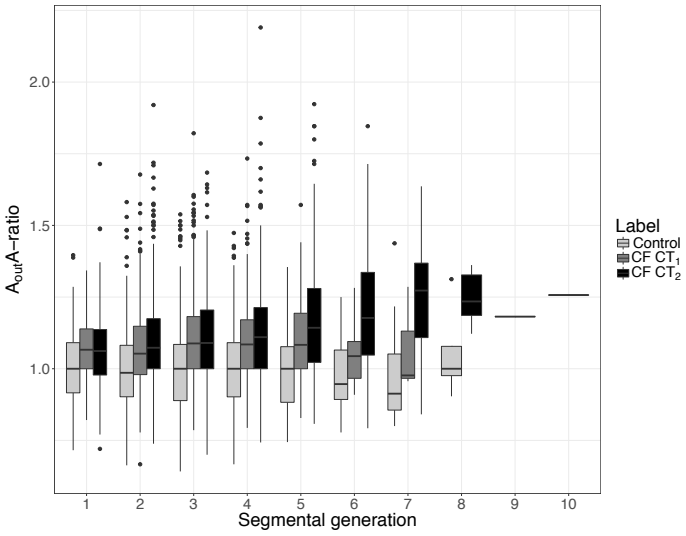

FIGURE 4. Boxplots of the A_{out}A-ratio in the control group (light gray) and in the CF group at CT_1 (gray) and CT_2 (black). Each box shows median (horizontal line), interquartile range (solid box), 1.5*interquartile range (whiskers) and outliers (points). Table 2 describes the mean differences and p-values for each generation as plotted in the A_{out}A-ratio graph. Note that the A_{out}A-ratio increases in the CF CT_2 group by segmental generation compared to controls. Secondly note that the number of AA-pairs observed decreases in the higher segmental generation for all three groups as shown in Figure 1 and Table 2.

TABLE 3. AA-pairs and AA-ratios for each segmental generation

1. Number of AA-pairs	Segmental generation							
	1	2	3	4	5	6	7	8
Controls	151	364	456	333	102	29	11	4
CF CT_1	158	368	493	338	121	38	3	0
CF CT_2	155	391	526	406	193	78	21	6
2. A_{in}A-ratio								
Control vs CT_1	0.00, -0.05-0.05 (p=0.91)	-0.01, -0.06-0.03 (p=0.65)	-0.01, -0.06-0.03 (p=0.56)	-0.02, -0.06-0.02 (p=0.36)	-0.03, -0.09-0.02 (p=0.23)	-0.08 -0.16-0.00 (p=0.06)	-0.08, -0.27-0.11 (p=0.35)	
Control vs CT_2	0.03, -0.02-0.08 (p=0.22)	0.02, -0.02-0.07 (p=0.37)	0.01, -0.03-0.06 (p=0.55)	0.01, -0.03-0.01 (p=0.59)	-0.01, -0.06-0.05 (p=0.84)	-0.01, -0.09-0.07 (p=0.78)	0.11, -0.01-0.24 (p=0.08)	0.16, -0.25-0.58 (p=0.24)
CT_1 vs CT_2	0.03, 0.01-0.05 (p=0.002)*	0.03, 0.02-0.04 (p<0.001)*	0.03, 0.01-0.04 (p<0.001)*	0.03, 0.02-0.05 (p<0.001)*	*0.03, 0.01-0.05 (p=0.017)*	0.07, 0.03-0.11 (p<0.001)*	*0.19, 0.01-0.38 (p=0.046)*	
3. A_{out}A-ratio								
Control vs CT_1	*0.07, 0.02-0.11 (p=0.009)*	0.08, 0.03-0.13 (p=0.002)*	0.10, 0.05-0.14 (p<0.001)*	0.08, 0.03-0.13 (p<0.001)*	*0.09, 0.02-0.16 (p=0.012)*	0.00, -0.11-0.11 (p=0.99)	0.08, -0.16-0.33 (p=0.53)	
Control vs CT_2	*0.06, 0.01-0.11 (p=0.016)*	0.10, 0.05-0.15 (p<0.001)*	0.10, 0.05-0.14 (p<0.001)*	0.11, 0.07-0.16 (p<0.001)*	0.12, 0.05-0.18 (p<0.001)*	*0.12, 0.02-0.23 (p=0.019)*	*0.26, 0.12-0.40 (p=0.006)*	0.21, -0.34-0.75 (p=0.24)
CT_1 vs CT_2	-0.01, -0.03-0.02, (p=0.65)	0.02, 0.00-0.04 (p=0.04)	0.00 -0.02-0.02 (p=0.83)	*0.03, 0.01-0.05 (p=0.006)*	0.03, -0.01-0.07 (p=0.10)	0.12, 0.07-0.18 (p<0.001)*	0.18, -0.05-0.41 (p=0.16)	
4. A_{WT}A-ratio								
Control vs CT_1	0.07, 0.03-0.10 (p<0.001)*	0.09, 0.05-0.12 (p<0.001)*	0.11, 0.07-0.15 (p<0.001)*	0.10, 0.06-0.14 (p<0.001)*	0.12, 0.08-0.17 (p<0.001)*	*0.08, 0.01-0.16 (p=0.026)*	0.17, -0.04-0.37 (p=0.10)	
Control vs CT2	0.03, 0.00-0.07 (p=0.08)	0.08, 0.04-0.11 (p<0.001)*	0.09, 0.05-0.13 (p<0.001)*	0.10, 0.06-0.14 (p<0.001)*	0.13, 0.08-0.17 (p<0.001)*	0.13, 0.06-0.20 (p<0.001)*	*0.13, 0.02-0.25 (p=0.029)*	0.04, -0.21-0.29 (p=0.57)
CT_1 vs CT_2	-0.04, -0.05--0.02 (p<0.001)*	-0.01, -0.02-0.00 (p=0.18)	-0.02, -0.04--0.01 (p<0.001)*	0.00, -0.02-0.01 (p=0.78)	0.00, -0.02-0.03 (p=0.86)	*0.05, 0.01-0.10 (p=0.022)*	-0.03, -0.22-0.16 (p=0.72)	

This table shows the number of AA pairs (1), differences in A_{in}A-ratio (2) , differences in A_{out}A-ratio (3) and differences in A_{WT}A-ratio (4) for each segmental generation. Differences in A_{in}A-ratio, A_{out}A-ratio and A_{WT}A-ratio were analyzed for control vs CF CT_1; control vs CF CT_2; and progression of CF in CT_1 vs CT_2. Differences were assessed with the mixed effects model for each generation demonstrating the mean difference, 95% confidence interval and p-values (an * indicates significant difference).

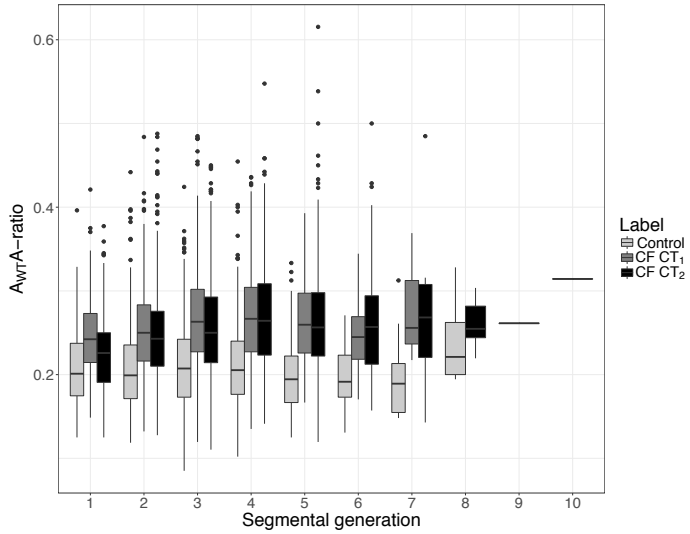

FIGURE 5. Boxplots of the A_{WT}A-ratio in the control group (light gray) and in the CF group at CT_1 (gray) and CT_2 (black). Each box shows median (horizontal line), interquartile range (solid box), 1.5*interquartile range (whiskers) and outliers (points). Table 2 describes the mean difference and p-value for each generation as plotted in the A_{WT}A-ratio graph. Note that the A_{WT}A-ratio is higher in the CF groups at CT_1 and CT_2 compared to controls. The number of AA-pairs observed decreases in the higher segmental generation for all 3 groups as shown in Figure 1 and Table 2.

Reproducibility of airway measurements

388 AA-pairs were re-measured in total. ICC and 95% confidence interval for intra-observer variability was 0.62 (0.60-0.64) for inner airway diameter; 0.63 (0.63-0.65) for outer airway diameter; 0.55 (0.53-0.56) for artery diameter.

Sample size estimates

Mean (SD) A_{out}A-ratio for SG 3, 4 and 5 combined was 1.12 (0.18) in CF at CT_2 and 1.00 (0.14) in controls. Sample sizes of 21, 33, 58 and 131 per treatment arm were calculated based on 50, 40, 30 and 20% reduction in A_{out}A-ratio respectively in difference between CF CT_2 and controls. Mean (SD) A_{WT}A-ratio for SG 3, 4 and 5 combined was 0.47 (0.08) in CF at CT_2 and 0.42 (0.07) in controls. Sample sizes of 53, 83, 148 and 331 per treatment arm were calculated based on 50, 40, 30 and 20% reduction in A_{WT}A-ratio respectively in difference between CF CT_2 and controls. Mean number of AA-pairs with A_{out}A-ratio>1.1 for SG 3, 4 and 5 combined was 0.51 in CF at CT_2 and 0.22 in controls. Sample sizes of 30, 46, 82 and 184 per treatment arm were calculated based on 50, 40, 30 and 20% reduction in number of AA-pairs with A_{out}A-ratio>1.1 respectively in difference between CF CT_2 and controls.

DISCUSSION

This study presents an unique dataset with all visible AA-pairs detected in 3D bronchial trees reconstructed from CT scans of young patients with CF. We compared AA-ratios between CF patients and disease controls and assessed progressive changes with time in children with CF.

This study confirms our previous study in older CF patients that the outer airway diameter should be used for comparison with the adjacent artery rather than the inner airway diameter in order to separate diseased CF airways from non-diseased CF airway.[11] A_{in}A-ratio did not show a significant difference between the disease control and CF group at CT_1 or CT_2. Relative to disease controls the A_{out}A-ratio in CF patients was significantly higher in segmental generation two to four at CT_1 and higher in segmental generation two to five for CT_2. A_{out}A-ratio > 1.06 was the best threshold to detect bronchiectasis in young children when using outer airway diameter for comparison to the artery diameter. This is in contrast to previous studies that have suggested a smaller AA-ratio to define bronchiectasis.[3,18] This difference could be explained as these studies used the inner airway diameter to determine the AA-ratio. An additional finding of this study is that wall thickening was detected in our young CF population compared to disease controls. A_{WT}A-ratio was significantly higher in CF at segmental generation one to five for CT_1, and in segmental generation two to six for CT_2. Similar but more apparent changes have been demonstrated in the A_{out}A,- and A_{WT}A-ratios of older children with CF compared to controls.[11] Furthermore, AA-, and A_{WT}A-ratios of disease controls in this study were independent of age and gender, which is in concordance to previous control studies.[11,18,19]

Another important finding of this study is that in the longitudinal analysis of children with CF, a progressive increase in A_{out}A-ratio on CT_2 relative to CT_1 was seen in the peripheral airways after a two-year interval (segmental generation ≥ 4), with a significant increase in segmental generation six. For the A_{in}A-ratio, small but significant changes over the two-year interval were detected for segmental generation one to four and six. This could be interpreted as the outer diameter reflecting irreversible airway dilation i.e., bronchiectasis and this diameter is, in contrast to the inner diameter, less influenced by lung volume and/or mucus impaction.[20] The systematic increase in A_{out}A-ratio by segmental generation after an interval of two years suggests that there is progressive bronchiectasis in the peripheral airways of young children with CF, although not statistically significant due to the small number of patients observed in this study. Based on our observations, larger studies that separately compare outer wall and inner wall to artery ratios could help to determine whether mucous impaction precedes the development of irreversible bronchial dilatation. For these studies automated analyses would be particularly useful.[21] Structural lung changes has been reported in young

children with CF previously,[1,22–25] and this study supports previous observations that the small airways play an important role in early CF lung disease.[11,26,27] In the longitudinal analysis of A_{WT}A-ratio, no changes in airway wall thickness were detected after two years, except for a very small but significant reduction observed in segmental generation three. Similarly, airway wall thickness did not increase significantly over a two years interval in older CF patient using visual CF-CT scoring.[22] These observations differ to those by de Jong et al.[13] who demonstrated progression of airway wall thickening over two years in older children and adolescents with CF using quantitative measures. This discrepancy between our study and that of de Jong et al. is likely to be explained by differences in the study populations. The study by de Jong et al. investigated a cohort of patients between 4 and 18 years of age. Disease progression at that time was likely to be more severe relative to our patient population diagnosed through newborn screening and evaluated between 0 and 6 years old. Furthermore, A_{WT}A-ratio in early CF lung disease is relatively stable and progression too small to be detected in the small group of patients in our study, even with very sensitive quantitative assessment in a large number of airways.

Previous studies suggested that the number of visible AA-pairs could be used as a novel CT outcome measure to establish CF lung disease severity.[11,12,28,29] In our cross-sectional analysis we did not observe a significant difference in number of AA-pairs between CF and disease controls, nor did the longitudinal analysis between the two time points in CF patients demonstrate significant differences in number of AA-pairs. Age was found to be positively correlated to the number of AA-pairs in these young CF and disease controls. Number of airways that can be detected is highly dependent on lung volume during CT acquisition and on image resolution of the CT.[30,31] All CF and control patients in this study had identical volume control protocol during CT acquisition. Hence, this did not likely influence our results. It was possible that due to the resolution limitations of even modern CT scanners we were not able to pick up sufficient number of high generation small airways in these young patients, as airways with a diameter less than 1 mm were mostly not measureable on CT. Hence, based on our findings we do not recommend to use number of visible airways as an outcome measure in patients below the age of 6. Number of airways as outcome measure in studies of these young children could be confounded by age and resolution of chest CT.[32] Nonetheless, in a cross-sectional study in children 6 years and older a sufficient amount of (small) airways can be sampled in CF and a control population to detect significant differences between those two groups.[11] We believe that in older children the size of airways, and therefore the detection of number of AA-pairs is to a lesser extent confounded by age or CT resolution.

Lastly, this study suggests that with objectively quantified AA-ratios, small sample sizes are needed to test effects of interventions or disease progression. A sample size of 21

per treatment arm was estimated based on 50% reduction in A_{out}A-ratio at age 6. In comparison, the semi-quantitative scoring technique PRAGMA-CF estimated a sample size of 100 per treatment arm based on 50% reduction in total airway disease at age 3.[25] However, it must be noted that the smaller sample size required with objective AA-ratios could have been caused by the older age of the patients studied. Additionally, the sample size estimation is likely an underestimation of the true sample size needed due to the comparison between CF and non-CF airways as baseline. Nonetheless, the AA-method appears to be sensitive for detecting abnormal airway dimensions on chest CT compared to controls, supporting the potential for AA-ratio determination as an outcome measure in clinical trials in young patients.

We acknowledge a number of limitations with the study. First, we have only studied a relative small population, due to the time consuming task to quantify AA dimensions manually. However, with 3,297 AA-pairs in CF and 1,450 in controls we had sufficient power to demonstrate differences in AA-dimensions between CF and disease controls. For the longitudinal analysis a larger number of patients are needed to determine whether progressive increase in AA-ratios and in the number of AA-pairs can be detected. Second, our control group cannot be considered healthy, as they were patients referred by the pediatric pulmonologist for respiratory complaints. However, their chest CTs were considered to be normal as evaluated by an experienced pediatric radiologist. The constant AA-ratios in disease controls over successive generations observed in this study and in relation to age, is consistent with reported measures in controls.[3,11,13] In addition, it is likely that the use of disease controls underestimates differences between CF and controls. Unfortunately, despite the low radiation dose of modern scanners there are still ethical barriers for studying healthy children with chest CT, due to the potential risks from ionizing radiation. For this reason we were only able to collect single control CTs over the same age range covering the age range of CF patients with each two CTs.

Third, the measurements made in the smaller airways are near the resolution limits of the CT scanner. However, with edge-enhancing reconstruction kernel and high image contrast between airway wall tissue and surrounding air or soft tissue, measurements of sub-millimeter structures were feasible. In addition, the accuracy of the measurements were improved by fixing the window width and level settings.

Finally, the intra-observer analysis was difficult to standardize as the manual measurements at mid-airway positions could have been made at different anatomic locations leading to the ICC of 0.62. However, this is being compensated by the large number of airway-artery pairs that could be sampled per patient (on average 132 pairs) resulting in small confidence intervals. The variability between the airway measurements can be improved when using automated analysis. Algorithms to do so are feasible and currently under development.[21]

Summary

Our study demonstrates that young children with early CF lung disease have more dilated airways and thicker walls than disease controls. In CF, progression in outer diameter AA-ratio was detected after two years, especially in the peripheral airways. Results of this study are in concordance with previous literature reporting structural airway changes early in life of patients with CF on chest CT.[2,3] AA-ratios are an objective tool for measuring CF related airway disease severity in early life, and a sensitive outcome measure for use in clinical trials aiming to prevent early SLD. A larger study population of CF patients is needed to accurately define the progression of SLD on chest CT in young children, which will be the next step using automatic analysis techniques.[21]

ACKNOWLEDGEMENTS

The authors like to thank Conor Murray (Department of Diagnostic Imaging, Princess Margaret Hospital for Children, Perth, WA, Australia) for his contribution to the assessment of the control group.

REFERENCES

1. Mott LS, Park J, Murray CP, Gangell CL, de Klerk NH, Robinson PJ, Robertson CF, Ranganathan SC, Sly PD, Stick SM. Progression of early structural lung disease in young children with cystic fibrosis assessed using CT. Thorax. 2012;67(6):509–516.
2. Sly PD, Brennan S, Gangell C, De Klerk N, Murray C, Mott L, Stick SM, Robinson PJ, Robertson CF, Ranganathan SC. Lung disease at diagnosis in infants with cystic fibrosis detected by newborn screening. American Journal of Respiratory and Critical Care Medicine. 2009;180(2):146–152.
3. Long F, Williams R, Castile R. Structural airway abnormalities in infants and young children with cystic fibrosis. J Pediatr. 2004;144:156–161.
4. Tiddens HAWM, Puderbach M, Venegas JG, Ratjen F, Donaldson SH, Davis SD, Rowe SM, Sagel SD, Higgins M, Waltz D a. Novel outcome measures for clinical trials in cystic fibrosis. Pediatric Pulmonology. 2015;50(3):302–315.
5. Schultz A, Stick S. Early pulmonary inflammation and lung damage in children with cystic fibrosis. Respirology. 2015;20(4):569–578.
6. Sanders DB, Li Z, Brody AS. Chest computed tomography predicts the frequency of pulmonary exacerbations in children with cystic fibrosis. Annals of the American Thoracic Society. 2015;12(1):64–69.
7. Stick S, Tiddens H, Aurora P, Gustafsson P, Ranganathan S, Robinson P, Rosenfeld M, Sly P, Ratjen F. Early intervention studies in infants and preschool children with cystic fibrosis: are we ready? The European respiratory journal. 2013;42(2):527–38.
8. Ciet P, Serra G, Bertolo S, Spronk S, Ros M, Fraioli F, Quattrucci S, Assael MB, Catalano C, Pomerri F, et al. Assessment of CF lung disease using motion corrected PROPELLER MRI: a comparison with CT. European Radiology. 2016;26(3):780–787.
9. Sileo C, Corvol H, Boelle PY, Blondiaux E, Clement A, Ducou Le Pointe H. HRCT and MRI of the lung in children with cystic fibrosis: Comparison of different scoring systems. Journal of Cystic Fibrosis. 2014;13(2):198–204.
10. Lee KS, Primack SL, Staples CA, Mayo JR, Aldrich JE, Müller NL. Chronic infiltrative lung disease: comparison of diagnostic accuracies of radiography and low- and conventional-dose thin-section CT. Radiology. 1994;191(3):669–73.
11. Kuo W, de Bruijne M, Petersen J, Nasserinejad K, Ozturk H, Chen Y, Perez-Rovira A, Tiddens HAWM. Diagnosis of bronchiectasis and airway wall thickening in children with cystic fibrosis: Objective airway-artery quantification. European radiology. 2017:In press.
12. Kuo W, Andrinopoulou E-R, Perez-Rovira A, Ozturk H, de Bruijne M, Tiddens HAWM. Objective airway artery dimensions compared to CT scoring methods assessing structural cystic fibrosis lung disease. Journal of Cystic Fibrosis. 2016;16(1):116–123.
13. De Jong PA, Nakano Y, Hop WC, Long FR, Coxson HO, Paré PD, Tiddens H a. Changes in airway dimensions on computed tomography scans of children with cystic fibrosis. American Journal of Respiratory and Critical Care Medicine. 2005;172(2):218–224.
14. Sly PD, Gangell CL, Chen L, Ware RS, Ranganathan S, Mott LS, Murray CP, Stick SM. Risk factors for bronchiectasis in children with cystic fibrosis. The New England journal of medicine. 2013;368(21):1963–70.
15. Netter FH. Atlas of human anatomy. 6th ed. Saunders Elsevier; 2014. 197-198 p.

16. Rutterford C, Copas A, Eldridge S. Methods for sample size determination in cluster randomized trials. International Journal of Epidemiology. 2015;44(3):1051–1067.

17. R Foundation for statistical Computing. R Development Core Team. R: A Language and Environment for Statistical Computing. Vienna; 2005.

18. Kapur N, Masel JP, Watson D, Masters IB, Chang AB. Bronchoarterial ratio on high-resolution CT scan of the chest in children without pulmonary pathology: Need to redefine bronchial dilatation. Chest. 2011;139(6):1445–1450.

19. Rao L, Tiller C, Coates C, Kimmel R, Applegate KE, Granroth-Cook J, Denski C, Nguyen J, Yu Z, Hoffman E, et al. Lung Growth in Infants and Toddlers Assessed by Multi-slice Computed Tomography. Academic Radiology. 2010;17(9):1128–1135.

20. O'Connor OJ, Vandeleur M, McGarrigle AM, Moore N, McWilliams SR, McSweeney SE, O'Neill M, Ni Chroinin M, Maher MM. Development of low-dose protocols for thin-section CT assessment of cystic fibrosis in pediatric patients. Radiology. 2010;257(3):820–829.

21. Perez-Rovira A, Kuo W, Petersen J, Tiddens HAWM, de Bruijne M. Automatic airway–artery analysis on lung CT to quantify airway wall thickening and bronchiectasis. Medical Physics. 2016;43(10):5736–5744.

22. Tepper LA, Caudri D, Utens EMWJ, van der Wiel EC, Quittner AL, Tiddens HAWM. Tracking CF disease progression with CT and respiratory symptoms in a cohort of children aged 6-19 years. Pediatric Pulmonology. 2014;1189(February):1182–1189.

23. de Jong PA, Lindblad A, Rubin L, Hop WCJ, de Jongste JC, Brink M, Tiddens HAWM. Progression of lung disease on computed tomography and pulmonary function tests in children and adults with cystic fibrosis. Thorax. 2006;61(1):80–85.

24. de Jong PA, Nakano Y, Lequin MH, Mayo JR, Woods R, Paré PD, Tiddens H a WM. Progressive damage on high resolution computed tomography despite stable lung function in cystic fibrosis. European Respiratory Journal. 2004;23(1):93–97.

25. Rosenow T, Oudraad MCJ, Murray CP, Turkovic L, Kuo W, de Bruijne M, Ranganathan SC, Tiddens HAWM, Stick SM. PRAGMA-CF. A Quantitative Structural Lung Disease Computed Tomography Outcome in Young Children with Cystic Fibrosis. American journal of respiratory and critical care medicine. 2015;191(10):1158–1165.

26. Tiddens HAWM, Donaldson SH, Rosenfeld M, Paré PD. Cystic fibrosis lung disease starts in the small airways: Can we treat it more effectively? Pediatric Pulmonology. 2010;45(2):107–117.

27. Ratjen F. Cystic Fibrosis: The role of the small airways. Journal of Aerosol Medicine and Pulmonary Drug Delivery. 2012;25(5):261–264.

28. DeBoer EM, Swiercz W, Heltshe SL, Anthony MM, Szefler P, Klein R, Strain J, Brody AS, Sagel SD. Automated ct scan scores of bronchiectasis and air trapping in cystic fibrosis. Chest. 2014;145(3):593–603.

29. Boon M, Verleden SE, Bosch B, Lammertyn EJ, McDonough JE, Mai C, Verschakelen J, Kemner-Van De Corput M, Tiddens HAW, Proesmans M, et al. Morphometric analysis of explant lungs in cystic fibrosis. American Journal of Respiratory and Critical Care Medicine. 2016;193(5):516–526.

30. Mott LS, Graniel KG, Park J, De Klerk NH, Sly PD, Murray CP, Tiddens HAWM, Stick SM. Assessment of early bronchiectasis in young children with cystic fibrosis is dependent on lung volume. Chest. 2013;144(4):1193–1198.

31. Kuo W, Kemner-van de Corput MPC, Perez-Rovira A, de Bruijne M, Fajac I, Tiddens HAWM, et al. Multicentre chest CT standardisation in children and adolescents with cystic fibrosis : the way forward. European Respiratory Journal. 2016:1–12.

32. Ménache MG, Hofmann W, Ashgarian B, Miller FJ. Airway geometry models of children's lungs for use in dosimetry modeling. Inhalation toxicology. 2008;20(2):101–126.

APPENDIX

Results

Excluded outliers

36 outliers due to typos in the manual annotations were excluded. This was determined as follows: outer airway diameter < inner airway diameter; generation > 40; A_{out}A-ratio >8; A_{in}A-ratio> 2; difference surface area as annotated and surface area calculated with the short and long diameter > 3.

14 measurements before the segmental branches were excluded in the analysis as well.

APPENDIX TABLE E1. CT settings

CT setting	Prior to 2012	From 2012
CT Scanner	Philips Brilliance 64	Siemens Definition Flash
Scan type	Inspiratory	Inspiratory
Acquisition	Volumetric	Volumetric
Rotation time (ms)	400	280
Pitch	0.61	3
Slice thickness (mm)	0.9	1.0
Increment (mm)	0.45	0.7
Collimation (mm)	0.63	0.63
Tube voltage (kVp)	120	100
Current-time product (mAs)	25	10
$CTDI_{vol}$ (mGy)	1.51 (0.06)	0.46 (0.00)
Dose-Length Product (mGy cm)	34.75 (4.01)	12.33 (0.58)

$CTDI_{vol}$ and Dose-Length Product were based on a 32-cm phantom and reported as mean (standard deviation).

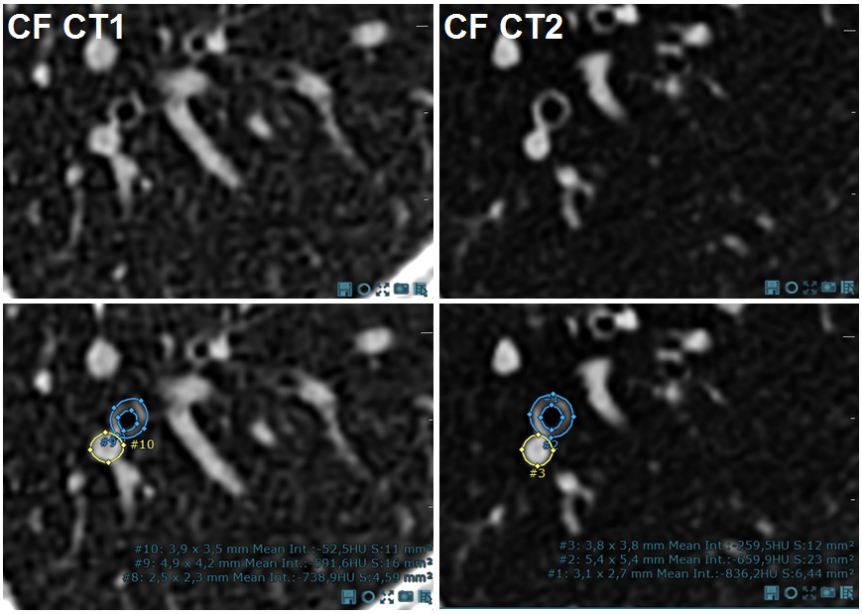

APPENDIX FIGURE E1. Example of a CF airway and artery pair (top row) measured with the ellipse tool (bottom row) in Myrian®. The airway and artery measurement are made during baseline (left) and follow up (right).

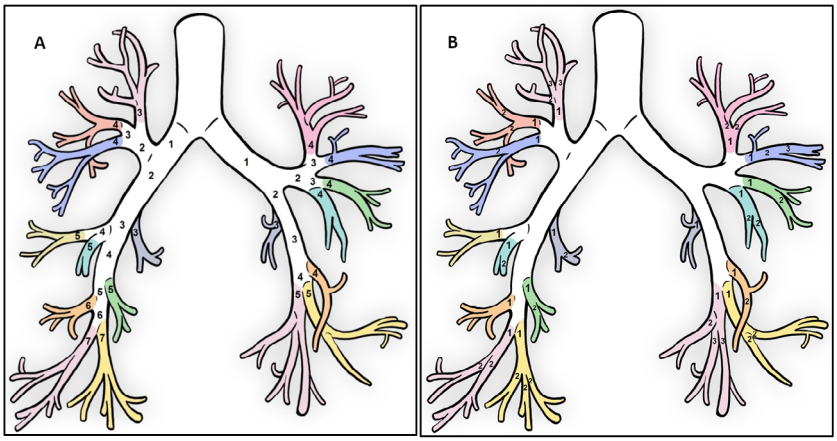

APPENDIX FIGURE E2. Anatomy of the airways. A) The segmental branches are shown in the different colors and the numbering stands for the airway generation. As shown in figure 1A each segmental branch starts with a different generation, eg generation 3-4 in the upper segmental branches whereas it starts at generation 5-7 in the lower segmental branches. B). To correct for this discrepancy we computed the segmental generation which ensured all segmental bronchi to start at segmental generation 1 (Artist: K. Rubenis).

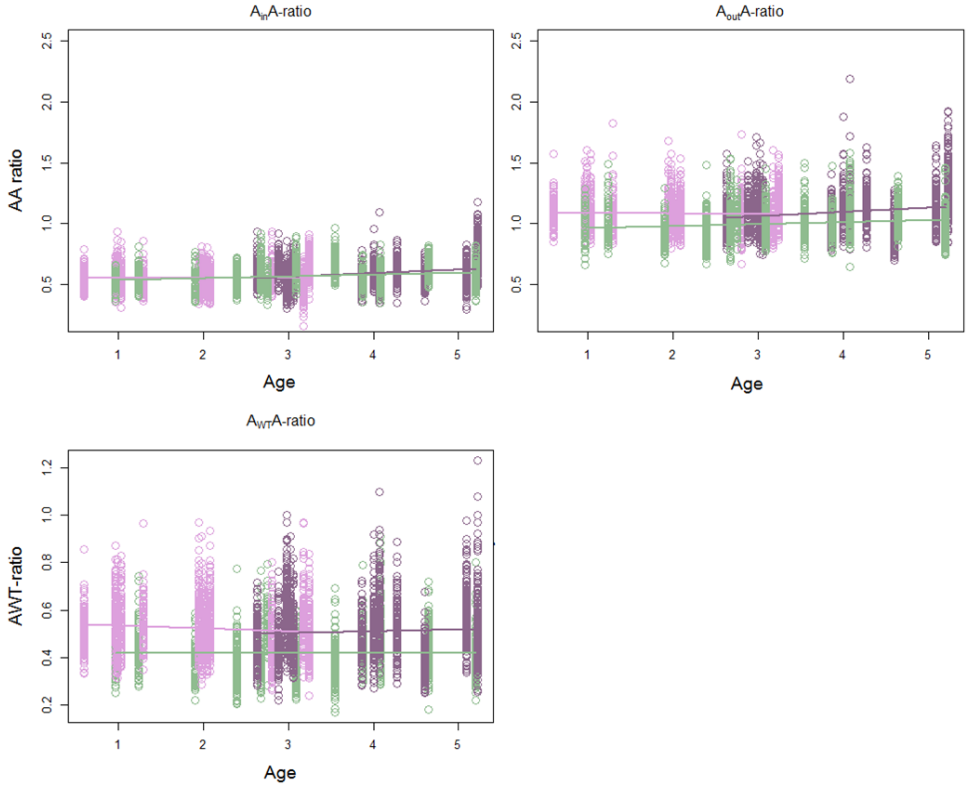

APPENDIX FIGURE E3. The airway artery ratio is plotted as a function of age, for $A_{in}A$-,(top left) and $A_{out}A$-ratio (top right) with the regression line based on the mixed model. Age was not significant in the mixed-effect model for $A_{in}A$-ratio for the CF CT_1 (p=0.78), CF CT_2 (p=0.22) or control group (p=0.15). The $A_{out}A$-ratio in the CF CT_1 (p=0.78), CF CT_2 (p=0.23), and control group (p=0.22) do not increase significantly either with age. The airway wall ratio is plotted as a function of age, for $A_{WT}A$-, (bottom left). Age was not significant in the mixed-effect model for $A_{WT}A$ ratio in the CF CT1 (p=0.41), CF CT2 (p=0.80), and control group (p=0.97).

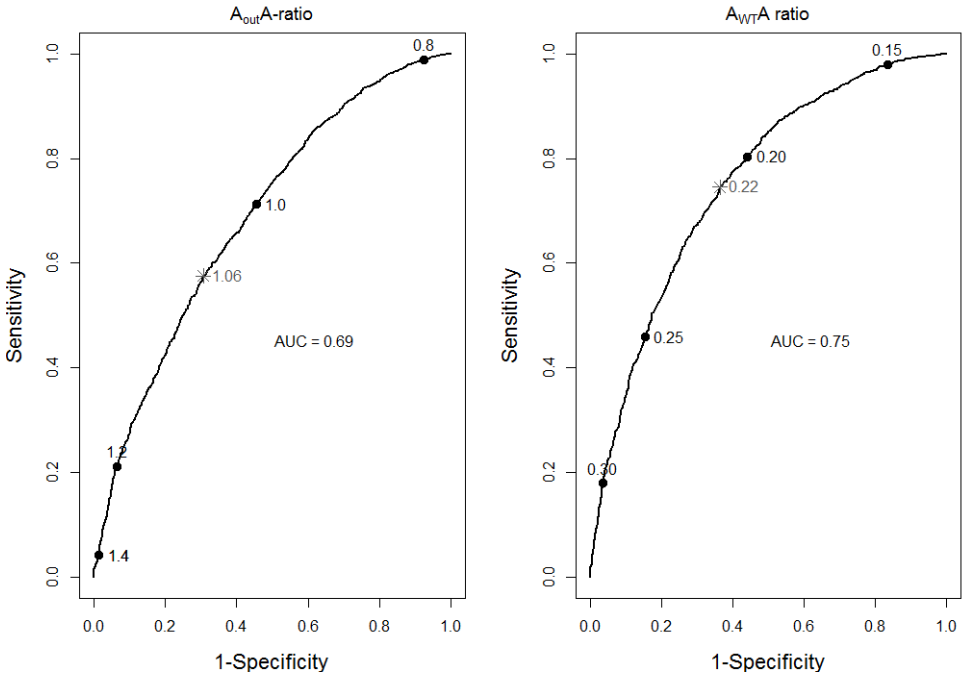

APPENDIX FIGURE E4. Receiver-operating characteristic (ROC) curves to distinguish the most optimal A_{out}A- (left) and A_{WT}A-ratio (right) between patients with CF and the control patients. The gray stars indicate the AA ratio with the optimal sensitivity + specificity.

CHAPTER 6

OBJECTIVE AIRWAY ARTERY DIMENSIONS COMPARED TO CT SCORING METHODS ASSESSING STRUCTURAL CYSTIC FIBROSIS LUNG DISEASE

Wieying Kuo, Eleni-Rosalina Andrinopoulou, Adria Perez-Rovira, Hadiye Ozturk, Marleen de Bruijne, Harm A.W.M. Tiddens

Journal of Cystic Fibrosis.
2016;16(1):116–123

ABSTRACT

Background

CF-CT and PRAGMA-CF are commonly used scoring methods to quantify the severity of bronchiectasis (BE) and airway wall thickening (AWT) on chest CTs of children with cystic fibrosis (CF). We aimed to validate CF-CT and PRAGMA-CF sub-scores for BE and AWT against quantitative airway-artery (AA) dimensions.

Methods

This is a retrospective study with 23 spirometer guided inspiratory chest CTs (11 CF, 12 controls; age range 6 to 16 years old) included. AA-, and $A_{WT}A$-ratios of all visible AA pairs were computed by dividing diameters of the outer airway and wall (outer-inner airway) by the accompanying artery diameter, respectively. BE, AWT and total airway disease (TAD) were scored using CF-CT (% max score) and PRAGMA-CF (% extent). Correlations were computed using Spearman rank. Akaike information criterion (AIC) from the mixed-effects models were used to investigate whether CF-CT or PRAGMA-CF was a better predictor for AA-, and $A_{WT}A$-ratios (lower AIC equals a better fitted model).

Results

4,861 AA pairs were measured in total. Correlations between CF-CT and PRAGMA-CF: BE ($r=0.93$, $P<0.001$); AWT ($r=0.62$, $P<0.001$); TAD ($r=0.88$, $P<0.001$). PRAGMA-CF TAD sub-score had lowest AIC in the mixed-model predicting AA-ratio. CF-CT AWT and PRAGMA-CF TAD sub-score had equal low AIC in the mixed-model predicting $A_{WT}A$-ratio.

Conclusion

PRAGMA-CF TAD sub-score was more precise predicting BE. CF-CT AWT and PRAGMA-CF TAD sub-scores predicted AWT equally well. CF-CT and PRAGMA-CF were both sensitive methods to score BE and AWT in children with CF lung disease, with PRAGMA-CT TAD sub-score being most accurate predicting AA dimensions.

INTRODUCTION

Lung disease is the leading cause of morbidity and mortality in cystic fibrosis (CF) patients.[1] Bronchiectasis (BE) and airway wall thickening (AWT) are two important components of CF lung disease.[2] Currently chest CT is the gold standard and most sensitive imaging tool to assess these structural lung changes.[3,4] To quantify disease severity, different CT scoring systems have been developed to score CF related components such as BE, AWT, mucous plugging (MP) and trapped air.[5–7] The CF-CT is a well standardized scoring system with extensive instruction module and standardized training sets.[3,5,8,9] A disadvantage of this system is that it is not sensitive to quantify early CF lung disease as the extent of disease is scored as absent; less than 33%, between 33 and 67%, or more than 67%. Hence, lung disease in young children will mostly be scored as either absent or less than 33%. More recently PRAGMA-CF was developed as a more sensitive alternative to quantify structural lung abnormalities in early CF lung disease.[6] However, this scoring method requires validation and independent verification.

A downside of CF-CT and PRAGMA-CF scoring methods is that they are subjective and have not been properly validated against an objective system measuring airway dimensions.[10]

For objective measurements of BE and airway dimensions several systems have been used to measure airway and artery (AA) dimensions of AA pairs on axial slices of CT scans.[11–13] A disadvantage of this approach is that it can cause inaccuracy due to a projection or parallax error,[14] which is an error that causes the AA dimensions to be perceived larger or smaller depending on the plane it is visualized in. More recently an improved method was developed to manually measure AA dimensions perpendicular to the airway centerline.[15] This AA-method is currently the most objective quantitative method to measure AA dimensions. Therefore, we used the AA-method as reference standard and compared it with BE, AWT, and total airway disease (TAD) scored with CF-CT and PRAGMA-CF.

This study compares quantitative AA dimensions with semi-quantitative CF-CT and PRAGMA-CF scores for BE, AWT and TAD in children and adolescents with CF and controls. We hypothesized that PRAGMA-CF is a better predictor of the quantitative AA- and A_{WT}A-ratios, hence a better suited tool for disease quantification in children with CF than the CF-CT scoring system.

METHODS

Study population

The dataset for this study was initially used for the development of the AA-method and was reported separately.[15] In summary, CF patients were between 6 and 16 years of age and were treated at the Erasmus MC-Sophia Children's Hospital between 2007 and 2012. Chest CTs of 12 CF patients with a routine spirometer guided inspiratory chest CT were randomly selected and analyzed. However, one subject in the CF group was excluded since the patient appeared to be mislabeled and diagnosed with common variable immunodeficiency.

The control group consisted of patients referred by the pediatric pulmonology department, Erasmus MC-Sophia Children's Hospital, for a spirometer guided chest CT. Patients were included if they had no visible lung abnormalities on chest CT according to two independent radiologists. Out of 16 normal chest CTs available, 12 CTs of the subjects with best matching ages to CF patients were selected.

CT scanning and scoring

End-inspiratory spirometer guided volumetric CT of all patients with CF and the control subjects were obtained in supine position with a SOMATOM® Definition Flash CT scanner (Siemens Healthcare, Forchheim, Germany). Detailed scan parameters were reported separately[15] and described in the Appendix Table E1. All CTs were anonymized and analyzed using the AA-method in random order by observer (WK) and a random subset by a second observer (HO).[15] CF-CT and PRAGMA-CF scoring was performed by a single scorer (HO) with 1-year experience in scoring. Table 1 summarizes CT components (BE, AWT and TAD) scored with the three different methods.

TABLE 1. Scoring algorithms

	AA-method	CF-CT	PRAGMA-CF
Bronchiectasis	AA-ratio = $\frac{\text{outer airway diameter}}{\text{artery diameter}}$	% of max BE sub-score including severity and extent of BE	% of BE extent
Airway wall thickening	A_{WT}A-ratio = $\frac{\text{outer–inner airway diameter}}{\text{artery diameter}}$	% of max AWT sub-score including severity and extent of AWT	% of AWT extent
Total airway disease		% of max BE, AWT and MP sub-score including severity and extent of BE, AWT and MP	% of BE, MP, AWT extent

Scoring components of bronchiectasis (BE), airway wall thickening (AWT) and total airways disease (TAD) using the AA-method, CF-CT and PRAGMA-CF scoring technique.

Quantitative analysis of airways and arteries

Dimensions of all visible AA pairs were measured with image analysis platform Myrian®, version 1.16.2 (Intrasense, Montpelier, France). The bronchial trees were interactively reconstructed in 3D for each CT. Next, AA dimensions of all visible AA pairs were measured in the middle of each branch perpendicular to the longitudinal airway axis. All measurements were made with an ellipse tool which was adjusted manually to the edges of the AA dimensions, in a window width of 1500 HU centered at -200 HU. Of each visible airway branch, areas of the inner-, outer airway and adjacent artery were measured.

Average diameters (*d*) were computed from annotated surface areas (*a*) using the following formula: $d = 2 \times \sqrt{\frac{a}{\pi}}$. Outer airway diameters were divided by the artery diameters to compute AA-ratio. Wall thickness (difference between outer and inner airway diameter) was divided by the artery diameter to compute A_{WT}A-ratio. Number of AA pairs was defined as the number of AA observations visible per CT scan.

CF-CT scoring

CF-CT scoring system evaluates the five lung lobes and lingula for severity and extent of central and peripheral CT components. The following sub-scores were assessed: BE; AWT; MP; opacities (atelectasis, consolidation, ground glass pattern) [5]. More detail on scoring algorithm for BE, AWT and MP are provided in Appendix Table E2. TAD sub-score was computed as the sum of BE, AWT and MP. BE, AWT and TAD sub-scores are expressed as percentage of maximum score (0-100%).

PRAGMA-CF scoring

PRAGMA-CF computes the volume fraction of CT components using a grid overlaying 10 equally spaced axial slices between lung apex and base.[6] Each grid cell that contains at least 50% coverage of the lung is scored. Any sign of the disease component in the grid cell will be scored with the following hierarchical system (highest to lowest priority): 1. BE, 2. MP, 3. AWT, 4. atelectasis or 5. normal lung. Atelectasis was subtracted from the total lung volume.[6] TAD was computed as the sum of BE, MP and AWT. We used volume fraction of the lung with BE, AWT and TAD sub-scores.

Statistical Analysis

Descriptive statistics of the patient's key characteristics are displayed as median (range). Receiver operating characteristic (ROC) curves with corresponding area under curves (AUC) were plotted to identify the AA- and A_{WT}A-ratio thresholds with the highest combined sensitivity and specificity to differentiate CF from controls.

Spearman rank correlation was used to describe the relationship between CF-CT and PRAGMA-CF scoring methods. To compare CF-CT and PRAGMA-CF with AA related components graphically, we standardized BE, AWT and TAD sub-scores by converting them into a Z-score using the following formula: ($\frac{Observed\ (sub)score\text{-}mean\ (sub)score}{standard\ deviation\ (sub)score}$). Univariable linear regression analysis was used to evaluate relation between BE, AWT and TAD sub-scores for each scoring module with AA parameters: the number of AA pairs; and the percentage AA pairs above ROC cut-off value for AA and $A_{WT}A$-ratio. Adjusted R^2 was used to compare the models, with higher adjusted R^2 equaling better fit.

Effects of the BE, AWT and TAD sub-scores derived from CF-CT and PRAGMA-CF, on AA- and $A_{WT}A$-ratios were investigated using mixed-effect models. The mixed-effects models took correlation between multiple AA ratios obtained from the same patients into account. Akaike information criterion (AIC) was used to compare models fit using the two scoring methods, where a lower AIC equals a better prediction model. An AIC with 5 points difference or more was regarded as a significant difference.[16,17] To account for multiple repeated testing for 14 linear regressions and 8 mixed-effect models, a p-value ≤ 0.002 was considered significant using the Bonferroni correction.

Intra-observer agreement of CF-CT and PRAGMA-CF sub-scores were calculated using intraclass correlation coefficients (ICCs). All analyses were conducted using R version 3.1.0,[18] except for the ICC analysis which was performed using SPSS version 21 for windows.

This retrospective study was approved by the institutional review board (MEC-2014-255). Written informed consent was waived for all patients because of the retrospective nature of the study.

RESULTS

Study population

11 patients with CF (6 males) were included aged 11 (7-16) years and 12 control subjects (7 males) aged 13.9 (6-16) years. There was no significant demographic difference between the CF and control group in age, gender height and weight (Appendix Table E3).

CT scoring

Characteristics of CF-CT and PRAGMA-CF sub-scores are shown in Table 2. Intra-observer reliability with CF-CT was 0.95 for BE; 0.9 for AWT; 0.94 for MP; 0.95 for TAD. Intra-observer reliability with PRAGMA-CF was 0.87 for BE; 0.5 for AWT; 0.98 for MP; 0.94 for TAD.

TABLE 2. Summarized characteristics of the scoring parameters

	CF-CT % of max score			PRAGMA-CF % extent			Number of AA pairs	AA pairs with AA ratio > 1.11 (%)	AA pairs with $A_{WT}A$ ratio > 0.58 (%)
	BE	AWT	TAD	BE	AWT	TAD			
CF	5.2	5.5	4.8	1.3	1.2	4.9	283	0.52	0.51
n=11	(0-68.1)	(0-26.4)	(0-44.6)	(0-13.2)	(0.2-4.6)	(0.6-16.7)	(149-503)	(0.15-0.82)	(0.34-0.79)
Control	0	0	0	0	0	0.1	130	0.22	0.26
n=12	(0-4.2)	(0-0)	(0-1.8)	(0-0.3)	(0-1.3)	(0-1.4)	(42-183)	(0.08-0.39)	(0.06-0.69)

Bronchiectasis (BE), airway wall thickening (AWT) and total airway disease (TAD) as scored with CF-CT and PRAGMA-CF. All results shown are median (range).

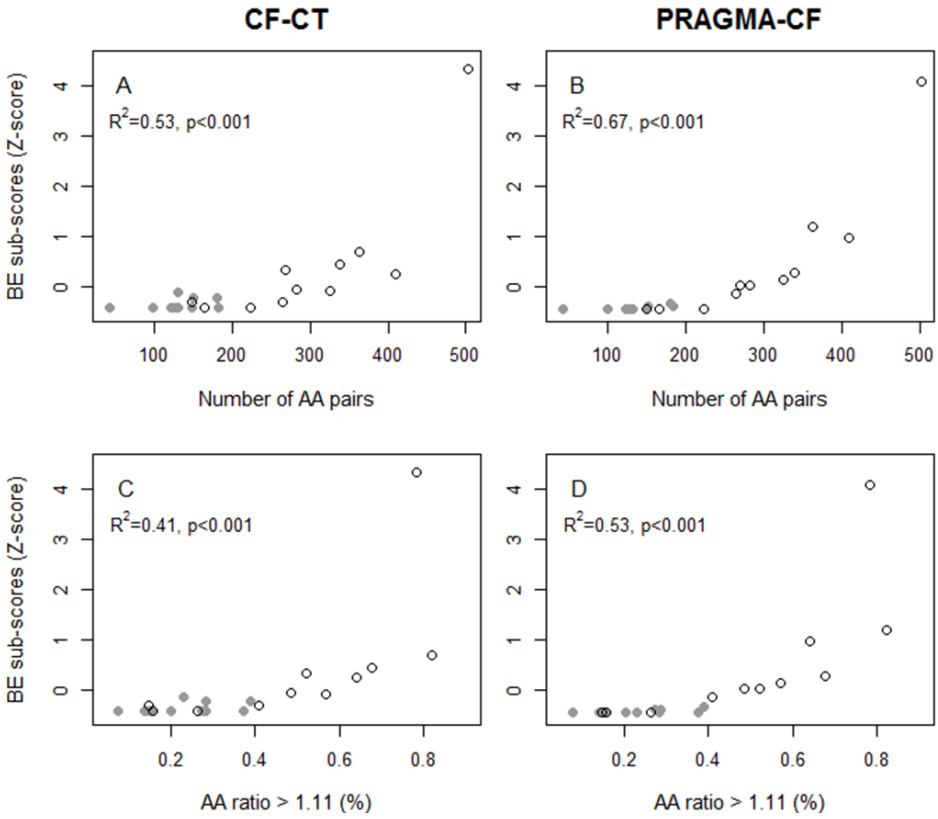

FIGURE 1. Scatterplots of CF-CT (left columns) and PRAGMA-CF (right columns) BE sub-scores (normalized into Z-scores), in relation to the number of AA pairs (top row) and the percentage of AA ratios above 1.11 (bottom row). CF patients are shown in black open circles and the control subjects in filled gray circles. All control subjects have a number of AA pair below 183 and percentage AA ratios > 1.11 of 0.4 or lower. The linear regressions were better fitted with PRAGMA-CF than with CF-CT in the CF and control subjects (Table 3).

AA parameters

A total of 4861 AA pairs were annotated perpendicular to the airway axis, 3293 in CF and 1568 in controls (see Table 2). AA-ratio with the most optimal threshold differentiating CF from control patients was determined to be 1.11 (AUC=0.72; sensitivity = 0.56; specificity=0.77). The optimal threshold for A_{WT}A-ratio was 0.58 (AUC = 0.7; sensitivity = 0.56; specificity = 0.75).

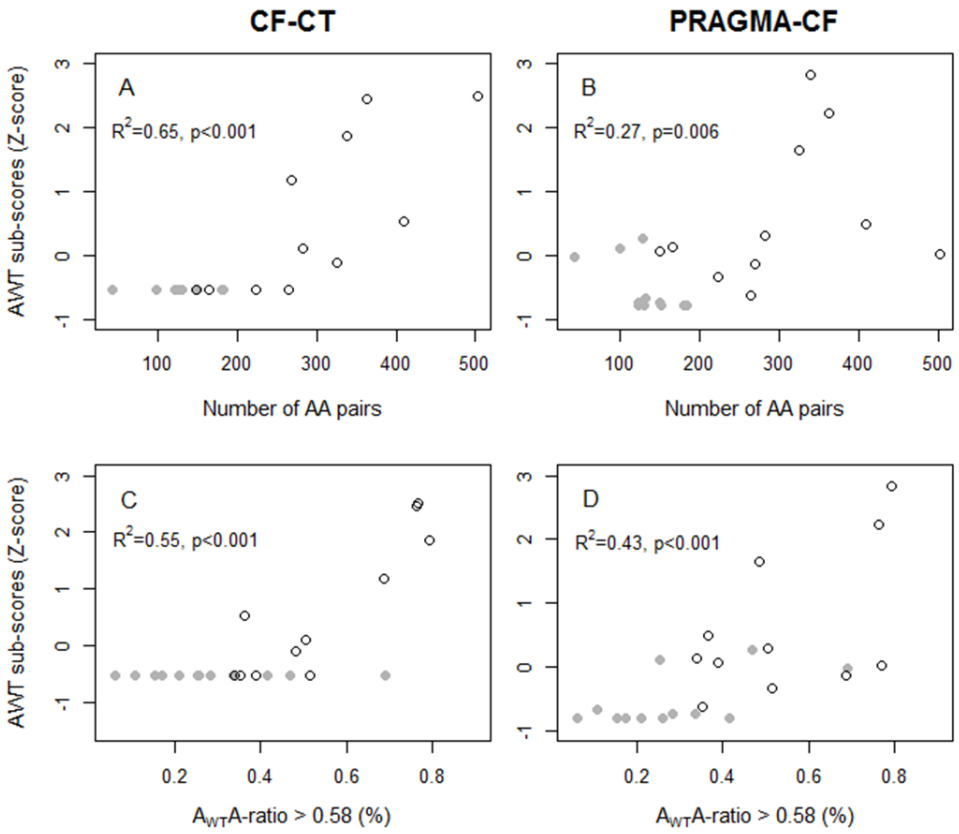

FIGURE 2. Scatterplots of CF-CT (left columns) and PRAGMA-CF (right columns) AWT sub-scores (normalized into Z-scores), to the number of AA pairs (top row) and the percentage of AA ratios above 1.11 (bottom row). CF patients are shown in black open circles and the control subjects in filled gray circles. The linear regressions were better fitted with CF-CT than PRAGMA-CF in the CF and control subjects (Table 3).

Bronchiectasis

CF-CT and PRAGMA-CF BE sub-scores were strongly correlated ($r = 0.93$, $p < 0.001$) (Appendix Figure E1a). Summary of all linear regressions is shown in Table 3. CF-CT (Figure 1a) and PRAGMA-CF BE sub-score (Figure 1b) were associated with the number of AA pairs ($R^2 = 0.53$, $p < 0.001$; $R^2 = 0.67$, $p < 0.001$, respectively). CF-CT (Figure 1c) and PRAGMA-CF BE sub-scores (Figure 1d) were associated with the percentage of AA pairs with AA-ratios > 1.11 ($R^2 = 0.41$, $p < 0.001$; $R^2 = 0.53$, $p < 0.001$, respectively).
Mixed-effect model with AA-ratios as outcome showed an AIC of -1034 with CF-CT BE, -1042 with PRAGMA-CF BE, -1048 with CF-CT TAD and -1055 with PRAGMA-CF TAD sub-score. PRAGMA-CF TAD sub-score was highest predicting AA-ratios.

Airway wall thickening

CF-CT AWT was correlated with PRAGMA-CF AWT sub-scores ($r = 0.64$, $p < 0.001$) (Appendix Figure E1b). CF-CT AWT sub-score (Figure 2a) was associated with the number of AA pairs ($R^2 = 0.65$, $p < 0.001$). PRAGMA-CF AWT sub-score (Figure 2b) was not significantly associated with the number of AA pairs ($R^2 = 0.27$, $p = 0.006$). CF-CT (Figure 2c) and the PRAGMA-CF AWT sub-score (Figure 2d) were associated with the percentage of AA pairs with an A_{WT}A-ratio > 0.58 ($R^2 = 0.55$, $p < 0.001$; $R^2 = 0.43$, $p < 0.001$, respectively).
Mixed-effect model with A_{WT}A-ratio as outcome showed an AIC of -4919 with CF-CT AWT sub-score, -4908 with PRAGMA-CF AWT sub-score, -4908 with CF-CT TAD and -4919 with PRAGMA-CF TAD. CF-CT AWT and PRAGMA-CF TAD performed equally well predicting A_{WT}A-ratio.

Total airway disease

CF-CT TAD was correlated with PRAGMA-CF TAD sub-score ($r = 0.88$, $p < 0.001$) (Appendix Figure E1c). CF-CT (Figure 3a) and PRAGMA-CF TAD sub-score (Figure 3b) were associated with the number of AA pairs ($R^2 = 0.62$, $p < 0.001$; $R^2 = 0.71$, $p < 0.001$, respectively). CF-CT (Figure 3c) and PRAGMA-CF TAD sub-score (Figure 3d) were associated with the percentage of AA pairs with AA-ratios > 1.11 ($R^2 = 0.60$, $p < 0.001$; $R^2 = 0.72$, $p < 0.001$, respectively). CF-CT (Figure 3e) and PRAGMA-CF TAD sub-score (Figure 3f) were associated with the percentage of AA pairs with A_{WT}A-ratios > 0.58 ($R^2 = 0.42$, $p < 0.001$; $R^2 = 0.57$, $p < 0.001$, respectively).

TABLE 3. AA related parameters to CT scores.

AA Method	CF-CT BE sub-score				PRAGMA-CF BE sub-score			
	Coefficient	Standard error	P-value	Adjusted R^2	Coefficient	Standard error	P value	Adjusted R^2
Number of AA pairs	5.9	1.2	<0.001*	0.53	32.3	4.8	<0.001*	0.67
Percentage AA ratio > 1.11	.01	<0.01	<0.001*	0.41	0.06	0.01	<0.001*	0.53
	CF-CT AWT sub-score				PRAGMA-CF AWT sub-score			
Number of AA pairs	10.7	1.7	<0.001*	0.65	49.2	16.2	0.006	0.27
Percentage AWT ratio > 0.58	0.02	<0.01	<0.001*	0.55	0.12	0.03	<0.001*	0.43
	CF-CT TAD sub-score				PRAGMA-CF TAD sub-score			
Number of AA pairs	8.5	1.4	<0.001*	0.62	21.1	2.8	<0.001*	0.71
Percentage AA ratio > 1.11	0.02	<0.01	<0.001*	0.60	0.04	<0.01	<0.001*	0.72
Percentage AWT ratio > 0.58	0.01	<0.01	<0.001*	0.42	0.04	<0.01	<0.001*	0.57

Results of the linear regression analysis evaluating the AA related parameters as an outcome with bronchiectasis (BE), airway wall thickening (AWT) and total disease (TAD) (sub-) score of the CF-CT and PRAGMA-CF as variables. Coefficient, standard error and p-value are of the variables in the regression and adjusted R^2 as the fit of the model. Significant p-value after Bonferroni correction is indicated by *.

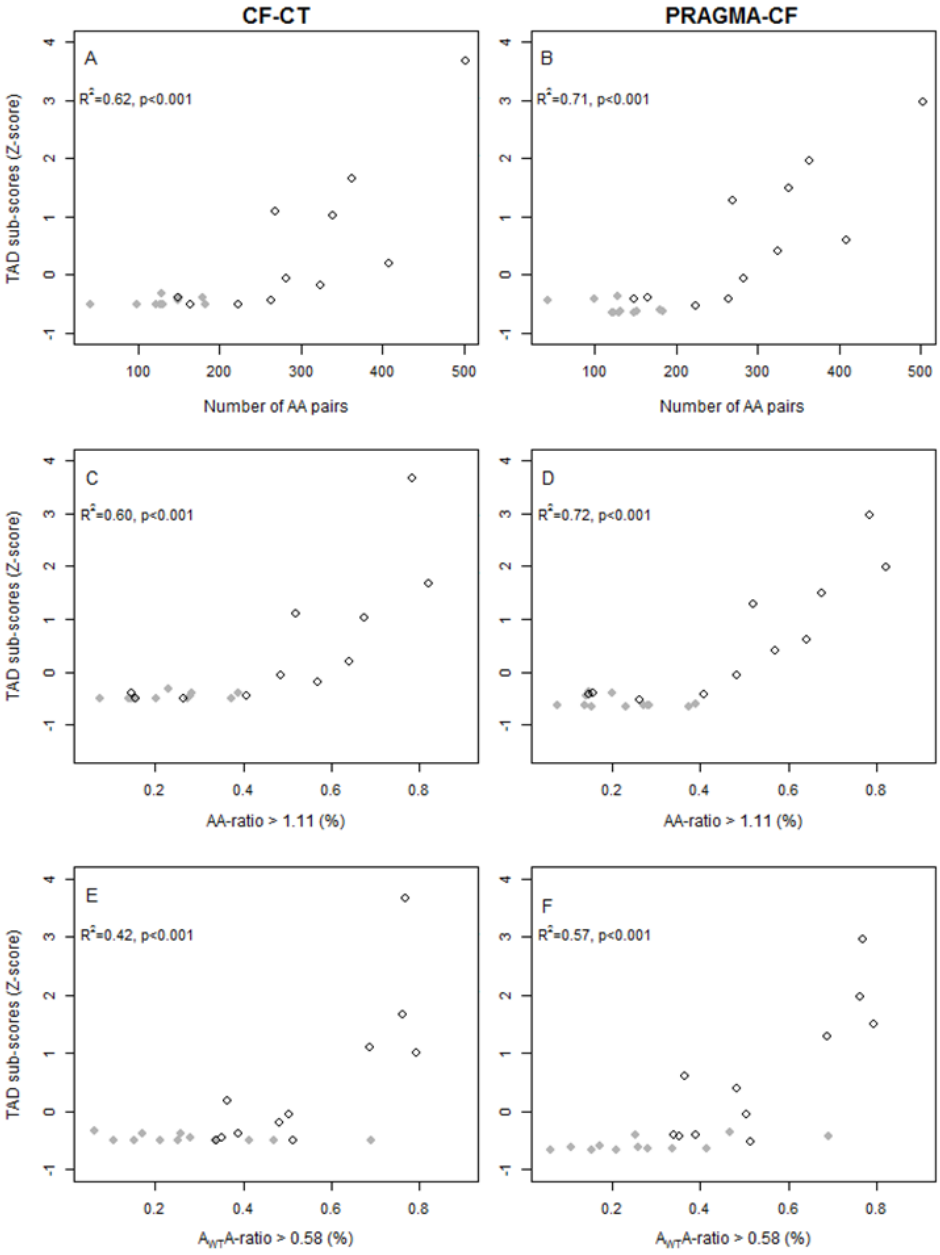

FIGURE 3. Scatterplots of CF-CT (left columns) and PRAGMA-CF (right columns) total airway disease (TAD) sub-score (normalized into Z-scores), to the number of AA pairs (top row), AA-ratio above 1.11 in percentage (middle row) and A_{WT}A-ratio>0.58 in percentage (bottom row). CF patients are shown in black open circles and the control subjects in filled gray circles. The linear regressions were better fitted with PRAGMA-CF than with CF-CT in the CF and control subjects (Table 3).

DISCUSSION

CF-CT is a frequently used CT scoring technique to quantify structural lung disease in children with CF.[3,8,19,20] PRAGMA-CF has been developed specifically for young children to quantify structural changes better in children with early CF lung disease,[6] but this has not been validated against other scoring methods previously. This study compares semi quantitative CF-CT and PRAGMA-CF sub-scores with quantitative AA dimensions in children with CF and a control group.

Our study showed that BE in children and adolescents can be scored reliably with both CF-CT and PRAGMA-CF scoring systems. CF-CT and PRAGMA-CF BE sub-scores correlated well with the number of AA pairs and with AA-ratios. Previous study by de Jong et al. also showed a correlation between AA-ratio and the Brody score (on which CF-CT scoring system was based) even when only limited AA pairs were assessed.[21] For quantification of BE in children with CF, our study showed that performance of PRAGMA-CF was better than the CF-CT scoring system.

Another important finding is that AWT can be scored using CF-CT and PRAGMA-CF AWT sub-scores as they correlated with objectively quantified A_{WT}A-ratios. Quantitatively assessed AWT was more accurately predicted with the CF-CT scoring system compared to PRAGMA-CF. This is probably due to the hierarchical system used in PRAGMA-CF.[6] Extent of airways disease is determined by grid cells overlaying axial CT images. For each grid cell only one disease component is scored using a hierarchical order. When both BE and AWT are present in the grid cell, only bronchiectasis will be scored even though bronchiectatic airways are often accompanied by AWT. This is demonstrated in our results showing that PRAGMA-CF TAD correlated better than CF-CT TAD sub-score with the number of AA pairs, AA- and A_{WT}A-ratios. PRAGMA-CF is a more quantitative method to determine structural lung disease in children compared to CF-CT.

Visual scoring of AWT is known to be difficult as illustrated by low intra- and inter-observer reproducibility of AWT sub-scores using various scoring systems,[7,22–24] and as shown with the PRAGMA-CF scoring of this study. This is likely a consequence of the airway wall being a thin structure making it more difficult to visually compare it to the adjacent artery. Manual AA-method is currently used for the development of an automated AA-system.[25] Clearly, it will be beneficial to have sensitive objective automated AA system to assess AWT in children with CF.

Next, our study confirms previous observations that the number of AA pairs visible on chest CT could be a marker for severity in CF lung disease. In a number of studies a higher number of AA pairs was observed in CF patients with more severe lung disease,[15,26] confirming the importance of small airways in CF lung disease.[27–29] Our dataset showed 299 AA pairs on average in patients with CF relative to 131 AA pairs in control subjects.[15] Elevated numbers of AA pairs in CF can easily be missed in routine clinical care, as

numbers of AA pairs are not counted and no reference values are available. Both CF-CT and PRAGMA-CF correlated significantly with the number of AA pairs, but do not take this component into account in their scorings algorithm. An important issue to address with using the number of AA pairs as a disease marker is that the number of airway branches is determined by the CT resolution. Variations in CT scanning protocol, lung volume during acquisition, patient size and growth can all affect the number of visible airways.[11,30] With standardized CT protocols and lung volume, number of AA pairs could be a sensitive marker for CF lung disease in older children without detectable airway growth on CT.[26,29]

Another unique feature of our study is that CF-CT and PRAGMA-CF scores were compared in control patients with normal chest CTs for the first time.[10] For CF-CT and PRAGMA-CF sub-scores there was a slight overlap in CF and control patients (Table 2). Similarly, AA-ratios showed overlap between CF and control patients. To some extent this overlap might be related to the fact that control patients were not healthy, as they were referred for chest CT through the pediatric respiratory department. Unfortunately, it is not feasible to study healthy children using chest CT due to ionizing radiation exposure.[31] Importantly, CTs of control and CF patients were collected from the same center using the same CT scanner. In addition, control CTs were reported as normal by two independent chest radiologists. Hence, we think that some overlap in AA-ratios between normal and abnormal subjects exists, similarly to most biomarkers.[32]

A limitation of this study was that we only studied a relatively small population. This was related to the time consuming task to quantify AA dimensions. However, due to the large numbers of AA pairs we had enough power to compare the AA-method with CF-CT and PRAGMA-CF scoring techniques.

In conclusion, both CF-CT and PRAGMA-CF were valid scoring techniques to evaluate airway disease in children aged 6 years and older with CF lung disease. Once the AA-method is automated, it can replace manual AA measurements, BE and AWT scoring for spirometer controlled inspiratory chest CTs.

ACKNOWLEDGEMENTS

The authors thank Marcel Koek from the Erasmus MC, Rotterdam, the Netherlands, for the development of the grid software used for PRAGMA-CF, and Yong Chen from General Hospital of Ningxia Medical University, Yichuan, China, for involvement of data acquisition of the control CTs.

REFERENCES

1. Foundation CF. Cystic Fibrosis Foundation Patient Registry Annual Data Report 2014. Accessed March 31, 2016. 2014.

2. Newell JD. Bronchiectasis. In: Contemporary Medical imaging. CT of the. 2008. p. 213–235.

3. Ciet P, Serra G, Bertolo S, Spronk S, Ros M, Fraioli F, Quattrucci S, Assael MB, Catalano C, Pomerri F, et al. Assessment of CF lung disease using motion corrected PROPELLER MRI: a comparison with CT. European Radiology. 2016;26(3):780–787.

4. Sileo C, Corvol H, Boelle PY, Blondiaux E, Clement A, Ducou Le Pointe H. HRCT and MRI of the lung in children with cystic fibrosis: Comparison of different scoring systems. Journal of Cystic Fibrosis. 2014;13(2):198–204.

5. Brody AS, Kosorok MR, Li Z, Broderick LS, Foster JL, Laxova A, Bandla H, Farrell PM. Reproducibility of a scoring system for computed tomography scanning in cystic fibrosis. Journal of thoracic imaging. 2006;21(1):14–21.

6. Rosenow T, Oudraad MCJ, Murray CP, Turkovic L, Kuo W, de Bruijne M, Ranganathan SC, Tiddens HAWM, Stick SM. PRAGMA-CF. A Quantitative Structural Lung Disease Computed Tomography Outcome in Young Children with Cystic Fibrosis. American journal of respiratory and critical care medicine. 2015;191(10):1158–1165.

7. Loeve M, van Hal PTW, Robinson P, de Jong PA, Lequin MH, Hop WC, Williams TJ, Nossent GD, Tiddens HAWM. The spectrum of structural abnormalities on CT scans from patients with CF with severe advanced lung disease. Thorax. 2009;64(10):876–882.

8. Tepper LA, Caudri D, Utens EMWJ, van der Wiel EC, Quittner AL, Tiddens HAWM. Tracking CF disease progression with CT and respiratory symptoms in a cohort of children aged 6-19 years. Pediatric Pulmonology. 2014;1189(February):1182–1189.

9. Wainwright CE, Vidmar S, Armstrong DS, Byrnes CA, Carlin JB, Cheney J, Cooper PJ, Grimwood K, Moodie M, Robertson CF, et al. Effect of bronchoalveolar lavage-directed therapy on Pseudomonas aeruginosa infection and structural lung injury in children with cystic fibrosis: a randomized trial. JAMA : the journal of the American Medical Association. 2011;306(2):163–171.

10. Calder AD, Bush A, Brody AS, Owens CM. Scoring of chest CT in children with cystic fibrosis: state of the art. Pediatric radiology. 2014;44(12):1496–506.

11. Mott LS, Graniel KG, Park J, De Klerk NH, Sly PD, Murray CP, Tiddens HAWM, Stick SM. Assessment of early bronchiectasis in young children with cystic fibrosis is dependent on lung volume. Chest. 2013;144(4):1193–1198.

12. De Jong PA, Nakano Y, Hop WC, Long FR, Coxson HO, Paré PD, Tiddens H a. Changes in airway dimensions on computed tomography scans of children with cystic fibrosis. American Journal of Respiratory and Critical Care Medicine. 2005;172(2):218–224.

13. Kapur N, Masel JP, Watson D, Masters IB, Chang AB. Bronchoarterial ratio on high-resolution CT scan of the chest in children without pulmonary pathology: Need to redefine bronchial dilatation. Chest. 2011;139(6):1445–1450.

14. Dournes G, Laurent F. Airway Remodelling in Asthma and COPD: Findings, Similarities, and Differences Using Quantitative CT. Pulmonary Medicine. 2012;2012:1–8.

15. Kuo W, de Bruijne M, Petersen J, Nasserinejad K, Ozturk H, Chen Y, Perez-Rovira A, Tiddens HAWM. Diagnosis of bronchiectasis and airway wall thickening in children with cystic fibrosis: Objective airway-artery quantification. European radiology. 2016:In press.

16. Lesaffre E, Lawson AB. Information theoretic measures for model selection. In: Bayesian Biostatistics. 1st ed. Wiley & Sons; 2012. p. 274–285.

17. Nishio M, Matsumoto S, Tsubakimoto M, Nishii T, Koyama H, Ohno Y, Sugimura K. Paired Inspiratory/Expiratory Volumetric CT and Deformable Image Registration for Quantitative and Qualitative Evaluation of Airflow Limitation in Smokers with or without COPD. Academic radiology. 2014;22(3):1–7.

18. R Foundation for statistical Computing. R Development Core Team. R: A Language and Environment for Statistical Computing. Vienna; 2005.

19. Loeve M, Lequin MH, de Bruijne M, Hartmann IJC, Gerbrands K, van Straten M, Hop WCJ, Tiddens H a WM. Cystic fibrosis: are volumetric ultra-low-dose expiratory CT scans sufficient for monitoring related lung disease? Radiology. 2009;253(1):223–229.

20. Tepper LA, Utens EMWJ, Caudri D, Bos AC, Gonzalez-Graniel K, Duivenvoorden HJ, Van Der Wiel ECW, Quittner AL, Tiddens HAWM. Impact of bronchiectasis and trapped air on quality of life and exacerbations in cystic fibrosis. European Respiratory Journal. 2013;42(2):371–379.

21. de Jong PA, Ottink MD, Robben SGF, Lequin MH, Hop WCJ, Hendriks JJE, Paré PD, Tiddens HAWM. Pulmonary disease assessment in cystic fibrosis: comparison of CT scoring systems and value of bronchial and arterial dimension measurements. Radiology. 2004;231(2):434–439.

22. de Jong PA, Lindblad A, Rubin L, Hop WCJ, de Jongste JC, Brink M, Tiddens HAWM. Progression of lung disease on computed tomography and pulmonary function tests in children and adults with cystic fibrosis. Thorax. 2006;61(1):80–85.

23. Stick SM, Brennan S, Murray C, Douglas T, von Ungern-Sternberg BS, Garratt LW, Gangell CL, De Klerk N, Linnane B, Ranganathan S, et al. Bronchiectasis in Infants and Preschool Children Diagnosed with Cystic Fibrosis after Newborn Screening. Journal of Pediatrics. 2009;155(5):623–628.e1.

24. Mott LS, Park J, Gangell CL, De Klerk NH, Sly PD, Murray CP, Stick SM. Distribution of early structural lung changes due to cystic fibrosis detected with chest computed tomography. Journal of Pediatrics. 2013;163(1):243–248.e3.

25. Perez-Rovira A, Kuo W, Petersen J, Tiddens H a. WM, de Bruijne M. Automated Quantification of Bronchiectasis, Airway Wall Thickening and Lumen Tapering in Chest CT. Insights Imaging. 2015;6(1):S1804-NaN-1117.

26. DeBoer EM, Swiercz W, Heltshe SL, Anthony MM, Szefler P, Klein R, Strain J, Brody AS, Sagel SD. Automated ct scan scores of bronchiectasis and air trapping in cystic fibrosis. Chest. 2014;145(3):593–603.

27. Ratjen F. Cystic Fibrosis: The role of the small airways. Journal of Aerosol Medicine and Pulmonary Drug Delivery. 2012;25(5):261–264.

28. Tiddens HAWM, Donaldson SH, Rosenfeld M, Paré PD. Cystic fibrosis lung disease starts in the small airways: Can we treat it more effectively? Pediatric Pulmonology. 2010;45(2):107–117.

29. Boon M, Verleden SE, Bosch B, Lammertyn EJ, McDonough JE, Mai C, Verschakelen J, Kemner-Van De Corput M, Tiddens HAW, Proesmans M, et al. Morphometric analysis of explant lungs in cystic fibrosis. American Journal of Respiratory and Critical Care Medicine. 2016;193(5):516–526.

30. Kuo W, Kemner-van de Corput MPC, Perez-Rovira A, de Bruijne M, Fajac I, Tiddens HAWM, et al. Multicentre chest CT standardisation in children and adolescents with cystic fibrosis : the way forward. European Respiratory Journal. 2016:1–12.

31. Kuo W, Ciet P, Tiddens HAWM, Zhang W, Guillerman RP, Van Straten M. Monitoring cystic fibrosis lung disease by computed tomography: Radiation risk in perspective. American Journal of Respiratory and Critical Care Medicine. 2014;189(11):1328–1336.

32. Kent L, Reix P, Innes JA, Zielen S, Le Bourgeois M, Braggion C, Lever S, Arets HGM, Brownlee K, Bradley JM, et al. Lung clearance index: Evidence for use in clinical trials in cystic fibrosis. Journal of Cystic Fibrosis. 2014;13(2):123–138.

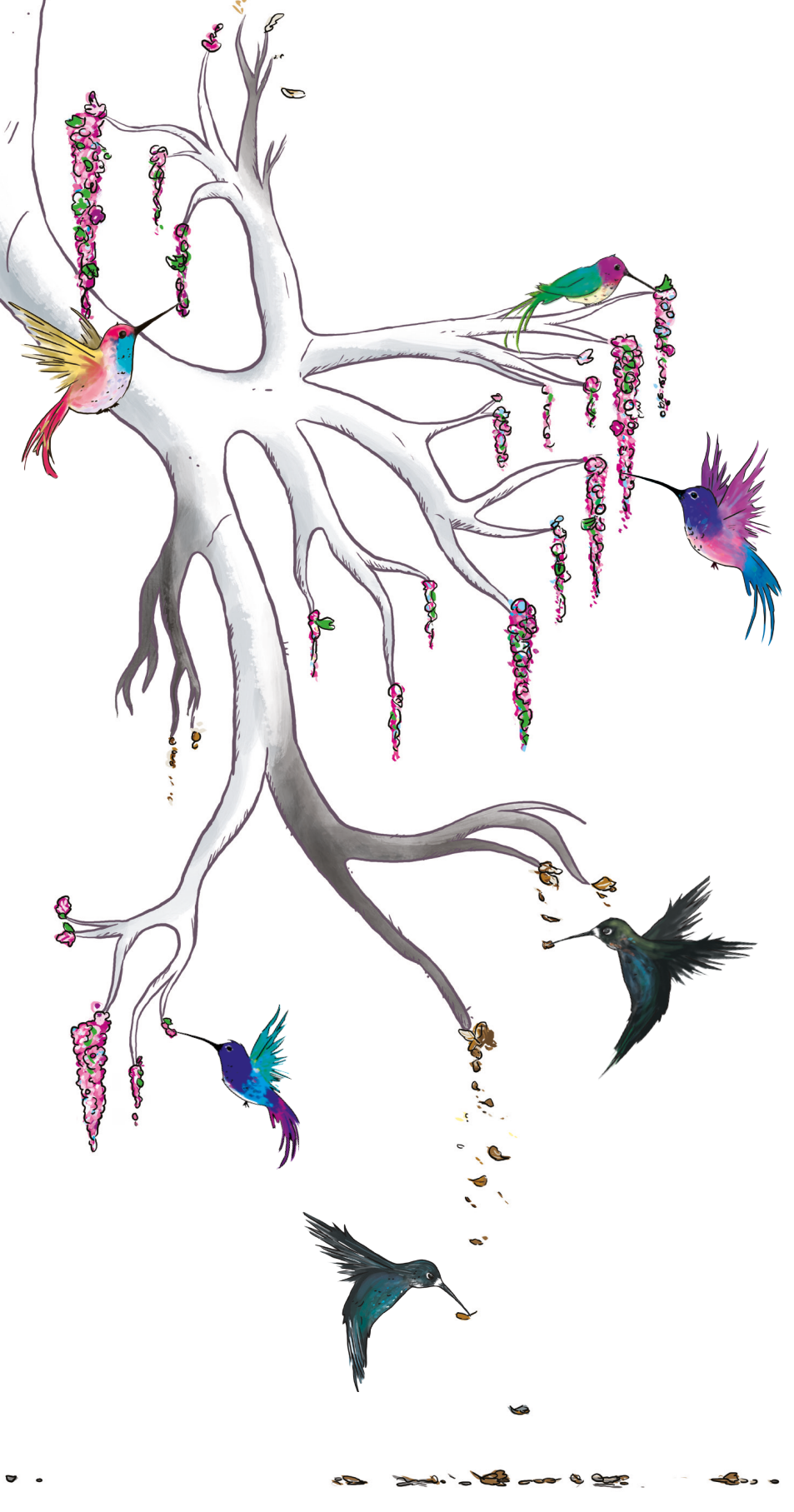

CHAPTER 7

AIRWAY TAPERING REVISITED: AN IMAGE BIOMARKER FOR BRONCHIECTASIS

Adria Perez-Rovira, Wieying Kuo, Harm A.W.M. Tiddens,
Marleen de Bruijne, on behalf of the Normal Chest CT study group

Normal Chest CT study group (in alphabetic order):
Lauren Akesson, Silvia Bertolo, Alan S. Brody, Kris de Boeck, Pim A. de Jong,
Robert J. Fleck, Francesco Fraioli, Pilar Garcia-Peña, Silvia Gartner, Edward Y. Lee,
Anders Lindblad, Michael McCartin, Christian P. Mol, Giovanni Morana, Arlette E. Odink,
Matteo Paoletti, Stephen M. Stick, Els van der Wiel, Francois Vermeulen.

Submitted

ABSTRACT

Purpose

To establish reference values for airway tapering and to assess the usability of tapering as a bronchiectasis biomarker in paediatric populations.

Methods

Reference airway tapering values were obtained from 156 computed tomography (CT) scans of an international multicentre cohort. Airway tapering as a bronchiectasis biomarker was assessed on spirometer-guided inspiratory CTs from 12 patients with bronchiectasis (11 cystic fibrosis, 1 common variable immunodeficiency) and 12 age- and gender-matched controls.

Automatic image analysis software was used to quantify intra-branch tapering (reduction in airway diameter along the branch), inter-branch tapering (reduction in airway diameter before and after bifurcation), and airway-artery ratios on chest CTs. Visual bronchiectasis sub-scores were collected for the 12 patients and matched controls.

Results

Bronchiectatic subjects showed significantly reduced inter-branch and intra-branch tapering as well as increased airway-artery ratios compared to controls. When airways were stratified by size only tapering measurements were significantly different between diseased and controls across all airway size groups. Bronchiectasis visual scores correlated better with tapering measurements than with airway-artery ratios.

Conclusion

Airway tapering is a promising biomarker for bronchiectasis, as subjects with bronchiectasis show a significant reduction in airway tapering across all airway sizes and it does not require comparison with pulmonary arteries.

INTRODUCTION

Bronchiectasis is an important characteristic of diseases such as cystic fibrosis (CF) lung disease,[1,2] chronic obstructive pulmonary disease (COPD),[1] common variable immunodeficiency (CVID),[3] tuberculosis,[4] and human immunodeficiency virus (HIV).[4] Chest computed tomography (CT) is currently the most sensitive imaging tool to detect bronchiectasis[5,6] and is a sensitive outcome measure in CF for both clinical and research purposes.[7-9]

In healthy subjects the diameter of an airway branch is similar to that of the accompanying artery[10] and there is subtle but progressive diameter reduction along the branch named intra-branch tapering.[4] In addition, diameter of the airway branch is reduced compared to the airway branch before bifurcation[11] and this is named inter-branch tapering.

Bronchiectasis is defined as an irreversible dilation of the bronchial lumen accompanied with lack of tapering.[4] Bronchiectasis is commonly quantified by comparing the airway diameter to the diameter of the accompanying artery and computing the Airway-Artery Ratio (AA-Ratio).[12-16] Lack of tapering, defined as an unchanged airway diameter for two cm after branching,[4] is also a recognized criterion for diagnosing bronchiectasis, in particular for the identification of cylindric bronchiectasis.[17] In accordance, tapering has been included in various semi-quantitative visual scoring systems for bronchiectasis.[14] Nevertheless, quantification of airway tapering has received very limited attention.

Bronchiectasis is associated with an enlargement of peripheral airways but not of the trachea or central airways[18.] We hypothesize that an abnormally dilated peripheral airway might coincide with reduced tapering further up in the bronchial tree, as shown in Figure 1. Thus, reduction in airway tapering should be observable in larger, more central airways than changes in AA-Ratio.

In this study we used newly developed state-of-the-art automated image analysis software to 1) obtain reference values for intra-branch and inter-branch tapering in patients with a normal chest CT; and to 2) assess differences in airway tapering between control patients and bronchiectatic patients, comparing the diagnostic value of airway tapering and AA-Ratios.

MATERIALS AND METHODS

This study was approved by institutional review board (MEC-2014-254 and MEC-2011-494). Written informed consent was waived for all patients because of the retrospective nature of the study.

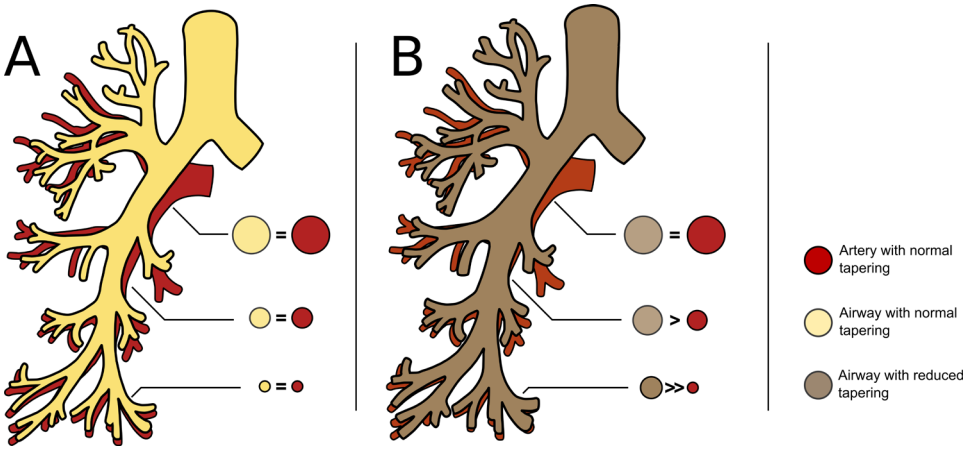

FIGURE 1. A: Bronchial tree with tapering similar to its accompanying artery, showing approximately constant airway-artery ratio. **B**: Same bronchial tree with reduced airway tapering uniformly distributed across the entire bronchial tree, showing an increased airway-artery ratio more pronounced in the more peripheral airways.

Study population

A total of 180 CT scans from three datasets were used.

Airway tapering reference values were obtained in the NormalCT dataset. This dataset consisted of 156 CTs acquired during free breathing or after a voluntary breath-hold of paediatric subjects (0 to 18 years old) found to be normal by the centre radiologist and a second radiologist (Dr. Chen Yong, 20 years experience). 42 of these 156 subjects were scanned with contrast. This NormalCT dataset is a subset from three centres participating in the international multicentre Normal Chest CT Study.

To assess differences between bronchiectatic patients and controls, the Matched-Bronchiectasis and Matched-Controls datasets were collected retrospectively. The Matched-Bronchiectasis consisted of spirometer-guided inspiratory chest CTs of 12 patients between 8 and 16 years old (11 CF and 1 non-CF bronchiectatic patient with CVID; 7 females) with visible signs of bronchiectasis. The Matched-Controls consisted of 12 spirometer-guided inspiratory scans of age- and gender-matched control patients referred for several clinical indications but found to be normal on chest CT by the Erasmus MC radiologists and a second radiologist (CY). Both groups were treated at the Erasmus MC-Sophia Children's Hospital; See Appendix for scanning and patient details. The Matched-Bronchiectasis and Matched-Controls datasets have been previously used to study changes in AA-Ratios,[10,19,20] but airway tapering has not been investigated.

Visual scores were obtained for all CTs from both Matched datasets using the CF-CT scoring module,[10,14] as detailed in the Appendix.

Automatic quantification of airways and arteries

In-house developed software (written in C++ and MATLAB) was used to measure AA-Ratio and airway tapering. The method, which has previously been validated,[20] automatically extracts the arteries and the bronchial tree using a classifier approach,[21] obtains diameter measurements every 0.5 mm via a graph-based method,[22] and pairs airway and artery branches according to their proximity and similarity in size and orientation. Because of the large variations in inspiration level and scanning protocols in the NormalCT dataset, the automatic extraction of initial airway centrelines was replaced by manually drawn airway centrelines, as detailed in the Appendix. For each airway-artery pair, the following measurements were obtained for the inner and outer airway diameter measurements separately:

Airway-artery ratio (AA-Ratio)

Ratio between airway diameter and the diameter of its accompanying artery, measured at the point where outer airway and artery were most similar in terms of size, orientation, and position.

Intra-branch tapering (intraBT)

A line ($y = mx + n$, where m is the slope of the line and n the y-intercept) was fitted to the diameters measured along the airway branch, using the bi-square weights method (see Figure 2). Intra-branch tapering was obtained as $intraBT = 100 * (-m / n)$, demonstrating the percentage reduction in airway diameter per mm along the centreline. For example, a value of 2 means that the airway diameter is reduced 2% each mm.

Inter-branch tapering (interBT)

$interBT = 100 * (1 - (d / d\_p))$, where d is the average diameter of the analysed airway branch and d_p is the average diameter of the parent airway (the airway branch one generation previously). A value of 20% would indicate that the airway branch is 20% smaller than before bifurcation.

Tapering was measured for all airways, but for ease of comparison with AA-Ratio, only measurements of airways paired with an artery are reported, unless otherwise stated.

Reference values

The median was used to summarize all airway-artery measurements per subject. For each population, the median and inter-quartile ranges were then reported as reference values.

Image biomarkers for bronchiectasis quantification

Per-subject median AA-Ratio, interBT and intraBT of inner and outer airway were compared between Matched-Bronchiectasis and Matched-Control populations to assess their value as biomarkers for bronchiectasis.

To assess changes in biomarkers for varying airway sizes, all airways from the Matched-Controls dataset were divided in three equally sized groups according to the diameter of their accompanying artery. Airways with an accompanying artery smaller than 3.08 mm, between 3.08 mm and 4.23 mm, and greater than 4.23 mm were considered small, medium, and large airways respectively. These thresholds were also applied to the Matched-Bronchiectasis and NormalCT datasets. Per subject median values of each airway size group were compared between datasets.

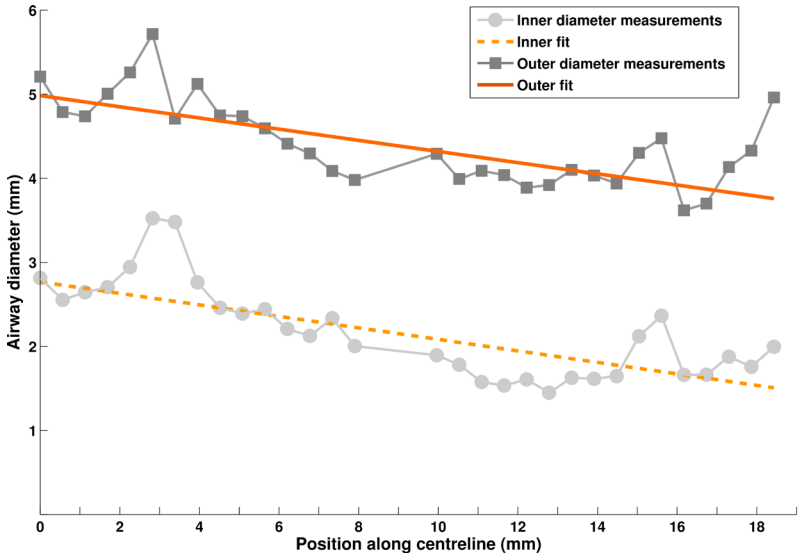

FIGURE 2. Diameter measurements along an airway branch in a control subject showing progressive reduction of diameter due to intra-branch tapering. Left (0) corresponds to the point after bifurcation (closest to the trachea), and right (19) to the point before the next bifurcation.

Stability of biomarkers under varying scanning conditions

In order to assess the stability of the extracted biomarkers to variations in scanning conditions, biomarkers extracted from the single-centre spirometry-controlled inspiration CTs from the Matched-Bronchiectasis dataset were compared to the biomarkers obtained in the CTs from the multicentre NormalCT group that included large variation in inspiration level and scanning protocols.

Statistical analysis

Differences between patient groups were assessed with Mann-Whitney U test. Spearman correlation coefficient (SCC) was used to assess correlations. P-values < 0.05 were considered significant.

RESULTS

Table 1 describes the demographics of all subjects in this study. A total of 22,275 airway branches and 153,238 artery branches were automatically extracted in the 180 CT scans analysed. Of these, 13,987 airway-artery pairs were detected and their AA-Ratio and tapering measurements were automatically measured.

TABLE 1. Demographics and visual scores

	Matched-Bronchiectasis	Matched-Controls	NormalCT
Age at CT (years)	10.58 [9.74, 11.73]	13.85 [8.72, 15.02]	10.66 [5.52, 14.99]
Gender	7 males; 5 females	7 males; 5 females	101 males; 54 females
Height (cm)	143.7 [137.4, 146.2]	149 [136.6, 170.9]	Not Available
Weight (kg)	34.25 [29.52, 40.75]	40.1 [28.58, 65.78]	Not Available
BMI	17.22 [15.64, 18.47]	18.05 [15.89, 20.19]	Not Available
CFCT BE (%) †	7.5 [1.4, 13.3]	0.0 [0.0, 0.7] *	Not Available
CFCT AWT (%) †	5.1 [0.0, 16.3]	0.0 [0.0, 0.0] *	Not Available
CFCT MP (%) †	1.4 [0.0, 18.8]	0.0 [0.0, 0.0] *	Not Available
CFCT AT (%) †	46.3 [22.2, 66.7]	3.7 [0.0, 8.3] *	Not Available
CFCT Total (%) †	8.4 [7, 17.8]	1.2 [0.4, 1.4] *	Not Available

All values are expressed as median [lower quantile, upper quartile].
* Statistically significant differences with Matched-Bronchiectasis (p-value < 0.05)
† CFCT categories are as follows BE: Bronchiectasis; AWT: Airway wall thickening; MP: Mucus plugging, AT: Air trapping.

Reference values

In the NormalCT dataset, median inner intraBT and outer intraBT were 1.16% and 0.94% respectively, expressed as a percentage reduction in diameter each mm. Median inner interBT and outer interBT were 38.54% and 23.75% respectively, expressed as the percentage diameter reduction for each airway branching.
Stratified by size, inner intraBT was 1.33%, 1.33%, 0.95%; outer intraBT was 0.94%, 1.00%, 0.93%; inner interBT was 42.02%, 39.35%, 34.20%; and outer interBT was 25.39%, 25.08%, 22.08% for small, medium and large airways respectively. See Appendix Tables E3,E4 and E5 for details.

Image biomarkers for bronchiectasis quantification

Bronchiectatic patients from the Matched-Bronchiectasis group did not show a significant difference ($p<0.470$) in inner AA-Ratio compared to the Matched-Controls population. Outer AA-Ratio was significantly increased ($p<0.022$) in Matched-Bronchiectasis compared to Matched-Controls.

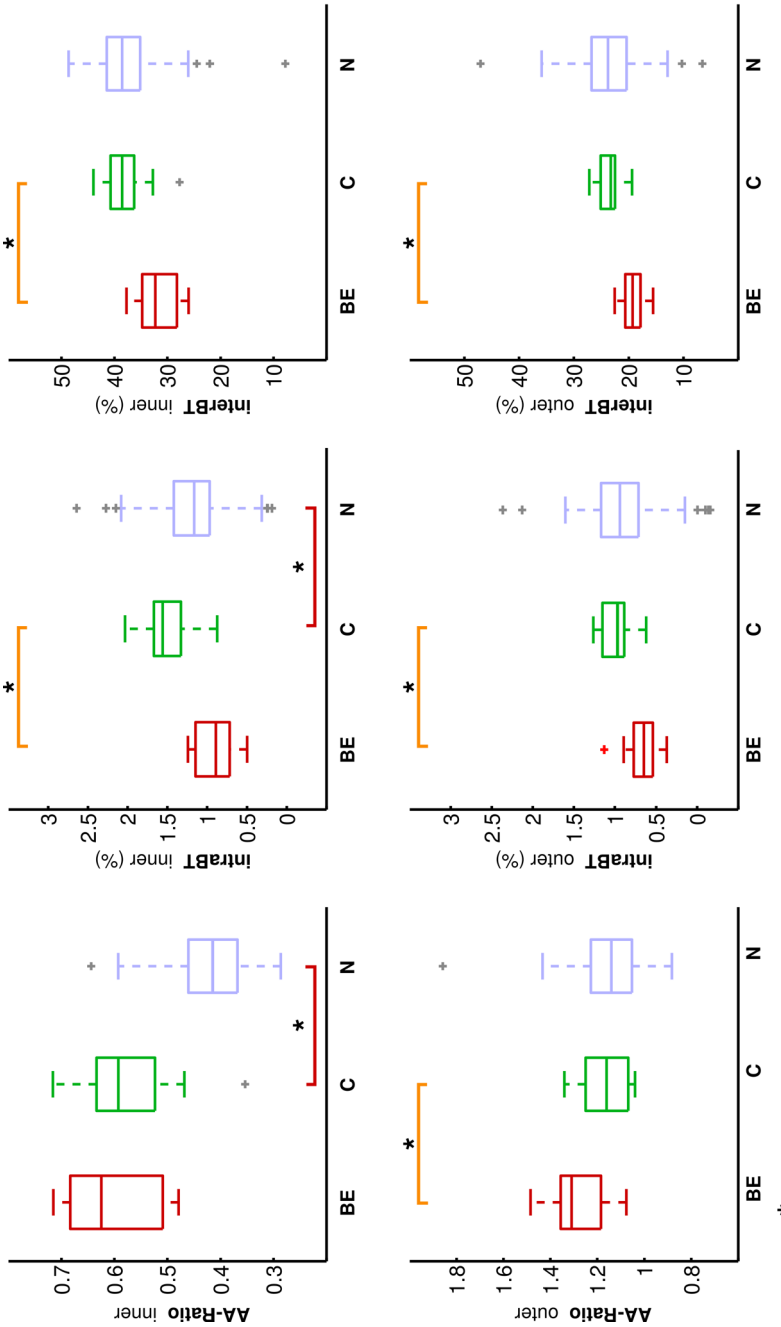

FIGURE 3. Distributions of airway-artery ratio, intra-branch tapering, and inter-branch tapering for each dataset. **BE**: Matched-Bronchiectasis; **C**: Matched-Controls **N**: NormalCT. Note that bronchiectatic subjects show significantly lower airway tapering than controls.

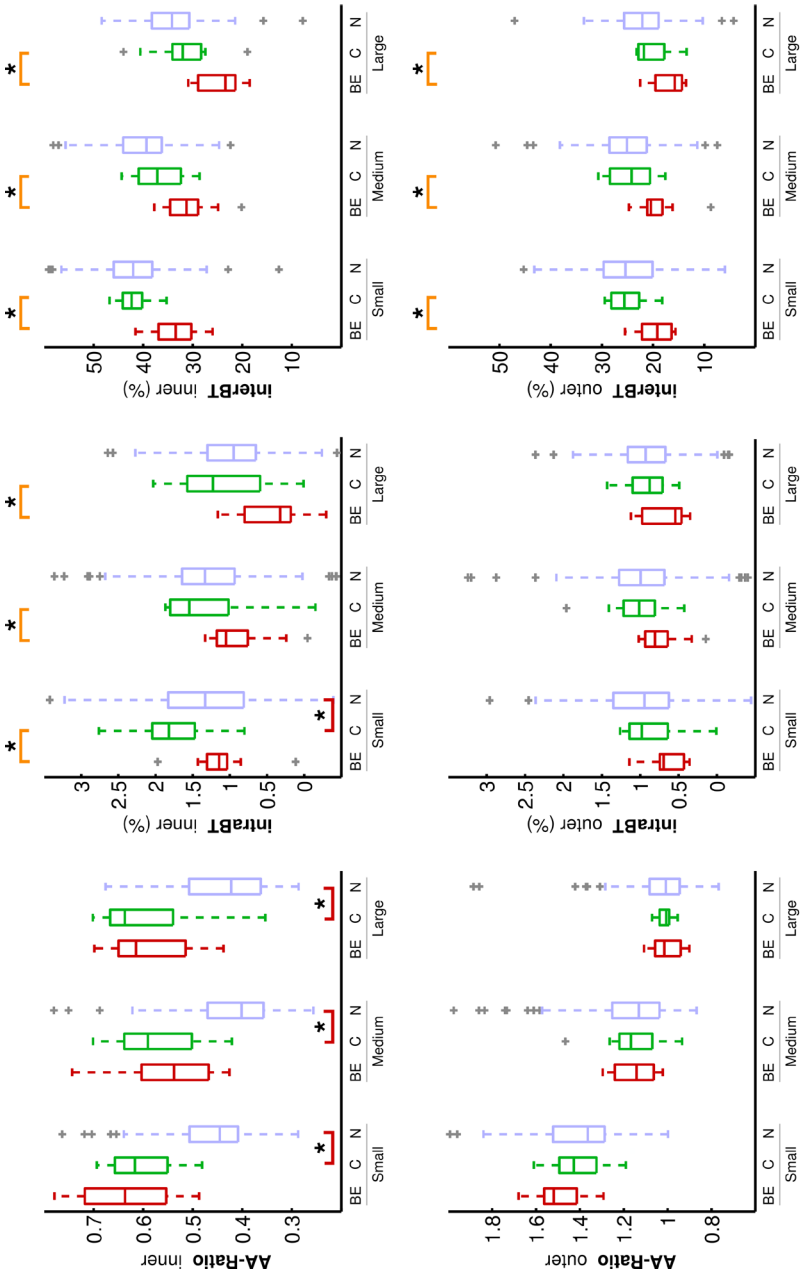

FIGURE 4. Distributions of Airway-Artery ratio, inter-branch tapering, and intra-branch tapering for small, medium and large airways, grouped by dataset. **BE**: Matched-Bronchiectasis; **C**: Matched-Controls **N**: NormalCT. Some outliers in the NormalCT that fell outside the axes range have been removed from this plot for clarity. Note that changes in airway tapering are observed across all airway sizes between bronchiectatic subjects and controls.

TABLE 2. Median, inter-quartile range, and p-values between groups for image biomarkers extracted from all airway-artery pairs

		Matched-Bronchiectasis (BE)	Matched-Controls (C)	NormalCT (N)	BE vs C	C vs N
AA-Ratio	inner	0.62 [0.51, 0.68]	0.59 [0.52, 0.63]	0.41 [0.37, 0.46]	0.4705	**0.0000**
AA-Ratio	outer	1.31 [1.18, 1.36]	1.16 [1.07, 1.25]	1.14 [1.05, 1.23]	**0.0226**	0.5173
intra-branch tapering	inner	0.89 [0.72, 1.14]	1.56 [1.33, 1.67]	1.16 [0.97, 1.42]	**0.0003**	**0.0049**
intra-branch tapering	outer	0.65 [0.54, 0.77]	0.97 [0.89, 1.15]	0.94 [0.72, 1.17]	**0.0029**	0.6757
inter-branch tapering	inner	32.28 [28.19, 34.75]	38.54 [36.26, 40.73]	38.54 [35.12, 41.43]	**0.0024**	0.9778
inter-branch tapering	outer	19.31 [17.86, 20.65]	23.23 [22.45, 25.08]	23.75 [20.41, 26.75]	**0.0005**	0.9087

TABLE 3. Correlation coefficient with visual scores of bronchiectasis (and p-value) for the different image biomarkers. Significant values ($p < 0.05$) are highlighted in bold.

Inner inter-branch tapering				**Outer inter-branch tapering**			
All	Small	Medium	Large	All	Small	Medium	Large
-0.67 (0.0004)	**-0.57 (0.0042)**	**-0.49 (0.0175)**	**-0.52 (0.0094)**	**-0.65 (0.0005)**	**-0.51 (0.0139)**	-0.31 (0.1465)	**-0.53 (0.0076)**
Inner intra-branch tapering				**Outer intra-branch tapering**			
All	Small	Medium	Large	All	Small	Medium	Large
-0.75 (0.0000)	**-0.70 (0.0002)**	**-0.65 (0.0009)**	**-0.60 (0.0021)**	**-0.56 (0.0046)**	-0.35 (0.1041)	**-0.50 (0.0144)**	**-0.44 (0.0334)**
Inner AA-Ratio				**Outer AA-Ratio**			
All	Small	Medium	Large	All	Small	Medium	Large
0.53 (0.0083)	**0.64 (0.0011)**	0.28 (0.1904)	0.14 (0.5142)	**0.75 (0.0000)**	**0.73 (0.0001)**	**0.46 (0.0272)**	0.24 (0.2631)

All inter-branch and intra-branch tapering measurements were significantly lower ($p<0.003$) in bronchiectatic subjects, compared to the matched controls.
Figure 3 shows the distribution of each image biomarker, with the descriptive statistics detailed in Table 2.
Since tapering measurements do not require a paired artery, tapering measurements for all 22,275 airways (13,987 AA-pairs and 8,288 airways without a matching artery) are also reported in Appendix Table E2. No significant differences in tapering were observed between measurements obtained from all airways and measurements obtained using only airways for which a matching artery was found.

Image biomarkers for bronchiectasis quantification, stratified by airway size

Inner and outer AA-Ratio were not significantly different between Matched-Bronchiectasis and Matched-Controls for any airway size group. In contrast, inner intraBT, inner interBT, and outer interBT were significantly lower in Matched-Bronchiectasis than in Matched-Controls for all airway size group. Outer intraBT trended to be lower ($p<0.08$) in Matched-Bronchiectasis than in Matched-Controls for all airway size groups.
Figure 4 shows the image biomarkers distribution in the three datasets divided in small, medium, and large airways. See Appendix Tables E3 to E5 for detailed values.

Stability of biomarkers under varying scanning conditions

When all airways were analysed together, inner AA-Ratio and inner intraBT were significantly different between control groups. See Figure 3 and Table 2.
When airways were stratified by size, all inner AA-Ratios and intraBT for small airways were significantly different between the spirometry-controlled subjects of the Matched-Controls and the free-breathing subjects of the NormalCT dataset. See Appendix Figure E4, and Tables E3-E5.

Correlations with visual scoring

Per-subject median values correlated well with CF-CT bronchiectasis sub-score for all biomarkers (Table 3). Only inner interBT and intraBT showed a strong and significant correlation with CF-CT bronchiectasis across all airway size groups.

DISCUSSION

Reduced airway tapering has long been known to be an important criterion to define bronchiectasis in clinical practice.[24] However, to our knowledge, this is the first study to obtain reference values for intra- and inter-branch airway tapering and to quantify tapering differences between patients with bronchiectasis and control patients.

An important finding of this study was that a significant reduction in intra-branch and inter-branch tapering was observed in bronchiectatic patients in comparison to a matched control group, for both inner and outer airway diameter. This is in concordance to the lack of tapering described visually in bronchiectatic airways in previous studies.[4,14,17]

More importantly, tapering measurements were significantly reduced in bronchiectatic subjects across all airway size groups (Figure 4) and correlated well with visual scores (Table 3). This is a clinically important finding because it suggests that lack of tapering of the larger airways (with an accompanying artery diameter larger than 4.23 mm) is associated with lack of tapering in the smaller airways reflecting a diffuse process throughout the bronchial tree. This is in contrast with AA-Ratio, which in this study was significantly increased in patients with bronchiectasis only in small airways. Previous studies also observed a more pronounced changes in AA-Ratio in the small airways of patients with bronchiectasis than in larger airways.[10,18] Hence, an increase in AA-Ratio of the small airways parallels reduced airway tapering across the bronchial tree and both can be used as independent biomarkers reflecting airway disease.

Tapering measurements offer two important advantages over AA-Ratios. First, tapering measurements do not require extraction and quantification of arteries, pairing airways with arteries, or airway generation labelling. These steps are all likely to introduce errors in an automated system. Second, and more importantly, AA-Ratio measurements assume that artery size is not affected by disease. This assumption might not hold for example in patients with pulmonary hypertension, which is commonly associated with COPD,[25] or for smokers, where increase in AA-Ratios has been shown to be driven by a reduction in vessel diameter.[26]

Another interesting finding was that significant differences in inner AA-Ratio and inner intraBT were observed between the spirometry-controlled inspiration scans of the Matched-Controls and the CTs acquired without lung volume control of the NormalCT dataset, while none of the outer airway measurements differed significantly between control groups. This is in line with previous studies[10] that reported that biomarkers derived from the outer diameter are more robust to variations in lung volume and scanning protocol.

While no reported values exist for inner and outer intra-branch tapering or outer inter-branch tapering, inner inter-branch tapering (also known as homothety ratio) has been previously reported in adult healthy subjects measured in bronchial casts[11] and CT scans[27,28] ranging between 21% and 29%. These values are lower than the median inner inter-branch tapering of 38.5% reported as reference value in this study. A possible explanation for this difference is that the automatic diameter measurements are consistently lower than measured by human observers.[20] The same absolute reduction

in diameter will then lead to higher values expressed as a percentage. Additionally, these studies analysed healthy adults while the present study analysed paediatric diseased-controls. Two previous studies have measured airway tapering in bronchiectatic subjects, focusing solely on inner inter-branch tapering computed over multiple airway branches and correlatingchanges in airway tapering with changes in visual scores. In line with the results of this study, both studies found a significant correlation between taper indices and visual scores: Odry *et al.*[29] found a correlation between inner airway tapering and visual inspection of bronchiectasis in one healthy and 8 diseased subjects. Weinheimer *et al.*[30] found a correlation between lobar inner airway taper indices and visual scores in 144 CTs of paediatric CF patients. Finally, Venkatraman *et al.*[31] detailed a method to quantify airway tapering but no measurements were reported.

This study has several limitations. A first limitation is the small number of subjects with bronchiectasis analysed. However the high number of airways analysed per CT meant that 2,398 airways were analysed on the 12 Matched-Bronchiectasis CTs. A second limitation is that the control groups might be affected by other diseases. All control subjects were checked by two independent radiologists who discarded any subject with signs of lung abnormalities or bronchiectasis on the CT scan, but we cannot exclude that subtle signs of lung abnormality may have been missed which could have reduced the differences between bronchiectatic and control groups. A third limitation is that median values were analysed, and therefore pathological changes that affect only a minority of airways in each subject or each airway size group within a subject might have been missed. A fourth and final limitation is that a previous study that used the same dataset[10] found significant differences in outer AA-Ratio between healthy and bronchiectatic subjects when airways were stratified by generation. This differs from the current study, where no significant differences in outer AA-Ratio were found between diseased and controls when airways where stratified by size. This discrepancy might be explained because in this study the median outer AA-Ratio of each airway group and subject was used to assess differences between diseased and controls in order top cope with spurious measurements, while the previous study included all AA-Ratio measurements in a mixed model analysis, leading to higher statistical power.

In conclusion, we demonstrated that with the use of automated medical image analysis techniques it is possible to quantify airway tapering in chest CTs of paediatric patients with and without bronchiectasis. We reported tapering reference values, showed that tapering changes associated with CF bronchiectasis occur nearly uniformly across all airway sizes, and that airway tapering changes can be readily observed in larger airways than changes in AA-Ratios.

REFERENCES

1 King PT. The pathophysiology of bronchiectasis. *Int. J. Chron. Obstruct. Pulmon. Dis.* 2009;4:411–9.

2 Loeve M, van Hal PThW, Robinson P, et al. The spectrum of structural abnormalities on CT scans from patients with CF with severe advanced lung disease. *Thorax*. 2009; 4(10):876–82.

3 Maarschalk-Ellerbroek LJ, de Jong PA, van Montfrans JM, et al. CT Screening for Pulmonary Pathology in Common Variable Immunodeficiency Disorders and the Correlation with Clinical and Immunological Parameters. *J Clin Immunol.* 2014;34(6):642–654.

4 Newell JD. Contemporary Medical Imaging: CT of the Airways. Totowa, NJ: Humana Press 2008.

5 Dodd JD, Souza CA, Muller NL. Conventional high-resolution CT versus helical high-resolution MDCT in the detection of bronchiectasis. *AJR Am J Roentgenol.* 2006;187(2):414–20.

6 Ciet P, Serra G, Bertolo S, et al. Assessment of CF lung disease using motion corrected PROPELLER MRI: a comparison with CT. *Eur Radiol.* 2016;26(3):780-787.

7 Tepper L, Caudri D, Utens EMWJ, et al. Tracking CF disease progression with CT and respiratory symptoms in a cohort of children aged 6-19 years. *Pediatr Pulmonol.* 2014;1189:1182–9.

8 Tiddens HAWM, Rosenow T. What did we learn from two decades of chest computed tomography in cystic fibrosis? *Pediatr Radiol.* 2014;44(12):1490-5.

9 Bortoluzzi CF, Volpi S, D'Orazio C, et al. Bronchiectasis at early chest computed tomography in children with cystic fibrosis are associated with increased risk of subsequent pulmonary exacerbations and chronic pseudomonas infection. *J Cyst Fibros* 2014;13(5):564–571.

10 Kuo W, de Bruijne M, Petersen J, et al. Diagnosis of bronchiectasis and airway wall thickening in children with cystic fibrosis: Objective airway-artery quantification. European Radiology. 2017. [*Ahead of print*]

11 Weibel E, Gomez M. Architecture of the human lung. *Science,* 1962;137:577-585.

12 Wielpütz MO, Eichinger M, Weinheimer O, et al. Automatic Airway Analysis on Multidetector Computed Tomography in Cystic Fibrosis: Correlation With Pulmonary Function Testing. *J. Thorac. Imaging* 2013;28(2):104–113.

13 Smith BM, Hoffman E, Rabinowitz D, et al. Comparison of spatially matched airways reveals thinner airway walls in COPD. The Multi-Ethnic Study of Atherosclerosis (MESA) COPD Study and the Subpopulations and Intermediate Outcomes in COPD Study (SPIROMICS). *Thorax* 2014;69(11):987–996.

14 Brody AS, Kosorok MR, Li Z, et al. Reproducibility of a scoring system for computed tomography scanning in cystic fibrosis. *J Thorac Imaging* 2006;21(1):14–21.

15 Kapur N, Masel JP, Watson D, et al. Bronchoarterial ratio on high-resolution CT scan of the chest in children without pulmonary pathology: Need to redefine bronchial dilatation. *Chest* 2011;139(6):1445–50.

16 Mott LS, Graniel KG, Park J, et al. Assessment of early bronchiectasis in young children with cystic fibrosis is dependent on lung volume. *Chest* 2013;144(4):1193–8.

17 Naidich DP, Webb WR, Muller NL, et al. Computed Tomography and Magnetic Resonance of the thorax. Philadelphia, PA: Lippincott Williams & Wilkins 2007.

18 Tiddens HW, Donaldson SH, Rosenfeld M, et al. Cystic fibrosis lung disease starts in the small airways: can we treat it more effectively?, *Pediatr. Pulmonol.* 2010;45(2):107–117.

19 W. Kuo, E-R. Andrinopoulou, A. Perez-Rovira A, et al. Objective airway artery dimensions compared to CT scoring methods assessing structural cystic fibrosis lung disease. *Journal of Cystic Fibrosis* 2016.

20 Perez-Rovira A, Kuo W, Petersen J, et al. Automatic airway-artery analysis on lung CT to quantify airway wall thickening and bronchiectasis. *Medical physics* 2016;43(10):5736-5744.

21 Lo P, Sporring J, Ashraf H, Pedersen J, et al. Vessel-guided airway tree segmentation: A voxel classification approach. *Med Image Anal* 2010;14(4):527–538.

22 Petersen J, Nielsen M, Lo P, et al. Optimal surface segmentation using flow lines to quantify airway abnormalities in chronic obstructive pulmonary disease. *Med Image Anal* 2014;18(3):531-541.

23 Hamutcu R, Rowland JM, Horn MV, et al. Clinical findings and lung pathology in children with cystic fibrosis. *Am J Respir Crit Care Med* 2002; 165:1172–1175.

24 Kang EY, Miller RR, Müller NL. Bronchiectasis: comparison of preoperative thin-section CT and pathologic findings in resected specimens. *Radiology* 1995;195(3):649–654.

25 Chaouat A, Naeije R, Weitzenblum E. Pulmonary hypertension in COPD. *J Eur Soc Clin Respir Physiol* 2008;32(5):1371–1385.

26 Diaz AA, Young TP, Maselli DJ, et al. Quantitative CT measures of bronchiectasis in smokers. *Chest* 2016. [*Ahead of print*]

27 Tawhai M. CT-based geometry analysis and finite element models of the human and ovine bronchial tree. *J Appl Physiol* 2004;97:2310-2321.

28 Montaudon M, Desbarats P, Berger P, et al. Assessment of bronchial wall thickness and lumen diameter in human adults using multi-detector computed tomography: comparison with theoretical models. *J Anat* 2007;211:579-588.

29 Odry BL, Kiraly AP, Novak CL, et al. Automated airway evaluation system for multi-slice computed tomography using airway lumen diameter, airway wall thickness and broncho-arterial ratio. *SPIE, Medical Imaging: Physiology, Function, and Structure from Medical Images* 2006;6143:11.

30 Weinheimer O, Wielpütz MO, Konietzke P, et al. Fully automated lobe-based airway taper index calculation in a low dose MDCT CF study over 4 time-points. SPIE Medical Imaging: Image Processing 2017; 101330U. [*Ahead of print*]

31 Venkatraman R, Raman R, Raman B, et al. Fully automated system for three-dimensional bronchial morphology analysis using volumetric multidetector computed tomography of the chest. *J Digit Imaging* 2006;19(2):132–139.

APPENDIX

MATERIALS AND METHODS

Detailed description of datasets used

Matched-Bronchiectasis: Spirometer-guided inspiratory chest computed tomography (CTs) of 12 patients with bronchiectasis (11 cystic fibrosis and 1 common variable immunodeficiency) on CT were selected retrospectively between 2007 and 2012. All patients were treated at Erasmus MC-Sophia Children's Hospital. Inclusion criteria were: age between 6 and 17 years old, spirometer guided chest CT acquired with SOMATOM® Definition Flash CT scanner (Siemens Healthcare, Forchheim, Germany). Exclusion: bad image quality due to motion artefacts; negative remark on breath hold performance by lung function technician. The dataset initially consisted of 12 randomly selected CF patients that meet the selection criteria of which the subject with common variable immunodeficiency was mislabelled.

Matched-Controls: Spirometer guided inspiratory chest CTs of 12 subjects without lung abnormalities on CT acquired with SOMATOM® Definition Flash scanner. Subjects were referred to Erasmus MC-Sophia Children's Hospital due clinical reasons for CT other than CF with the Erasmus MC radiology report stating chest CT to be normal, and confirmed as normal by a second independent radiologist (Dr. Chen Yong, 20 years of experience in thoracic imaging) who was blinded to patient identifiers and information. Out of 16 chest CTs that met the above mentioned criteria, we selected the 12 CTs with best matched ages to the Matched-Bronchiectasis group.

NormalCT: The Children Chest CT Study Group is a group of 10 multinational centres who retrospectively collected chest CTs of children aged 0-19 years old. Inspiration and expiration Chest CTs were made for various diagnostic indications but reported as normal by the centre's radiologist. All patient data was anonymized, with the exception of gender and age at the time of exam. Scans were sent to Erasmus MC where a second radiologist (CY, 20 years experience in thoracic imaging) discarded any scans not assessed as normal. A subset of 156 CTs from 3 different centres were ready to be analysed at the time of this study: Barcelona (Spain), Boston (United States), and Utrecht (the Netherlands). 42 scans (27.10%) were obtained with contrast. 82 scans (52.90%) were not spirometry-controlled or pressure-controlled and no information was available for the rest.

CT scanning parameters

End-inspiratory volumetric acquisitions from the Matched cohorts were obtained with a SOMATOM® Definition Flash scanner (Siemens Healthcare, Forchheim, Germany) under spirometry-guided conditions. Subjects from the NormalCT cohort were scanned in 6 different scanners mainly without lung volume control. Details of the scan parameters are provided in e-Table 1 of this Appendix.

CF-CT visual scores

All de-identified CTs from the Matched datasets (both diseased and controls) were scored (Hadiye Ozturk, 1 year experience) in random order for structural changes using the CF-CT scoring module.[1,2] The CF-CT scoring system evaluates the five lung lobes and lingula for severity and extent of bronchiectasis, airway wall thickening, mucous plugging, and opacities on inspiratory CT. Only the CF-CT score component regarding bronchiectasis is reported in this study.

Automatic quantification of airways and arteries

Initial coarse segmentations of airway lumen for both Matched datasets, and for arteries in all scans, were obtained automatically using a voxel classifier approach.[3]

For the Normal CT dataset, where large variability exists between CTs in terms of scanning protocols and levels of inspiration, we opted for a semi-automated approach to obtain the initial coarse segmentation of airway lumen. First an automatic segmentation was obtained using the region growing algorithm tool of Myrian® (v1.16.2, Lung XP module) image analysis platform (Intrasense, Montpellier, France) and then the segmentation was refined manually using the same platform to include all airway branches and remove false positives. A full CT was annotated in around 1 hour.

All initial segmentations were automatically refined using a graph-cut method to detect the inner and outer surfaces of the airways and the artery surfaces.[4] Next, artery and inner and outer airway diameter measurements were extracted every 0.5 mm along the centrelines. Diameter measurements of airway and artery branches shorter than 5 mm were not considered reliable and were discarded. Airway and artery branches located in close proximity and with similar orientation and size were automatically paired together as airway-artery pairs, using the formulation described in Perez-Rovira *et al.*[5]

To adjust for variations in lung size due to differences in subject size, gender, and inspiration level, all centrelines and associated diameter measurements were isotropically rescaled using the cubic root of the lung volume measured in CT to correspond to a lung of 4 litres in volume, which is close to the mean measured lung volume of all scans.

RESULTS

Image biomarkers for bronchiectasis quantification, stratified by airway size

Appendix Tables E3 to E5 detail the descriptive statistics of the Figure 4 shown in the main document. In these the median and distribution of each image biomarker are shown for each datasets divided in small, medium, and large airways.

APPENDIX TABLE E1. Scan parameters used to obtain the CTs.

	Matched-Bronciectasis	Matched-Controls	NormalCT
Scanner model	SOMATOM Definition Flash	SOMATOM Definition Flash	Brilliance 16P (x18), Brilliance 64 (x90), Mx8000 IDT 16 (x1), SOMATOM Definition AS+ (x12), Sensation 16 (x2), Sensation 64 (x19)
Slice thickness (mm)	1.00 (0.75, 1.00)	1.00 (1.00, 1. 00)	1.50 (0.75, 2.00)
Reconstruction increment (mm)	0.60 (0.30, 1.00)	0.80 (0.60, 0.80)	1.00 (0.40, 1.50)
Reconstruction kernel	B70f (x5), B75f (x7)	B75f (x5), I70f\3 (x7)	B (x5), B20f (x5), B30f (x1), B50f (x4), B60f (x7), B70f (x16), C (x20), D (x1), L (x14), YA (x81), YB (x2)
Tube voltage (kV)	80 (80 - 80)	100 (80, 120)	120 (80, 120)
CTDI	0.74 (0.57, 0.83)	0.76 (0.32, 1.13)	1.90 (0.40, 17.60) *

Values expressed as: median (min, max).
** 21 scans did not include CTDI data*

APPENDIX TABLE E2. Median, lower and upper quartiles, and p-values between groups of image biomarkers extracted from all airways, including airways not paired to artery.

		Matched-Bronchiectasis (BE)	Matched-Controls (C)	NormalCT (N)	BE vs C	C vs N
intra-branch tapering	inner	0.91 [0.73, 1.12]	1.55 [1.29, 1.71]	1.10 [0.92, 1.33]	**0.0007**	**0.0006**
intra-branch tapering	outer	0.62 [0.54, 0.78]	1.03 [0.89, 1.14]	0.98 [0.79, 1.18]	**0.0009**	0.6912
inter-branch tapering	outer	30.62 [26.88, 32.01]	36.73 [34.84, 38.13]	36.76 [33.03, 39.26]	**0.0011**	1.0000
inter-branch tapering	outer	18.40 [18.19, 19.29]	23.01 [22.23, 24.82]	22.60 [19.98, 25.28]	**0.0001**	0.3971

APPENDIX TABLE E3. Median, lower and upper quartiles, and p-values between groups for image biomarkers extracted from small airways paired to an artery.

		Matched-Bronchiectasis (BE)	Matched-Controls (C)	NormalCT (N)	BE vs C	C vs N
AA-Ratio	inner	0.64 [0.55, 0.72]	0.62 [0.55, 0.66]	0.45 [0.41, 0.51]	0.3099	**0.0000**
AA-Ratio	outer	1.52 [1.41, 1.56]	1.43 [1.32, 1.49]	1.36 [1.29, 1.52]	0.0605	0.7304
intra-branch tapering	inner	1.14 [1.04, 1.31]	1.82 [1.47, 2.04]	1.33 [0.81, 1.83]	**0.0028**	**0.0414**
intra-branch tapering	outer	0.69 [0.43, 0.75]	0.98 [0.64, 1.14]	0.94 [0.63, 1.35]	0.0794	0.8461
inter-branch tapering	inner	33.42 [30.29, 36.89]	42.32 [40.19, 44.15]	42.02 [38.17, 45.95]	**0.0006**	0.8968
inter-branch tapering	outer	19.18 [16.39, 22.16]	25.60 [22.70, 28.16]	25.39 [20.08, 29.65]	**0.0028**	0.9612

APPENDIX TABLE E4. Median, lower and upper quartiles, and p-values between groups for image biomarkers extracted from medium airways paired to an artery.

		Matched-Bronchiectasis (BE)	Matched-Controls (C)	NormalCT (N)	BE vs C	C vs N
AA-Ratio	inner	0.54 [0.47, 0.60]	0.59 [0.50, 0.64]	0.40 [0.36, 0.47]	0.4060	**0.0000**
AA-Ratio	outer	1.14 [1.06, 1.24]	1.17 [1.07, 1.22]	1.13 [1.04, 1.25]	0.9755	0.8498
intra-branch tapering	inner	1.05 [0.76, 1.18]	1.54 [1.02, 1.80]	1.33 [0.94, 1.64]	**0.0247**	0.4786
intra-branch tapering	outer	0.81 [0.64, 0.93]	1.01 [0.81, 1.22]	1.00 [0.69, 1.28]	0.0605	0.8278
inter-branch tapering	inner	31.26 [28.90, 34.58]	37.13 [32.37, 40.93]	39.35 [36.26, 44.04]	**0.0210**	0.0849
inter-branch tapering	outer	20.41 [18.14, 21.12]	24.19 [20.58, 28.42]	25.08 [21.23, 28.52]	**0.0289**	0.7511

APPENDIX TABLE E5. Median, lower and upper quartiles, and p-values between groups for image biomarkers extracted from large airways paired to an artery.

		Matched-Bronchiectasis (BE)	Matched-Controls (C)	NormalCT (N)	BE vs C	C vs N
AA-Ratio	inner	0.61 [0.51, 0.65]	0.64 [0.54, 0.67]	0.42 [0.36, 0.51]	0.5444	**0.0000**
AA-Ratio	outer	1.02 [0.94, 1.06]	1.01 [0.99, 1.04]	1.01 [0.95, 1.08]	0.8852	0.9679
intra-branch tapering	inner	0.32 [0.18, 0.80]	1.23 [0.59, 1.57]	0.95 [0.65, 1.30]	**0.0086**	0.2633
intra-branch tapering	outer	0.54 [0.46, 0.97]	0.88 [0.71, 1.10]	0.93 [0.67, 1.16]	0.0606	0.9038
inter-branch tapering	inner	23.41 [21.38, 28.89]	32.01 [28.31, 34.10]	34.20 [30.67, 38.24]	**0.0086**	0.1699
inter-branch tapering	outer	15.75 [14.32, 19.54]	21.78 [17.79, 22.85]	22.08 [18.90, 25.65]	**0.0262**	0.1532

REFERENCES

1 Kuo W, de Bruijne M, Petersen J, et al. Diagnosis of bronchiectasis and airway wall thickening in children with cystic fibrosis: Objective airway-artery quantification. European Radiology. 2017. [*Ahead of print*]

2 Brody AS, Kosorok MR, Li Z, et al. Reproducibility of a scoring system for computed tomography scanning in cystic fibrosis. *J Thorac Imaging* 2006;21(1):14–21

3 Lo P, Sporring J, Ashraf H, Pedersen J, et al. Vessel-guided airway tree segmentation: A voxel classification approach. *Med Image Anal* 2010;14(4):527–538.

4 Petersen J, Nielsen M, Lo P, et al. Optimal surface segmentation using flow lines to quantify airway abnormalities in chronic obstructive pulmonary disease. *Med Image Anal* 2014;18(3):531-541.

5 Perez-Rovira A, Kuo W, Petersen J, et al. Automatic airway-artery analysis on lung CT to quantify airway wall thickening and bronchiectasis. *Medical physics* 2016;43(10):5736-5744.

PART III

PEDIATRIC REFERENCE VALUES FOR CHEST CT BASED BIOMARKERS

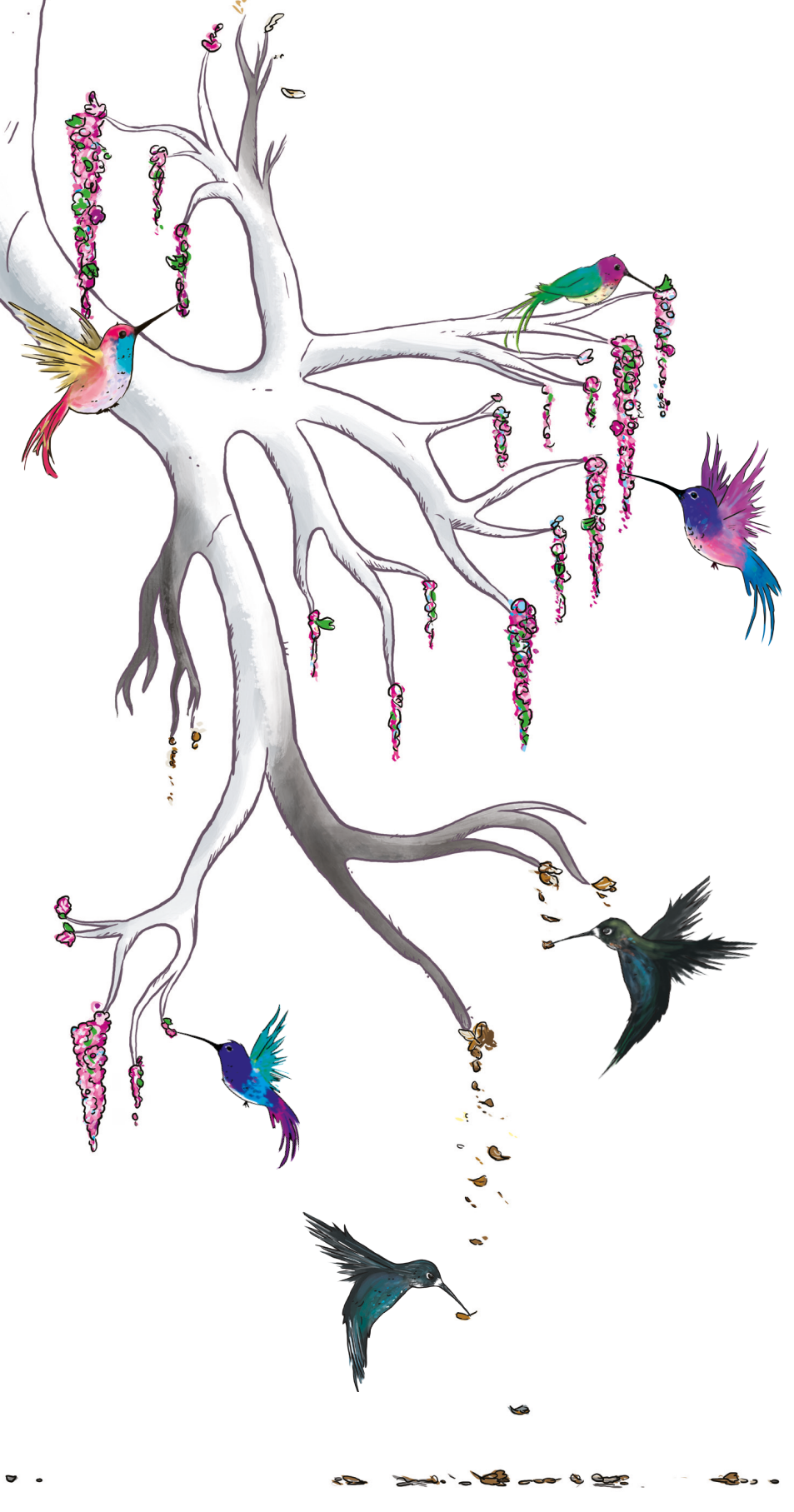

CHAPTER 8

REFERENCE VALUES FOR CENTRAL AIRWAY DIMENSIONS ON CT OF CHILDREN AND ADOLESCENTS

Wieying Kuo, Pierluigi Ciet, Eleni-Rosalina Andrinopoulou, Chen Yong, Bas Pullens, Pilar Garcia-Peña, Robert J. Fleck, Matteo Paoletti, Michael McCartin, Francois Vermeulen, Giovanni Morana, Edward Y. Lee, Harm A.W.M. Tiddens on behalf of the Normal Chest CT study group.

Normal Chest CT study group (in alphabetic order):
Lauren Akesson, Silvia Bertolo, Alan S. Brody, Kris de Boeck, Pim A. de Jong, Robert J. Fleck, Francesco Fraioli, Pilar Garcia-Peña, Silvia Gartner, Edward Y. Lee, Anders Lindblad, Michael McCartin, Christian P. Mol, Giovanni Morana, Arlette E. Odink, Matteo Paoletti, Stephen M Stick, Els van der Wiel, Francois Vermeulen.

American Journal of Roentgenology.
2017; in press

ABSTRACT

Objective

To provide normative data of central airway dimensions on chest CT in the pediatric population.

Methods

Chest CTs reported as normal by a radiologist were collected retrospectively in ten international centers. An experienced and independent thoracic radiologist reevaluated all CTs for image quality and for normality. Semi-automated image analysis (Myrian®, Intrasense, Montpelier, France) was performed to measure dimensions of trachea, right (RMB) and left main bronchus (LMB) at inspiration. Intrathoracic tracheal length was measured from carina to thorax inlet. Cross sectional area, short and long axes were measured perpendicular to the longitudinal airway axis starting from carina every cm upwards for the trachea and every 0.5 cm downwards for the main bronchi. The effect of age, gender, intrathoracic tracheal length and distance from carina on airway diameters was investigated using mixed-effect models analysis.

Results

Out of 1160 CTs collected, 390 (33.6%) were evaluated normal by the independent radiologist with sufficient image quality and adequate inspiratory volume level. Central airways were successfully semi-automatically analyzed in 294 (75.4%) out of 390 CTs. Age, gender, intrathoracic tracheal length and distance from carina were all significant predictors in the models for tracheal, RMB and LMB diameters ($p<0.001$). The central airway dimensions increased with age up to 20 years and dimensions were larger in adolescent males compared to females.

Conclusion

Normative data were determined for the central airways of children and adolescents. Central airway dimensions were dependent on distance from the carina and on the patient's intrathoracic tracheal length.

INTRODUCTION

Currently, central airway dimensions can be accurately assessed with chest computed tomography (CT). Unlike bronchoscopy, chest CT is a non-invasive method and can allow objective measurements of the central airway dimensions.[1] Configuration and dimensions of the central airways have shown to be dependent on age in children.[2–4] The integrity of the central airways is an important determinant for lung health. Several congenital and acquired abnormalities of the intrathoracic airways cause reduction in the dimensions of the trachea or mainstem bronchi, which can lead to mortality and morbidity such as severe and chronic respiratory symptoms.[5] For the objective assessment of central airway dimensions, comparison to a reference population is needed.[6] Normative data can be used to assess and diagnose various central airway structural abnormalities such as trachea-broncho-megaly,[7] tracheobronchomalacia,[8] congenital or acquired stenosis[9,10] or extrinsic compression by surrounding mediastinal masses or vascular anomalies.[11,12] Reference values can especially be valuable for radiologists, anesthesiologists, pediatricians, otolaryngologists and thoracic surgeons.

Normative dimensions of the trachea are currently based on studies with small sample sizes,[13] studies in adults[14] or on studies more than 30 years old using older generation CT scanners.[4,15] To the best of our knowledge, mainstem bronchus dimensions have never been assessed on CT of pediatric patients. In addition, the dimensions of the trachea have only been assessed at few tracheal points and not over its entire intrathoracic length from the carina to the thoracic inlet. Finally, in the previous studies, central airway dimensions were obtained with manual measurements, and not with semi-automatic segmentation software, which reduces operator dependency and lead to more objective measurements.[16]

Prospective and systematic assessment of central airways in healthy growing children using chest CT would involve exposure to ionizing radiation and may therefore be considered unethical.[17] In order to overcome these limitations while obtaining pediatric CT reference values, the *Children Chest CT study group* was founded to collect chest CTs, obtained for various clinical indications, and eventually considered to be normal by the reporting radiologist. This study aimed to provide normative data of central airway dimensions on chest CT in the pediatric population.

METHODS

This study was approved by institutional review board (IRB) at the Erasmus Medical Center (MEC-2011-494), followed by approval by the local IRB from each participating institution. Written informed consent was waived for all subjects because of the retrospective study design.

Study population

Chest CTs of children and adolescents were collected retrospectively by the international multicenter *Children Chest CT study group*. Details on participated centers are included in the Appendix. CT data were collected between December 2011 and March, 2013 and CT scans were made from 2003 to 2013 for various diagnostic indications. Inclusion criteria were: all chest CT protocols, age at the time of CT between 0 and 20 years old; normal trachea, lung and heart according to the radiologist's report.

CT scanning and scoring

All CTs were anonymized for patient specific and clinical information by the participating centers and sent to the Erasmus MC LungAnalysis core laboratory for further analysis. An independent radiologist (CY, 20 years of experience in pediatric thoracic imaging) reevaluated all CTs made in supine position for image quality and abnormalities. CTs were included for this study if they fulfilled the following requirements: no pulmonary, thoracic cavity or cardiac abnormalities; contiguous helical CT acquisition overlap in the images defined as slice thickness > reconstruction increment; sufficient inspiratory lung volume as defined by a round shape of the trachea and presence of lung parenchyma between the heart and sternum; no visible endotracheal tube; no artifacts or mild artifacts with minimal effect on the visualization of the central airways. More detailed information on the scan parameters is provided in Appendix Table E1.

The measurements of the central airways were conducted by two trained observers (A.H. and N.E., both medical students with two months training in thoracic CT image analysis). The CTs were divided in 2 equal batches which were scored by the two observers supervised by a PhD-student (W.K.) with 4 years' experience in thoracic imaging research. Detection of the central airways was done automatically using Myrian® v1.19.1 (XP Lung module, Intrasense, Montpelier, France) designed to segment the bronchial tree on CT with a soft kernel reconstruction filter which suppresses image noise at the cost of image resolution (See Appendix Table E1 for all the specific kernels used). The algorithm worked in three phases: 1. Detection of seed points belonging to the trachea. 2. Launch of a region growing based algorithm from previously adapted seed points. 3. Computation of a centerline for all branches of the segmented region of interest. An example of the inner airway segmentation and the measurements of the central airways is shown in Appendix Figure E1. The CTs that failed automatic detection of the entire central airways including the trachea, RMB and LMB by Myrian were excluded. A three-dimensional (3D) volume rendering reconstruction of the trachea and main bronchi pathway was generated. The length of the segmented central airway could not be measured automatically therefore the . intrathoracic tracheal length was measured manually with a digital ruler from the thorax inlet, defined as the first image slice where

both lung apices became visible, to the carina. Cross-sectional area (CSA), longest and shortest diameters were automatically measured perpendicular to the centerline of the airway lumen. A digital ruler was positioned manually on the 3D segmentation to annotate the dimensions for the trachea at every cm starting from the thoracic inlet to the carina. Similarly, dimensions were annotated for the right (RMB) and left (LMB) main bronchi every 0.5 cm (since these structures are shorter than the trachea) from the carina to the origin of the upper lobe bronchus, which was considered the end of each mainstem bronchus. Since the software could not measure the anterior-posterior and lateral diameter, the diameter of the trachea, RMB and LMB at each location were computed using the mean of the longest and shortest diameter,.

The intrathoracic trachea, RMB and LMB were divided in several sections as demonstrated in Figure 1. For each patient, the length of the intrathoracic trachea was divided in three equal sections; i.e. proximal, middle and distal. Length of the relatively shorter RMB was divided in two equal sections (proximal and distal) and the relatively longer LMB was divided in three equal sections (proximal, middle and distal).

In addition, ratios between the median LMB and tracheal diameter and between median RMB and tracheal diameter were calculated for each subject.

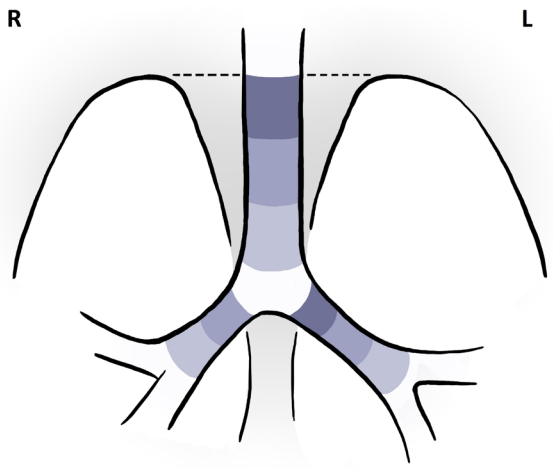

FIGURE 1. This figure shows the trachea, right (RMB) and left main bronchus (LMB) with the sections it was divided in. The intrathoracic trachea starts when both apical lungs are visible and was divided in 3 equal sections; i.e. proximal, middle and distal section (from dark to light grey, respectively). The relatively shorter RMB was divided in 2 equal sections to define the proximal (dark grey) and distal (light grey) section of the main bronchi. The relatively longer LMB was divided in 3 equal sections to define the proximal, middle and distal section (from dark to light grey, respectively) of the main bronchi (Artist: K. Rubenis).

Intra-, and inter-observer reliability

To assess intra-observer variability of the central airway measurements both observers repeated measurements on 25 randomly selected CTs after one month of completion. To assess the inter-observer variability, the measurements of 25 randomly selected CTs from observer 1 were repeated by observer 2.

Statistical Analysis

Patients were divided into ten age groups by 2 year intervals to express the central airway dimensions as median and interquartile range (IQR). Boxplots were made with 1.5 times IQR whiskers to demonstrate the range of the reference values without the outliers.

Mixed-effect models were performed to model the diameters of the central airways (trachea, RMB and LMB) accounting for age, gender, intrathoracic tracheal length and distance from carina. A multivariable linear regression model was used assuming one measurement per patient to assess the relationship between the ratios of LMB to trachea and RMB to trachea with age and gender. A p value < 0.05 was considered significant and correction for multiple testing was not performed.

Intraclass correlation coefficient (ICC) was calculated to measure inter-, and intra-observer agreement using mixed-effects models. In these models the structure of the data was taken into account, specifically the repeated location measurements and repeated patient measurements. Generally, ICC values between 0.4 and 0.6, 0.6 and 0.8, and ≥ 0.8 are considered to represent moderate, good and very good agreement, respectively.[18]

RESULTS

Study population

In total, 1160 CTs were collected by the *Children Chest CT study group* of which 258 were excluded by the independent thoracic radiologist (CY) since they were defined abnormal for reasons such as regions of low attenuations suggestive for pulmonary trapped air, pleural thickening and consolidations. 286 CTs were excluded due to insufficient overlap of the images (slice thickness > reconstruction increment). Of the remaining 616 CTs, 388 met the criteria for a good inspiratory lung volume level without artifacts impairing the visualization of the central airways. These 388 CTs were analyzed using semi-automatic detection of the central airways of which 94 failed related to variations in image acquisition settings and reconstruction kernel used (see Appendix Table E1). Finally, 294 CTs were included in the analysis (see Appendix Figure E2 for flow chart).

Demographics of the subjects and median diameters of the trachea and main bronchi are presented according to age group and gender in Table 1. The 95% confidence intervals are shown for the intrathoracic tracheal length (Figure 2A) and the diameter of the trachea (Figure 2B), RMB (Figure 2C) and LMB (Figure 2D) for each age group and gender. Older age, male gender, longer intrathoracic tracheal length and closer distance from the carina were all significant predictors for larger tracheal, LMB and RMB diameters in the mixed-effect model ($p<0.001$). Moreover, the effect of age on the tracheal, LMB and RMB diameters is found to be different for males and females since the interaction between gender and age was found to be significant ($p<0.001$). As shown in Fig 2B, C and D, the diameters of the trachea and main bronchi were all increasing equally in male and female subjects until the age of 14. After that diameters were greater for male compared to female.

TABLE 1. Dimensions of the central airways by age and gender

Age, range (in years)	Gender	N patients	Age median, IQR (in years)	Tracheal length, median, Q1-Q3 (in mm)	Tracheal diameter, median, Q1-Q3 (in mm)	LMB diameter, median, Q1-Q3 (in mm)	RMB diameter, median, Q1-Q3 (in mm)
≥0 and <2	Male	5	1.3, 0.6	32.7, 32.3-35.4	6.8, 6.2-7.5	4.2, 4.1-4.5	5.2,4. 7-5.5
	Female	0					
≥2 and <4	Male	7	3.6, 0.5	45.5, 37.0-45.9	7.8, 7.3-8.1	5.1, 4.5-5.7	6.7,6.4-7.0
	Female	1	3.4, 0.0	30.9, 30.9-30.9	6.7, 6.7-6.7	4.0, 4.0-4.0	5.6,5.6-5.6
≥4 and <6	Male	5	5.2, 0.7	45.6, 43.5-46.5	7.9, 7.6-9.2	5.0, 4.7-5.8	7.0,5.9-7.2
	Female	1	5.5, 0.0	45.9, 45.9-45.9	8.3, 8.3-8.3	5.4, 5.4-5.4	7.1,7.1-7.1
≥6 and <8	Male	7	6.8, 0.7	52.2,47.2-56.6	9.0, 8.6-9.2	6.3, 5.9-6.7	8.1,8.0-8.3
	Female	9	7.3, 1.1	52.7, 50.5-57.4	9.9, 8.9-11.2	6.4, 6.2-6.8	8.2,7.3-9.5
≥8 and <10	Male	9	9.4, 0.6	60.1, 56.8-62.3	10.5, 10.4-10.9	6.7, 6.2-7.3	8.7,8.1-8.9
	Female	6	9.3, 0.9	49.5, 47.8-52.9	10.3, 9.6-10.8	7.1, 6.4-7.3	9.3,8.4-9.7
≥10 and <12	Male	22	11.3, 1.1	63.8, 58.6-71.0	10.6, 10.2-11.3	7.0, 6.6-7.2	8.9,8.6-9.4
	Female	13	11.1, 0.8	56.1, 54.4-60.4	11.2, 10.6-11.5	6.7, 6.3-7.4	8.9,8.3-10.2
≥12 and <14	Male	35	13.3, 0.8	71.0, 65.5-77.4	12.7, 11.6-13.5	8.5, 7.7-9.2	10.8,9.7-11.4
	Female	14	13.2, 1.1	68.2, 63.0-72.7	12.2, 11.8-13.2	8.4, 7.3-9.0	10.9,10.2-11.1
≥14 and <16	Male	29	14.9, 0.6	77.9, 72.2-83.4	14.8, 13.2-15.8	9.7, 8.6-10.6	12.1,10.9-13.6
	Female	28	15.3, 0.8	68.1, 66.6-73.0	11.8, 11.5-13.4	8.0, 7.4-8.8	10.6,9.8-11.7
≥16 and <18	Male	36	17.1, 0.9	76.0, 69.2-84.8	14.9, 14.3-16.4	10.1, 9.1-10.7	12.3,11.8-14.0
	Female	13	17.2, 1.0	73.9, 65.5-82.1	12.7, 12.5-13.7	8.4, 7.9-8.8	11.3,10.6-11.9
≥18 and <20	Male	28	18.8, 1.1	81.8, 69.2-87.3	15.8, 15.3-16.9	10.4, 9.4-11.6	13.1,12.7-14.4
	Female	26	18.7, 0.8	71.2, 65.2-78.9	13.6, 12.5-14.3	9.0, 7.9-9.5	11.5,10.8-12.5
All	Male	183	14.2, 5.7	70.6, 59.8-80.4	13.2, 10.7-15.4	8.7, 7.0-10.2	11.2,8.9-12.8
	Female	111	15.2, 5.9	66.9, 58.6-72.9	12.0, 11.1-13.4	7.8, 6.9-8.9	10.6,9.6-11.7

Dimensions of the trachea, left (LMB) and right main bronchus (RMB) separated by age groups and by gender. Age is described as median and the 25th to 75th percentile (Q1-Q3). Tracheal length from carina to the thorax inlet is described as the median, first and third quartile. The tracheal, LMB and RMB dimensions are described as median, first and third quartile of the diameter of the shortest and longest diameter.

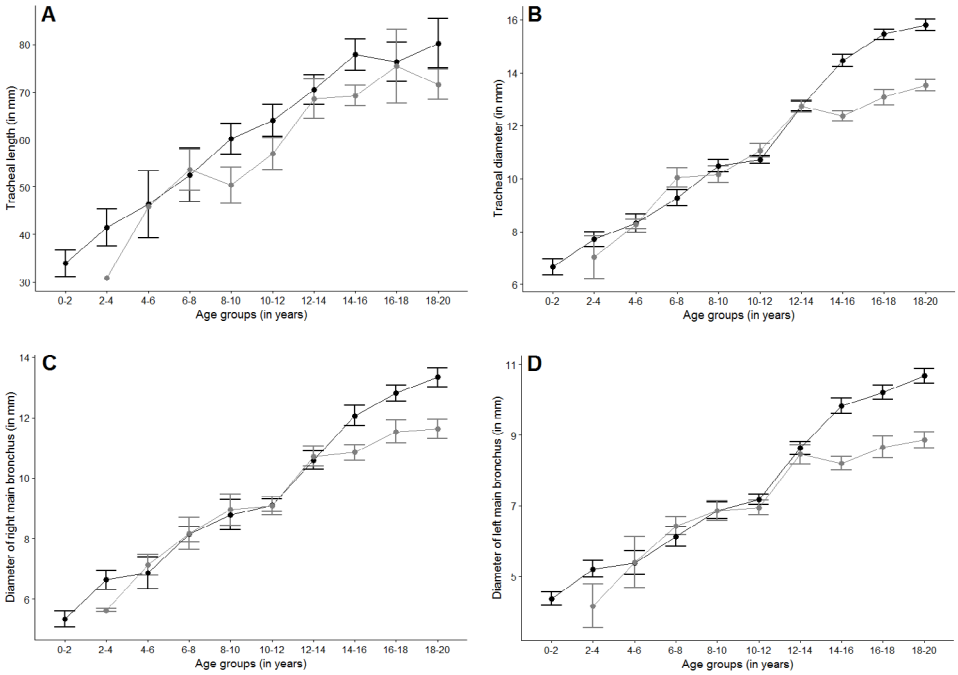

FIGURE 2. The mean and 95% confidence interval for each age group in males (black) and females (gray) subjects are demonstrated for the tracheal length (**A**), tracheal diameter (**B**), diameter of the right main bronchus (**C**) and diameter of the left main bronchus (**D**). An apparent difference in the diameter of the trachea, right main bronchus and left main bronchus is visible between male and female subjects after the age group of 12-14 year olds.

The diameter of the central airways are depicted for each section in table 2 and cross sectional areas of the central airways according to the age group and gender are depicted for every distance from the carina in Appendix Table E2. Diameters of the trachea (Figure 3), RMB (Figure 4) and LMB (Figure 5) are plotted in boxplots for male and female subjects for each section in ten age groups. The mixed-effect model showed that the distal section was significantly larger than the middle and proximal section of the trachea ($p<0.001$). Mixed-effect model predicting RMB dimensions showed that the proximal section was also significantly larger than the distal section ($p<0.001$). Lastly, the mixed-effect model prediction for LMB dimensions showed that the proximal part was significantly larger than the middle and distal sections ($p<0.001$). In addition, the distal section of LMB was larger than the middle section ($p=0.002$). Diameters of the trachea (Appendix Figure E3), RMB (Appendix Figure E4) and LMB (Appendix Figure E5) are demonstrated as a function of the distance from the carina for both the male and female subjects in the ten age groups.

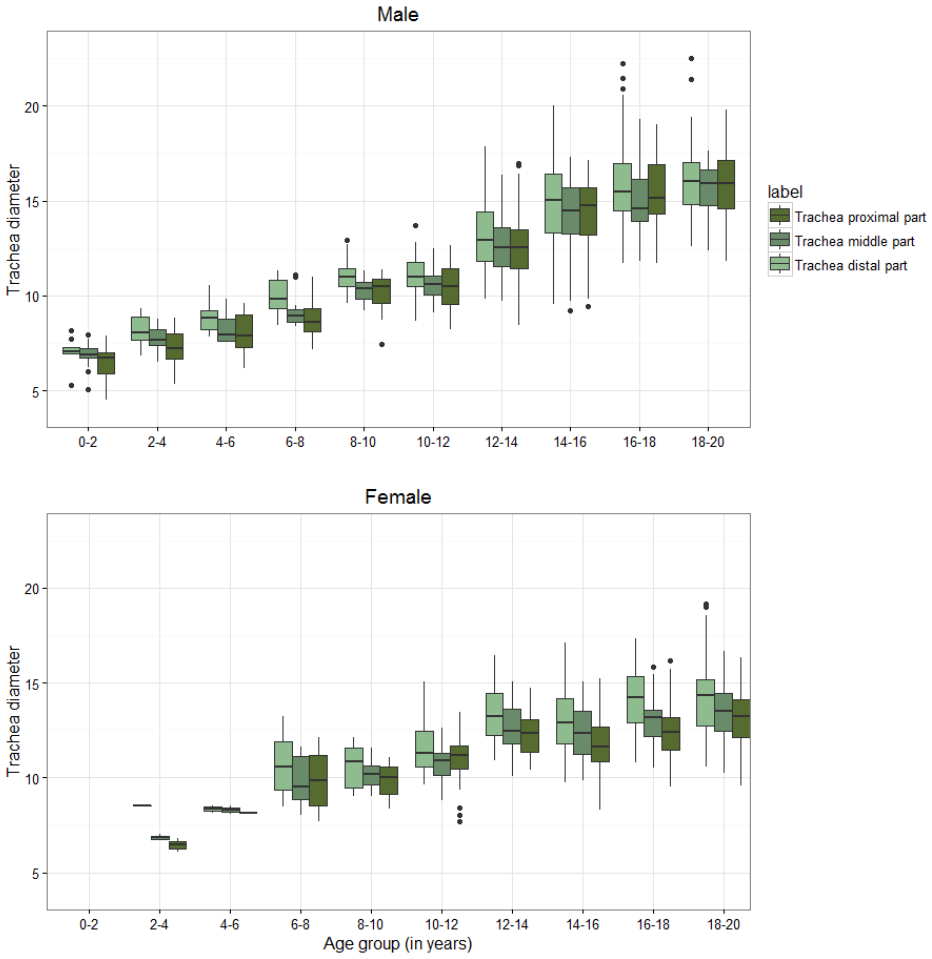

FIGURE 3. Boxplots are shown of the mean tracheal diameter for each age group in male (top) and female (bottom) subjects in each section of the trachea. The green color scheme demonstrated from dark to light represent the proximal, middle and distal section of the trachea. Each box shows median (horizontal line), interquartile range (solid box), 1.5*interquartile range (whiskers) and outliers (points).

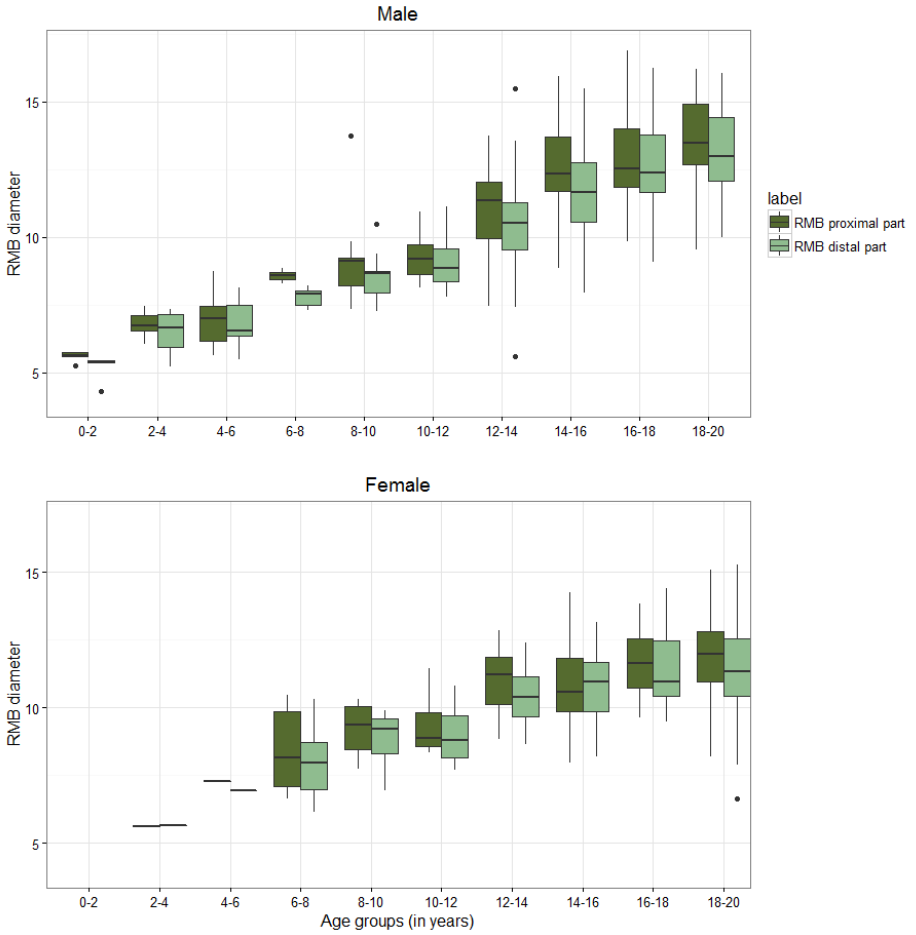

FIGURE 4. Boxplots are shown of the mean right main bronchi diameter for each age group in male (top) and female (bottom) subjects in section of the main bronchi. Dark and light green represents the proximal and distal section of the right main bronchi, respectively. Each box shows median (horizontal line), interquartile range (solid box), 1.5*interquartile range (whiskers) and outliers (points).

Ratios between median RMB and tracheal diameter and between the median LMB and tracheal diameter were calculated for each subject. The mean ± standard deviation was 0.85 ± 0.06 for RMB to trachea ratio and was 0.66 ± 0.06 for LMB to trachea ratio. The multivariable linear regression model showed that age, gender and the interaction between age and gender were not significant determinants of the RMB to trachea ratio ($p>0.30$) and were not significant determinants for the LMB to trachea ratio ($p>0.20$).

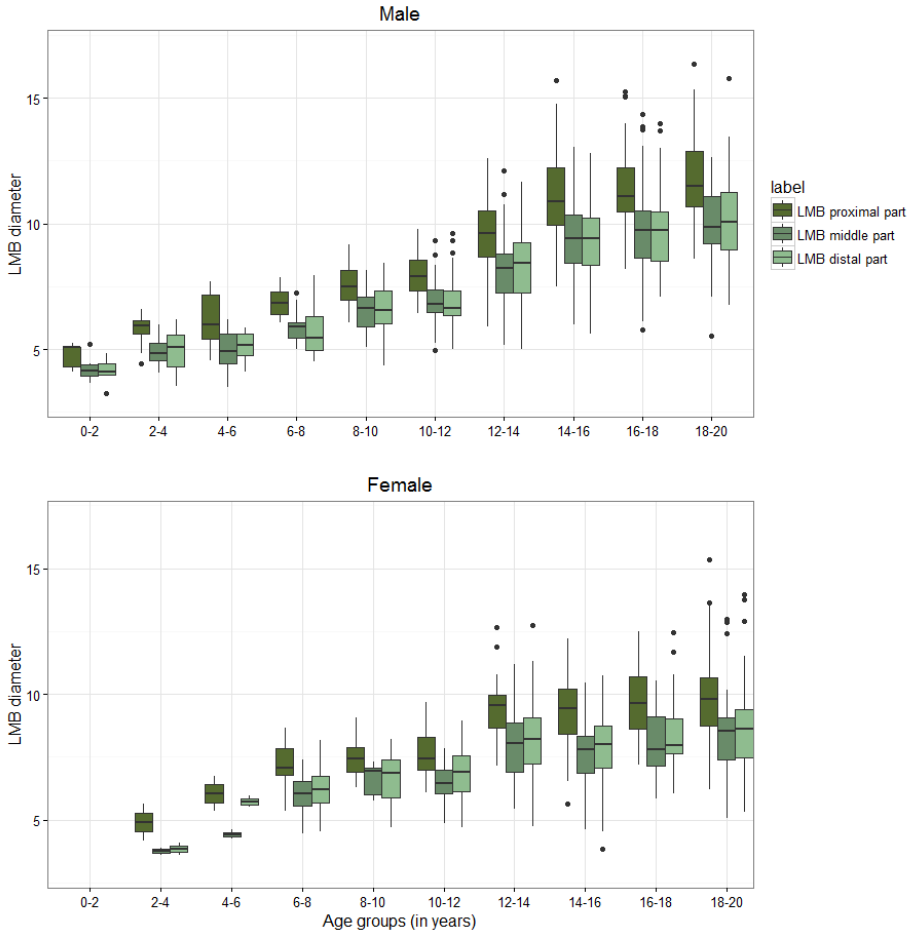

FIGURE 5. Boxplots are shown of the mean left main bronchi diameter for each age group in male (top) and female (bottom) subjects in each section of the main bronchi. The green color scheme demonstrated from dark to light represent the distal, middle and proximal section of the main bronchi. Each box shows median (horizontal line), interquartile range (solid box), 1.5*interquartile range (whiskers) and outliers (points).

Reproducibility of measurements

ICCs intra-observer 1: Tracheal CSA = 0.81; diameter = 0.92. RMB CSA = 0.77; diameter = 0.79. LMB CSA = 0.81; diameter = 0.83. Intrathoracic tracheal length = 0.99

ICCs intra-observer 2: Tracheal CSA = 0.99; diameter = 0.98. RMB CSA = 1; diameter = 0.99. LMB CSA = 1; diameter = 0.99. Intrathoracic tracheal length = 0.99

ICCs inter-observer: Tracheal CSA = 0.79; diameter = 0.88. RMB CSA = 0.91; diameter = 0.94. LMB CSA = 0.98; diameter = 0.97. Intrathoracic tracheal length = 0.98.

TABLE 2. Tracheal diameter by age and gender for each location

Age range (in years)	Gender	n	Tracheal diameter (in mm) for each section. Measurements are in median; IQR		
			distal	middle	proximal
≥0 and <2	Male	5	7.1; 0.8	6.9; 1.3	6.3; 1.2
	Female	0	NA	NA	NA
≥2 and <4	Male	7	8.1; 1.3	7.7; 0.8	7. 3; 1. 3
	Female	1	8.6; 0.0	6.9; 0.2	6. 5; 0.4
≥4 and <6	Male	5	8.9; 1.0	8.0; 1.2	7.9; 1.8
	Female	1	8.4; 0.2	8.3; 0.2	8.2; 0.1
≥6 and <8	Male	7	9.9; 1.5	9.0; 0.6	8.6; 1.3
	Female	9	10.6; 2.6	9.5; 2.3	9.9; 2.7
≥8 and <10	Male	9	11.0; 1.0	10.4; 0.9	10.5; 1.3
	Female	6	10.9; 2.1	10.2; 1.0	10.0; 1.5
≥10 and <12	Male	22	11.0; 1.3	10.6; 1.0	10.5; 1. 9
	Female	13	11.3; 1.9	10.9; 1.2	11.2; 1.3
≥12 and <14	Male	35	13.0; 2.6	12.6; 2.1	12.5; 2.0
	Female	14	13.3; 2.2	12.5; 1.8	12.3; 1.7
≥14 and <16	Male	29	15.1; 3.1	14.5; 2.4	14.9; 2.5
	Female	28	12.9; 2.4	12.4; 2.3	11.7; 1.9
≥16 and <18	Male	36	15.5; 2.5	14.6; 2.2	15.1; 2.6
	Female	13	14.3; 2.5	13.2; 1.4	12.4; 1.8
≥18 and <20	Male	28	16.1; 2.2	15.9; 1. 9	15.9; 2.6
	Female	26	14.5; 2.4	13.5; 2.0	13.3; 2.0
All	Male	183	14.2; 4.3	13.4; 4.4	13.6; 4.6
	Female	111	13.0; 2.9	12.4; 2.4	11.9; 2.2

Diameter of the trachea separated by age groups and by gender for each location of the measurement. Results are expressed in median; interquartile range (IQR).

DISCUSSION

Normative data for central airway dimensions are provided as a function of age and gender, in a large cohort of normal pediatric chest CTs.

This is the first study to show tracheal and main stem bronchial dimensions to be largest near the bifurcations: central airway dimensions are larger near the carina and the mainstem bronchi bifurcations. The dimensional increase near a bifurcation is presumed to be due to the division into the following two airway branches.

Secondly, our study in children up to 20 years old shows that central airway dimensions increase gradually with age. In particular, male and female subjects have similar dimensions of the airways from birth until approximately age 14. After this age, there is an apparent difference between genders in terms of the tracheal, LMB and RMB dimensions, with significantly larger dimensions found in boys compared to girls. This

difference is likely a resultant size differences between boys and girls after puberty,[19] where the growth of the central airways in boys continues and start to declines in females. Changes in the tracheal dimensions with age and gender in this study are in agreement with a previous smaller study by Griscom et al.[4], except gender differences were observed only after age 15. Similar cross-sectional dimensions of the trachea were shown previously in 38 infants below the age of 2.5 years by Rao at al. [20] however, the CSA of the RMB were slightly smaller and the reference values on the LMB were not presented[20]. The entire mainstem bronchi dimensions have not been assessed on CT and published in children previously.

Lastly, this study also confirms that the LMB to trachea ratio is not dependent on age and gender in children. Brodsky et al.[21] showed that the LMB to trachea ratio was constant for 30 adults. A slightly smaller mean ratio of 0.66 was found in children and adolescents in this study compared to a 0.75-0.77 ratio found previously in adults.[21] This relatively small difference could be secondary to slightly different ratios existing in adults relative to children, or better CT image quality. The main bronchi to trachea ratio is relevant for anesthesiologists for the selection of the appropriate double-lumen endobronchial tube for selective intubation of the LMB or RMB.[22,23] RMB to trachea ratio is provided in the present paper for children and adolescents and demonstrated to be constant as well.

This study, however, comes with several limitations. First, CTs were made for clinical reasons and despite our strict selection criteria, we may not be able to completely exclude some degree of underlying potential pathology involving central airways. Second, the CTs were not acquired using a standardized CT scanning protocol or standardized lung volume during CT acquisition, as the dataset was collected retrospectively. This resulted in different image qualities which could have impact the reference values presented in this study. However, an advantage of this approach was a larger study population. In addition, the heterogeneity of several CT scanners is related with a superior translation in the clinical practice where CT scanners and image quality of CTs are also diverse, and therefore and improved external validity. Regarding the lung volume during CT acquisition, the majority of CT studies were obtained at end-inspiratory which is current standard. Shape and dimensions of the central airways are known to be influenced by lung volume level during CT acquisition.[24,25] In this dataset there was however variance in lung volume protocols including scans acquired from free breathing to inspiratory and expiratory breath holds in cooperative children or with pressure control in younger children. In order to overcome this limitation in this retrospective study, we only included CTs with features of an appropriate inspiratory volume level. As more centers are nowadays implementing spirometer guided chest CTs in children,[26] it should be noted that observed dimensions are likely to be somewhat larger on spirometer guided

CTs, with lung volume near the total lung capacity, compared to our findings. Third, this diverse dataset did not collect information about patient's height, weight, BMI, size of the chest or ethnicity. These factors could be confounders of central airways dimensions. However, we believe that our patient's population who includes patients with various height, weight, BMI and ethnicity may be beneficial, because the results of study can be more easily generalized to other pediatric populations. Fourth, we were not able to measure the entire trachea starting from the vocal cords as this region was frequently outside the CT scan range. Therefore, we decided to use the intrathoracic length of the trachea. It should be noted that with older age a larger part of the entire trachea is measured. Fifth, the results of this study only included CT data retrieved automatically using Myrian®, which was 76% of the available data. Lower image quality due to lower radiation exposure might be the reason of the failed automated analysis.[27] In fact, radiation exposure in the scans that failed automated analysis was significantly lower. However we believe the exclusion of CT scans did not lead to substantial bias in the results as age and gender did not differ significantly between the failed scans and the scans included in this study. Lastly, the final sample sizes were smaller in females compared to males and smaller in the younger age group. This might have led to a somewhat unbalanced comparison between genders and young children. Additionally, there was insufficient data to make smaller interval groups in the first two years of life when there is the greatest period of lung growth. Therefore, there is still a need for additional normative values in the younger age groups.

In the future, normative values for central airway dimensions could be ideally collected prospectively in healthy children using MRI which is a radiation free alternative for chest CT. However, it is currently still challenging to acquire high resolution chest MRI under sufficiently standardized conditions from infancy into adolescence. Acquisition of chest MRI in young children is challenging and will likely require ethical approval similar to chest CT in case sedation is needed.[28] In addition, current MRI spatial resolution is between 1-2 mm in breath-hold condition and below in 1 mm using the newest free breathing ultra-short echo time scans.[29,30] Unfortunately, free breathing scans are acquired around functional residual capacity; therefore, underestimating the maximal dimensions of airway's lumen.

CONCLUSIONS

In our study, CT normative data were determined for the central airways in a large group of children and adolescents. Central airway dimensions were dependent on the location of the measurement relative to the location of the carina. The dimensions of the central airways increase with age and intrathoracic tracheal length and were larger in males compared to females after approximately 13 – 14 years old.

ACKNOWLEDGEMENTS

The authors would like to acknowledge Niels Erkelens, Abdullah Horiakhill and Hadiye Ozturk (Dept. of Pediatric Pulmonology and Dept. of Radiology, Erasmus MC-Sophia Children's Hospital, Rotterdam, the Netherlands) for their involvement in data acquisition.

REFERENCES

1. Williamson JP, James AL, Phillips MJ, Sampson DD, Hillman DR, Eastwood PR. Quantifying tracheobronchial tree dimensions: methods, limitations and emerging techniques. The European respiratory journal. 2009;34(1):42–55.
2. Seo JH, Hwang SH, Kang JM, Kim CS, Joo YH. Age-related changes of the larynx and trachea assessed by three-dimensional computed tomography in children: Application to endotracheal intubation and bronchoscopy. Clinical Anatomy. 2014;27(3):360–364.
3. Herek D, Herek O, Ufuk F. Tracheobronchial Angle Measurements in Children : An Anthropometric Retrospective Study With Multislice Computed Tomography. Clinical and experimental otorhinolaryngology. 2016:1–5.
4. Griscom NT, Wohl MEB. Dimensions of the growing trachea related to age and gender. American Journal of Roentgenology. 1986;146(2):233–237.
5. Desir A, Ghaye B. Congenital Abnormalities of Intrathoracic Airways. Radiologic Clinics of North America. 2009;47(2):203–225.
6. O'Connor PJ. Normative data: their definition, interpretation, and importance for primary care physicians. Family medicine. 22(4):307–11.
7. Enriquez G, Cadavid L, Garcés-Iñigo E, Castellote A, Piqueras J, Peiró JL, Carreras E. Tracheobronchomegaly following intrauterine tracheal occlusion for congenital diaphragmatic hernia. Pediatric Radiology. 2012;42(8):916–922.
8. Carlos Fraga J, Jennings RW, Kim PCW. Pediatric tracheomalacia. Seminars in Pediatric Surgery. 2016;25(3):156–164.
9. Lam WW, Tam PKH, Chan F, Chan K. Esophageal Atresia and Tracheal Stenosis. American Journal of Roentgenology. 2000;174:1009–1012.
10. Hewitt RJ, Butler CR, Maughan EF, Elliott MJ. Congenital tracheobronchial stenosis. Seminars in Pediatric Surgery. 2016;25(3):144–149.
11. Watanabe N, Hayabuchi Y, Inoue M, Sakata M, Nabo MMH, Nakagawa R, Saijo T, Kagami S. Tracheal compression due to an elongated aortic arch in patients with congenital heart disease: Evaluation using multidetector-row CT. Pediatric Radiology. 2009;39(10):1048–1053.
12. Fawcett SL, Gomez AC, Hughes JA, Set P. Anatomical variation in the position of the brachiocephalic trunk (innominate artery) with respect to the trachea: A computed tomography-based study and literature review of innominate artery compression syndrome. Clinical Anatomy. 2010;23(1):61–69.
13. Chen SJ, Shih TTF, Liu KL, Chiu IS, Wu MH, Chen HY, Lee WJ. Measurement of tracheal size in children with congenital heart disease by computed tomography. Annals of Thoracic Surgery. 2004;77(4):1216–1221.
14. Diaz AA, Rahaghi FN, Ross JC, Harmouche R, Tschirren J, San Jose Estepar R, Washko GR. Understanding the contribution of native tracheobronchial structure to lung function: CT assessment of airway morphology in never smokers. Respiratory research. 2015;16:23.
15. Griscom NT, Wohl MEB. Dimensions of the growing trachea related to body height. The American Review of Respiratory Disease. 1985;131:840–844.

16. Perez-Rovira A, Kuo W, Petersen J, Tiddens HAWM, de Bruijne M. Automatic airway–artery analysis on lung CT to quantify airway wall thickening and bronchiectasis. Medical Physics. 2016;43(10):5736–5744.

17. Kuo W, Ciet P, Tiddens HAWM, Zhang W, Guillerman RP, Van Straten M. Monitoring cystic fibrosis lung disease by computed tomography: Radiation risk in perspective. American Journal of Respiratory and Critical Care Medicine. 2014;189(11):1328–1336.

18. Portney L, Watkins M. Foundations of clinical research: applications to practice. Prentice Hall; 2000. p. 560–567.

19. Abbassi V. Growth and normal puberty. Pediatrics. 1998;102(2 Pt 3):507–11.

20. Rao L, Tiller C, Coates C, Kimmel R, Applegate KE, Granroth-Cook J, Denski C, Nguyen J, Yu Z, Hoffman E, et al. Lung Growth in Infants and Toddlers Assessed by Multi-slice Computed Tomography. Academic Radiology. 2010;17(9):1128–1135.

21. Brodsky JB, Malott K, Angst M, Fitzmaurice BG, Kee SP, Logan L. The relationship between tracheal width and left bronchial width: Implications for left-sided double-lumen tube selection. Journal of Cardiothoracic and Vascular Anesthesia. 2001;15(2):216–217.

22. Campos JH. Which device should be considered the best for lung isolation: double-lumen endotracheal tube versus bronchial blockers. Current opinion in anaesthesiology. 2007;20(1):27–31.

23. Hammer GB. Pediatric thoracic anesthesia. Anesthesiology Clinics of North America. 2002;20(1):153–180.

24. O'Donnell CR, Bankier AA, O'Donnell DH, Loring SH, Boiselle PM. Static end-expiratory and dynamic forced expiratory tracheal collapse in COPD. Clinical Radiology. 2014;4(164):357–362.

25. Yamashiro T, San José Estépar R, Matsuoka S, Bartholmai BJ, Ross JC, Diaz A, Murayama S, Silverman EK, Hatabu H, Washko GR. Intrathoracic tracheal volume and collapsibility on inspiratory and end-expiratory CT scans: Correlations with lung volume and pulmonary function in 85 smokers. Academic Medicine. 2011;18(3):299–305.

26. Salamon E, Lever S, Kuo W, Ciet P, Tiddens HAWM. Spirometer guided chest imaging in children: It is worth the effort! Pediatric Pulmonology. 2016;56(September 2015):48–56.

27. Kuo W, Kemner-van de Corput MPC, Perez-Rovira A, de Bruijne M, Fajac I, Tiddens HAWM, et al. Multicentre chest CT standardisation in children and adolescents with cystic fibrosis : the way forward. European Respiratory Journal. 2016:1–12.

28. Lee EY, Boiselle PM, Shamberger RC. Multidetector computed tomography and 3-dimensional imaging: preoperative evaluation of thoracic vascular and tracheobronchial anomalies and abnormalities in pediatric patients. Journal of Pediatric Surgery. 2010;45(4):811–821.

29. Baez JC, Ciet P, Mulkern R, Seethamraju RT, Lee EY. Pediatric Chest MR Imaging: Lung and Airways. Magnetic resonance imaging clinics of North America. 2015;23(2):337–49.

30. Dournes G, Grodzki D, Macey J, Girodet P-O, Fayon M, Chateil J-F, Montaudon M, Berger P, Laurent F. Quiet Submillimeter MR Imaging of the Lung Is Feasible with a PETRA Sequence at 1.5 T. Radiology. 2015;276(1):258–65.

APPENDIX

Methods

The following centers contributed to the *Children Chest CT study group* dataset (ordered according the number of CT scan provided, from highest to lowest): University Medical Center Utrecht, Utrecht, the Netherlands; Hospital Universitari Vall d'Hebron, Barcelona, Spain; Erasmus Medical Center- Sophia Children's Hospital, Rotterdam, the Netherlands; University of Rome Sapienza, Rome, Italy; Cincinnati Children's Hospital Medical Center, Cincinnati, Ohio, USA; Boston Children's Hospital and Harvard Medical School, Boston, MA, USA; Queen Silvia Children's Hospital, University of Gothenburg, Gothenburg, Sweden; University of Leuven, Leuven, Belgium; General Hospital, Ospedale Ca'Foncello, Treviso, Italy; Princess Margaret Hospital for Children and Telethon Kids Institute, Perth, WA, Australia

APPENDIX TABLE E1. Scan parameters of included and excluded CTs.

	Included scans	Excluded scans	P-value
n	294	94	
Age	11.79 (7.16-25.96)	13.95 (9.84- 16.76)	0.10
Gender	108 males, 186 females	52 males, 42 females	0.24
CT scanners	14x GE; 109x Philips; 152x Siemens; 19x Toshiba	7x GE; 42x Philips; 39x Siemens; 6x Toshiba	-
Tube voltage (kV)	120 (100-120)	120 (100-120)	0.09
Pitch	1 (1-1) *	5 (5-6) #	0.45
Slice thickness (mm)	1 (1-2.5)	1.5 (1-1.5)	0.51
Reconstruction increment (mm)	0.8 (0.7-1.2)	1 (0.7-1.24)	0.13
Reconstruction kernel	GE: 9x LUNG; 2x SOFT; 3x STANDARD Philips: 17x B; 40x C; 2x D; 28x L; 18x YA; 3x YB; 1x YD Siemens: 6x B20; 2x B26; 14x B30; 21x B31; 1x B46; 2x B50; 29x B60; 54x B70; 13x B75; 4x B80; 6x I30 Toshiba: 1x FC05; 1x FC10; 10x FC12; 7x FC18	GE: 5x LUNG; 1x SOFT; 1x DETAIL Philips: 2x B; 13x C; 1x L; 25x YA; 1x YC Siemens: 2x B31; 7x B60; 8x B70; 6x B75; 6x I70 Toshiba: 1x FC05; 4x FC12; 1x FC18	-
Current-time product (mAs)	56.36 (36.48-101.2) *	44.55 (23.56-97.36) #	0.03
CTDI (mGy)	3.53 (1.7-5.4) *	2.16 (0.96-4.95) #	0.45

Summary of the scan parameters of the CTs included in this study (middle column) and the scan parameters of the excluded CT scans with failed automatic reconstruction (right column). The parameters are shown with median, interquantile range. * 238 scans did not include pitch; 4 scans did not include current-time product; 127 scans did not include CTDI. # 70 scans did not include pitch; 1 scan did not include current-time product; 30 scans did not include CTDI. The Wilcoxon rank sum test was performed to test difference between the scans included and excluded.

APPENDIX TABLE E2. Tracheal dimensions by age, gender and distance to the carina.

Age range (in years)	Gender	n	Tracheal CSA (in mm²). Distance given from carina bifurcation to location of measurements in median; IQR											
			1 cm	2 cm	3 cm	4 cm	5 cm	6 cm	7 cm	8 cm	9 cm	10 cm	11 cm	12 cm
≥0 and <2	Male	5	39; 9	37;13	36; 16	39; 11	29; 6							
	Female	0												
≥2 and <4	Male	7	62;19	51; 14	45; 7	51; 15	43; 20	39; 6	39; 4	20; 0				
	Female	1	52; 0	35; 0	36; 0	35; 0	31; 0							
≥4 and <6	Male	5	62; 6	51; 19	50; 18	55; 8	50; 12	39; 20	37; 18					
	Female	1	58; 0	52; 0	52; 0	56; 0	53; 0	49; 0						
≥6 and <8	Male	7	85;15	65; 9	65; 9	64; 9	60; 15	60; 9	52; 7	50; 0				
	Female	9	85; 38	68; 46	79; 39	75; 35	76; 33	76; 44	89; 26					
≥8 and <10	Male	9	96; 17	86; 6	88; 13	88; 14	90; 5	83; 16	70; 28	66; 0				
	Female	6	101; 20	86; 2	86; 14	85; 15	84; 13	75; 14	61; 5	67; 0				
≥10 and <12	Male	22	97; 25	87; 22	88; 18	87; 11	91; 17	101; 15	94; 17	84; 19	81; 28	75; 18	78; 13	66; 0
	Female	13	105; 30	95; 15	92; 21	94; 16	99; 21	98; 23	87; 34	99; 19				
≥12 and <14	Male	35	147; 46	127; 39	118; 32	122; 38	128; 43	131; 38	132; 38	121; 46	124; 44	144; 40	131; 46	106; 9
	Female	14	152; 55	124; 45	117; 36	124; 37	121; 19	129; 35	122; 45	124; 19	118; 29	112; 16	109; 0	
≥14 and <16	Male	29	196; 74	166; 59	164; 68	163; 68	167; 55	173; 42	173; 50	175; 43	158; 59	180; 36	198; 26	158; 0
	Female	28	148; 57	118; 45	118; 45	109; 5	113; 48	124; 42	113; 37	102; 29	109; 35	117; 13	107; 9	45; 0
≥16 and <18	Male	36	208; 77	179; 49	167; 47	166; 41	170; 53	184; 49	197; 63	186; 66	176; 82	187; 30	209; 45	207; 28
	Female	13	177; 35	141; 42	137; 49	131; 37	128; 38	131; 31	133; 33	131; 17	116; 21	114; 23	134; 22	
≥18 and <20	Male	28	228; 61	189; 36	194; 42	199; 51	198; 56	208; 50	214; 61	203; 41	185; 56	189; 48	201; 33	216; 40
	Female	26	179; 57	156; 48	150; 56	142; 47	139.5; 31	137; 38	144; 37	136; 35	142; 44	133; 35	150; 24	137; 3
All	Male	183	163; 113	135; 94	133; 87	130; 82	136; 86	145; 86	157; 93	164; 91	161; 73	172; 59	191; 60	174; 101
	Female	111	142; 70	118; 58	110; 54	111; 50	114; 50	121; 45	120; 46	122; 35	115; 38	121; 34	140; 39	134; 48

Cross sectional area (CSA) of the trachea separated by age groups and by gender for each location of the measurement to the distance from the carina location. Results are expressed in median; interquartile range (IQR).

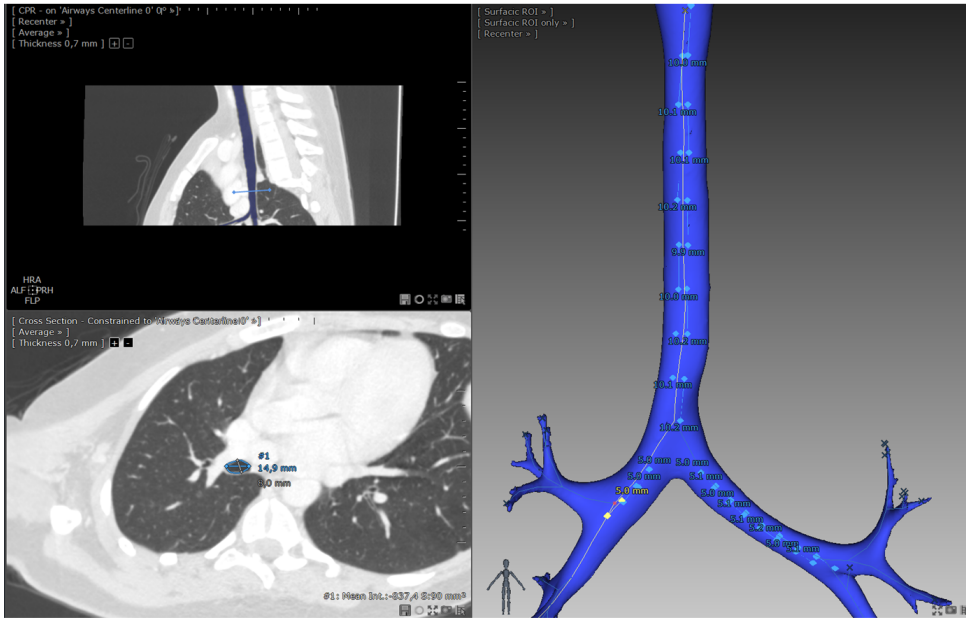

APPENDIX FIGURE E1. Example of the segmentation of the central segmentation (right figure in blue) with the yellow airway centerline and red dot indicating the position of the cross sectional area measurement in the left bottom figure. A manual digital ruler was used to indicate each 1 cm position of the trachea and each 0.5 cm in the main bronchi (blue diamonds).

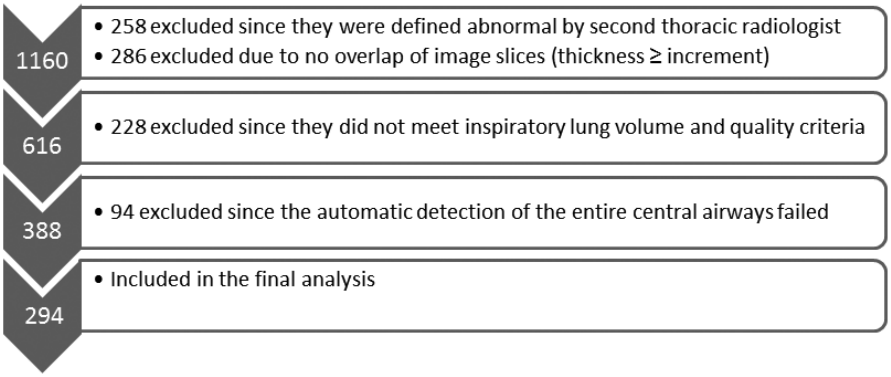

APPENDIX FIGURE E2. Flowchart of the scans excluded in this study.

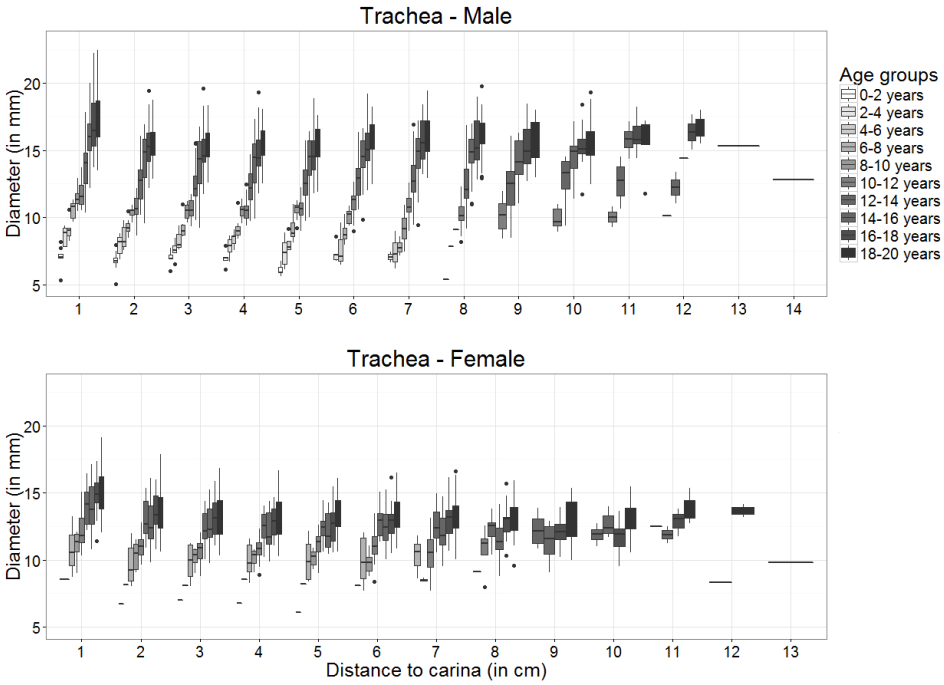

APPENDIX FIGURE E3. Boxplots show the diameter of the trachea relative to the distance from the carina for male (top graph) and female (bottom graph) subjects. Each box shows median (horizontal line), interquartile range (solid box), 1.5*interquartile range (whiskers) and outliers (points) for every age group (lighter to darker colors represent younger to older age groups). Note that the diameter of the trachea is larger when closer to the carina.

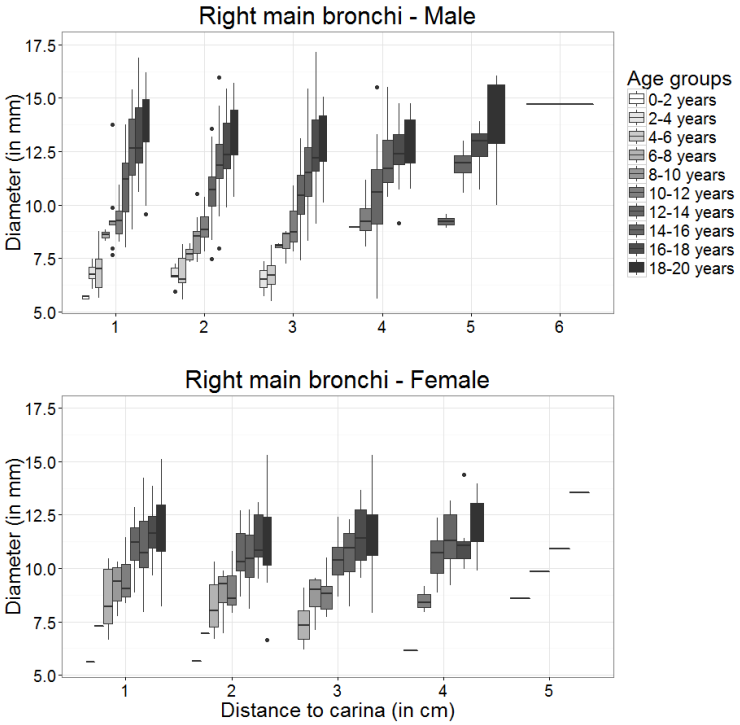

APPENDIX FIGURE E4. Boxplots show the diameter of the right main bronchi relative to the distance from the carina for male (top graph) and female (bottom graph) subjects. Each box shows median (horizontal line), interquartile range (solid box), 1.5*interquartile range (whiskers) and outliers (points) for every age group (lighter to darker colors represent younger to older age groups).

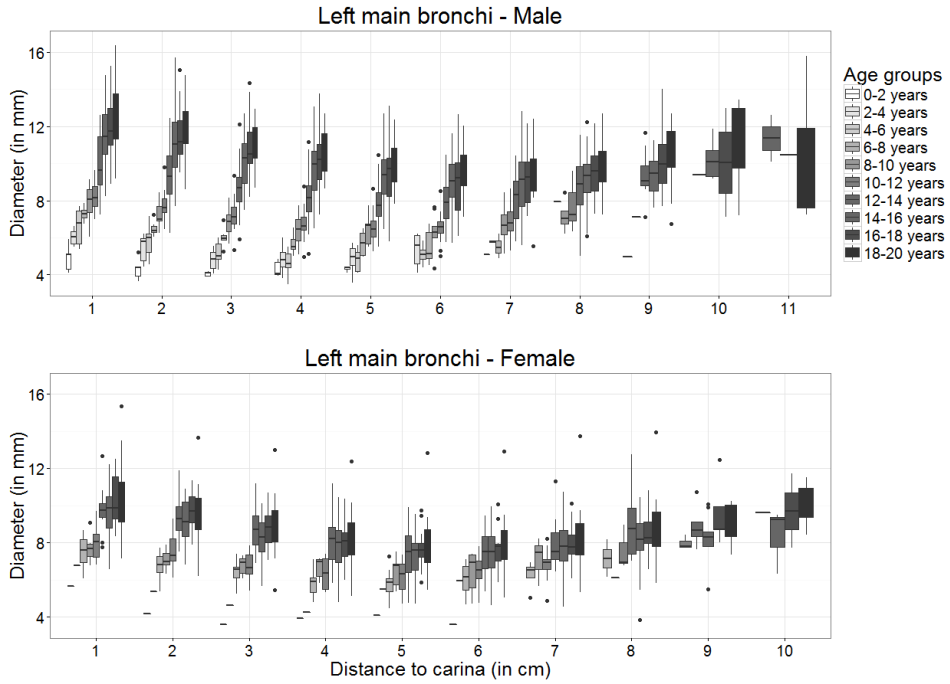

APPENDIX FIGURE E5. Boxplots show the diameter of the left main bronchi relative to the distance from the carina for male (top graph) and female (bottom graph) subjects. Each box shows median (horizontal line), interquartile range (solid box), 1.5*interquartile range (whiskers) and outliers (points) for every age group (lighter to darker colors represent younger to older age groups). Note that the diameter of the left main bronchi is larger when closer to the carina and when closer to the bifurcation into the upper lobes.

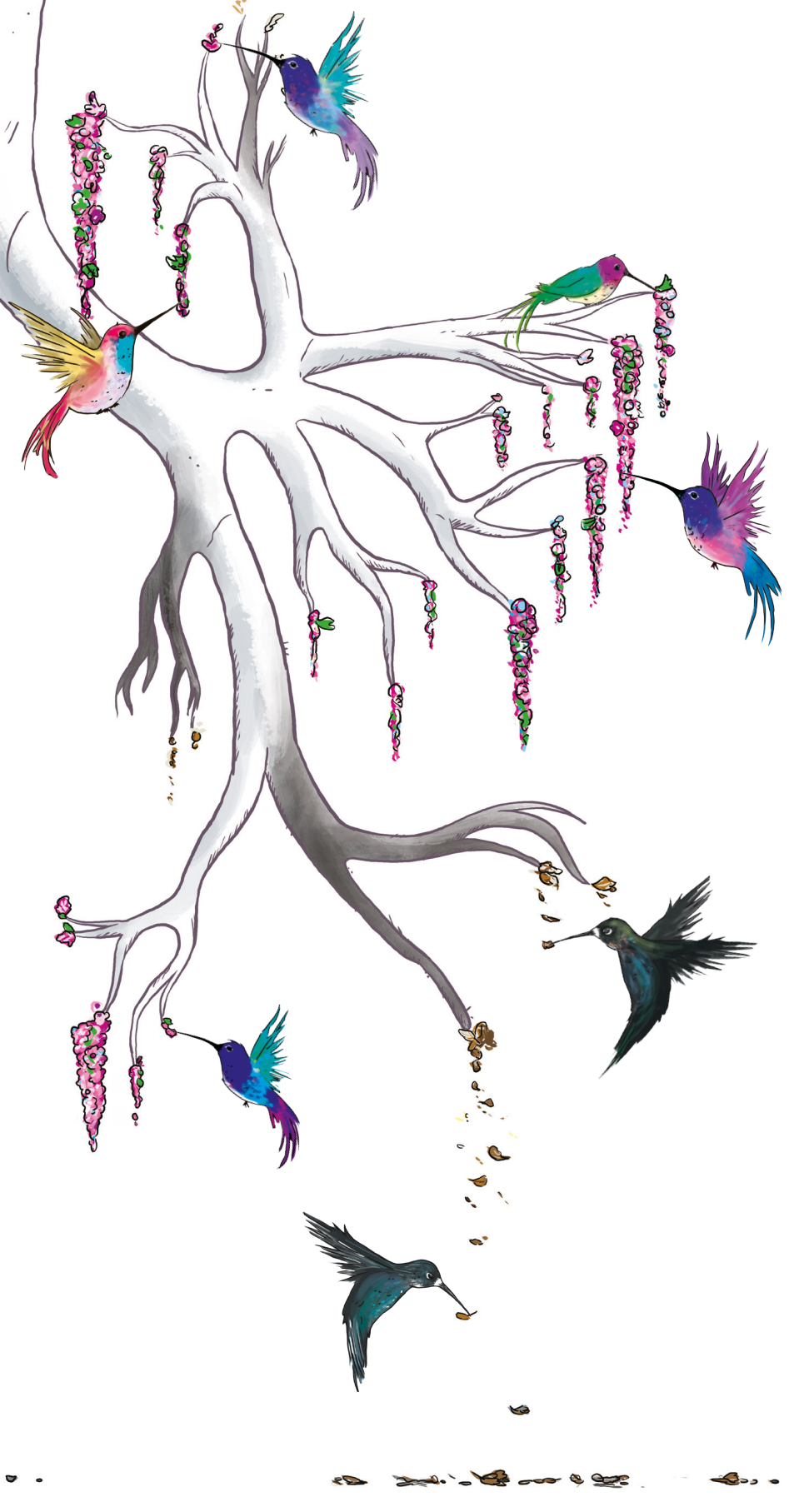

CHAPTER 9

REFERENCE VALUES FOR AIRWAY AND ARTERY DIMENSIONS ON CT OF CHILDREN AND ADOLESCENTS

Wieying Kuo *, Adria Perez-Rovira *, Eleni-Rosalina Andrinopoulou, Chen Yong, Silvia Gartner, Alan S. Brody, Kris de Boeck, Silvia Bertolo, Lauren Akesson, Stephen M. Stick, Harm A.W.M. Tiddens, Marleen de Bruijne on behalf of the Children Chest CT Study Group

* Both authors contributed equally

Children Chest CT Study Group (in alphabetic order):
Lauren Akesson, Silvia Bertolo, Alan S. Brody, Kris de Boeck, Pim A. de Jong, Robert J. Fleck, Francesco Fraioli, Pilar Garcia-Peña, Silvia Gartner, Edward Y. Lee, Anders Lindblad, Michael McCartin, Christian P. Mol, Giovanni Morana, Arlette E. Odink, Matteo Paoletti, Stephen M Stick, Els van der Wiel, Francois Vermeulen.

In preparation

ABSTRACT

Rationale

To provide normative values of airway dimensions measured on chest CT in children and adolescents.

Methods

Chest CTs evaluated as normal were collected retrospectively in ten international centers. The airway tree was interactively extracted and airway dimensions were automatically quantified using image analysis software. Airway to artery (AA)-ratios, intra-branch tapering (reduction in airway diameter along the branch) and inter-branch tapering (reduction in airway diameter before and after bifurcation) were determined. Four airway groups were established based on lumen diameter: the largest 18 (central), the second largest 18 (segmental), the following 36 (subsegmental) and the remaining airways (peripheral). Effect of age, gender and airway group on the AA-ratios and tapering values were investigated using mixed-effect models.

Results

516 (80%) out of 645 CTs were successfully analyzed automatically. Mean of 0.5 for inner and 1.2 for outer AA-ratio; 1% for inner and outer intra-branch tapering; 36% for inner and 23% for outer inter-branch tapering was found. Age and gender were not significant predictors of the AA-ratios ($p>0.36$), intra-branch tapering ($p > 0.68$) or inter-branch tapering ($p > 0.59$). Airway group was a significant predictor for inner AA-ratio (value = -0.09, $p < 0.0001$), inner intra-branch tapering (value = 0.29, $p = 0.0005$), inner inter-branch (value = 6.43, $p < 0.0001$) and outer intra-branch tapering (value = 2.78, $p < 0.0001$).

Conclusion

AA-ratio and tapering measures for children and adolescents were not dependent on age or gender. Inner AA-ratio decreased from central to peripheral airways, while inner intra-branch and both inner and outer inter-branch tapering increased from central to peripheral airways.

INTRODUCTION

Various imaging modalities can be used to assess airway and artery dimensions in the lungs, with the most sensitive being chest computed tomography (CT).[1] Airways and accompanying arteries are routinely imaged on chest CT in children to assess structural changes such as bronchiectasis and airway wall thickening. An airway to artery ratio larger than one is considered a sign of bronchiectasis.[2,3] Another important sign for bronchiectasis is lack of tapering with only a few studies defining objective criteria.[4–6] Wall thickening is defined by an enlarged airway wall to artery ratio,[7] or as an enlarged airway wall to the overall airway area.[8] Even though semi quantitative criteria are being used in day to day radiological reports reference values in the pediatric population is lacking. Ideally, to generate such reference values a large number of CT scans from healthy children from infancy into the adolescent age is needed. However, due to the radiation exposure related to CT scanning is only performed in children with known or suspicion of thoracic diseases. Performing CT scans in healthy children to generate normative values is not justified. As a consequence, only a few studies have reported normative airway and artery dimensions and only in small study populations.[7–9] Previous study showed that hundreds of airway artery pairs could reliable be measured on each chest CT and that major differences could be detected between patients with CF and a control group.[7] To generate reliable reference data of airway and artery dimension in children from infancy into adolescence the *Children Chest CT Study Group* was established aiming to collect a sufficiently large number of control CTs, assessed to be free of any disease signs. Manual quantification of hundreds of airway-artery pairs per CT in such a large dataset would be unfeasible due to the laborious and time consuming nature of the task, and (semi-) automated image analysis tools need to be used instead. To our knowledge the cross-sectional airway and artery dimensions of the entire pulmonary airway tree visible on CT have never been studied in a large pediatric control population before. The aim of this study is to derive normative values for airway and artery dimensions, inter-, and intra-branch tapering and airway to artery ratios in children and adolescents.

METHODS

This study was approved by institutional review board (MEC-2011-494). Written informed consent was waived for all patients because of the retrospective nature of the study.

Study population

Chest CTs of children aged 0 to 19 were collected retrospectively in an international multicenter study group, the *Children Chest CT Study Group*. The CTs were acquired

between 2003 and 2013 for various diagnostic indications but were reported as normal by the radiologist. All CTs were anonymized for patient specific and clinical information and send to LungAnalysis (Erasmus MC, Rotterdam) for further analysis. A second independent thoracic radiologist (CY, 20 years of experience in thoracic imaging) checked all the CTs for pulmonary and cardiac abnormalities.

CT acquisition parameters

All CTs that were defined as normal by the second radiologist were further selected for our current study when they met the following: volumetric CT; slice thickness ≥ increment; field of view (FOV) encapturing the entire lungs. More detailed information on the scan parameters is provided in Appendix Table E1.

Quantitative analysis of airways and arteries

In-house developed software was used to segment airway branches and their accompanying artery, and to quantify their diameters, the airway tapering and the airway-artery ratio in a fully 3D manner. The method has been previously described and validated with the use of 8,000 manual annotations [6,10] and can be summarized as follows: Firstly, airways were automatically segmented in all CTs. Pathways of additional visible airways not automatically segmented were added manually using Myrian® (v1.16.2, Lung XP module) image analysis platform (Intrasense, Montpelier, France) [7]. Secondly, the lung fields were extracted automatically using thresholding and morphological smoothing.[11] A multi-scale Hessian Eigen analysis approach was used to extract an initial segmentation of the lung vasculature, as implemented in Lo *et al*.[11] Then, accurate surface of the initial airway and vessel segmentations were automatically corrected using a graph-cut method.[12] Centerlines of the segmented airway and vessel trees were extracted using a front-propagation method [LO12]. Centerline branching points were then located and used to split the whole segmentation into individual branches. Inner, outer airway and vessel diameters were then extracted every 0.5 mm along their centerlines with subvoxel accuracy. With trachea considered generation 0, airway generation was increased at each branching. Airway and artery branches shorter than 5 mm, and airways from generation 15 onwards were considered not reliable and discarded. Airway and artery branches located in close proximity, with similar orientation and size were automatically paired together as an airway-artery pair. Of each airway and artery branch the average diameter for the full branch was determined to compute the normative airway and artery dimensions. Normative tapering biomarkers were obtained for all airway branches (including those without artery pair). Intra-branch tapering (intraBT) is defined as the percentage reduction in airway diameter per mm along the

centerline. For example, a value of 2 means that the airway diameter is reduced 2% each mm. Inter-branch tapering (interBT) is defined as the percentage that the average diameter of the analyzed airway is reduced compared to the average diameter of the airway branch before bifurcation. For example, a value of 20% would indicate that the child branch is 20% smaller than the parent branch. Finally, for each airway-artery pair the following biomarkers were obtained at the point where airway and artery were most similar in terms of size, orientation and position: $A_{in}A$-, $A_{out}A$- and $A_{WT}A$-ratios as computed by dividing the inner, outer, and airway wall diameter (difference between outer and inner) by the adjacent artery diameter, respectively. Wall area percentage (WAP), is the percentage of airway wall in the total area.

Statistical Analysis

Patients were grouped by age, with 1 year intervals. Airways of each subject were grouped in four categories depending on lumen diameter: the largest 18 (central), the second largest 18 (segmental), the following 36 (subsegmental) and the remaining airways (peripheral).

All projections of the CT segmentations were visually inspected and excluded if they were considered a failed segmentation (more than 50% erroneous airways). In addition, any airway measurement with AA-ratios or tapering values above and below 1.5 times the inter-quartile range (IQR) was considered an extreme outlier likely due to errors in the automated analysis and was excluded from the main analysis. Mixed-effect models under heavy-tailed distributions were used to predict AA dimensions, AA ratios and tapering measures using age, gender and the airway group as covariates. A p-value of <0.05 was considered significant.

RESULTS

Study population

In total, 1160 CTs were collected by the *Children Chest CT study group* of which 258 were considered abnormal by the independent thoracic radiologist (CY) and were excluded. An additional 257 CTs were excluded due to slice gap (slice thickness ≥ reconstruction increment).

Manual segmentation was performed on the remaining 645 CTs prior to the automatic analysis. All 645 CTs were automatically analyzed of which 516 CTs (80%) returned with a visual projection of the inner and outer airway. The visual inspection of all 516 CT projections resulted into 29 CT scans to be excluded. 39 branches were omitted due an airway generation >15. After outlier omission, 487 subjects with a total of 46,306 airway measures and 24,618 AA pairs were included in this study. Details on the extreme

TABLE 1. Airway dimensions by age and airway group

Age	N patients	Sex (% males)	Inner airway diameter, median (Q1-Q3)				Outer airway diameter, median (Q1-Q3)			
			Central	Segmental	Subsegmental	Peripheral	Central	Segmental	Subsegmental	Peripheral
0	2	50	1.8 (1.2-2.8)	1.0 (0.9-1.1)	0.8 (0.7-0.8)	-	4.7 (3.2-5.8)	3.1 (2.8-4.7)	2.8 (2.6-2.9)	-
1	15	67	2.2 (1.9-2.6)	1.4 (1.2-1.7)	1.0 (0.8-1.1)	0.7 (0.7-0.8)	4.9 (4.4-5.6)	3.6 (3.1-4.2)	2.8 (2.5-3.2)	2.4 (2.2-2.6)
2	15	60	2.2 (1.8-2.6)	1.3 (1.1-1.7)	1.0 (0.8-1.2)	0.7 (0.6-0.8)	4.8 (4.4-5.4)	3.6 (3.1-4.3)	3.0 (2.6-3.5)	2.3 (2.1-2.5)
3	15	80	2.5 (2.0-3.1)	1.4 (1.2-1.8)	1.0 (0.8-1.2)	0.7 (0.7-0.8)	5.5 (4.9-6.2)	4.0 (3.4-4.6)	3.0 (2.6-3.7)	2.5 (2.2-3.0)
4	16	50	2.7 (2.3-3.2)	1.6 (1.3-2.0)	1.2 (1.0-1.5)	0.8 (0.7-0.9)	5.7 (5.2-6.3)	4.2 (3.7-4.9)	3.3 (2.9-3.7)	2.6 (2.5-2.9)
5	15	73	2.6 (2.3-3.1)	1.7 (1.5-1.9)	1.1 (0.9-1.4)	0.8 (0.7-0.9)	5.5 (4.9-6.3)	4.1 (3.5-4.6)	3.2 (2.7-3.7)	2.6 (2.3-2.8)
6	22	41	2.8 (2.4-3.4)	1.8 (1.5-2.0)	1.2 (0.9-1.4)	0.8 (0.7-1.0)	5.6 (4.9-6.5)	4.1 (3.6-4.6)	3.1 (2.8-3.5)	2.6 (2.4-2.8)
7	18	44	3.3 (2.6-3.8)	2.0 (1.7-2.4)	1.4 (1.2-1.7)	0.9 (0.8-1.1)	5.9 (5.2-6.8)	4.4 (3.9-5.2)	3.6 (3.2-4.0)	2.8 (2.4-3.1)
8	22	32	3.3 (2.7-4.0)	2.0 (1.6-2.4)	1.3 (1.0-1.6)	1.0 (0.9-1.2)	6.0 (5.4-6.8)	4.4 (4.0-5.1)	3.5 (3.0-4.0)	3.0 (2.7-3.3)
9	26	42	3.2 (2.7-3.8)	2.1 (1.8-2.5)	1.4 (1.1-1.7)	1.0 (0.8-1.2)	6.1 (5.3-6.7)	4.6 (4.1-5.1)	3.6 (3.1-4.2)	3.1 (2.7-3.5)
10	32	62	3.4 (2.9-4.0)	2.2 (1.9-2.5)	1.4 (1.1-1.7)	0.9 (0.8-1.1)	6.1 (5.4-6.8)	4.6 (4.1-5.1)	3.5 (3.1-4.0)	2.9 (2.6-3.2)
11	33	58	3.5 (3.1-4.3)	2.4 (2.0-2.7)	1.5 (1.2-1.8)	1.0 (0.9-1.2)	6.4 (5.7-7.2)	4.9 (4.5-5.5)	3.8 (3.4-4.4)	3.0 (2.7-3.4)
12	25	64	3.6 (3.0-4.2)	2.4 (1.7-2.8)	1.5 (1.2-1.9)	1.0 (0.8-1.3)	6.3 (5.5-7.1)	4.8 (4.3-5.3)	3.6 (3.2-4.2)	3.0 (2.6-3.3)
13	32	66	3.6 (3.0-4.4)	2.4 (2.0-2.8)	1.6 (1.3-1.9)	1.1 (0.9-1.3)	6.5 (5.6-7.2)	4.9 (4.4-5.4)	3.9 (3.4-4.4)	3.1 (2.8-3.5)
14	41	66	3.6 (3.2-4.4)	2.4 (2.0-2.8)	1.6 (1.3-1.9)	1.1 (0.9-1.3)	6.4 (5.8-7.2)	5.0 (4.5-5.6)	3.9 (3.5-4.4)	3.1 (2.8-3.5)
15	38	41	3.9 (3.1-4.8)	2.5 (2.0-2.9)	1.6 (1.2-2.0)	1.2 (0.9-1.4)	6.7 (5.9-7.7)	5.1 (4.4-5.7)	4.0 (3.4-4.6)	3.3 (2.9-3.7)
16	32	69	4.1 (3.4-4.9)	2.7 (2.1-3.2)	1.7 (1.3-2.2)	1.2 (1.0-1.4)	7.0 (6.2-8.0)	5.4 (4.8-6.1)	4.3 (3.7-5.0)	3.4 (3.1-3.9)
17	33	52	4.3 (3.6-5.2)	2.8 (2.3-3.3)	1.9 (1.5-2.3)	1.2 (1.0-1.5)	7.4 (6.5-8.4)	5.7 (5.0-6.3)	4.6 (3.9-5.2)	3.6 (3.2-4.1)
18	30	50	4.1 (3.5-4.7)	2.8 (2.2-3.1)	1.6 (1.3-2.0)	1.2 (0.9-1.4)	7.0 (6.4-7.8)	5.4 (4.8-6.0)	4.1 (3.5-4.7)	3.3 (2.9-3.8)
19	25	52	4.0 (3.4-4.9)	2.6 (2.0-3.1)	1.7 (1.3-2.1)	1.1 (0.9-1.3)	7.1 (6.2-7.9)	5.3 (4.6-5.9)	4.2 (3.6-4.8)	3.3 (3.0-3.7)
All	487	56	3.5 (2.9-4.9)	2.2 (1.8-3.1)	1.5 (1.2-2.1)	1.1 (0.9-1.3)	6.4 (5.5-7.9)	4.8 (4.2-5.9)	3.8 (3.3-4.8)	3.2 (2.8-3.7)

Dimensions of inner and outer airway diameter for each age separated by airway group. Airway diameters are described as the median, first and third quantile.

outliers of the AA-ratio and tapering values that were omitted are described in the Appendix. The mean (range) age was 11.85 (0.45-19.9) with 272 males (56%). Detailed demographics of the airway dimensions are shown in table 1 and the AA ratios and tapering values in table 2.

TABLE 2. Characteristics of AA-ratio and tapering by airway size

Airway size	AA-ratio			Intra-branch tapering			Inter-branch tapering		
	n	Inner	Outer	n	Inner	Outer	n	Inner	Outer
Central	3562	0.7±0.2	1.2±0.2	8759	0.8±1.8	1.0±1.4	5953	25.6±13.1	17.6±10.0
Segmental	5817	0.5±0.2	1.2±0.3	8653	0.7±1.9	1.1±1.4	5697	31.9±13.9	22.0±10.5
Sub-segmental	11879	0.5±0.1	1.2±0.3	15495	1.2±2.0	1.0±1.4	11696	37.6±14.4	24.4±11.5
Peripheral	11523	0.4±0.1	1.2±0.3	15330	1.5±1.9	0.9±1.5	12333	42.6±13.2	25.0±11.3
All airways	32781	0.5±0.2	1.2±0.3	48237	1.1±1.9	1.0±1.4	35679	36.4±14.9	23.1±11.3

This table shows the mean ± standard deviation for the AA-ratio and tapering for each airway size.

Airway and artery dimensions

The mean number of visible airways and visible AA pairs are shown by age in Figure 1. The number of airways increased with age (estimate = 4.3, $p < 0.0001$) and was higher in males (estimate = -7.7, $p = 0.005$) in the linear model. The number of AA pairs increased with age (estimate = 4.6, $p < 0.0001$) and was higher in males (estimate = -7.1, $p = 0.01$) in the linear model.

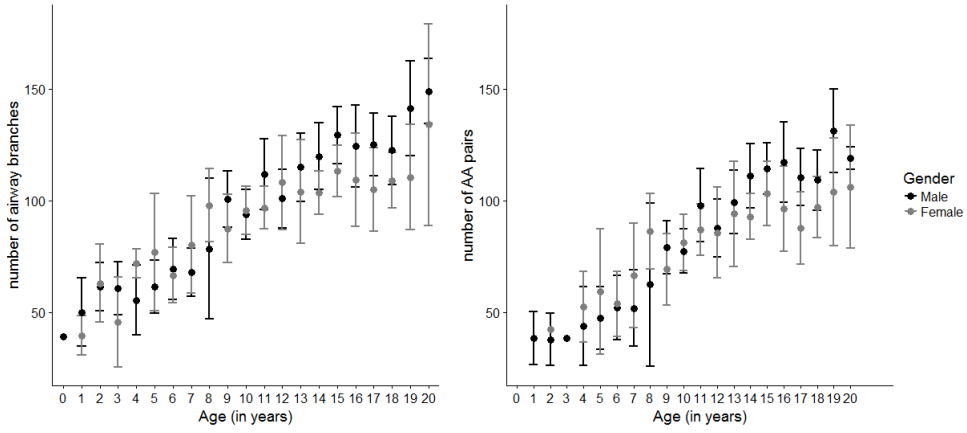

FIGURE 1. The 95% confidence interval for number of airway branches (left) and number of AA pairs (right) for each age group for male subjects (black) and female subjects (gray).

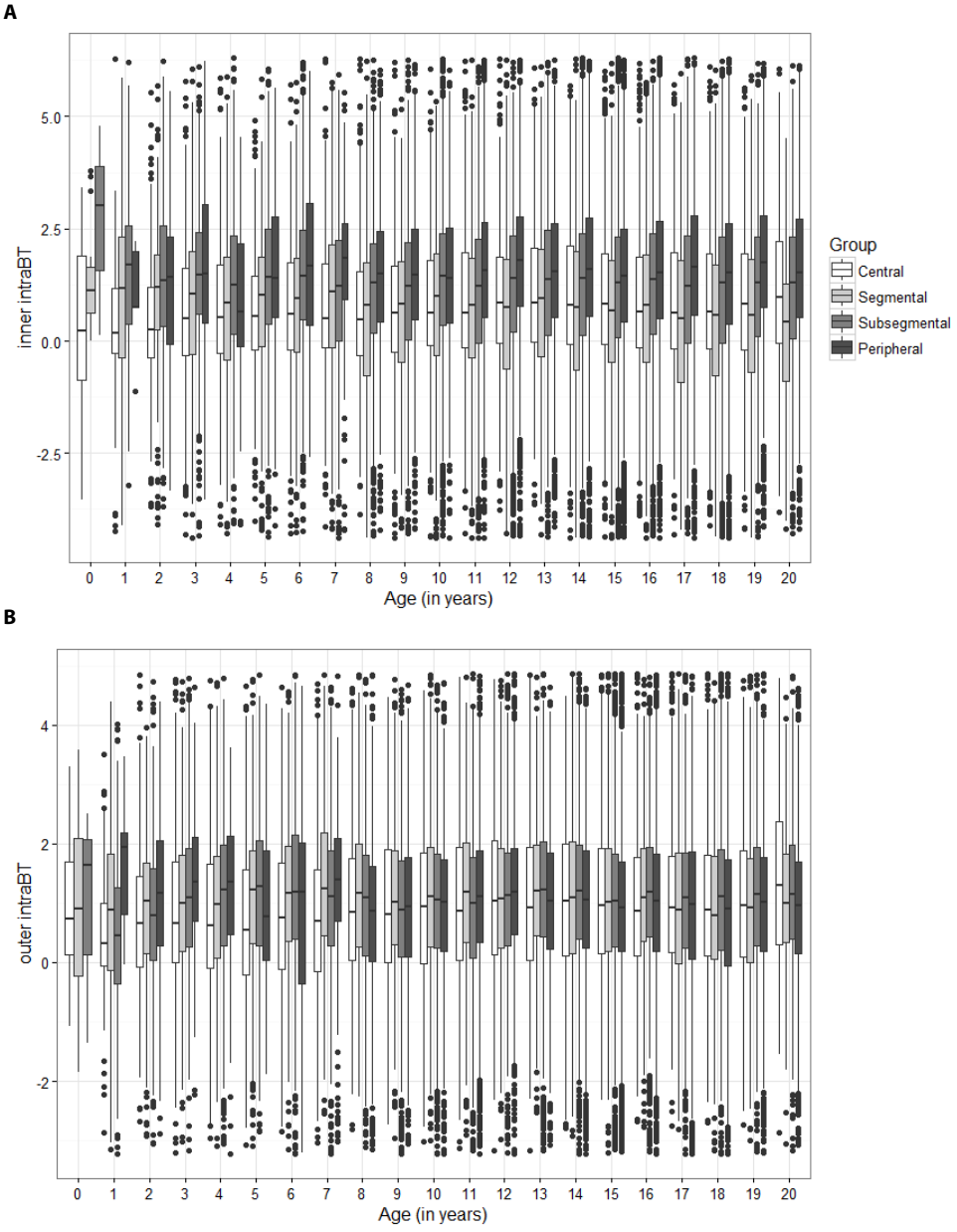

FIGURE 2. Boxplots of the **a.** inner intra-branch and **b.** outer intra-branch tapering is shown by age for the central (white), segmental (light grey), subsegmental (grey) and peripheral airways (dark grey). Each box shows median (horizontal line), interquartile range (solid box), 1.5*interquartile range (whiskers) and outliers (points). Note that the inner intra-branch tapering is uniformly decreased from the central airways to the peripheral airways across all ages. The outer intra-branch tapering is more consistent among the airway groups across most ages.

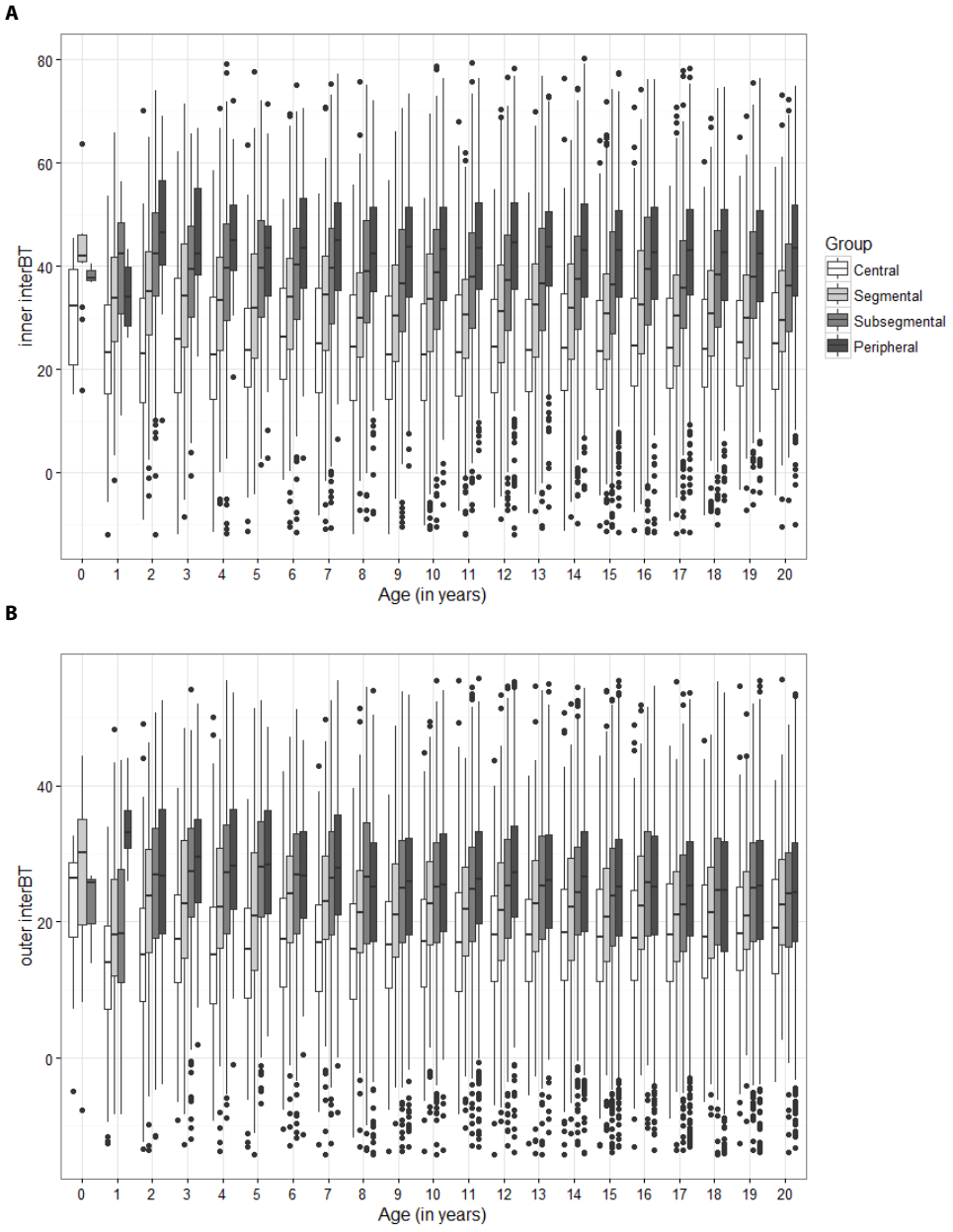

FIGURE 3. Boxplots of the **a.** inner inter-branch and **b.** outer inter-branch tapering is shown by age for the central (white), segmental (light grey), subsegmental (grey) and peripheral airways (dark grey). Each box shows median (horizontal line), interquartile range (solid box), 1.5*interquartile range (whiskers) and outliers (points). Note that the inner inter-branch and the outer inter-branch tapering is uniformly decreased from the central airways to the peripheral airways across all ages.

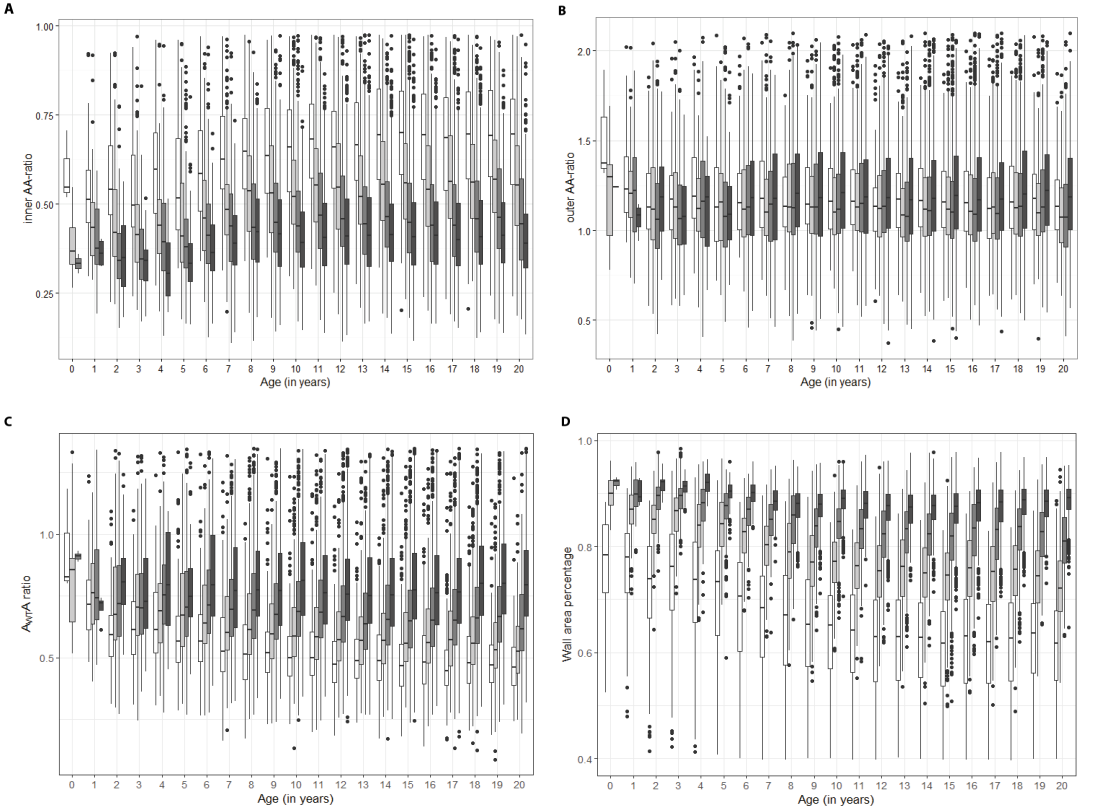

FIGURE 4. Boxplots of the **a.** inner and **b.** outer AA-ratio, **c.** A_{WT}A-ratio and **d.** wall area percentage (WAP) is shown by age for the central (white), segmental (light grey), subsegmental (grey) and peripheral airways (dark grey). Each box shows median (horizontal line), interquartile range (solid box), 1.5*interquartile range (whiskers) and outliers (points). Note that the inner AA-ratios are uniformly increased from the central airways to the peripheral airways across all ages. The outer AA-ratios showed to be consistent among the airway groups across most ages. The A_{WT}A-ratio and WAP are uniformly decreased from the central airways to the peripheral airways across all ages.

Airway intra-branch tapering

The inner and outer intra-branch tapering values are demonstrated for each age group and airway group in Figures 2a and 2b, respectively. Age and gender were not significant predictors of the inner and outer intra-branch tapering ($p > 0.68$). The airway group was a significant predictor for the inner intra-branch tapering (value = 0.29, $p = 0.0005$), with increasing intra-branch tapering from central to peripheral airways. The airway group was not a significant predictor for the outer intra-branch tapering ($p=0.78$).
The airway generation was not a significant predictor in the mixed-effect model for the inner intra-branch tapering ($p = 0.72$) nor the outer intra-branch tapering ($p = 0.14$).

Airway inter-branch tapering

After outlier exclusion, 34,187 inter-branch tapering measurements were analyzed. The inner and outer inter-branch tapering values are demonstrated for each age group and airway group in Figures 3a and 3b, respectively. Age and gender were not significant predictors of the inner and outer inter-branch tapering ($p > 0.59$). The airway group was a significant predictor for both the inner inter-branch (value = 6.43, $p < 0.0001$) and outer intra-branch tapering (value = 2.78, $p < 0.0001$), with an increasing inter-branch tapering from central to peripheral airways.
The airway generation was a significant predictor in the mixed-effect model for the inner inter-branch tapering (value = 0.85, $p = 0.007$), with increasing inter-branch tapering by generation. The airway generation was not a significant predictor in the mixed-effect model for the outer inter-branch tapering ($p = 0.93$).

Airway to artery ratio

The inner and outer AA-ratios, A_{WT}A-ratio and WAP are demonstrated for each age group and airway group in Fig 4a-d respectively. Age and gender were not significant predictors of the inner and outer AA-ratio or the A_{WT}A-ratio ($p>0.36$). Age was a predictor of WAP (value -0.005, $p = 0.02$). In the mixed-effect model the airway group was a significant predictor for: inner AA-ratio (value = -0.09, $p < 0.0001$), with decreasing AA-ratios from central to peripheral airways; A_{WT}A-ratio (value 0.09, $p < 0.0001$) and WAP (0.07 $p < 0.0001$), with increasing A_{WT}A-ratio and WAP from central to peripheral airways. The airway group was not a significant predictor for the outer AA-ratio ($p=0.45$).
The airway generation was a significant predictor in the mixed-effect model for: inner AA-ratio (value = -0.03, $p<0.0001$) and outer AA-ratio (value = -0.02, $p=0.012$), with decreasing AA-ratios by generation; WAP (value = 1.4, $p<0.0001$), with increasing WAP by generation. The airway generation was not a significant predictor in the mixed effect model for A_{WT}A-ratio ($p = 0.11$).

DISCUSSION

This study provides normative data for the airway and artery dimensions and tapering measures based on a large dataset with normal pediatric chest CTs. Normative data of AA dimensions are provided and the AA-ratios, intra-, and inter-branch tapering values have been determined by central, segmental, subsegmental and peripheral airway groups in children and adolescents.

The most important finding of this study is that the AA-ratios, intra- and inter-branch tapering values are not dependent on age or gender from birth to 20 years old. These findings confirm previous studies[7,9,13] reporting that AA-ratios in control patients are constant regardless of age and gender. A mean inner AA-ratio of 0.5 and an outer AA-ratio of 1.2 was found in this study, which is in concordance with previous studies assessing the AA-ratios in studies with smaller sample sizes.[7,13,14] Both the intra-, and inter-branch tapering values are similar to the findings by Perez-Rovira et al. using a subset of 168 CTs from the Children Chest CT Study Group dataset.[6] A mean inner and outer intra-branch tapering of 1% was found, however with large standard deviations, indicating a low signal to noise ratio that highlights the difficulty to measure such a small change in airway size. The mean inter-branch tapering was 36% for the inner airway and 23% for the outer airway diameter. The inner inter-branch tapering reference values of 36% in the *Children Chest CT Study Group* is higher than previous studies in adults and with small sample sizes reporting an inner inter-branch tapering value of around 26%.[4,5]

The next important finding of this study is that the airway group influences the AA ratio and tapering values. The inner AA-ratio was lower in the subsegmental and peripheral airways compared to the central and segmental airways. However, the outer AA-ratio remained constant by airway group. Wall thickening defined as A_{WT}A-ratio and WAP were found to be higher from peripheral to central airways. The inner intra-branch, inner and outer inter-branch tapering were higher in the peripheral airways compared to the central airways, but the outer intra-branch tapering remained constant. The outer AA-ratio and outer intra-branch tapering were uniform across all airway sizes, which make the reference values easy to use in clinical practice.

Lastly, the number of visible airways and AA pairs that could be measured with automated analysis algorithms increases with age. The number of visible AA pairs was previously suggested to be a potential biomarker for disease severity.[7,15] However, as shown with this study age should be taken into account as the number of AA pairs increase at least till the age of 15 years old for both male and females.

This study has some limitations. First, the control patients could not be considered truly healthy as they were referred for chest CT for clinical indications. Even though all CTs were reported to be normal by two independent radiologists, we cannot exclude that subtle changes in AA dimensions could have been present.

Secondly, CTs were not acquired using a standardized protocol and were not standardized for lung volume during acquisition, as the dataset was collected retrospectively. Parameters in the scan protocol such as radiation dose, reconstruction kernels and slice thickness influence the image quality and spatial resolution of a CT scan.[16] With this heterogeneous dataset this may have affected the size measures. While the automated algorithm has been previously validated for CTs of diseased and controls subjects obtained with different scanning protocols, the method has only been validated using CTs form a single clinical center.[10] However to decrease the inclusions of erroneous values in this study extreme outliers were excluded. Standardization of lung volume during CT acquisition has shown to influence the AA ratios[7,17] and the inner intra-branch tapering.[6] AA ratios and intra-branch tapering were significantly higher in CT scans with inspiratory volume control.[7,10,17] The data presented in this study could be an underestimation of the values on volume controlled inspiratory CT scans. Yet, even with this variable dataset the AA ratios found in this study are comparable to previous studies using spirometer guided inspiratory volume control.[7]

Thirdly, as in all CT-based studies of airways, the limited image resolution on CT scans means that only airways larger than certain size would be visible. Thus, the peripheral airway group, and any of the other airway groups if fewer than 18, 36 or 72 airways were found, shows a bias towards larger airways. In addition, we included the analysis based on airway generation. However, as described previously,[7] a downside of the airway generation is that the generations found in the lower lobes are higher than generations in the upper lobes. The difference in airway generation of upper and lower lobes could not be corrected in the automated extracted data. This could therefore have led to different results between analysis with airway groups and generations. Since both grouping methods had limitations we included the reference values for both the airway group and generation.

The normative airway dimensions presented in this paper can be used to assess and diagnose various structural airway abnormalities such as bronchiectasis and airway wall thickening. The identification of bronchiectasis can be performed with the airway to artery ratio and the novel tapering values. Normative airway values could be of value for radiologists and pediatric pulmonologists, particularly when automated airway analysis will be incorporated in clinical practice.

CONCLUSION

In our study, normative airway and artery dimensions, airway-artery ratios and tapering values were quantified on chest CT of a large group of children and adolescents. All AA-ratios and tapering values were found to be independent of age and gender. Airway group influenced tapering values: the inner intra-branch tapering, inner and outer inter-

branch tapering were larger in the peripheral airways compared to the central airways. The reference values established in this study could be used for thresholds of diseased lungs and could be the groundwork for automated airway disease quantification in children.

ACKNOWLEDGEMENTS

We would like to thank Hadiye Ozturk, Dora Angyal, Niels Erkelens, Sarina A. Balentin (Dept. of Pediatric Pulmonology and Dept. of Radiology, Erasmus MC- Sophia Children's Hospital, Rotterdam, the Netherlands) for their involvement in manual annotation and segmentation of the airways.

REFERENCES

1. Ciet P, Serra G, Bertolo S, Spronk S, Ros M, Fraioli F, Quattrucci S, Assael MB, Catalano C, Pomerri F, et al. Assessment of CF lung disease using motion corrected PROPELLER MRI: a comparison with CT. European Radiology. 2015.
2. Newell JD. Bronchiectasis. In: Contemporary Medical imaging. CT of the. 2008. p. 213–235.
3. McGuinness G, Naidich D, Leitman B, Mccauley D. Pictorial Essay Bronchiectasis : CT Evaluation. Radiology. 1993;160:253–259.
4. Montaudon M, Desbarats P, Berger P, Dietrich G de, Marthan R, Laurent F. Assessment of bronchial wall thickness and lumen diameter in human adults using multi-detector computed tomography: comparison with theoretical models. Journal of anatomy. 2007;211(July):579--588.
5. Tawhai MH, Hunter P, Tschirren J, Reinhardt J, McLennan G, Hoffman E a. CT-based geometry analysis and finite element models of the human and ovine bronchial tree. Journal of applied physiology. 2004;97(6):2310–2321.
6. Perez-Rovira A, Kuo W, Tiddens HAWM, de Bruijne M. Airway tapering revisited: an objective image biomarker for bronchiectasis. European Respiratory Journal. 2017;submitted.
7. Kuo W, de Bruijne M, Petersen J, Nasserinejad K, Ozturk H, Chen Y, Perez-Rovira A, Tiddens HAWM. Diagnosis of bronchiectasis and airway wall thickening in children with cystic fibrosis: Objective airway-artery quantification. European radiology. 2016:In press.
8. Nakano Y, Muro S, Sakai H, Hirai T, Chin K, Tsukino M, Nishimura K, Itoh H, Pare PD, Hogg JC, et al. Computed tomographic measurements of airway dimensions and emphysema in smokers correlation with lung function. American Journal of Respiratory and Critical Care Medicine. 2000;162(3 I):1102–1108.
9. De Jong P a., Nakano Y, Hop WC, Long FR, Coxson HO, Paré PD, Tiddens H a. Changes in airway dimensions on computed tomography scans of children with cystic fibrosis. American Journal of Respiratory and Critical Care Medicine. 2005;172(2):218–224.
10. Perez-Rovira A, Kuo W, Petersen J, Tiddens HAWM, de Bruijne M. Automatic airway–artery analysis on lung CT to quantify airway wall thickening and bronchiectasis. Medical Physics. 2016;43(10):5736–5744.
11. Lo P, Sporring J, Ashraf H, Pedersen JJH, de Bruijne M. Vessel-guided airway tree segmentation: A voxel classification approach. Medical Image Analysis. 2010;14(4):527–538.
12. Petersen J, Nielsen M, Lo P, Nordenmark LH, Pedersen JH, Wille MMW, Dirksen A, de Bruijne M. Optimal surface segmentation using flow lines to quantify airway abnormalities in chronic obstructive pulmonary disease. Medical Image Analysis. 2014;18(3):531–541.
13. Kuo W, Soffers T, Andrinopoulou E-R, Rosenow T, Ranganathan SC, Turkovic L, Stick SM, Tiddens HAWM. quantitative assessment of airway dimensions in young children with cystic fibrosis lung disease using chest computed tomography. Pediatric Pulmonology. 2017;submitted.
14. Kapur N, Masel JP, Watson D, Masters IB, Chang AB. Bronchoarterial ratio on high-resolution CT scan of the chest in children without pulmonary pathology: Need to redefine bronchial dilatation. Chest. 2011;139(6):1445–1450.

15. Kuo W, Andrinopoulou E-R, Perez-Rovira A, Ozturk H, De Bruijne M, Tiddens HAWM. Assessment of bronchiectasis and airway wall thickening on chest CT of cystic fibrosis patients: Comparison between quantitative airway-artery method and two semi-quantitative scoring techniques. Journal of Cystic Fibrosis. 2016:Submitted.
16. Kuo W, Kemner-van de Corput MPC, Perez-Rovira A, de Bruijne M, Fajac I, Tiddens HAWM, van Straten M. Multicentre chest CT standardisation in children and adolescents with cystic fibrosis : the way forward. European Respiratory Journal. 2016:1–12.
17. Mott LS, Graniel KG, Park J, De Klerk NH, Sly PD, Murray CP, Tiddens H a WM, Stick SM. Assessment of early bronchiectasis in young children with cystic fibrosis is dependent on lung volume. Chest. 2013;144(4):1193–1198.

APPENDIX

Outliers:
39 measures deleted with generation ≥15
1.5*IQR A_{out}A-ratio: lower limit: 0; upper limit: 1639 (3.9%)
1.5*IQR A_{in}A-ratio: lower limit: 0; upper limit: 1909 (4.6%)
1.5*IQR A_{WT}A-ratio: lower limit: 34 (0.1%); upper limit: 1542 (3.7%)

1.5*IQR inner intraBT: lower limit:4289 (6.9%); upper limit: 1558 (2.5%)
1.5*IQR outer intraBT: lower limit: 4238 (6.8%); upper limit: 1201 (1.9%)
1.5*IQR WTR: lower limit: 870 (1.4%); upper limit: 0

1.5*IQR inner interBT: lower limit: 2048 (4.4%); upper limit: 114 (0.2%)
1.5*IQR outer interBT: lower limit: 2374 (5.1%); upper limit: 171 (0.4%)

- intraBT 62,567 -> 48,237
- interBT 46,988-> 35,679
- AA pairs 41,833-> 32,781

Appendix Table E1. Scan parameters.

CT scanners	17x GE; 228x Philips; 251x Siemens; 19x Toshiba
Tube voltage (kV)	110 (90-120)
Pitch*	1 (1-1)
Slice thickness (mm)	1 (1-1.5)
Reconstruction increment (mm)	0.8 (0.7-1)
Reconstruction kernel	GE: 15x LUNG; 2x STANDARD Philips: 18x B; 74x C; 1x D; 44x L; 82x YA; 6x YB; 3x YD Siemens: 7x B20; 2x B26; 12x B30; 20x B31; 1x B40; 2x B46; 4x B50; 76x B60; 78x B70; 35x B75; 1x B80; 1x I30; 12x I70 Toshiba: 16x FC12; 3x FC18
Current-time product (mAs)*	48.17 (25.36-83.38)
CTDI (mGy)*	2.2 (1.1-4.6)

Summary of the scan parameters used. The parameters are shown with median, interquantile range.
* 414 scans did not include pitch; 1 scan did not include current-time product; 189 scans did not include CTDI

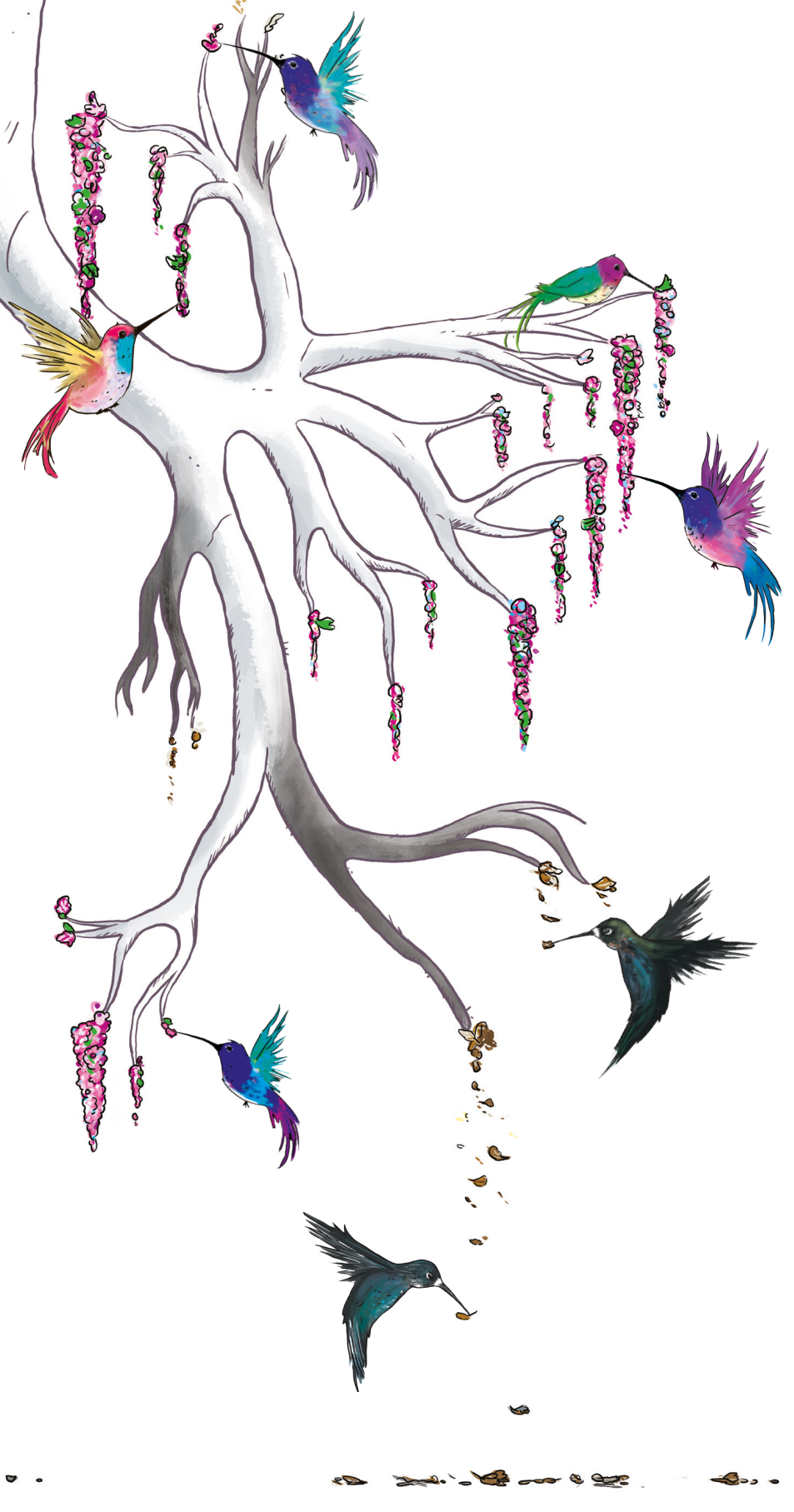

CHAPTER 10

GENERAL DISCUSSION

In patients with CF, progressive structural lung disease starts early in life and leads to respiratory symptoms. Eventually CF lung disease leads to a premature death in most CF patients. Close monitoring of CF lung disease using various outcome measures is essential to guide treatment and for clinical trials. CT is currently the most sensitive imaging technique to assess structural lung disease, such as bronchiectasis, airway wall thickening and mucous plugging. In children with CF it is important to detect structural lung changes at an early stage before irreversible alterations of the lung have established. The studies presented in this thesis address the challenges of chest CT usage in children with CF and the further validation of objective image analysis strategies to assess structural lung disease.

Image acquisition

The acquisition of CT images in the pediatric population and in multi-center studies comes with two challenges described in the first part of this thesis. The first challenge is the associated radiation exposure. Routine chest CT has shown to be beneficial for detecting and monitoring structural lung damage in children with CF. Unfortunately, chest CT exposes patients to ionizing radiation, which has potential carcinogenic risks. In the past decades the radiation dose for a volumetric chest CT has decreased substantially for which updated risk estimates were needed to adequately assess the risk to benefit ratio in patients with CF. In the review on this issue described in Chapter 2 we estimated that the additional life time mortality risk for routine biennial chest CT scanning from birth till the age of 18 years was 0.2%. This finding was in concordance with previous risk estimates by Gonzalez et al.[1] Most importantly the estimated risk is about 2.5 times lower when taking into account the reduced life expectancy of patients with CF. Our review allows the assessment of the risk to benefit ratio of chest CT scans acquired in children with chronic diseases such as CF.

The second challenge with chest CT usage in clinical trials is the large variety of CT scanners and CT protocols used in children with CF. Standardization is required to compare chest CTs of patients across different centers or even within centers when different scanners and/or protocols are being used. Previous standardization studies were only performed with adult sized phantoms.[2–4] For the study presented in Chapter 3, custom designed anthropomorphic thorax phantoms composed of human tissue equivalent material were developed specifically for pediatric patients. The infant, child and adult phantoms were scanned at 16 European CF centers. A large variation in image noise and radiation dose was found between centers when scanning protocols were not standardized. After correction for differences in spatial resolution, differences in image quality remained. We found that standardization can be achieved with equal image

quality across centers with proper adjustment of resolution and radiation dose. The findings of this study allow for standardization of chest CTs in multi-center clinical studies.

Image analysis

The second part of this thesis describes the sensitive and objective image analysis method to assess airways disease on chest CT scans. The studies described in Chapter 4 and 5 compare the objective quantification of airway and artery dimensions in children and adolescents with CF with control patients.

The main finding of our studies is that the diagnosis of bronchiectasis based on the inner airway diameter should be revisited. We found that diagnosis of bronchiectasis by diameter comparison with the adjacent artery was more reliable for the outer than for the inner airway diameter. In clinical practice and in recent studies, the inner airway diameter is generally compared with the adjacent artery for the diagnosis of bronchiectasis.[5–7] Our data show that the prevalence of bronchiectasis in children with CF is underestimated using the inner airway diameter since it does not show clear differences with a control group and is more influenced by lung volume. On the other hand, the outer airway diameter does differentiate CF from controls patients significantly from birth into adolescence.

The second finding is that more AA pairs are visible in children with CF compared to controls. The increase in AA pairs could be a consequence of airway inflammation with more dilated airways and bronchiectasis in patients with CF. Therefore the number of visible AA pairs could be a biomarker for disease severity in patients with CF. However, aside from disease severity it should be noted that the number of AA pairs is also dependent on age and inspiration level. Our studies demonstrate that the number of AA pairs is 2 to 3 times higher on spirometer guided inspiratory CT compared to expiratory CTs, which could subsequently affect the detection of bronchiectasis in the peripheral airways. The difference in number of AA pairs visible and in AA ratios between CF and control patients was larger in end-inspiration than in end-expiration CTs.

Chapter 4 and 5 also quantified the airway wall thickness to artery ratio in patients with CF compared to controls. The third finding is that airway wall thickness was better visible in end-expiratory compared to end-inspiratory CTs, likely because of a higher intensity on CT due to the folding of the airways. Findings related to bronchiectasis and airway wall thickness reiterate the need for lung volume standardization for sensitive detection and monitoring of structural lung disease in a consistent manner.[5]

Furthermore, Chapter 5 shows that differences as determined by the AA method between 12 CF and 12 control subjects is initially small in children around 3 years old, but increased after a follow up of 2 years. In the longitudinal comparison, the change in inner airway to artery ratio was small but significant over two years in these young

children with CF. However, the change in outer airway to artery ratio was not significant over two years. An explanation for this finding could be that the outer diameter reflects irreversible airway dilation accurately, and in contrast to the inner diameter, is less influenced by early inflammation.[8] However, another explanation for this finding could be that the studied population was too small to detect significant differences in the outer airway diameter.
Lastly, the AA ratios were more abnormal in peripheral airways than in central airways in infants, children, and adolescents with CF compared to normal subjects. This finding confirms previous studies that suggested that the small airways play an important role in CF lung disease.[9,10] Our findings suggest that the small airways more affected by chronic infection compared to the larger airways and we speculate that the small airways are affected first in infants with early CF lung disease. This however needs to be further investigated in a larger cohort.

The sixth important finding of our AA studies, as described in Chapter 6, is that established scoring techniques, such as the CF-CT[6] and PRAGMA-CF[11] can be used to assess airways disease in children and adolescents with CF. The CF-CT is a well-standardized scoring system but it is not sensitive to quantify early CF lung disease as the extent of disease is scored as absent, less than 33%, between 33 and 67%, or more than 67%. Hence, determinants of lung disease such as bronchiectasis in young children will mostly be scored as either absent or less than 33%. For this reason PRAGMA-CF was developed especially for scoring young children with early CF lung disease as a more sensitive alternative. We investigated the two scoring systems in children aged 6 to 16 years old and showed that both CF-CT and PRAGMA-CF scores correlated well with the number of AA pairs and outer AA-ratios. The outer AA-ratio for bronchiectasis correlated better with the bronchiectasis and total airways disease sub-score for PRAGMA-CF scoring than with the CF-CT scoring. The AA-ratio for airway wall thickening correlated better with the airway wall thickness sub-score of CF-CT scoring than with PRAGMA-CF. This is most likely due to the hierarchical system using in PRAGMA-CF, where only bronchiectasis is scored when both bronchiectasis and airway wall thickening are present. This explanation is supported since there is a higher correlation with the total airway disease sub-score by PRAGMA-CF than with CF-CT. The results of this study are important as they validate the role of scorings system for the assessment of CF lung disease in children and adolescents with CF.

The quantification of airway and artery dimensions in Chapter 4, 5 and 6 as discussed above, was performed largely manually. Quantifying thousands of airway and artery dimensions manually was a very time consuming task. Overall it took 15 hours on

average to analyze one CT scan, depending on the quality of the scan and severity of the lung disease. Manual assessment of the airway and artery dimensions was an important step for the validation of an automated analysis technique[12] which was used in Chapter 7 and 9. Automatic analysis of the airway and artery dimensions is essential to analyze larger sample sizes. It limits the timely and costly assessment of semi-automatic analysis and eliminates intra-, and interobserver variation.

The seventh important finding of our AA studies is that we developed an algorithm to objectively assess airway tapering as a determinant of airway disease. Lack of tapering is considered a determinant of bronchiectasis by radiologists, however objective automated methods to assess lack of tapering are lacking to date. In Chapter 7 we describe state-of-the-art medical image analysis software for the automated assessment of tapering. Unique of the method is that both the inter- and intra-branch tapering were assessed automatically. The intra-branch tapering is defined as reduction in diameter along an airway branch and inter-branch tapering is defined as reduction in diameter between an airway before and after bifurcation. For the validation of this algorithm we used spirometer guided inspiratory CTs of bronchiectatic patients and compared them with controls. A significant reduction in intra-, and inter-branch tapering was observed in the large, medium and small airway branches of bronchiectatic patients compared to controls. This result was in contrast with the AA-method which showed the AA-ratios of bronchiectatic patients to be increased compared to controls only in the small airways . These findings suggest that the analysis of the more central airways could suffice as a determinant of the overall severity of CF lung disease. This is a promising result which could mean that the use of tapering could improve sensitivity for the detection of airways disease in clinical care and for clinical trials. Additionally this study showed a difference in the control patients with and without volume control during acquisition with the inner AA-ratio and inner intra-branch tapering. This indicates that the inner airway diameter is more affected by the inspiration level than the outer diameter. This finding is line with the previous statement for the use of the outer airway diameter in Chapter 4.

Reference values

Airway dimensions can be assessed accurately and non-invasively using chest CT. In order to assess abnormal airway dimensions it is important to know the normal range of lung dimensions in children with growing lungs. Pediatric reference values are needed when using lung image parameters of patients for clinical management. For this reason, 1160 CTs have been collected in ten centers worldwide. In the third part of this thesis we describe the normative data on the trachea, central airways and airway to artery

dimensions. We determined the physiological anatomical growth of the lung structures on chest CT of children and adolescents and provided normative dimensions of the trachea, main bronchi and the airway tree.

In Chapter 8, the normative dimensions of the trachea and central airways showed the position relative to the carina to be of influence on the size of the trachea, left and right mainstem bronchi. The central airway dimensions were larger near the carina and near the mainstem bronchi bifurcation. In addition, the central airway dimensions increased similarly with age in both male and female subjects until the age of 13-14 years old. After this age, central airway dimensions are larger in male subjects than in female subjects. This finding could be related to the onset of puberty in males or the end of puberty in females.[13] Similar findings were observed for the trachea by Griscom et al.[14] Normative data on the entire main stem bronchi was not available and could not be compared.

In Chapter 9, the normative airway and artery dimensions were quantified automatically. AA-ratios were constant regardless of age and gender from birth to 20 years old, confirming previous findings in smaller control groups described in chapter 4 and 5. In addition to the AA ratio, intra- and inter-branch tapering values were also found to be independent of gender and age. However the inner AA-ratio, inner intra-branch, inner and outer inter-branch tapering were found to be dependent on airway size. The inner AA-ratio was lower in the peripheral airways compared to the central airways and the inner intra-branch, inner and outer inter-branch tapering were higher in the peripheral airways compared to the central airways. The outer AA-ratio and outer intra-branch tapering remained constant by airway group. The uniformity across all airway sizes makes these reference values easy to use in clinical practice. This indicates the robustness of the AA-ratios and tapering biomarkers and their reference values to detect airway abnormality in the pediatric population.

Future directions

Chest CT has become increasingly important in clinical practice for the diagnosis and monitoring of CF lung disease. The studies presented in this thesis have contributed to the objective assessment of CF lung disease with validation of fully-automated and semi-quantitative scoring techniques and improved our understanding of the pathogenesis of lung disease. In addition, we have generated normative data for central airways and airway to artery dimensions. Physical changes of the airways have been assessed in control subjects to improve our understanding of the normal thoracic growth. There are however many opportunities to further improve the image analysis of lung disease and the use of image analysis outcomes in the clinic and for clinical studies.

Minimizing radiation dose

Advances in CT technology and reconstruction techniques will allow further reduction of the radiation exposure. With the latest generation CT scanners, an ultra low-dose chest CT exposes the patient to a radiation dose which is in the range of a chest X-ray.[15] Hopefully, the radiation dose levels of chest CT can be reduced to the level where it becomes ethically possible to acquire chest CTs in the healthy population one day. To date, normative data have been generated using control patients who were referred for CT but did not show any abnormalities on their CT. Clearly this is not an optimal solution as these patients cannot with certainty be considered truly healthy. If radiation exposure levels of CT scanners decrease in the future and become irrelevant, the assessment of reference values should be repeated on a healthy cohort. On the other hand, the quality of radiation free alternatives, such as chest MRI is improving rapidly. Recent improvements in MRI pulse sequences allow for better detection and resolution of the airways.[16] If the resolution and signal to noise ratio of MRI images approach the level of the current CTs, normative imaging data of the airways can be generated for MRI based on a truly healthy population. Regardless of the resolution, scanning with MRI has a long acquisition time which is more challenging in the younger age group. Children aged 0 to 6 years old are not cooperative and have higher cardiac and respiratory rates resulting in more movement artifacts. Hence, for the next decade it is likely that chest CT will continue to be the preferred modality for these younger children.

CT standardization

We showed that standardization of CT protocols is feasible across international CF centers. For multi-center studies, it is of key importance to standardize CT protocols and lung volume during acquisition. Image quality and lung volume levels have shown to influence the detection and appearance of structural lung disease severity. In multi-center studies investigating the effect of expensive drugs it is important to have minimal variance on chest CTs to make an unbiased sensitive comparison between patients. In addition, standardization of CT protocols will streamline automated image analysis. Furthermore, standardization improves the quality and diagnostic yield of the CT scan. Hence, the medical community should embrace and implement lung volume standardization for routine chest CTs as standard care.

Image analysis

More quantitative analysis is needed to understand the pathophysiology of CF lung disease on the airways. In particular, image analysis of the longitudinal follow-up of young children with CF during end-inspiration and end-expiration is required. It would be interesting to determine the effect of inflammation in early CF lung disease in a

larger study population to assess the change on the inner and outer airway diameter. Furthermore, the small airways of the young children were near the resolution limits of a CT scanner. This affects the accuracy of the measurements of the small airways.[17] Accuracy of the measurements can be improved in future studies with better image quality of the CT scan and advanced automated measurement techniques that take the limited spatial resolution of the CT scanner into account.
A promising biomarker described in this thesis is the lack of tapering in patients with CF. Tapering showed to be more sensitive than the airway to artery ratio and occurs uniformly across all airway sizes. An additional advantage of the tapering method over the AA-method is that it does not require comparison to the pulmonary artery system. Hence, segmentation of the pulmonary artery system is not required which makes the automatic measurement of tapering less challenging and perhaps more robust as the outcome is not influenced by the artery. Tapering was assessed in a large control cohort but only in 12 patients with bronchiectasis and needs to be assessed in a larger CF study population. Lastly, it would be of interest to quantify tapering in adults with severe airway disease.

Reference values

A limitation of the normative data, in addition to the population not being truly healthy and not large enough, is the lack of information on height, weight and ethnicity of the patient. It is known that the patients' size and ethnicity can impact the size of the airways. However, it was not possible for us to collect this information retrospectively since the data for our study needed to remain anonymous and not retraceable to the patient. When prospective studies with a healthy population can be repeated, it is important to collect all relevant data including the subjects' height, weight, and ethnicity.

Automated image analysis for clinical practice

Chest CT is sensitive and provides highly relevant information on the presence of lung disease and its progression in children. With standardization of CT protocols and lung volume levels among multiple centers we can ensure standardized outcome measures on CTs for future studies. Standardization is an important condition to allow routine use of image analysis software for clinical care and for the analysis of large numbers of chest CTs in registries. It will generate longitudinal data which in turn will improve our understanding of the pathophysiology and treatment of CF lung disease. Evidently, automated lung imaging biomarkers need to be properly validated by comparing them with functional tests and clinical outcome measures, such as exacerbations. Adding image analysis information to the expert analysis by the radiologist will enhance the diagnostic yield of the chest CT.

REFERENCES

1. de Gonzalez AB, Kim KP, Samet JM. Radiation-induced cancer risk from annual computed tomography for patients with cystic fibrosis. Am J Respir Crit Care Med. 2007;176(10):970–973.
2. Newell JD, Sieren J, Hoffman EA. Development of quantitative computed tomography lung protocols. Journal of thoracic imaging. 2013;28(5):266–71.
3. Sieren JP, Newell JD, Judy PF, Lynch DA, Chan KS, Guo J, Hoffman EA. Reference standard and statistical model for intersite and temporal comparisons of CT attenuation in a multicenter quantitative lung study. Medical Physics. 2012;39(9):5757.
4. Robinson TE, Long FR, Raman P, Saha P, Emond MJ, Reinhardt JM, Raman R, Brody AS. An Airway Phantom to Standardize CT Acquisition in Multicenter Clinical Trials. Academic Radiology. 2009;16(9):1134–1141.e1.
5. Mott LS, Graniel KG, Park J, De Klerk NH, Sly PD, Murray CP, Tiddens HAWM, Stick SM. Assessment of early bronchiectasis in young children with cystic fibrosis is dependent on lung volume. Chest. 2013;144(4):1193–1198.
6. Brody AS, Kosorok MR, Li Z, Broderick LS, Foster JL, Laxova A, Bandla H, Farrell PM. Reproducibility of a scoring system for computed tomography scanning in cystic fibrosis. Journal of thoracic imaging. 2006;21(1):14–21.
7. Gaillard EA, Carty H, Heaf D, Smyth RL. Reversible bronchial dilatation in children: comparison of serial high-resolution computer tomography scans of the lungs. European Journal of Radiology. 2003;47(3):215–220.
8. Tepper LA, Caudri D, Utens EMWJ, van der Wiel EC, Quittner AL, Tiddens HAWM. Tracking CF disease progression with CT and respiratory symptoms in a cohort of children aged 6-19 years. Pediatric Pulmonology. 2014;1189(February):1182–1189.
9. Tiddens HAWM, Donaldson SH, Rosenfeld M, Paré PD. Cystic fibrosis lung disease starts in the small airways: Can we treat it more effectively? Pediatric Pulmonology. 2010;45(2):107–117.
10. Ratjen F. Cystic Fibrosis: The role of the small airways. Journal of Aerosol Medicine and Pulmonary Drug Delivery. 2012;25(5):261–264.
11. Rosenow T, Oudraad MCJ, Murray CP, Turkovic L, Kuo W, de Bruijne M, Ranganathan SC, Tiddens HAWM, Stick SM. PRAGMA-CF. A Quantitative Structural Lung Disease Computed Tomography Outcome in Young Children with Cystic Fibrosis. American journal of respiratory and critical care medicine. 2015;191(10):1158–1165.
12. Perez-Rovira A, Kuo W, Petersen J, Tiddens HAWM, de Bruijne M. Automatic airway–artery analysis on lung CT to quantify airway wall thickening and bronchiectasis. Medical Physics. 2016;43(10):5736–5744.
13. Abbassi V. Growth and normal puberty. Pediatrics. 1998;102(2 Pt 3):507–11.
14. Griscom NT, Wohl MEB. Dimensions of the growing trachea related to age and gender. American Journal of Roentgenology. 1986;146(2):233–237.
15. Gordic S, Morsbach F, Schmidt B, Allmendinger T, Flohr T, Husarik D, Baumueller S, Raupach R, Stolzmann P, Leschka S, et al. Ultralow-Dose Chest Computed Tomography for Pulmonary Nodule Detection. Investigative Radiology. 2014;49(7):465–473.

16. Ciet P, Tiddens HAWM, Wielopolski PA, Wild JM, Lee EY, Morana G, Lequin MH. Magnetic resonance imaging in children: common problems and possible solutions for lung and airways imaging. Pediatric radiology. 2015:1901–1915.

17. Marquering HA, Stoel BC, Dijkstra J, Geleijns K, Persoon M, Jukema JW, Streekstra GJ, Reiber JHC. CT blurring induced bias of quantitative in-stent restenosis analyses. Proc. SPIE 6913, Medical Imaging 2008: Physics of Medical Imaging, 69131J

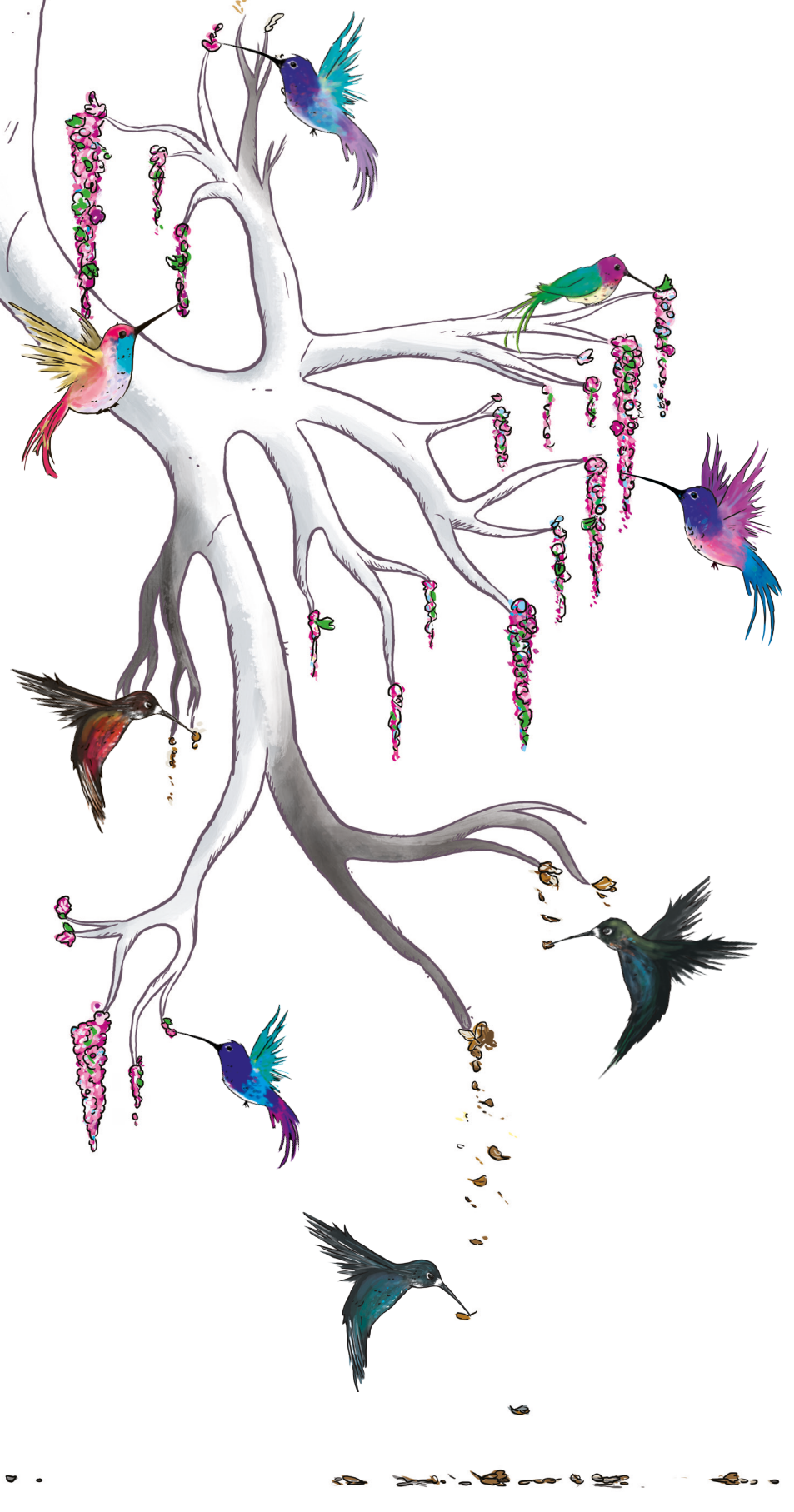

CHAPTER 11

SUMMARY / SAMENVATTING

SUMMARY

Children with cystic fibrosis (CF) routinely receive computed tomography (CT) scans in many centers to diagnose and monitor their lung disease. This thesis focuses on radiation safety, standardization and image analysis techniques related to chest CT of patients with CF.

Chapter 1 provides a general introduction and background to the hereditary disease CF, the safety and standardization of chest CT and monitoring and image analysis of CF lung disease using chest CT. Regarding radiation safety we aim to estimate the CT related radiation risks and put these risks into perspective. For standardization of chest CT we characterized and standardized pediatric chest CTs across multiple CF centers. To improve the image analysis we developed an objective airway quantification method for infants, children and adolescents with CF and to validate fully-automated and semi-quantitative scoring techniques.

Part 1 describes the safety and the standardization of routine chest CT. Chest CT is an important and sensitive image modality to assess structural changes related to CF lung disease. CT scanning, however, exposes the area of the body scanned with ionizing radiation and this could result in cancer later in life. **Chapter 2** describes the CT radiation dose terminology and complexities of estimating radiation risks for a pediatric population and reviews the risk estimates of routine chest CT usage in children. The estimated radiation induced risk for cancer mortality in a lifetime increases with younger ages at exposure. The estimated lifetime cancer mortality risk for nine routine chest CTs from birth till the age of 18 was calculated to be 0.2%. This risk is probably even 2.5 times lower, i.e. 0.08%, for CF patients since they have a lower life expectancy. To put this risk into perspective we compared this estimate to other CT indications, other radiation sources, CF-related risks and other "daily" risks. In conclusion, we estimated the risk associated with CF lung disease monitoring by CT to be relatively small. Nonetheless, the use of CT should always be justified and the radiation dose kept as low as reasonably achievable.

Different CT scanners and scan protocols lead to variations in image quality and radiation exposure among centers. To utilize chest CT as an outcome measure it is essential to standardize image acquisition. **Chapter 3** is about the standardization of chest CT for multi-center studies. The Standardized Chest Imaging Framework for Interventions and Personalized Medicine in CF (SCIFI CF) was founded to characterize chest CT image quality and radiation doses among 16 participating CF centers in 10 different European countries. The performance of the scanners in each center was assessed using three size specific chest phantoms. Considerable differences in CT protocols, image quality and

radiation dose were found among the participating centers. However, when adjusted for spatial resolution and radiation dose, the performance of the scanners was found to be quite similar. The SCIFI CF showed that standardization of chest CT is feasible in an international multicenter cohort.

The chapters in **Part 2** describe objective image analysis techniques to quantify lung disease on chest CT of pediatric CF patients. A sensitive and objective method to quantify the airway and artery dimensions on chest CTs was developed which is used in studies described in Chapter 4, 5 and 6. The objectively acquired dimensions of the airway and accompanying artery are used to assess structural airways disease, such as bronchiectasis and airway wall thickening.

In **Chapter 4**, airway and artery dimensions in patients with CF between 6 and 16 years old are compared with age- and gender-matched control patients. More than 6000 airway and artery pairs were measured in total up to the 15th airway generation in 11 CF and 12 control patients. The ratios of the inner airway diameter, outer airway diameter, and airway wall thickness to the adjacent artery diameter were all significantly larger on inspiratory compared to expiratory CTs in CF and control patients. The ratios of the outer airway diameter and airway wall thickness to the adjacent artery diameter were significantly larger in patients with CF compared to control patients, and this difference was increasingly greater in smaller airways. In conclusion, based on the objective quantification of the airways, the diagnosis of bronchiectasis was found to be most accurate on inspiratory chest CT. This study reiterates the need for lung volume standardization during chest CT acquisition. Secondly, the diagnosis of bronchiectasis was more reliable by comparing the outer airway diameter, instead of the inner airway diameter, with the adjacent artery. Lastly, the airway to artery ratio showed more prominent differences in the smaller airways than central airways of patients with CF.

In **Chapter 5**, the airway and artery quantification method is performed in young children with early CF lung disease below the age of 6 years, both cross-sectionally and longitudinally. In the cross-sectional analysis, CF patients were compared with control patients. In the longitudinal analysis, CF patients were compared at baseline (CT_1) and 2 years later (CT_2). In the cross-sectional analysis, the ratio of the inner airway diameter to artery diameter in the CF patients did not demonstrate a significant increase. The ratio of the outer airway diameter and airway wall thickness to artery diameter was significantly higher in patients with CF compared to controls. As was seen in the older children in Chapter 4, the outer airway diameter should be used to separate diseased CF airways from non-diseased CF airways in the young children with CF. Similarly to the older patients with CF, there are more dilated airways and thicker walls in the young children with CF compared to control patients. In the longitudinal analysis, a small but

significant progression could be detected in the ratio of the inner airway diameter to artery diameter after two years. In the longitudinal analysis over the two-year interval of children with CF: a small but significant change in the inner airway diameter to artery diameter was detected; a progressive increase was seen in the outer airway diameter to artery ratio for the peripheral airways; and no changes in airway wall thickness were detected after two years. This could be interpreted as the outer diameter reflecting irreversible airway dilation i.e., bronchiectasis and this diameter is, in contrast to the inner diameter, less influenced by lung volume and/or mucus impaction.

Our findings suggest that with the objective airway and artery quantification, smaller sample sizes could be required to test reduction by treatment than with semi-quantitative scoring methods. This supports the potential of objective airway and artery ratios as outcome measure in young children. We estimated that in young children with CF sample sizes of 21 and 33 per treatment arm would be needed to detect 50 and 40% reduction in outer airway to artery ratio between CF CT_2 and controls, with 80% power and α=0.05. In comparison, using the semi-quantitative scoring technique PRAGMA-CF a sample size of 100 per treatment arm would be needed, based on 50% reduction in total airway disease at age 3.

Scoring methods are less time consuming than measuring all airway and artery dimension manually but their accuracy has not been assessed in children. In **Chapter 6**, two semi-quantitative CT scoring systems are compared with objective quantification of airway and artery dimensions. CF and control patients with spirometer guided inspiratory chest CTs were scored with the two scoring methods and compared with the airway and artery dimension ratios as described in chapter 4. The CF-CT and PRAGMA-CF scoring methods both showed to be sensitive methods to score bronchiectasis and airway wall thickening in children and adolescents with CF. Bronchiectasis and total lung disease scores (defined as the sum of bronchiectasis, airway wall thickening and mucous plugging) were shown to be the most accurate predictor of airway and artery dimensions using the PRAGMA-CF scorings system. On a separate note, we found that the actual number of airway and artery pairs visible on the lung images correlated well with the CF-CT and PRAGMA-CF scores. Both airway dilation and wall thickening lead to a larger number of visible airway and artery pairs on CT. Thus, the number of airway and artery pairs on CT could be another potential marker for lung damage, but it should be noted that it is dependent on age and lung volume during CT acquisition.

In **Chapter 7**, airway tapering is investigated as a biomarker for bronchiectasis with the use of automated quantification. Tapering is a reduction in the airway diameters along the bronchial tree and it can be divided in two biomarkers: the intra-branch tapering defined as the progressive reduction in airway diameter along the branch;

and inter-branch tapering defined as the reduction in airway diameter before and after bifurcation. It is known by radiologists that there is a lack of tapering in bronchiectatic airways. Tapering has however not previously been assessed on chest CT using an objective automated method in children and adolescents with bronchiectasis. Tapering biomarkers and airway artery ratios were assessed on spirometer guided inspiratory CTs of patients with bronchiectasis and control patients. In addition, tapering biomarkers and airway to artery ratios were assessed in 156 control patients without volume control during CT acquisition. Significantly decreased airway tapering was found for both the inner and outer airway diameters of patients with CF compared to controls. This difference was found across all airway sizes including the central airways. Detecting significant change in the central airways could potentially facilitate the assessment of structural airway changes on CTs with low resolution and possibly also on chest MRIs. Additional advantages of using tapering to assess airways disease is that the airways alone are easier to extract automatically than airway artery pairs, and tapering is not influenced by changes in dimensions of the accompanying arteries. In addition, tapering was found to be less influenced by changes in lung volume levels than airway artery ratios. Automatic quantification of tapering is therefore a promising image biomarker for bronchiectasis.

Dimensions of the airways can accurately and non-invasively be assessed in children with chest CT. The shape and size of the central and main airways are important determinants for lung health. However, reference values based on large study populations are lacking to date. The chapters in **Part 3** provide reference values of the central and main airway structures on chest CT for children and adolescents. The retrospectively collected chest CTs were made for various indications but reported as normal by two radiologists. A total of 1160 CTs were collected in 10 international centers.
In **Chapter 8**, central airways dimensions are established in 294 children and adolescents. Semi-automated image analysis was performed to measure dimensions of trachea, right and left main bronchus. The intrathoracic tracheal length was measured manually with a ruler from carina bifurcation to the thorax inlet. Cross sectional area and diameters were measured perpendicular to the airway lumen starting from carina upwards every cm for the trachea and downwards every 0.5 cm for the main bronchi. Dimensions of the central airways such as the trachea and main stem bronchi were dependent on distance to the carina bifurcation. As can be expected the central airway dimensions are larger near the carina bifurcation and near the mainstem bronchi bifurcation of segmental bronchi into the upper lobes. The diameter of the trachea, left and right main bronchi also increased with intrathoracic length and age. Central airway dimensions were similar in males and females till the age of 13-14 years old but became higher in

males compared to females after this age. This result could be explained by changes between genders in relation to the pubertal growth spurt.
In **Chapter 9**, dimensions of the airways, arteries and tapering were determined automatically in 487 children and adolescents. The inner and outer AA-ratios, intra- and inter-branch tapering values were found not to be dependent on age or gender from birth to 20 years old. The airway groups (central, segmental, subsegmental and peripheral) influenced the AA ratio and tapering values. A lower inner AA-ratio was present in the peripheral airways compared to the central airways and the outer AA-ratio remained constant by airway group. The inner intra-branch, inner and outer inter-branch tapering were higher in the peripheral airways compared to the central airways. The outer intra-branch tapering remained constant. The reference values established in this chapter could be used for the detection of early lung disease and are the groundwork for the development of automated chest CT image analysis for the detection of airway disease in children.

Finally, **Chapter 10** discusses the main findings of the studies included in this thesis, their clinical implications, potential challenges and future suggestions for research. With respect to the latter: Quantitative image analysis should be performed on larger pediatric study populations to understand the pathophysiology of early CF lung disease and the treatment effect. Studies investigating the dimensions of the airway and arteries should be repeated in children with CF and in healthy children if radiation dose is negligible or when improvements in MRI allow better resolution of the airways. Automated airway analysis is advancing expeditiously and will provide valuable and more detailed information on the severity and progressions of lung disease.

SAMENVATTING

Cystische fibrose (CF), ook wel bekend als taaislijmziekte, is een ongeneeslijke erfelijke ziekte die veel organen in het lichaam aantast door een defect gen. Dit leidt ertoe dat alle klieren in het lichaam afwijkend, taai slijm produceren. De organen die hierdoor het meest zijn aangedaan, zijn de longen. Patiënten met CF kunnen door het taaie slijm hun longen niet goed schoon houden waardoor de luchtwegen chronisch geïnfecteerd en ontstoken zijn. Om deze schade zichtbaar te maken en te monitoren krijgen kinderen met CF periodiek een computertomografie (CT) scan. Dit proefschrift beschrijft studies naar de stralingsrisico's, standaardisatie en beeldanalyse van long CT scans bij kinderen met CF.

Hoofdstuk 1 is de introductie van dit proefschrift. Patiënten met CF krijgen in het Erasmus MC - Sophia kinderziekenhuis eens in de twee jaar een CT scan van de borstkas. Met de beelden van een CT scan kunnen we de inwendige organen, zoals het longweefsel en de luchtwegen duidelijk in beeld krijgen. Zo kan er op een long CT scan worden gezien wanneer er afwijkingen ontstaan in de longen en of deze af- of toenemen. Daardoor kan de long CT scan worden gebruikt om het effect van de behandeling te evalueren. Als de afwijkingen in een periode toenemen moet de therapie aangepast of geïntensiveerd worden om verdere, soms onomkeerbare, schade aan de longen te voorkomen.

In het eerste gedeelte van dit proefschrift worden de mogelijke onveiligheid en de noodzakelijke standaardisatie beschreven bij het gebruik van de CT scanner bij kinderen. In **hoofdstuk 2** worden de mogelijke stralingsrisico's van een tweejaarlijkse CT scan bij kinderen met CF beschreven. Het gebruik van CT scans brengt mogelijk risico's met zich mee vanwege de bijbehorende straling. Gelukkig is de straling van een long CT scan tegenwoordig erg laag, maar bij regelmatig gebruik neemt dit risico naar ratio toe. Het risico op sterfte op latere leeftijd door straling bij tweejaarlijks gebruik van long CT scans van de geboorte tot 19 jarige leeftijd hebben we geschat op minder dan 0.1%. De risico's van straling zijn verder vergeleken met: de risico's van andere CT indicaties, de risico's van andere stralingsbronnen en andere "dagelijkse" risico's.
Hoofdstuk 3 gaat over de standaardisatie van de uitvoering van een CT onderzoek bij kinderen met CF. De naam van de studie is 'Standardized Chest Imaging Framework for Interventions and personalized medicine in CF', oftewel SCIFI-CF. Deze studie was opgezet om de CT scanners van 16 verschillende CF centra binnen Europa te testen. Alle centra werden bezocht om de beeldkwaliteit van de verschillende CT scanners te meten met behulp van een drietal long fantomen (plastic longen) van verschillende groottes. Hiermee was het mogelijk om de kwaliteit van de beelden vast te leggen en kon de kwaliteit tussen de CT scanners worden vergeleken en geoptimaliseerd. Tussen

de deelnemende centra werden substantiële verschillen gevonden in de uitvoering van het CT onderzoek, de beeldkwaliteit en de stralingsdosis. Desalniettemin was de kwaliteit van de CT scanners voldoende om gebruikt te worden voor internationale studies, mits de CT onderzoeken worden gestandaardiseerd.

In het tweede gedeelte van dit proefschrift worden nieuwe objectieve beeldanalyse methodes beschreven om de longafwijkingen bij kinderen met CF te kwantificeren.
In de hoofdstukken 4,5 en 6 wordt de AA (airway and artery) methode beschreven waarbij de afmetingen van luchtwegen zijn gemeten op long CT scans. De afmetingen van de luchtwegen werden vergeleken met de bijbehorende bloedvaten. De afmetingen van de luchtwegen in gezonde personen zijn vergelijkbaar met de afmeting van de bloedvaten. Echter, in de zieke luchtwegen bij patiënten met CF kan door de ontsteking de afmeting van de luchtwegen groter worden dan de bijbehorende bloedvaten. Als de luchtwegen onomkeerbaar groter zijn spreken we van een bronchiëctasie.
In **Hoofdstuk 4** zijn de luchtweg- en bloedvatafmetingen van 11 kinderen met CF op CT vergeleken met 12 kinderen zonder zichtbare luchtwegziekten. Alle CT scans werden gemaakt bij kinderen tussen de 6 en 16 jaar oud met behulp van een spirometer om de volledige in- en uitademing te kunnen waarborgen. Op alle scans werden de verhoudingen tussen de luchtwegen en bloedvaten van elke aftakking van de luchtwegen gemeten. Opvallend was dat de afmeting van de luchtwegdiameter substantieel groter was bij patiënten met CF in vergelijking met patiënten zonder luchtwegziekten. Daarnaast was het aantal zichtbare luchtwegen bij kinderen met CF fors toegenomen ten opzichte van de kinderen zonder luchtwegziekte. Deze studie laat verder zien dat het erg belangrijk is om long CT scans te maken met behulp van spirometrie om de longvolumes te standaardiseren. Verder laten we zien dat bronchiëctasieën het beste gemeten kan worden door de buitenste luchtwegdiameter te vergelijken met het bijbehorende bloedvat, in plaats van de binnenste luchtwegdiameter wat in eerdere studies werd gebruikt. Tenslotte liet deze studie zien dat de AA methode betrouwbaar en een objectieve maat is voor luchtwegziekte bij kinderen met CF.
In **Hoofdstuk 5** zijn de luchtweg- en bloedvatafmetingen beoordeeld in kinderen jonger dan zes jaar met vroege longziekten door CF. De luchtweg- en bloedvatafmetingen werden wederom vergeleken met kinderen zonder zichtbare afwijkingen op CT en werden beoordeeld over een tussenperiode van twee jaar. Net zoals bij oudere kinderen werden er meer verwijde luchtwegen en verdikte luchtwegwanden gezien bij jonge kinderen met CF. Bij patiënten met CF was er over twee jaar een subtiele toename te zien in de ratio van de binnenste luchtweg diameter met het bijbehorende bloedvat. Ook was er een zichtbare toename in de ratio tussen de buitenste luchtwegdiameter en het bijbehorende bloedvatdiameter in de kleinere luchtwegen. Ten slotte suggereren de bevindingen in dit hoofdstuk dat door gebruik te maken van de AA methode als

uitkomstmaat, er minder patiënten nodig zijn voor klinische studies. Een nadeel van deze AA methode is dat deze erg veel tijd kost en daarom geautomatiseerd moet worden om bruikbaar te zijn in de praktijk.
Er zijn nu verschillende methodes om afwijkingen van de luchtwegen te kunnen meten zoals de CF-CT methode, PRAGMA-CF en de AA methode. De CF-CT-scoringsmethode is ontwikkeld voor patiënten met matig tot ernstige longziekten en is daardoor niet gevoelig genoeg voor het scoren van milde longafwijkingen bij met name jonge kinderen met CF. PRAGMA-CF werd daarom speciaal ontwikkeld om longziekte bij jonge kinderen te kunnen beoordelen. PRAGMA-CF scoort de afwijkingen met behulp van een raster dat over het longbeeld wordt geprojecteerd. Met deze methode kunnen de verschillende longafwijkingen die kenmerkend zijn voor CF als percentage van het longvolume worden uitgedrukt. De CF-CT en PRAGMA-CF scoring methodes kosten minder tijd dan de AA methode. In **Hoofdstuk 6** zijn de CT scans tijdens volledige inademing uit hoofdstuk 4 gescoord met CF-CT en PRAGMA-CF en vergeleken met de objectieve AA methode. De studie liet zien dat zowel CF-CT als PRAGMA-CF gevoelige methoden zijn om longziekten bij kinderen en adolescenten met CF te beoordelen. Scores voor bronchiëctasieën en voor alle afwijkingen aan de luchtwegen (som van bronchiëctasieën, luchtwegverdikking en slijmophoping) die werden bepaald met PRAGMA-CF, waren het meest nauwkeurig. Tevens is er met verwijding van de luchtwegen en luchtwegwandverdikking is er een grotere aantal luchtwegen zichtbaar op CT. Een hoger aantal zichtbare luchtweg- en bloedvatparen op CT was gecorreleerd met een hogere CF-CT en PRAGMA-CF ziektescore. Het aantal luchtwegen zichtbaar op CT kan ook een mogelijke marker zijn voor longschade, maar het aantal luchtwegen is ook afhankelijk van leeftijd en long volume op het moment van de CT.
In **Hoofdstuk 7** wordt luchtweg tapering bestudeerd als biomarker voor bronchiëctasieën door middel van een automatische methode. Tapering is de natuurlijke afname van luchtwegdiameter bij elke volgende generatie van de bronchiaal boom. Intra-branch tapering is de versmalling van een luchtweg tussen twee aftakkingen. Inter-branch tapering is de vermindering van luchtwegdiameter voor en na de splitsing van een luchtweg. Hoewel een afname van tapering een bekend fenomeen is van bronchiëctasieën is dit nooit objectief gemeten op CT scans van kinderen en adolescenten met CF. Wij vonden een duidelijke afname van tapering bij kinderen met CF in vergelijking met patiënten zonder zichtbare longafwijkingen. Deze afname was zichtbaar in alle luchtwegen van grote naar kleine luchtwegen. Een groot voordeel van de tapering methode is dat hiervoor alleen de luchtwegen gemeten hoeven te worden. De afmetingen van alleen de luchtwegen zijn geautomatiseerd makkelijker te bepalen dan de geautomatiseerde afmetingen van de luchtwegen met de bijbehorende bloedvaten. Ten slotte lijkt de tapering methode minder gevoelig te zijn voor verschillen

in longvolume tijdens de CT dan de AA-methode. De tapering methode lijkt een veelbelovende meetmethode te zijn om bronchiëctasieën op te sporen.
Het derde gedeelte van dit proefschrift gaat over de normale afmetingen van de luchtwegen bepaald op long CT van kinderen. Meer dan duizend CT scans werden hiervoor verzameld afkomstig uit tien verschillende CF centra over de hele wereld. De long CT scans zijn afkomstig van kinderen die voor verschillende indicaties een CT scan nodig hadden, maar achteraf als normaal werden beoordeeld door twee onafhankelijke radiologen. Deze unieke verzameling CT scans werd gebruikt om referentiewaarden te bepalen voor de centrale en algemene luchtwegstructuren. Dit werd gedaan door middel van geautomatiseerde technieken.
In **Hoofdstuk 8** zijn de centrale luchtwegafmetingen bepaald bij 294 kinderen en adolescenten. Geautomatiseerde beeldanalysetechnieken werden gebruikt om de afmetingen van de centrale luchtpijp en de aftakking naar rechter- en linkerlong te meten. De diameter van de luchtpijp en zijn aftakkingen bleken gerelateerd te zijn aan de lengte van de luchtpijp en de leeftijd. De afmetingen van deze centrale luchtwegen zijn even groot bij jongens en meisjes tot de leeftijd van 14 jaar. Hierna zijn de centrale luchtwegafmetingen bij de jongens groter dan bij de meisjes. Dit kan verklaard worden door veranderingen in groei in samenhang met de puberteit en geslacht.
In **Hoofdstuk 9** zijn de afmetingen van de luchtwegen, bloedvaten en tapering beschreven die met een automatische methode werden gemeten bij 487 kinderen en adolescenten. De luchtweg tot bloedvat ratio en intra- en inter-branch tapering waren niet afhankelijk van de leeftijd of geslacht vanaf de geboorte tot het 20ste jaar. De tapering waarden bleken lager te zijn in de centrale luchtwegen ten opzichte van de perifere luchtwegen. Dankzij dit onderzoek weten we nu wat de normale afmetingen zijn van de luchtwegen bij kinderen. Deze referentiewaarden zijn nodig om longziekten bij CF patiënten in een vroege fase op te kunnen sporen.
Hoofdstuk 10 bespreekt de belangrijkste bevindingen, de klinische implicaties, de mogelijke uitdagingen en suggesties voor toekomstige studies. Om een beter idee te kunnen krijgen van het ontstaan van afwijkingen in de luchtwegen en het effect van behandeling is vervolgonderzoek nodig. Studies naar de afmetingen van de luchtwegen en bloedvaten in de longen zouden uitgebreid moeten worden in grotere groepen gezonde kinderen. Dit kan alleen als de stralingsdosis van CT scans verwaarloosbaar is. Als alternatief kan dit onderzoek in de toekomst plaatsvinden met de stralingsvrije magneetscan. Verdere ontwikkeling van de beschreven geautomatiseerde luchtweg analyse methodes is belangrijk om waardevolle en gedetailleerde informatie over de ernst en progressie van longziekten te kunnen krijgen.

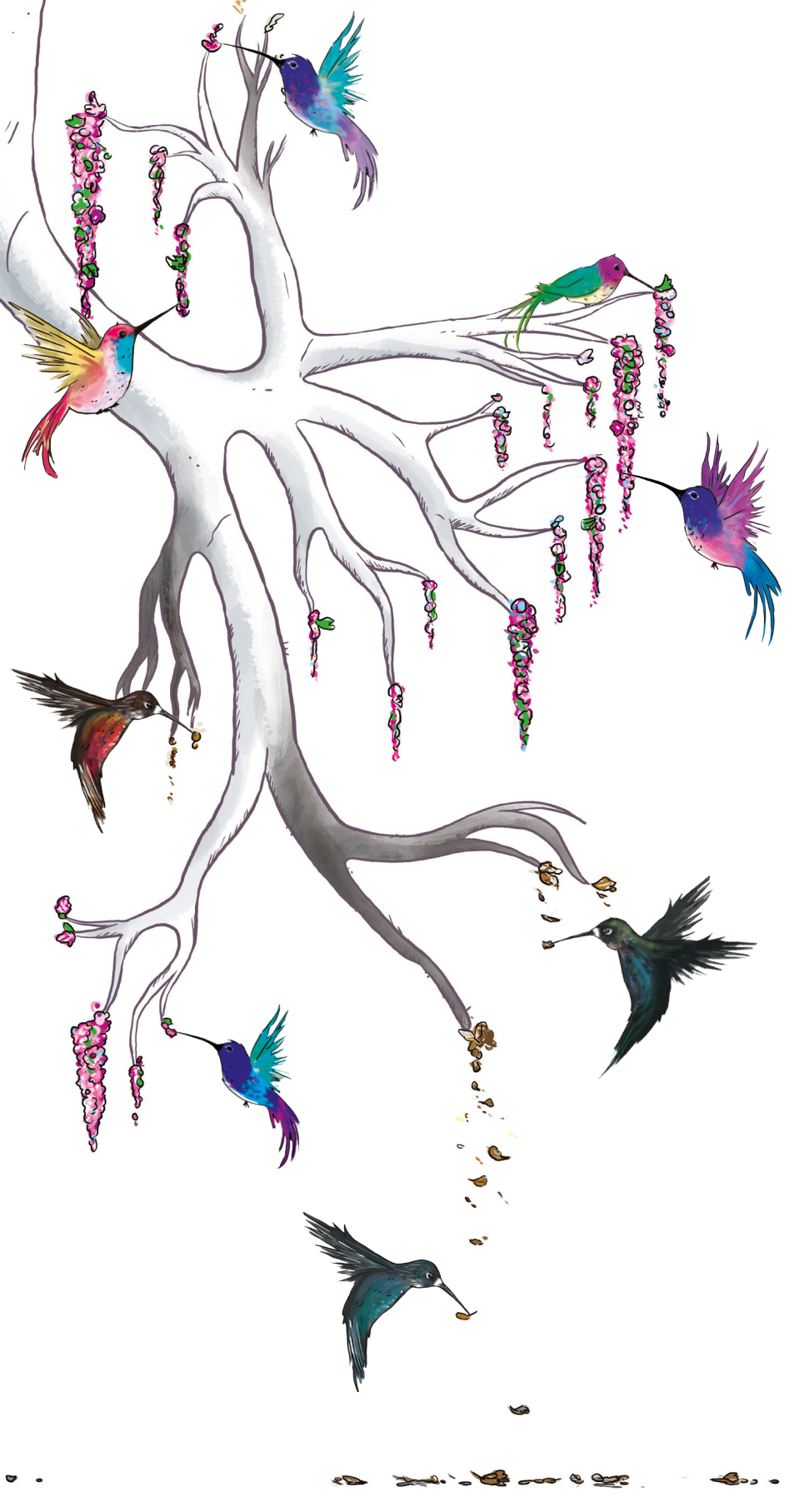

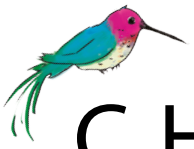

CHAPTER 12

APPENDICES

ACKNOWLEDGEMENT/DANKWOORD
LIST OF PUBLICATIONS
PHD PORTFOLIO
LIST OF ABBREVIATIONS
ABOUT THE AUTHOR

ACKNOWLEDGEMENT/DANKWOORD

This thesis has many chapters, and the chapters of this book are coming to an end. However, it cannot be finished without one of the most important chapters. That would be the chapter where I would like to thank all the people who have helped me in so many ways. In 2012 I starting my PhD as a youngling and now a few years later I am finishing another chapter in my life. I sense a great feeling of gratitude to have gotten this opportunity and all the assistance along the way preparing and completing this thesis, because let's be honest, I would not have been able to achieve all this on my own. I would like to acknowledge the ones contributing to me standing here today with a few sentences of appreciation and heartfelt gratitude in the different languages that deemed most fit.

Mijn eerste dank gaat naar mijn promotor, Prof. Dr. Harm Tiddens. Beste Harm, 5 jaar geleden heb je mij de mogelijkheid gegeven om verder te gaan in onderzoek. Ik ben je dankbaar voor de kans die ik heb gekregen om een promotietraject te volgen. De afgelopen jaren bestonden voor mij uit onbetaalbare ervaringen en ik heb ontzettend veel van je mogen leren. Je hebt mij door alle jaren heen gesteund ongeacht met welke moeilijkheden ik bij je aanklopte. Zo ook in mijn eerste jaar bij mijn eerste internationale congres. Dit vond ik des te spannender omdat de abstract die we hadden ingediend was geselecteerd voor een presentatie in een grote zaal. Jij fluisterde nog secondes voordat ik het podium op moest welke ademhaling manoeuvres het beste waren om de zenuwen te kunnen onderdrukken. Ik kan dit moment nog goed herinneren want het ging eigenlijk best redelijk met de zenuwen tot het moment dat mijn promotor opstond om vooraan foto's te kunnen maken. Ik ben in het diepe gegooid maar dankzij de veelvoudige buitenlandse werk visites en congressen die daarop volgde gingen de presentaties steeds wat makkelijker en kan ik hier bij mijn publieke verdediging met zelfvertrouwen staan. Je hebt altijd vertrouwen in mij gehad en ik waardeer de vrijheid die je mij hebt gegeven tijdens mijn onderzoeken hier in Nederland maar ook in Amerika. Ik kon altijd bij je terecht en het was ook altijd mogelijk even te bellen of skypen. Maar een volle droppot in de LungAnalysis kamer was tevens erg nuttig want bij binnenkomst voor een dropje was je ook altijd bereid even tussendoor van gedachten te wisselen. Bedankt voor jouw onbeperkte dosis aan inspiratie en ongekende enthousiasme voor onderzoek.

Mijn co-promotoren, Ass. Prof. Dr. Marleen de Bruijne en Dr. Ir. Marcel van Straten. Beste Marleen, ondanks jouw begeleiding in de vele projecten, promovendi en postdocs binnen de BIGR groep, had je altijd ook een kritisch oog in het werk wat verricht werd in het Sophia. Bij het schrijven van de artikelen had jij altijd de meest kritische vragen en ik kon jouw expertise goed waarderen. Als het eens allemaal te veel werk was,

was jij degene die het in de meetings aankaartte of we nu niet te veel hooi op onze vork hadden genomen en of het wel haalbaar zou zijn. Daarnaast liepen we vaak uit Harms kamer waarna jij zorgzaam naging of het allemaal bij mij wel ging lukken. Ik waardeer jouw ongekende ambities en jouw kritische blik vanuit de perspectief van de beeldanalyse mogelijkheden, waarvoor mijn oneindige dank.

Beste Marcel, ooit begonnen als jouw eerste promovenda. Ik kan me nog goed herinneren dat we op een van onze eerste meetings samen een checklist doornamen voor jouw cursus "supervisie". Ik kan je vertellen dat de promovendi die zullen volgen van geluk mogen spreken met een supervisor zoals jij. Als groentje heb ik mijn eerste artikelen met je samen mogen schrijven en dit was voor mij een zeer leerzaam proces geweest. Daarnaast verliep de submissie van mijn eerste twee artikelen erg soepel en heeft het ons twee mooie publicaties opgeleverd. Het was altijd een stukje lopen van het Sophia of Westzeedijk naar het Hs-gebouw maar dit was het altijd waard. Je wist mij altijd heel goed de complexe en technische onderwerpen in simpele termen of tekeningen uit te leggen. Je werkt erg secuur en ondanks mijn ongeduldigheid kon ik de precisie altijd zeer waarderen. Als ik weer een site visite had uitgevoerd en de CT scanner onder handen had genomen was jij ook altijd bereid om dit even te bepreken ook al was dat vaak na kantooruren en had je Florian net op bed gelegd. Daarnaast was jouw goed gedoseerde hoeveelheid relativerende humor ook precies genoeg om het ijs te breken, bedankt voor alles.

De leden van de promotie commissie, Prof. Dr. M. de Hoog, Prof. Dr. G.G.O. Brusselle, Prof. Dr. C. K. van der Ent en Dr. M. M. van der Eerden. Hartelijk bedankt voor het beoordelen van mijn proefschrift en uw bereidheid zitting te nemen in de commissie. Prof. Dr. J. S. Elborn, thank you for travelling all the way to Rotterdam. It is an honor to have you partake in my thesis dissertation as a committee member.

Prof. Dr. G. J. Redding, dear Greg, you were my first research supervisor and taught me the basics in the field of research. I can undoubtingly say that your enthusiasm inspired me to consider a future in research and the reason I choose to continue with a PhD. Thank you for your guidance and enthusiastic encouragements. Prof. Dr. M. Rosenfeld, dear Margaret, you have always been very welcoming whenever I visited Seattle and I will always remember the potlucks at your beautiful home. Thank you for your useful critiques to improve my studies.

Prof. Dr. A. L. Quittner, dear Alexandra, it was an honor participating in your grant writing class. Your course gave me a great advantage and confidence in critical writing, which is a quality I will benefit from for the rest of my life. It was always a pleasure seeing you again at conferences and thank you for your positive outlook and confidence in my research.

I would like to thank all the co-authors for their collaborations and all the valuable feedback. The studies would not have reached their current impact without your input. The following individuals I would like to acknowledge by name: Dr. A. Perez-Rovira. Dear Adria, working closely with you was a fruitful (or a cookie-full) business and has saved me many hours of manual work. I appreciate your creative thought processing and all the work you performed in the "magical black box". Thank you for making my endless hours of manual work obsolete and I look forward to the days we can start cashing in the dinners we owe each other.

Dr. P. Ciet, dear Pier, thank you for all the radiological teachings and explanations. Starting from my first study you always ploughed through the manuscript and gave me helpful feedback. It was great having you to discuss the perks of a PhD and I am grateful for all your advice. I enjoyed the wonderful Italian and Chinese dinners.

Dr. E.R. Andrinopoulou and Dr. K. Nasserinejad, dear Elrozy and Kazem, thank you for your essential statistical assistance and guidance. Learning to deal with R studio and understanding the basics of coding without any background in computer programming was a hefty challenge. I am therefore the more grateful for your helping hand in making graphs and solutions for error messages.

The SCIFI CF study was in collaboration with 20 centers across Europe and the United States of America. I would like to thank each CF center and in particular all the individuals who contributed to make the SCIFI CF site visits possible. Your hospitality and warm welcome to your CF center is something I will always remember dearly. I am aware that there were many people involved with arranging the visits and assisting in the scanning procedures so my gratitude goes out to each and every one of you. In particular, I would like to express my gratitude to the CF clinical trial network and to the following physicians of the participating centers: Laureline Berteloot, Kris de Boeck, Cesare Braggion, Torkel B. Brismar, Rosaria Casciaro, Matt Cooper, Desmond Cox, Jane C. Davies, Stephanie D. Davis C. Kors van der Ent, Thomas Ferkol, Pilar Garcia-Peña, Silvia Gartner, Kath Halliday, David Hansell, Lena Hjelte, Herma C. Holscher, Annmarie Jeanes, Pim A. de Jong, Ahmed Kheniche, Timothy Lee, Giorgio Lucigrai, Marco Di Maurizio, Anne Mehl, Anne Munck, Marianne Nuijsink, Jacqueline Payen de la Garanderie, David Rea, Isabelle Sermet, Veronika Skalicka, Florian Streitparth, Philippe Reix, Marleen Smet, Alan Smyth and Hana Vitouskova

The last part of my thesis consisted of studies part of the Normal Chest CT study group. This was a collaboration to collect normal chest CT scans retrospectively in order to facilitate reference values. I am thankful for the contribution of ten different centers across the world. Without your contribution these studies would not have been possible.

Many thanks to the following researchers for your contributions in the data collection: Lauren Akesson, Silvia Bertolo, Alan S. Brody, Kris de Boeck, Pim A. de Jong, Robert J. Fleck, Francesco Fraioli, Pilar Garcia-Peña, Silvia Gartner, Edward Y. Lee, Anders Lindblad, Michael McCartin, Christian P. Mol, Giovanni Morana, Arlette E. Odink, Matteo Paoletti, Stephen M Stick, Francois Vermeulen. Special gratitude is also extended to Chen Yong, thank you for reevaluating more than a thousand chest CT scans and building the foundation for several of my studies.

De medische staf van de afdeling kinderlongziekten, prof. dr. Johan de Jongste, dr. Hettie Janssens, dr. Marielle Pijnenburg, dr. Liesbeth Duijts, dr. Saskia ten Raa- Kwee, dr. Sanne Kloosterman dr. Ismee de Kleer, dr. Suzanne Terheggen, dr. Daan Caudri. Bedankt voor de leerzame patientenbesprekingen, pulmodagen, research besprekingen. Dankzij jullie input vanuit een klinisch oogpunt heb ik de vele cijfers, metingen en resultaten kunnen extrapoleren naar de kliniek. Ook hebben jullie mij uit kunnen dagen met de kritische vragen en sterke argumenten.

Lieve Els, in 2012 deed ik een paar studenten klusjes bij je om de tijd op te vullen voordat ik kon beginnen met de coschappen. Jij hebt mijn leven veranderd door Harm te adviseren dat ik een ideale kandidaat zou zijn voor promotieonderzoek en dat hij mij niet mis zou moeten lopen. Als zijn rechterhand volgde Harm jouw advies blindelings op en ik heb de afgelopen jaren mogen inzien waar dit (volkomen terecht!) vandaan komt. Daarnaast ben je onmisbaar geweest in het opstarten van de normal chest CT studies en ben ik je hier uitermate dankbaar voor. Naast de unieke inzichten heb je ook werkelijk altijd de beste adviezen klaarliggen. Bedankt dat ik altijd bij je binnen mocht lopen en dat je altijd vertrouwen had in mijn kunnen. Je hebt me altijd bijgestaan met jouw ongekend probleemoplossend vermogen en dit zal mij altijd bij blijven.

Beste Irma, je bent als secretaresse van de pulmo groep een onmisbaar deel van de groep. Voor mij was het altijd heel fijn dat ik altijd even bij je langs kon lopen en even kon spuien. Bedankt voor alle keren dat je mij in Harms drukke agenda hebt kunnen plannen, jouw hulp bij het afronden van de artikelen en het afronden van de promotie.

De longfunctie analisten, Sandra, Laura, Cheyenne en Sunny. Bedankt dat ik altijd bij jullie binnen mocht lopen om vragen te stellen over de long functie data of gewoon even mocht komen kletsen voor de gezelligheid. De CF (research) verpleegkundige, Eveline, Annelies, Inge en Jorien. Bedankt voor het luisterend oor, steun en adviezen. Daarnaast was het altijd erg gezellig met jullie op de CF congressen, waar een dansje wagen hoort bij het onderzoek doen. Jorien, ik hoop dat je er vandaag bij zult zijn en je weet het, je mag altijd de spotlight van me stelen tijdens de verdediging;)

Ik heb gedeeltelijk mijn promotie ook binnen de Radiologie mogen verwezenlijken en mijn dankbaarheid gaat natuurlijk ook uit iedereen die mij heeft geholpen binnen deze afdeling. In het bijzonder alle leden van de research commissie Radiologie en Nucleaire Geneeskunde, bedankt voor het waarborgen van de haalbaarheid van mijn promotieplanning en de waardevolle adviezen. Daarnaast zullen de vermakelijke radiologie PhD-diners, feesten en borrels mij altijd bij blijven. Beste Ton, als de grafisch ontwerper en fotograaf van de afdeling radiologie heb ook ik bij je aan mogen kloppen. Bedankt voor alle hulp bij het maken van de posters voor congressen de afgelopen jaren. Beste Mariette, in 2013 kwam jij het LungAnalysis team flink versterken. Bedankt voor je bijdrage aan de SCIFI CF studie, zonder alle data analyses was het niet gelukt. Daarnaast ook mijn dank aan de Kemner familie voor de gastplaatsing van Moose, ik weet zeker dat hij soms nog droomt over de vele treden en voetjes waar hij eindeloos mee plezier mee had.

My fellow PhD-colleagues, Leonie, Pierluigi, Aukje, Tim, Jennifer, Hamed, Yifan and Clara. Since the start of my PhD we have moved to different locations and offices for seven times: within the Sophia, to Westzeedijk, to the Na-building and back to the Sophia and within the Sophia another several times. With all these relocations we could almost co-author a paper entitled: "Moving efficiently". Besides the packing we did together, I am grateful for all the productive and valuable meetings we shared. The hard work we did during the long hours in the office, and more than one too many during the evenings or weekends. The lunches, coffee breaks, dinners and drinks were always a pleasant and much needed change of scenery. Research days, Conferences and Radiology events would not have been the same without each and every one of you. A particular memorable recollection I have was at the ECFS in Basel with Aukje and Jennifer where we were dubbed as "Harm's Angels". Lieve Aukje, samen in 2012 begonnen en direct een mooie vriendschap erbij. Het was erg fijn om samen met mijn "adoptiezusje" op de congressen te mogen trippelen. Bedankt voor alle adviezen, een luisterend oor en de presentaties die ik nog net voor het echte werk bij je mocht oefenen. Lieve Jennifer, je hebt Harms team vergezeld aan het eind van mijn promotie maar ik heb je gelukkig nog leren kennen in Knots voor een buitenlands werkbezoek. Samen met Sunny hebben we er een productieve werkbezoek, maar het was vooral ook erg gezellig om de stad en de verstopte barretjes te ontdekken. Bedankt voor jouw gezelligheid en je bruisende open persoonlijkheid. Dear Lizzie and Karla, without you guys the SCIFI CF visits would not have been the same. We have made quite some visits and I feel grateful being able to have shared so many new experiences together in-, and outside of the Netherlands. Thank you for your contributions, proof readings, support and the much needed distractions from time to time. America, Europe and who knows one day it will be time to explore Australia. Dear Giuseppe and Greta, it was short but a pleasure to have met you at

the end of my PhD. Thank you for the amazing many (I lost count) course Italian dinner and I hope to see you again in the Netherlands or Italy. Dear Gautam, thank you for all the USMLE documents, this might be useful for a potential future chapter. Alle overige promovendi van de afdeling kinderlongziekten, ook jullie erg bedankt voor alle leerzame research meetings, jullie feedback en de gezelligheid bij de borrels.

De studenten die ik met plezier heb mogen begeleiden, Pauline, Merel, Michelle, Thomas en Niels. Bedankt voor jullie inzet en interesse in het onderzoek. Ook wil ik alle LungAnalysis studenten bedanken, in het bijzonder Sarina, Hadiye, Dora, Elena en Anh. Ik wens jullie allen veel succes met jullie verdere loopbaan. Het gezellige co-groepje 16.30, bedankt voor de LSD's zonder OMA's en jullie support tijdens het afronden van mijn promotie.

Kenny Rubenis, bedankt voor het mooie ontwerp van dit proefschrift en de tekeningen die jij hebt gemaakt voor mijn publicaties. Als geen ander heb jij ingezien wat ik had ingebeeld en dit zo mooi uitgevoerd.

Mijn lieve vriendinnen, ik waardeer deze vriendschappen enorm en jullie zijn een onmisbaar deel van mijn leven. Lieve Inge, allereerst bedankt voor de mooie foto. Bij jou kan ik altijd terecht met al mijn verhalen en geniet ik nog meer van al jouw verhalen en ervaringen. Alle melige avonden waar we niet meer bij kunnen komen van de slappe lach zal ik nooit vergeten. Maar ook voor serieuze zaken kon ik altijd bij jou terecht, bedankt dat je er altijd voor me bent. Lieve Hanna en Daphna, jullie hebben me altijd gesteund en met de vele lekkere etentjes hebben we altijd heerlijk bij kunnen kletsen. Toen ik alleen in het buitenland was, of zelfs in het binnenland, waren jullie degene die elke avond van me wilde horen of ik wel goed terecht was gekomen. Bedankt voor jullie continue zorgzaamheid en het luisterend oor. En lieve Ellie, ik kom snel weer een keertje op je passen. Lieve Genesis, bedankt voor de gezelligheid, high tea's en de dansjes, dit heeft me altijd goed gedaan om er weer tegen aan te kunnen. Lieve Poonam, de bezoekjes aan Den Haag hebben mij altijd goed gedaan. Mijn middelbare school vriendinnetjes, bedankt voor jullie vele gezelligheden en de nodige ontspanning. Wie had gedacht dat we zo lang vriendinnetjes zouden zijn? Met alle drukte wordt het helaas steeds moeilijker om af te spreken maar al onze tripjes, feestjes en festivals zullen me altijd bij blijven en wie weet in de toekomst een mooi bezoekje naar Japan? Lieve Claar, bedankt voor jouw eindeloze hoeveelheid aan steun. Onze romantische ervaringen zijn weer te lang geleden. We moeten dit maar snel overdoen met onze uitbreiding(en). Lieve Denise G, een veel langere periode dan afgesproken zit jij nu al in Sydney en heb ik je moeten missen. Ondanks de grote afstand voel ik de nodige support en bedankt voor alle adviezen, we blijven FaceTimen. Lieve Denise R, bedankt voor de nodige ontspanning en jouw hulp met figuren en grafieken. Bezoekjes naar Amerika waren

altijd leuk en het was ook zeer leerzaam om een keer over de Braves te leren, chop chop! Ik hoop binnenkort weer wat meer tijd te hebben zodat we weer gezellig op de bank met wat popcorn kunnen zitten. Lieve Mann, wat hebben we veel meegemaakt en gereisd. Een uitje, feestje of vakantie met jou is nooit saai en ik kijk uit naar de volgende mooie momenten. Lieve Meen, bedankt voor je support en gezelligheid. Jij weet altijd waar de goede feestjes zijn en ik hoop binnenkort weer wat meer festivals mee te kunnen pakken.

My dear friends, thank you so much for the much needed fun the past few years and I am very glad with our friendships. Dear Allen & Eve, Christine & Peter, I am so happy you stayed in the Netherlands and Amsterdam is luckily only a quick train ride away. I enjoyed the many trips we made within and outside of the country, dinners, sleepovers, the uncontrollable laughter's and deep conversations and talks on what is most important in life. I look forward to many more. Dear Deppe, Eima, Sophie & Machiel and Stine, I have enjoyed the many dinners, game nights, parties, bike trips, tourist trips around the country while having great conversations. Thank you for the support. Dear Ying, I truly appreciate you coming all the way back from Sydney to be here at my thesis dissertation. Thank you for being there for me as family. I look forward to many more dinners with meaningful conversations, girls' night out and who knows maybe one day we will start a new life in Sydney. Dear Judith, I look forward for you to be back with Santosh so we can continue our many more outings.

I now understand why acceptance and Oscar speeches are so long. There are so many people that have been there for me in so many ways possible and made me who I am today. I undoubtingly have not mentioned every person that has contributed to me being here, but I still appreciate all that you have done for me and what you mean to me!

Mijn paranimfen, ik ben ontzettend trots en bof enorm dat jullie op deze belangrijke dag naast mij staan. Lieve Shoista, als geen ander wist jij hoe het is om je promotie af te ronden tijdens de coschappen en daarbij het sociale leven en relaties staande te houden. Voor alle problemen waar ik tegen aan liep stond jij altijd voor me klaar met waardevolle adviezen. Hoe druk jij het ook had, ik mocht altijd bij je aankloppen wanneer ik je het meest nodig had. Ik bewonder jouw onuitputbare doorzettingsvermogen en ik kan nog veel van jou leren. Bedankt voor je decennia aan vriendschap, de steun en alle momenten waar jij voor me klaar stond en niet te vergeten voor het delen van al het geluk en plezier tijdens de mooie gebeurtenissen in ons leven. Ik kijk uit naar de vele mooie decennia die zullen volgen. Lieve Yvonne, mijn kleine nichtje die zo ontzettend veel is gegroeid en zo wijs is geworden. Als jong meisje die alleen naar uitjes mee mocht als ik er ook zou zijn, tot jonge vrouw die mij op de sleeptouw nam om naar de bibliotheek

te gaan om de pathofysiologie van 130 ziektebeelden samen uit ons hoofd te leren. Je luisterde altijd zonder te oordelen en had altijd een heerlijke dosis nuchterheid en relativeringsvermogen klaar liggen. Ik heb dit altijd enorm kunnen waarderen. Bedankt voor de onvoorwaardelijke steun en dat extra steuntje op de momenten waar ik dit goed kon gebruiken. Ik kijk uit naar de dag dat we samen kunnen dokteren.

Mijn familieleden, bedankt voor jullie steun, begrip en de grenzeloze interesse die jullie in mij hebben getoond. For my family abroad, thank you for all your great care and hospitality whenever I visited. Weena, bedankt voor je begrip en zorgzaamheid. Ik weet dat je het niet altijd makkelijk hebt gehad en kijk daarom des te meer naar je op.

亲爱的妈妈,我想感谢你培养我成今天的我。对我有意义的一个经典语录是：‘时间不会愈合一切，但接受会’。我知道过去经历了很多坎坷，但是因为这些经历，我才变得更坚强。我非常感激你为我牺牲了很多，为我创造了很好的条件去取得事业上的成功。我希望我能成为你的骄傲。

My dear in-laws, appa 아빠 , eomma 엄마 , Dave, Angela and Justin, thank you so much for taking me in as your own daughter/sister and making me feel so comfortable within your loving family. Regardless of the distance I have always felt your love and good spirits. Thank you for believing in me. I love and miss you all. My grateful thanks are also extended to all the in-laws in South Korea. 감사하다.

Dear Daniel Drake, you have been the most avid guarantor of my true happiness; especially at times I did not realize myself what true happiness should be like. For all my PhD struggles you were a great and patient listener, no matter the distance. I want to express my great gratitude for your sacrifice to be here with me, without you I wouldn’t be half the person I am today. For several instances have you put me in situations outside my comfort zone, which are now my most valuable memories. You have taught me many practical and invaluable lessons in life and I hope to learn so much more from you. I can’t believe how far we have made it and I look forward to a happy life together with little jumps outside of the lines.

LIST OF PUBLICATIONS

Manuscript based on this thesis

Kuo W, Ciet P, Tiddens HAWM, Zhang W, Guillerman RP, Van Straten M. Monitoring cystic fibrosis lung disease by computed tomography: Radiation risk in perspective. Vol. 189, American Journal of Respiratory and Critical Care Medicine. American Thoracic Society; 2014. p. 1328–36.

Kuo W, Kemner-van de Corput MPC, Perez-Rovira A, de Bruijne M, Fajac I, Tiddens HAWM, van Straten M on behalf of the ECFS-CTN/SCIFI CF study group. Multicentre chest CT standardisation in children and adolescents with cystic fibrosis : the way forward. Eur Respir J. 2016;1–12.

Kuo W, de Bruijne M, Petersen J, Nasserinejad K, Ozturk H, Chen Y, Perez-Rovira A, Tiddens HAWM. Diagnosis of bronchiectasis and airway wall thickening in children with cystic fibrosis: Objective airway-artery quantification. Eur Radiol. 2017; In press.

Kuo W, Soffers T, Andrinopoulou ER, Rosenow T, Ranganathan SC, Turkovic L, Stick SM, Tiddens HAWM on behalf of AREST CF. quantitative assessment of airway dimensions in young children with cystic fibrosis lung disease using chest computed tomography. Pediatr Pulmonol. 2017; In press.

Kuo W, Andrinopoulou ER, Perez-Rovira A, Ozturk H, de Bruijne M, Tiddens HAWM. Objective airway artery dimensions compared to CT scoring methods assessing structural cystic fibrosis lung disease. J Cyst Fibros. 2016;16(1):116–23.

Perez-Rovira A, **Kuo W**, Tiddens HAWM, de Bruijne M on behalf of the Children Chest CT Study Group. Airway tapering revisited: an objective image biomarker for bronchiectasis. Eur Respir J. 2017 (submitted).

Kuo W, Ciet P, Andrinopoulou ER, Chen Y, Pullens B, Garcia-Pena P, Fleck RJ, Paoletti M, McCartin M, Vermeulen FL, Morana G, Lee EY, Tiddens HAWM on behalf of the Children Chest CT Study Group. Reference values for central airway dimensions on normative CT of children and adolescents. Am J Roentgenol. 2017; In Press.

Kuo W*, Perez-Rovira A*, Andrinopoulou ER, Chen Y, Gartner S, Brody AS, de Boeck K, Bertolo S, Akesson L, Stick SM, Tiddens HAWM, de Bruijne M on behalf of the Children Chest CT Study Group. Reference values for airway and artery dimensions on CT of children and adolescents (in preparation).

* contributed equally

Other manuscripts

Redding GJ, **Kuo W**, Swanson JO, Phillips GS, Emerson J, Yung D, Swanson JW, Sawin RS, Avansino JR. Upper thoracic shape in children with pectus excavatum: Impact on lung function. Pediatr Pulmonol. 2013;48(8):817–23.

Kuo W, Ciet P, Tiddens HAWM, Zhang W, Guillerman RP, Van Straten M. Reply: Cumulative radiation exposure to abdominal organs in patients with cystic fibrosis should not be forgotten. Am J Respir Crit Care Med. 2014;190(8):961–2.

Rosenow T, Oudraad MCJ, Murray CP, Turkovic L, **Kuo W**, de Bruijne M, Ranganathan SC, Tiddens HAWM, Stick SM. PRAGMA-CF. A quantitative structural lung disease computed tomography outcome in young children with cystic fibrosis. Am J Respir Crit Care Med. 2015;191(10):1158–65.

Rosenow T, Oudraad MCJ, Murray CP, Turkovic L, **Kuo W**, de Bruijne M, Ranganathan SC, Tiddens HAWM, Stick SM. Reply: Excess risk of cancer from computed tomography scan is small but not so low as to be incalculable. Am J Respir Crit Care Med. 2015;192(11):1397–9.

Salamon E, Lever S, **Kuo W**, Ciet P, Tiddens HAWM. Spirometer guided chest imaging in children: It is worth the effort! Pediatr Pulmonol. 2016;56:48–56.

Perez-Rovira A, **Kuo W**, Petersen J, Tiddens HAWM, de Bruijne M. Automatic airway–artery analysis on lung CT to quantify airway wall thickening and bronchiectasis. Med Phys. 2016;43(10):5736–44.

Tiddens HAWM, van Straten M, **Kuo W**, Ciet P. Clinical year in review, pediatric lung imaging: The times are a-changin'. European Respiratory Review. (submitted)

PHD PORTFOLIO

Name: WieYing Kuo
Erasmus MC Department:
1. Pediatric Pulmonology
2. Radiology

PhD period: 2012-2016
Promotor: Prof. dr. H. Tiddens
Co-Promotors: dr. M. de Bruijne and dr. ir. M. van Straten

1. PhD training	Year	Workload ECTS
General courses		
Grant writing course by prof. Quittner	2012	1.5
BROK (Basiscursus Regelgeving Klinisch Onderzoek)	2013	1.0
Nihes- Biostatistical Methods I : Basis principles	2013	5.7
Molmed – Basic course on 'R'	2015	1.8
Scientific integrity	2015	0.3
Seminars and workshops		
Research meetings dept. of Pediatrics, division of respiratory medicine	2012-2016	4.0
PhD day	2012	0.3
PhD day	2013	0.3
Sophia's 150th anniversary congress	2013	0.3
Presentations		
Sophia research day [poster presentation]	2013	0.3
ECFS CTN Steering committee (Lisbon, Portugal) [oral presentation]	2013	1.0
ECFS CTN Steering committee (Leuven, Belgium) [oral presentation]	2014	1.0
Longdagen [poster presentation]	2014	0.3
LEAD (Lectures Education Awareness & Discussion) in CF [oral presentation]	2015	1.0
Sophia research day [Slam Presentation]	2016	0.3

International Conferences

36th European CF Society Conference, Lisbon, Portugal [oral presentation]	2013	1.4
23rd European Respiratory Society International Congress, Barcelona, Spain [oral presentation]	2013	1.4
28th North American CF Conference, Atlanta, USA [poster presentation]	2014	0.3
European Congress of Radiology, Vienna, Austria [oral presentation, awarded Scientific Session Best Paper]	2015	1.4
European CF Young Investigator Meeting, Paris, [oral and poster presentation]	2015	1.7
North American CF Conference [poster presentation]	2015	0.3
39th European CF Society Conference, Basel Switzerland [2 oral presentations]	2016	2.8
29th North American CF Conference, Phoenix, USA [invited speaker and poster presentation]	2016	1.7

Grants and awards

Best Paper Scientific Session ECR 2015	2015
Travel grants for conference participation; Vereniging Trustfonds Erasmus Universiteit Rotterdam	2014-2015

2. Teaching	**Year**	**Workload ECTS**

Master Theses Supervision

Merel Oudraad, medical student, University Medical Center Utrecht	2013	3.0
Pauline Wesselman van Helmond, medical student, Erasmus Medical Center	2014	3.0
Michelle van den Berg, medical student, Erasmus Medical Center	2014	3.0
Thomas Soffers, medical student, Erasmus Medical Center	2015	3.0
Abdullah Horiakhill, medical student, Erasmus Medical Center	2015	3.0
Niels Erkelens, medical student, Erasmus Medical Center	2015-2016	3.0

Workshops

Site visits to 19 CF centers for standardized pediatric chest CT workshops.	2013	3.0
LEAD in CF workshop for pediatric pulmonologists	2015	0.3

Other

Peer review of articles for international scientific journals	2012-2016	2.0
Outpatient clinic pediatric pulmonology	2012-2016	3.0
Chairing biweekly PhD lunch meetings	2012-2016	2.0
TOTAL		**58.4**

LIST OF ABBREVIATIONS

3D	three-dimensional
AA	airway and accompanying artery
AIC	Akaike information criterion
A_{in}A-ratio	inner airway diameters divided by the accompanying artery diameter
A_{out}A-ratio	outer airway diameters divided by the accompanying artery diameter
AREST CF	Australian Respiratory Early Surveillance Team for Cystic Fibrosis
AT	air trapping
AUC	area under the curve
AWT	airway wall thickness
A_{WT}A-ratio	wall thickness divided by the accompanying artery diameter
A_{WT}-ratio	wall thickness divided by the outer airway diameter
BE	bronchiectasis
BEIR	Biological Effects of Ionizing Radiations
BERT	Background Equivalent Radiation Time
CF	cystic fibrosis
CF-CT	cystic fibrosis computed tomography
CFTR	cystic fibrosis transmembrane conductance regulator
CI	confidence interval
COPD	chronic obstructive pulmonary disease
CSA	cross-sectional area
CT	computed tomography
CTDI	Computed Tomography Dose Index
$CTDI_{vol}$	Volumetric Computed Tomography Dose Index
CVID	common variable immunodeficiency
DLP	dose-length-product
EAR	Excess absolute risk
ECFS-CTN	European Cystic Fibrosis Society-Clinical Trial Network
ERR	Excess relative risk
FEF_{25-75}	forced expiratory flow between 25 and 75% of forced vital capacity
FEV_1	forced expiratory volume in the first second
FOV	field of view
FVC	forced vital capacity

Gy	gray
HIV	human immunodeficiency virus
HU	hounsfield units
ICC	intraclass correlation coefficient
interBT	inter-branch tapering
intraBT	intra-branch tapering
IQR	interquartile range
IRB	institutional review board
LING	lingula
LLL	left lower lobe
LNT	linear no-threshold dose response model
LUL	left upper lobe
mGy	milligrays
MP	mucous plugging
MTF	modulation transfer function
PFT	pulmonary function tests
PRAGMA-CF	Perth-Rotterdam Annotated Grid Morphometric Analysis for CF
PSF	point spread function
Q_1-Q_3	first to third quartile
QIBA	Quantitative Imaging Biomarkers Alliance
Q_{NOISE}	image quality solely related to image noise
$Q_{NOISE,RES}$	image quality with relationship between image noise and spatial resolution
$Q_{NOISE,RES,DOSE}$	image quality with relationship between image noise and spatial resolution and relationship between image noise and radiation dose
QRM	Quality Assurance in Radiology and Medicine
RLL	right lower lobe
RML	right middle lobe
ROC	receiver-operating characteristic
RUL	right upper lobe
SALD	severe advanced lung disease
SCC	spearman correlation coefficient
SCIFI CF	Standardized Chest Imaging Framework for Interventions and personalized medicine in CF

SE	standard error
SEER	Surveillance, Epidemiology and End Results program
SG	segmental generation
SLD	structural lung disease
SSDE	size specific dose estimate
SSP	slice sensitivity profile
Sv	sievert
TAD	total airway disease
TLC	total lung capacity
WAP	wall area percentage

ABOUT THE AUTHOR

WieYing Kuo - Kim was born on the 1st of March 1989 in Rotterdam, the Netherlands. She grew up in Rotterdam and graduated from secondary school at the Montessori Lyceum Rotterdam in 2007. That same year she started her medical training at the Erasmus University, Medical Center in Rotterdam. During her studies WieYing worked in the psychiatry department as a team leader who supervised students that provided assisted care for patients. Her fourth year of medical school was spent abroad in the United States conducting an elective research at Seattle Children's Hospital. Under the supervision of Prof. Dr. G.J. Redding and Prof. Dr. H.A.W.M. Tiddens, she developed a strong inclination towards the fundamentals of her research. This research project of hers led to her first publication of an article in a medical journal, and eventuated into continued work with Dr. H. Tiddens through a PhD program before starting her clinical rotations. She obtained her *doctoraal examen* (Master's Degree) April of 2012 and started her PhD project in May at the departments of Pediatric Pulmonology and Radiology, Erasmus MC, Rotterdam, the Netherlands (Promotor: Prof. Dr. H.A.W.M. Tiddens; Co-promotors: Dr. M. de Bruijne and Dr. M. van Straten). She has also supervised several medical students while they were conducting their elective research projects.

WieYing worked on the studies described in this thesis and published her work in several peer-reviewed international journals. She has presented her findings at several national and international conferences and won the Best Paper Scientific Session in 2015 at the European Conference of Radiology, Vienna, Austria. While pursuing her doctorate degree, she also coordinated an international multi-center multi-city study in Europe and USA, traveling to many Cystic Fibrosis care centers to present her study and to characterize the CT scanners.

Since August 2016, WieYing has continued her clinical rotations of her medical training. She plans to graduate medical school August 2018.